Analysis of the Role of the Cohesin Regulatory Proteins Pds5, Esco1, and Esco2 in DNA Replication

A Thesis submitted to the College of Medicine, Biological Sciences, and Psychology of the University of Leicester

by

Lubinda Mukololo

in accordance with the requirements for the award of the Degree of

Doctor of Philosophy

in

Biochemistry

Department of Molecular and Cell Biology
Henry Wellcome Building
Lancaster Road
Leicester
LE1 7RH, UK

September 2016

Declaration

The accompanying thesis submitted for the degree of Doctor of Philosophy, titled 'Analysis of the Role of the Cohesin Regulatory Proteins Pds5, Esco1, and Esco2 in DNA replication', is my own work based on the research I conducted in the Department of Molecular and Cell Biology (formerly Biochemistry) at the University of Leicester during the period between September 2013 and September 2016. The material in this thesis has not been copied from any other person's work (published or unpublished) and has not been previously submitted for assessment for another degree in this or any other University. Where secondary data is used, this has been clearly acknowledged in text or by references.

Signed: ……..

Date: ……01/09/2016…….

University of Leicester

Department of Molecular and Cell Biology

Henry Wellcome Building

Lancaster Road

Leicester

LE1 7RH

Abstract

Sister chromatid cohesion (SCC) is mediated by the cohesin complex whose core components are Smc1, Smc3, Scc1, and Scc3 (SA1 and SA2 in vertebrates) and is regulated by associated factors that include Pds5 (Pds5A and Pds5B in vertebrates) and the acetyltransferases Esco1 and Esco2. The correct establishment and maintenance of sister chromatid cohesion is important in safeguarding genome integrity. Previous studies have shown that Pds5 is important in the establishment and maintenance of SCC (in yeast and fungi) as well as sister chromatid resolution (in humans and *Xenopus*). In humans, both Esco1 and Esco2 acetylate Smc3 during DNA replication to establish SCC.

Cohesin participates in DNA replication by modulating higher-order organisation of replication factories. Although disputed in *Xenopus* egg extracts, cohesin acetylation is reported to speed replication forks in human somatic cells. However, the mechanistic consequences of cohesin acetylation are still poorly understood and while Pds5's role in SCC maintenance and resolution has been explored, no study to date has reported its role in DNA replication. Pilot studies (unpublished) in our lab have implicated Pds5 in DNA replication. In light of the foregoing, the aim of this project was to analyse the role of Pds5, Esco1, and Esco2 in DNA replication.

Here, using an siRNA approach and DNA combing techniques in mammalian cells, I show that Pds5, Esco1, and Esco2 are functionally important in DNA replication. Depletion of either Esco1 or Esco2 results in precocious separation of sister chromatids, delay in DNA replication, apoptosis, or senescence. Depletion of Pds5 proteins is characterised by DNA damage which eventually activates the intra-S-phase DNA damage checkpoint that delays replication fork progression. Depletion of the anti-establishment complex, Pds5A and Wapl, rescues the defect in DNA replication observed when Pds5A is depleted alone. These results provide a novel insight into the role of Esco1, Esco2, and Pds5 in the regulation of DNA replication and suppression of aneuploidy in mammalian cells.

Acknowledgement

I am sincerely grateful to my supervisor, Dr Raj Patel, not only for his adept tutelage and flexibility, but also for his patience and encouragement throughout this project. I would also like to record my sincere gratitude to my second supervisor, Dr Sally Prigent, for her support and generous supply of secondary antibodies.

I owe earnest thankfulness to my committee members, Dr Salvador Macip and Dr Shaun Cowley, for their guidance. Special thanks go to Dr Salvador Macip's lab for the help and guidance with the senescence protocol, reagents, and antibodies. I am also thankful to Dr Don Jones' lab for the help with the comet assay.

Many thanks go to Dr Kees Straatman for his help with confocal image acquisition and analysis. I would also like to sincerely thank Dr Lucia Pinon for her invaluable guidance and training with flow cytometry. I thank Katie White and Nitika Gupta for their help with the RPE1 and HeLa cell growth curves.

I am truly indebted to my sponsors, the Commonwealth Scholarship Commission, for funding my PhD.

To my wife Mercy and son Imasiku, thank you for your unrivalled support; my time in the UK would not have been as enjoyable without your care and warm company.

Table of Contents

List of Tables

Table of Figures

List of Abbreviations

%	Percentage
°C	Degree celsius
53BP	p53 binding protein
A. nidulans	*Aspergillus nidulans*
a.a	Amino acid
Ac-Smc3	Acetylated structural maintenance of chromosomes 3
ACT	Acetyltransferase binding motif
AML	Acute myeloid leukaemia
APC/C	Anaphase-promoting complex/cyclosome
APS	Ammonium persulphate
ASP	Aspartic acid
ATM	Ataxia telangiectasia mutated
ATP	Adenosine triphosphate
ATPase	Adenosine triphosphatase
ATR	Ataxia telangiectasia and Rad3 related
BRCA1	Breast cancer 1
BrdU	5'-Bromo-2'-deoxyuridine
BSA	Bovine serum albumin
Bub1/3	Budding uninhibited by benzimidazole proteins 1/ 3
C-terminal	Carboxyl terminal
C. elegans	*Caenorhabditis elegans*
C2H2	Cys (2) His (2) zinc finger domain
CAF	Chromatin assembly factor
CAR	Cohesion attachment regions

CBS	Cohesin binding site
Cdc2	Cell division control protein 2 homolog
Cdc20	Cell division cycle protein 20
Cdc25A	Cell division cycle protein homolog A
Cdc6	Cell division cycle 6 protein
Cdh1	Cdc20 homologue 1
Cdk	Cyclin dependent kinase
CDKI	Cyclin dependent kinase inhibitor
CdLS	Cornelia de Lange Syndrome
Cdt1	Chromatin licensing and DNA replication factor 1
Chk1/2	Checkpoint kinase 1/2
Chl1	chromosome loss 1
CIdU	Chlorodeoxyuridine
CIP	Ctf4-interaction peptide motif
CML	Chronic myeloid leukaemia
CO_2	Carbon Dioxide
CPC	Chromosome passenger complex
CSC	Checkpoint sliding clamp
Csm3	Chromosome segregation in meiosis 3
CTCF	CCCTC binding factor
Ctf4	Chromosome transmission fidelity 4
D. melanogaster	*Drosophila melanogaster*
DMEM	Dulbecco's Modified Eagle's Medium
DNA	Deoxyribonucleic acid
DSB	DNA double-strand breaks

EDTA	Ethylenediaminetetraacetic acid
EGTA	Ethylene glycol tetraacetic acid
EJ p21/53	A human bladder carcinoma with a tetracycline-regulated p21/ p53
ESCO1/2	Establishment of sister chromatid cohesion N-acetyltransferase homolog 1/2
FACS	Fluorescence-activated cell sorting
FBS	Foetal bovine serum
FGF	Phenylalanine-Glycine-Phenylalanine
Fitc	Fluorescence isothiocyanate
g	Gram
G1	Gap 1
G2	Gap 2
GBM	Glioblastoma multiforme
GINS	Go, Ichi, Nii, and San (five, one, two, and three in Japanese)
ɣ	Gama
h	Hour
H. sapiens	*Homo sapiens*
HCl	Hydrochloric acid
HDAC8	Histone deacetylase 8
HEAT	Huntington, Elongation Factor 3, PR65/A, TOR
HeLa	Henrietta Lacks
HP1	Heterochromatin protein 1
HRP	Horseradish peroxidase
IdU	Iododeoxyuridine
INCENP	Inner centromere protein

kb	Kilobase
KCl	Potassium chloride
kDa	kilo Daltons
LBA	Lysis buffer A
LBB	Lysis buffer B
LBC	Lysis buffer C
M (unit)	Molarity
M-phase	Mitotic phase
mA	Miliampere
Mad2	Mitotic arrest deficient protein 2
MCC	Mitotic checkpoint complex
Mcm	Minichromosome maintenance
MDC1	Mediator of DNA damage checkpoint 1
MEFs	Mouse embryonic fibroblasts
MeOH	Methanol
min	Minute
ml	Millilitres
Mm	*Mus musculus*
mm	Millimetre
mM	Millimolar
Mrc1	Mediator of replication checkpoint
MRE11	Meiotic recombination protein 11
mRNA	Messenger RNA
N- terminal	NH_2 terminal
NBS1	Nijmegen breakage syndrome 1

nM	Nanomolar
NP40	Nonyl phenoxypolyethoxylethanol 40
ns	Not significant
ORC	Origin recognition complex
p16/21/53	Protein 16/21/53
PARP	Poly (ADP-ribose) polymerase
PBS	Phosphate buffered saline
PCNA	Proliferating cell nuclear antigen
Pds5	Precocious dissociation of sisters protein 5
Pen/Strp	Penicillin/Streptomycin
PI	Propidium iodide
PIP	PCNA-interacting Protein
Plk1	Polo-like kinase 1
PMSF	Phenylmethylsulphonly fluoride
PP2A	Protein phosphatase 2A
pre-RC	Prereplicative complex
R. norvegicus	*Rattus norvegicus*
RAD1/9/17/50	Radiation sensitive protein 1/9/17/50
RB	Retinoblastoma protein
RBS	Robert's Syndrome
RFC	Replication factor C
RIPA	Radio-immunoprecipitation assay buffer
RNA	Ribonucleic acid
RNAse	Ribonuclease A
RPE1	Retinal pigment epithelial 1 cells

rpm	Revolution per minute
RT	Room temperature
S	Serine
s	Second
S-phase	Synthesis-phase
S. cerevisiae	*Saccharomyces cerevisiae*
S. macrospora	*Sordaria macrospora*
S. pombe	*Schizosaccharomyces pombe*
s.e.m	Standard error of the mean
SA- β-Gal	Senescence-associated endogenous β-galactosidase activity
SA1/2/3	Stromal antigens 1/2/3
SAC	Spindle assembly checkpoint
SCC	Sister chromatid cohesion
Scc1/2/4	Sister chromatid cohesion protein 1/2/4
SDS	Sodium dodecyl sulphate
SDS-PAGE	Sodium dodecyl sulphate polyacrylamide gel electrophoresis
Ser	Serine
Sgo1	Shugoshin 1
siRNA	Small interfering ribonucleic acid
Smc	Structural maintenance of chromosomes
T	Threonine
TADs	Topologically associating domains
Temed	Tetramethylethylenediamine
Tof1	Topoisomerase I interacting factor
TopBP1	Topoisomerase binding protein 1

TST	Tris-saline tween 20
V	Voltage
v/v	Volume in volume ratio
w/v	Weight in volume ratio
WABS	Warsaw breakage syndrome
Wapl	Wings apart-like protein
WHD	Winged-helix domain
X. laevis	*Xenopus laevis*
α	Alpha
β	Beta
µ	Micron
µg	Microgram
µl	Microliter
µm	Micrometre
µM	Micromolar

Chapter 1 - Introduction

1.1 Sister Chromatid Cohesion

During the mitotic cell cycle, cells execute two important events: precise duplication of each chromosome and partitioning of the duplicated chromosomes between two identical daughter cells (Yu & Tang, 2005). Maintenance of genome integrity is dependent upon the accuracy of these processes (Shen, 2011). The original and the duplicated copy of each chromosome (sister chromatids) are associated with each other physically through the sister chromatid cohesion (SCC) complex (Chatterjee et al., 2013). The cohesion of sister chromatids is important for the prevention of precocious separation of sister chromatids and the regulation of gene expression and development (Dorsett, 2007).

In normal cells, the establishment and dissolution of SCC is a tightly regulated process and aberrant regulation can lead to missegregation and aneuploidy (a hallmark of cancer cells) (Shen, 2011; Pfau & Amon, 2012), as well as development of congenital birth defects such as Robert's Syndrome (RBS), Cornelia de Lange Syndrome (CdLS), and Down's syndrome (Shen, 2011; Pfau & Amon, 2012). An in-depth understanding of the molecular mechanisms that regulate the dissolution of SCC should therefore provide an important insight into how cell division is regulated and how aberrant regulation may lead to the development of cancer. This can be achieved by studying the functional properties of regulatory proteins that have been implicated in SCC regulation.

A number of proteins have so far been identified as key regulators of SCC and its dissolution (Losada & Hirano, 2005; Nasmyth & Haering, 2005; Nasmyth, 2005; Hirano, 2005). Previous studies (unpublished) in our lab have shown that some of these proteins may be functionally important in SCC resolution, DNA replication, and DNA damage repair processes. This project is aimed at investigating the role of cohesin regulatory proteins, Pds5, Esco1, and Esco2, in S-phase and mitosis in mammalian cells. This introduction explains the basic principles of the cell cycle, the cohesin complex, and our current understanding of the roles and mechanisms of the regulatory proteins associated with the cohesin complex.

1.2 The Mammalian Cell Cycle

The cell cycle is a sequence of events by which a growing cell duplicates its DNA and all other cellular components and divides into two daughter cells, each with the same amount of DNA. These sequences of events are divided into four phases (Figure 1.1). The cell generates a single and faithful copy of its genetic material during the synthetic or S-phase and accurately separates the replicated DNA between the two daughter cells at mitosis or M-phase (Yu, 2002). The other two phases of the cycle, G1 and G2, represent 'gap' phases, during which cells continue to grow in readiness for successful completion of S and M phases, respectively. When cells cease to proliferate, either due to the presence of specific anti-mitogenic signals or the absence of proper mitogenic signalling, they exit the cycle and enter a non-dividing, quiescent state known as G0 (Yu and Tang, 2005). Furthermore, in the face of aberrant regulation, cells undergo senescence or apoptosis to ensure that defective DNA is not propagated and passed on to new daughter cells.

Re-entry into the cell cycle from quiescence, through the G1-phase, is mediated by a highly conserved family of proteins called cyclin-dependent kinases (cdks), whose activation requires binding to specific regulatory subunits called cyclins (Malumbres & Barbacid, 2009). Biochemical events that prompt quiescent cells to enter the cell cycle involve phosphorylation of target proteins e.g. retinoblastoma protein (RB) and degradation of cdk inhibitors (CDKIs) (Malumbres & Barbacid, 2009). Extra-cellular stimuli such as growth factors and hormones elevate D-type cyclins which bind to and activate cdk4 and cdk6. The cyclin D/cdk4/6 complex is the central cell cycle regulator and once formed, is sufficient to convert unphosphorylated RB/E2F-1/DP complex to the hypophosphorylated form (Malumbres & Barbacid, 2009).

Upon activating cyclin D/cdk4/6, growth factors also activate other genes that include cyclin E. Once activated, cyclin E binds to cdk2 and causes the hyperphosphorylation of RB, which then dissociates from E2F-1 (Malumbres & Barbacid, 2009). The dissociation of hyperphosphorylated RB from the E2F-1/DP complex enables activation of the E2F-1 responsive gene, which drives the cell cycle through the G1/S transition and induces DNA synthesis (Hinds et al., 1992; Lundberg & Weinberg, 1998).

After replication, DNA is packed into condensed chromatin fibres and the basic packing unit is a nucleosomal repeat which consists of 147 DNA base pairs wrapped around an octamer of histones (Olins & Olins, 1974; Olins & Olins, 2003). With the aid of proteins such as the chromatin assembly factors (CAFs) which are associated with the replication fork machinery, nucleosomes mediate assembly of newly replicated DNA. During S-phase in eukaryotes, five basic types of histones are synthesised; these are histones H1, H2A, H2B, H3, and H4 (Olins & Olins, 1974; Olins & Olins, 2003). Histone H1 is the linker, while the H2A, H2B, H3, and H4 are the core histones. Two copies of each of the core histones come together to form a central octamer which binds and wraps approximately 146 base pairs of DNA. The linker histones then bind to DNA on the outside of the nucleosomes and interact with each other, causing close packaging of chromatin into higher order structures (Olins & Olins, 1974; Olins & Olins, 2003). There are two distinct types of eukaryotic chromatin: euchromatin and heterochromatin. Of these two types, euchromatin is the more accessible and easily transcribed type because it is less condensed and contains more genes and unique sequences (Olins & Olins, 2003). Heterochromatin, on the other hand, is highly condensed and contains highly repetitive satellite sequences. It forms structural components of centromeres and telomeres (Olins & Olins, 1974; Olins & Olins, 2003).

After S-phase, cells enter the G2-phase where they continue to grow and prepare for cell division in M-phase. Cyclin A is induced shortly after cyclin E and binds to cdk2 in S-phase and to cdk1 in G2 and mitosis (Hinds et al., 1992). Mitosis is a highly regulated process and occurs in six distinguishable stages: prophase, prometaphase, metaphase, anaphase, telophase, and cytokinesis (Figure 1.1) (Malumbres & Barbacid, 2009). During prophase, centrosomes (microtubule-organising structures) separate, forming the mitotic spindle. In prometaphase, kinetochores attach to the chromosomes and microtubules attach to the kinetochores. Chromosomes are aligned and organised between the spindle microtubules at metaphase, and separated at anaphase by moving to the opposite sides of the cell through the shortening and depolymerisation of the mitotic spindle. This is followed by cytokinesis, when the cell divides into two daughter cells, each having equal amount of DNA and the necessary biochemical machinery to repeat the process of cell division (Malumbres & Barbacid, 2009).

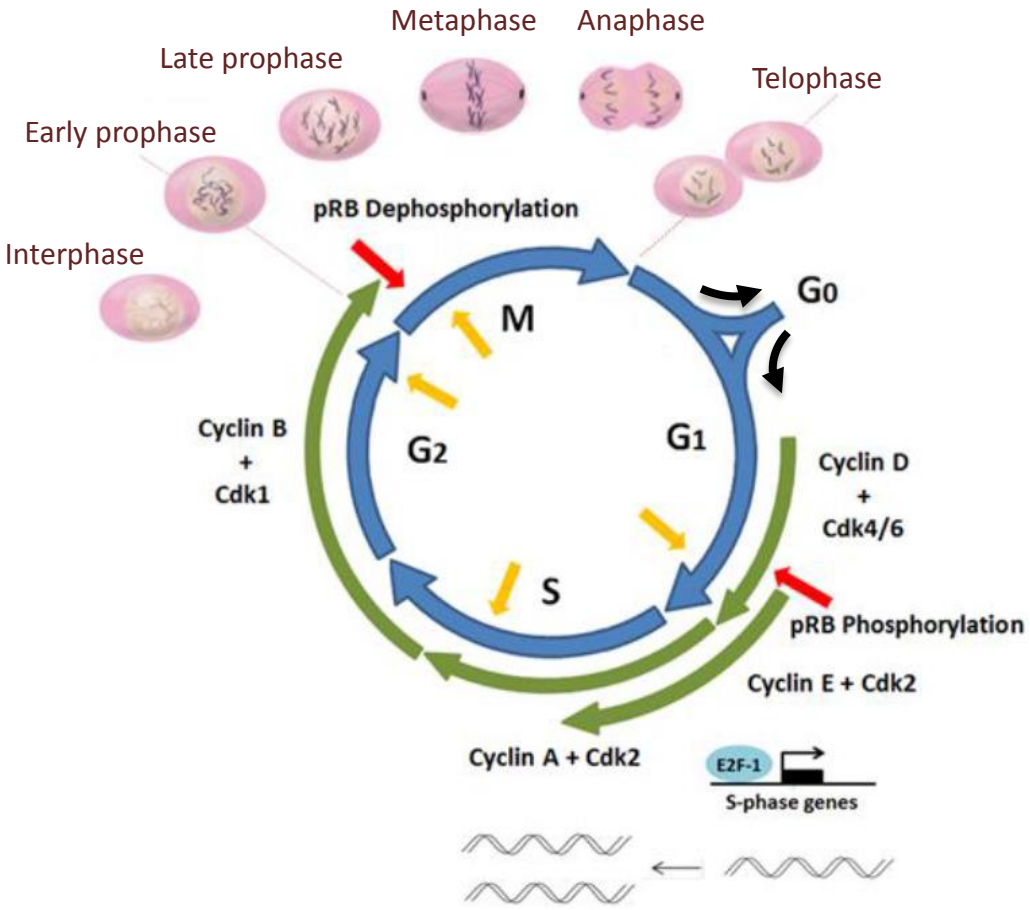

Figure 1.1 The regulation of the eukaryotic cell cycle

The cell cycle consists of interphase and mitosis (M). Interphase is divided into three distinct phases: Gap 1 (G1), Synthesis (S) and Gap 2 (G2). Interphase is monitored by three DNA damage checkpoints during the cell cycle, while mitosis is monitored by one spindle assembly checkpoint (yellow arrows). Non-proliferative cells exit the cell cycle and enter G0, where they remain quiescent until growth factors are available to prompt them back into cell cycle. Growth factors also activate Cdk4/6 and Cdk2, which hyperphosphorylate and dissociate Rb from E2F-1. E2F-1 then allows the G1-to-S-phase transition. Cells enter the G2-phase after DNA synthesis, where they continue to grow and prepare for cell division in mitosis. During mitosis, chromosomes condense (Early prophase), the nuclear envelope breaks down, and spindle microtubules attach to kinetochores (Prophase). The chromosomes then align at the metaphase plate (Metaphase), separate and pull apart to the spindle poles (Anaphase). The nuclear envelope reforms for each daughter cell (Telophase) and the two daughter cells are now divided (Cytokinesis) (Alberts, 2008; Malumbres & Barbacid, 2009).

1.2.1 Cell Cycle Checkpoints

During the eukaryotic cell cycle, a set of feedback control mechanisms monitor the successful completion of events in one phase of the cell cycle before allowing the cell to proceed to the next phase. For example, the Start/Restriction point in late G1 monitors cell size and nutrients before allowing cells to enter S-phase (Bertoli et al., 2013). These regulatory pathways, commonly referred to as cell cycle checkpoints, ensure that genetic information is copied faithfully and transmitted from the mother cell to the daughter cells. This regulation involves monitoring and detecting damaged DNA through the DNA damage checkpoint at G1 and G2; detecting improper alignment of chromosomes at the metaphase plate and failure of the spindle microtubule attachment to kinetochores through the spindle assembly checkpoint (SAC). When an anomaly is detected, progression through the cell cycle is halted in order to prevent replication of damaged DNA or propagation of the damaged chromosomes. Progression through the cell cycle only resumes after the errors have been corrected.

1.2.1.1 The DNA Damage Checkpoint

When damaged DNA is detected in the G1-phase, sensor genes RAD17, RAD9, Rad1, and HUS1 (in yeast) form a heterotrimeric checkpoint sliding clamp (CSC) which has structural similarities with the DNA polymerase clamp, the Proliferating Cell Nuclear Antigen (PCNA) (Figure 1.2) (Shiomi et al., 2002). Rad17 then forms a complex with four replication factor C (Rfc) subunits, Rfc2, Rfc3, Rfc4, and Rfc5, which act as a clamp loader that is related to PCNA (Kondo et al., 1999; Griffith et al., 2002).

Recruitment of these complexes to the damage site triggers the DNA damage response by activating the signal transducer kinases ATM and ATR. Activated ATM/ATR in turn phosphorylate and activate kinases such as Chk1 and Chk2 (Liu et al., 2000; Matsuoka et al., 2000). Once activated, Chk1 phosphorylates the C-terminal portion of cdc25A, resulting in inhibition of its phosphatase activity towards cdk2 and cdk4 (Chen et al., 2003). This stops the progression of the cell cycle until the damaged DNA is repaired. Chk2 phosphorylates cdc25A, BRCA1, and p53 at different sites compared to Chk1 (Bartek & Lukas, 2003).

Activation of p53 induces expression of p21, the cdk inhibitor, which then inhibits cyclin E-cdk2 activity, resulting in the blockage of the G1/S-phase transition (Bartek & Lukas, 2003).

Chk1 and Chk2 are also the major effectors of the G2/M DNA damage checkpoint response (Furnari et al., 1997; Matsuoka et al., 2000; Sanchez et al., 1997). Entry into mitosis is triggered through the rapid activation of the cdk1/cyclin B complex. The cdk1/cyclin B complex is under the control of Wee1 and Myt1, which phosphorylate cdk1 on two residues, Thr14 and Tyr15 (Lindqvist et al., 2009), to prevent its activation. The inhibitory phosphorylation of cdk1 is rapidly removed by cdc25 family phosphatases (cdc25A, cdc25B, and cdc25C) to trigger cdk1/cyclin B activation and mitotic entry (Lindqvist et al., 2009). In response to DNA damage, the target of the G2 arrest is cdk1/cyclin B. Chk1 phosphorylates and inhibits cdc25 family phosphatases via a combination of protein degradation (Mailand et al., 2000; Chen et al., 2003) and association with 14-3-3 proteins (Peng et al., 1997) while simultaneously phosphorylating and stimulating the activity of Wee1 (Lee et al., 2001). This allows the accumulation of inhibitory cdK1 phosphorylation while DNA damage persists, thus effectively blocking entry to mitosis (Smits et al., 2015).

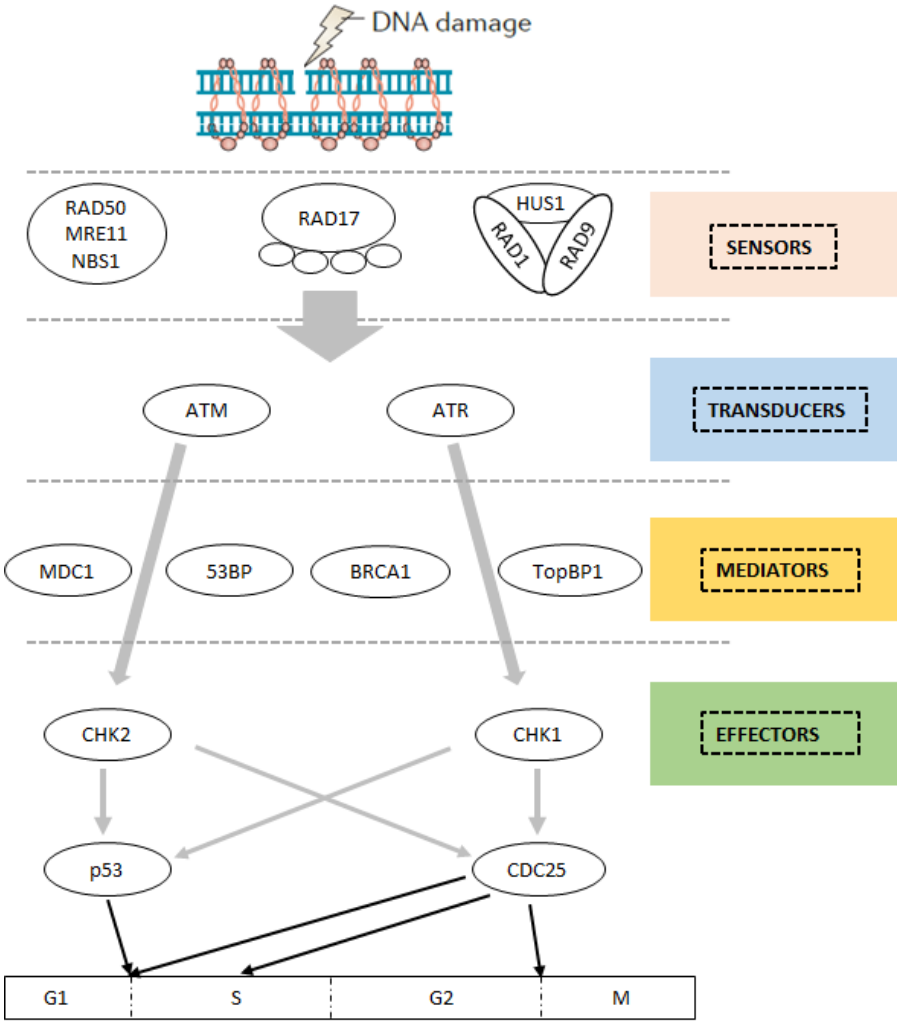

Figure 1.2 The DNA damage checkpoint signalling

In the presence of damaged DNA, sensor genes Rad9, Hus1, and Rad1 form a ring structure (the 9-1-1 complex) that can encircle DNA, similar to PCNA. The 9-1-1 complex is loaded onto damaged DNA by a protein complex that consists of four Replication Factor C (RFC) subunits (RFC_{2-5}) and Rad17, (the Rad17-RFC_{2-5} complex). The Rad50/Mre11/NBS1 complex, ATM and ATR, Rad17-RFC_{2-5}, and the 9-1-1 complex localise to sites of DNA damage independently but interact to trigger the checkpoint signalling cascade. Increased amounts of 9-1-1 on the damaged site triggers the DNA damage checkpoint response by activating the signal transducer kinase ATM/ATR, which in turn activates several kinases by phosphorylation, including Chk1 and Chk2. ATM and ATR also phosphorylate mediator proteins that include MDC1, 53BP, BRCA1, and TopBP1. Rad50/Mre11/NBS1 complex functions as a DSB sensor for ATM. Activated Chk1 phosphorylated the C-terminal portion of Cdc25 and inhibits its phosphatase activities towards Cdk2 and Cdk4, thus stopping the progression of the cell cycle until the damage is repaired. Activated Chk2 phosphorylates Cdc25 and p53. Once activated, p53 induces the expression of the Cdk inhibitor, p21, which inhibits cyclin E-Cdk2 activity, thereby inhibiting G1/S transition (Liu et al., 2000; Matsuoka et al., 2000; Houtgraaf et al., 2006).

1.2.1.2 The Spindle Assembly Checkpoint

The SAC is a signalling cascade that ensures that cells do not enter anaphase until chromosomes have lined-up at the metaphase plate and bipolar spindle attachment is accomplished (Yu, 2002). The main components of the SAC pathway include the mitotic-arrest deficient proteins (Mad1, Mad2, and Mad3/BubR1 in humans), the budding uninhibited by benzimidazole proteins (Bub1 and Bub3), and Mps1 (Figure 1.3) (Hoyt et al., 1991; Earnshaw & Mackay, 1994; Uhlmann et al., 1999; Cheeseman & Desai, 2008; Logarinho & Bousbaa, 2008; Kops, 2009). The principal target of the SAC is Cdc20, an activator of the Anaphase Promoting Complex/Cyclosome (APC/C) ubiquitin ligase that targets proteins for degradation by the 26S proteosome (Morgan, 1999; Reddy et al., 2007; Stegmeier et al., 2007).

The SAC gets constitutively activated as soon as cells enter mitosis (Barbosa et al., 2011). In the presence of non-attached or mis-attached kinetochores to microtubules, failure by chromosomes to align at the metaphase plate, or if spindle microtubules attached to kinetochores fail to generate appropriate bipolar tension, the cell cycle is blocked at the metaphase-to-anaphase transition (Figure 1.3) (Musacchio & Salmon, 2007). This allows time for correction of errors (Musacchio & Salmon, 2007). Mad2, Bub3, and Mad3/BubR1 are recruited to unattached kinetochores and form the mitotic checkpoint complex (MCC) (Sudakin et al., 2001). The MCC sequesters Cdc20. By sequestering Cdc20, the MCC inactivates APC/C, thereby enabling cyclin B to bind to Cdk1 and Securin to bind to Separase and prevent it from cleaving cohesin. Inactivation of the APC/C also ensures that Cyclin B is not targeted for degradation by the APC/C. Prevention of Separase activation and Cyclin B degradation ensures that cohesins are intact and the cell cycle is arrested. After bipolar spindle attachment to kinetochores is achieved, the SAC is silenced to allow the cell to progress to anaphase (Li et al., 1997). This involves disassembly of the MCC, which releases Cdc20. Free Cdc20 then binds and activates APC/C, which in turn ubiquitinates Securin and Cyclin B. Degradation of Securin activates Separase, which then cleaves the Scc1 subunit of cohesin, allowing sister chromatids to separate. Proteolysis of Cyclin B by the APC/C is required for the inactivation of cyclin-dependent kinase 1 (Cdk1), the master mitotic kinase whose down-regulation is required for exit from mitosis (Bharadwaj & Yu, 2004; Peters, 2006).

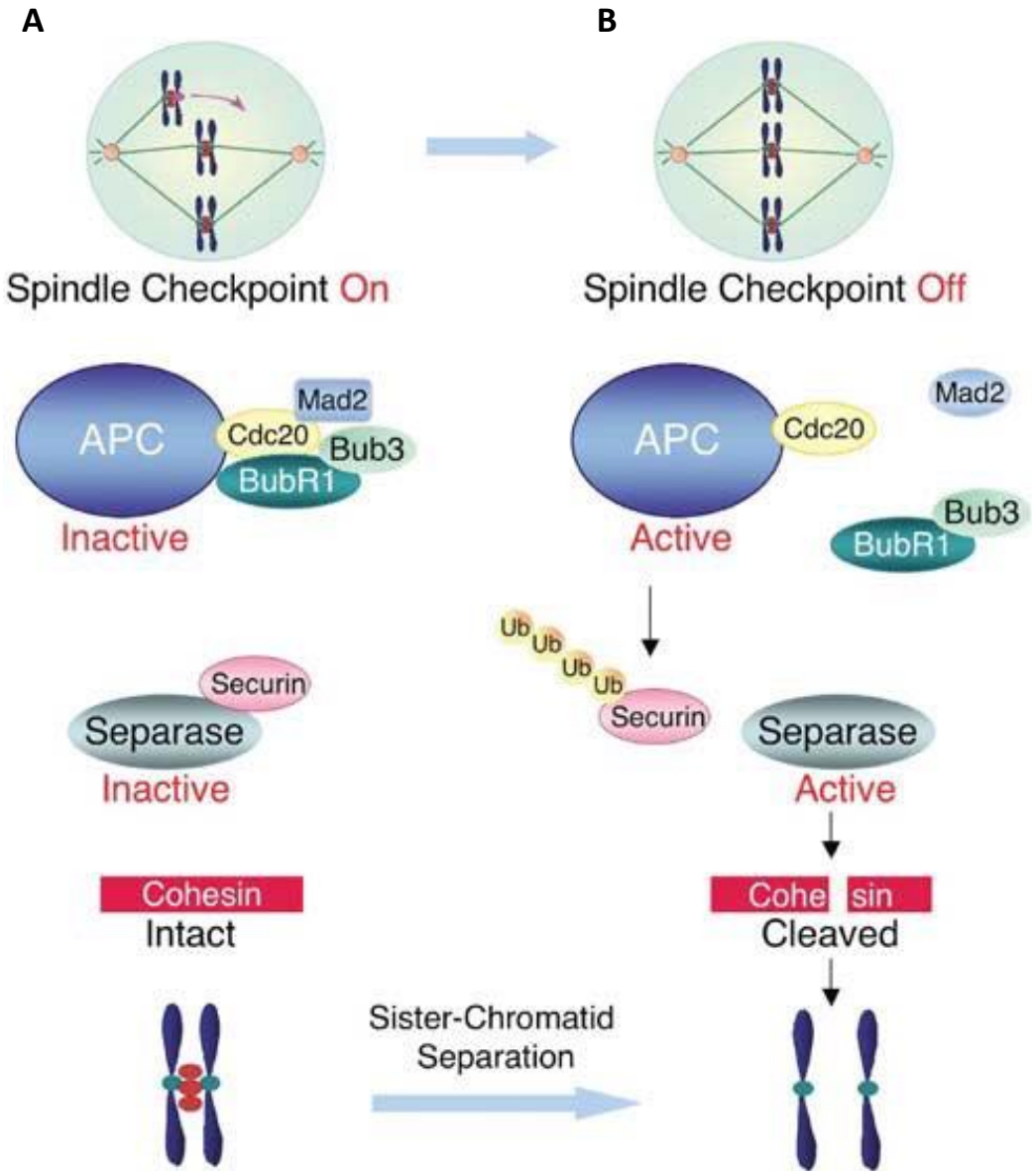

Figure 1.3 Spindle assembly checkpoint signalling

(**A**) In the presence of non-attached kinetochore to microtubules, Mad2, Bub3, and Mad3/BubR1 are recruited to unattached kinetochores and sequester Cdc20. This inactivates APC/C which depends on Cdc20 for its ubiquitin ligase activities, thereby enabling Securin to bind to Separase and prevent it from cleaving cohesins. (**B**) After bipolar spindle attachment to kinetochores is achieved, Mad2, Bub3, and Mad3/BubR1 disassemble, releasing Cdc20, which then binds and activates APC/C. Activated APC/C ubiquitinates Securin. Degradation of Securin activates Separase, which then cleaves the Scc1 subunit of cohesin, allowing sister chromatids to separate (Bharadwaj & Yu, 2004).

1.3 The Cohesin Complex

Within the cell cycle there is the chromosome cycle which is mediated by the cohesin complex. Originally discovered in genetic screens in yeast as a multi-subunit protein complex that regulates sister chromatid cohesion, the cohesin complex comprises two flexible structural maintenance of chromosomes (Smc) family of ATPases, Smc1/Psm1 (in humans) and Smc3/Psm3 (in humans), and two accessory subunits, the sister chromatid cohesion protein-1 (Scc1/Mcd1/Rad21) and stromal antigens Scc3/Psc3/SA (Figure 1.4) (Haering et al., 2002; Gruber et al., 2003). In vertebrates, Scc3 has three isoforms: SA1, SA2, and SA3 (reserved for meiotic cohesion) (Losada et al., 2000; Sumara et al., 2000). Cohesin is highly conserved in all eukaryotes (Table 1.1) (Guacci et al., 1997; Michaelis et al., 1997; Losada et al., 1998; Sumara et al., 2000; Losada et al., 2000; (White & Erickson, 2006).

Several studies have shown that the cohesin complex is a ring-shaped tripartite structure with a diameter of 50 nm created by a direct head-to-head interaction between the hinge domains of the Smc1 and Smc3 coiled coils, and a tail-to-tail interaction with Scc1/Mcd1/Rad21, a member of the kleisin protein family (see Figure 1.4) (Guacci et al., 1997; Michaelis et al., 1997; Losada et al., 1998; Sumara et al., 2000; Losada et al., 2000; Gligoris et al., 2014; Huis et al., 2014). Scc3/Psc3/SA serves as a scaffold for binding of several accessory subunits that regulate cohesin functions.

It has been shown that the C-terminal region of Scc1 forms a winged-helix domain (WHD) that interacts directly with the Smc1 ATPase head (Haering et al., 2004), while the N-terminal region of Scc1 folds into two helices, which form a four-helix bundle with the coiled-coil region adjacent to the Smc3 ATPase head (Gligoris et al., 2014). The central region of Scc1 folds into several short helices and binds to HEAT repeat-containing Scc3/Psc3/SA2 through an extensive binding interface of highly conserved residues (Hara et al., 2014). The cohesin complex topologically embraces and holds sister chromatids together from telophase/G1 until mitosis when it is removed from chromatin and chromosomes separate (Ivanov et al., 2005; Haering et al., 2008; Nishiyama et al., 2010).

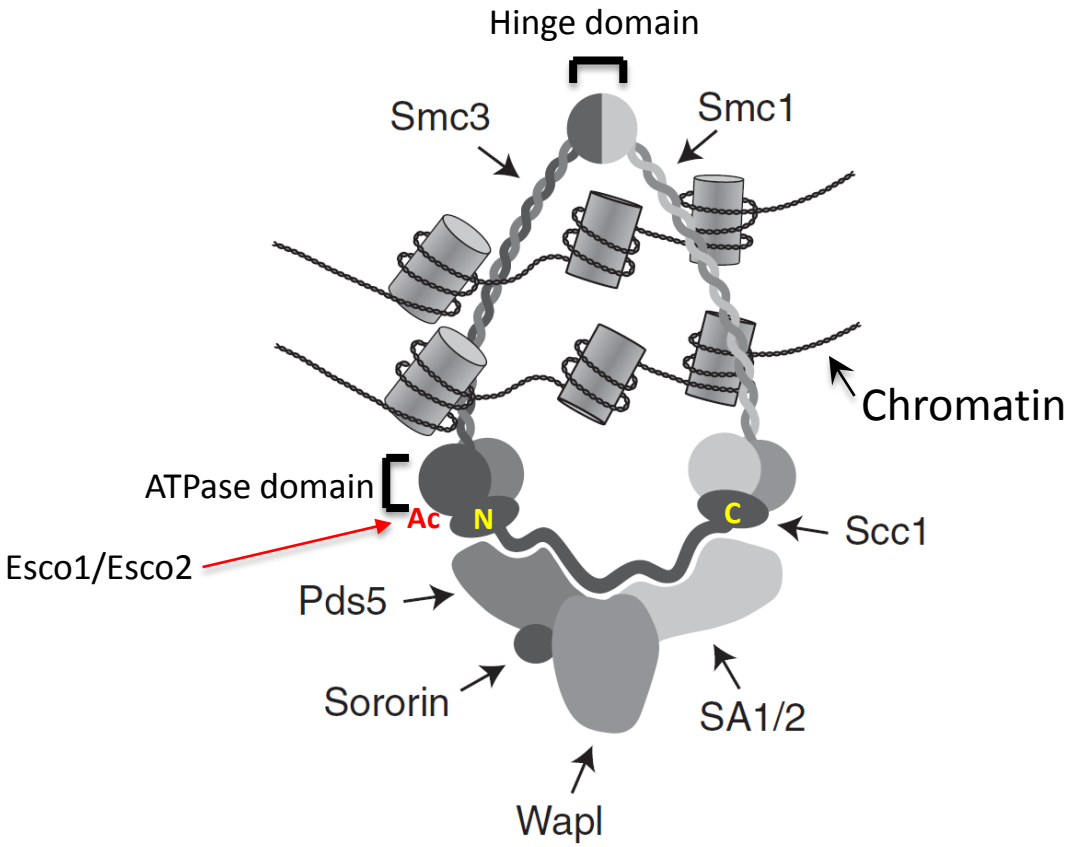

Figure 1.4 The cohesin complex

Cohesin is a ring-shaped tripartite protein complex made up of flexible coiled coils of the structural maintenance of chromosome proteins, Smc1 and Smc3; these two heterodimers bind to each other head to head through the hinge domain and tail to tail through their interaction with Scc1 and SA1 or 2. It is associated with regulatory proteins such as Pds5, Sororin, and Wapl, which bind cohesin via the Scc1 and SA1/2 subunits. Pds5 binds both Sororin and Wapl and regulates the function of Cohesin. The Pds5-Sororin complex is important in the maintenance of sister chromatid cohesion, in conjunction with Smc3 acetylation by Esco1 and Esco2. Wapl binds to Pds5 and removes cohesin from chromatin. Ac= acetylation; N= N-terminus of Scc1; C= C-terminus of Scc1 (Adapted, with modifications, from Peters, 2012).

Table 1-1 Conservation of cohesin subunits and cohesin regulatory proteins

Function	*H. sapiens*	*S. cerevisiae*	*S.pombe*	*D.melanogaster*	*X.laevis*
Cohesin subunits	Smc1 α Smc1 β* Smc3 RAD21/Scc1 SA1/STAG1 SA2/STAG2 SA3*/STAG3 Rec8*/Scc1	Smc1 Smc3 MCD1 Scc3 Rec8*	Psm1 Psm3 Rad21 Psc3 Rec11* Rec8*	Smc1 Smc3 Rad21 SA SA2 c(2)M*	Smc1 Smc3 Rad21 SA1 SA2 Rec8*
Loading factors	Nipbl hScc4 (Mau2)	Scc2 Scc4	Mis4 Ssl3	Nipped-B Scc4	Scc2 Scc4
Acetyltransferases	Esco1 Esco2	Eco1/Ctf7	Eso1	Deco San	XEsco1 XEsco2
Cohesin deacetylases	HDAC8**	Hos1			
Cohesion Establishment	Sororin/CDCA5			Dalmatian	
Cohesin maintenance	PDS5A PDS5B	PDS5	Pds5	Pds5	PDS5A PDS5B
Cohesion dissolution	WAPAL Plk1 Separin	Wpl1/Rad61 CDC5 ESP1	Wapl Plo1 Cut1	Wapl Polo Separase	Wapl Plx1 Separin

* Meiotic cohesin subunits
** Histone deacetylase 8
(Onn et al., 2008; Peters et al., 2008).

1.3.1 Cohesin Regulation during the Chromosome Cycle

1.3.1.1 Loading of Cohesin onto Chromatin

In every cell cycle chromosomes undergo a series of dynamic changes called the chromosome cycle, which involves replication, cohesion, and segregation, all mediated by the cohesin complex. Cohesin is recruited and loaded onto chromatin by the loader complex comprising Scc2 and Scc4 heterodimers (Kollerin complex/Nipbl/Mau) (Ciosk et al., 2000) and requires pre-replication complexes in vertebrates (Gillespie & Hirano, 2004; Guillou et al., 2010; Higashi et al., 2012; Takahashi et al., 2008) and ATP hydrolysis by the Smc3 head domains (Gruber et al., 2006). The cohesin complexes are assembled prior to loading onto chromatin (Losada et al., 1998; Waizenegger et al., 2000), and according to the logic of the ring model the cohesin ring must transiently open up to allow entry of DNA (Gruber et al., 2006). The cohesin ring has three possible gates, the Smc1–Smc3 hinge, the Smc1–Scc1 gate, and the Smc3–Scc1 gate (Figure 1.4). Studies in both yeast and human cells suggest that cohesin loading takes place via the Smc1–Smc3 hinge domain while the interface between Smc3 and Scc1 serves as the DNA exit gate (Gruber et al., 2006; Buheitel et al., 2013).

In vertebrates, cohesin is loaded onto chromatin during telophase while in budding yeast it is loaded in late G1 (Gillespie & Hirano, 2004; Takahashi et al., 2004); (Guacci et al., 1997). In yeast, cohesin cannot be loaded onto chromatin before G1 because of Separase's continuous destruction of cohesin through G1 (Uhlmann et al., 1999). In *S. cerevisiae* cohesin binds chromatin both at the centromeric region and the cohesion attachment regions (CARS), which are typically 500-800 base pairs long and occur nearly every nine kilobases along the chromosomes arms (Cohen-Fix, 2001; Wang & Christman, 2001). CARS have an increased A/T content (Blat & Kleckner, 1999). Before S-phase, the cohesin that associates with chromatin has high turnover due to the Wapl-Pds5 sub-complex-orchestrated cycle of chromatin entrapment and release (Eichinger et al., 2013; Gerlich et al., 2006; Nishiyama et al., 2010).

1.3.1.2 Cohesion Establishment and Maintenance

The recruitment and loading of cohesin onto chromatin by the Scc2-Scc4 loader complex is essential but not sufficient for the establishment of sister chromatid cohesion. Establishment of sister chromatid cohesion depends on acetyltransferase Eco1/Ctf7 (Esco1/Esco2 in humans), which is conserved from yeast to humans (Skibbens et al., 1999; Toth et al., 1999; Ivanov et al., 2002; Unal et al., 2007; Zhang et al., 2008), and acetylates Smc3 on two Lysine residues (K105/106 in humans) and renders cohesin insensitive to Wapl (Rolef et al., 2008; Rowland et al., 2009; Sutani et al., 2009; Unal et al., 2008; Zhang et al., 2008), following the passage of the replication fork (Nishiyama et al., 2010). In humans, acetylation of Smc3 is coupled with the recruitment of Sororin to chromatin, which displaces Wapl from Pds5, and establishes sister chromatid cohesion (Lafont et al., 2010; Nishiyama et al., 2010). Both Wapl and Sororin contain FGF (Phenylalanine-Glycine-Phenylalanine) motifs, via which they bind to Pds5 (Nishiyama et al., 2010).

Locking of cohesin's exit gate through the fusion of Smc3 to Scc1 allows stable sister chromatid cohesion in the absence of Eco1 (Chan et al., 2012), suggesting that Eco1-mediated Smc3 acetylation establishes cohesion by locking cohesin's exit gate. The establishment of sister chromatid cohesion is intimately linked to DNA replication and Eco1 has been shown to associate with the replication fork (Skibbens et al., 1999; Toth et al., 1999; Ivanov et al., 2002; Unal et al., 2007) and is specifically required in S-phase (Skibbens et al., 1999). Eco1 accumulates at sites of DNA replication and has been found to bind many factors involved in DNA replication including PCNA (Kenna & Skibbens, 2003; Lengronne et al., 2006; Moldovan et al., 2006; Song et al., 2012). Both Esco1 and Esco2 are required for Sororin-dependent stabilisation of cohesin on chromatin in G2 (Laduner et al., 2016).

Various models of chromatin entrapment by cohesin have been proposed (Figure 1.5). Among these is a model (Figure 1.5A) that proposes that cohesin entraps single DNAs before S-phase and that the replication fork passes through the cohesin rings, thereby automatically coentraping sister chromatids (Haering et al., 2002). Another model (Figure 1.5B) suggests that cohesin rings, loaded onto chromatin earlier, transiently

open to allow the passage of the replication forks and then reclose to coentrap sister chromatids (Lengronne et al., 2006). The third (Figure 1.5C) model proposes that cohesin *de novo* coentraps two sister chromatids at once after the passage of the replication forks. In each of these models, Eco1 (Esco1/Esco2) may be required for sister chromatid cohesion.

Sister chromatid cohesion can also be established in G2 in response to DNA damage in a manner that depends on Scc1 acetylation, but not Smc3, by Eco1/Esco1, suggesting that coentrapment of sister chromatids by cohesin does not strictly depend on DNA replication (Lyons & Morgan, 2011; Strom et al., 2007; Unal et al., 2007). Once established in S-phase, sister chromatid cohesion is maintained until mitosis. This notion is supported by the finding that there is a pool of chromatin-associated cohesin complexes that has little-to-no turnover throughout G2 (Chan et al., 2012; Gerlich et al., 2006; Lopez-Serra et al., 2013).

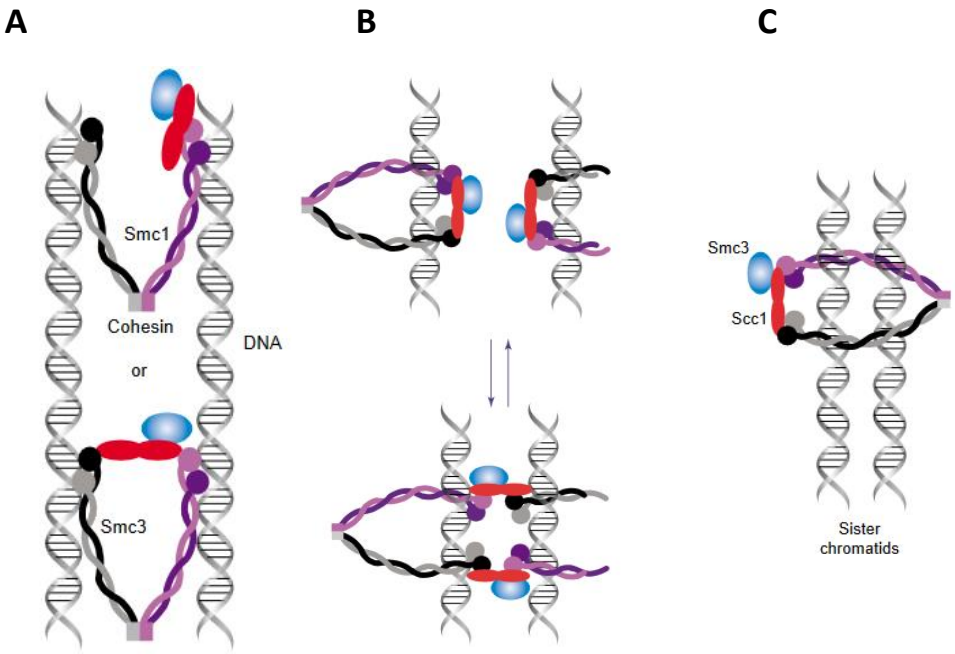

Figure 1.5 Models of cohesin interaction with chromatin

(**A**) The direct binding model. The SMC proteins interact directly with chromatin to form a physical bridge between the sister chromatids (Anderson et al., 2002, Haering et al., 2002). (**B**) The double-ring model. Cohesin complex loops around individual chromatids and cohesion is established by a change in the Scc1 association from intra-complex interactions (top panel) to inter-complex interactions (bottom panel). (**C**) The ring model. It is the currently accepted cohesin-chromatin interaction model, which proposes that the cohesin complex binds by encircling and embracing the two sister chromatids (Haering et al., 2002).

1.3.1.3 Cohesin Dissociation from Chromatin

Dissolution of sister chromatid cohesion takes place in mitosis. In yeast, sister chromatid cohesion is maintained until the metaphase-to-anaphase transition (Losada et al., 1998; Waizenegger et al., 2000). However, in animal cells, two distinct pathways, the prophase pathway and the SAC-mediated pathway, are responsible for the two-stage dissociation of cohesin from chromosomes; cohesin is removed from chromosome arms during prophase, and from the centromere during the metaphase-to-anaphase transition (Figure 1.6) (Losada et al., 1998; Waizenegger et al., 2000). A number of Serine/Threonine (S/T) protein kinases regulate the removal of cohesin from chromatin at mitosis; these include Aurora B, Cdk1, and Plk1 (Taylor & Paters, 2008; Hochegger et al., 2008; Takaki et al., 2008). While the role of Aurora B in the prophase pathway is still obscure, Cdk1 and Plk1 have been shown to phosphorylate Sororin and SA2, respectively, facilitating the removal of cohesin by Wapl from chromosome arms (Sumara et al., 2002; Rivera & Losada, 2009; Nishiyama et al., 2010).

Recent evidence suggests that the Smc3–Scc1 interface is the DNA exit gate of cohesin (Buheitel et al., 2013). Studies in yeast showed that fusion of Smc3 to the N-terminal region of Scc1 blocks the release of DNA from cohesin in interphase (Chan et al., 2012), while mutations in the Smc3–Scc1 interface in human cells destabilises the interaction between cohesin and chromatin, and disrupt sister chromatid cohesion (Huis et al., 2014), suggesting that the Smc3–Scc1 interface is the conserved DNA exit gate of cohesin. Why cohesin has distinct DNA entry and exit gates is not yet clear. Since the Smc1 and Smc3 coiled coils contain ATPase domains and are related to ABC transporters (Guacci et al., 1997; Michaelis et al., 1997; Losada et al., 1998; Sumara et al., 2000; Losada et al., 2000), a possible explanation of having separate entry and exit gates is to allow for a more specific level of regulation, conferring a sense of directionality to cohesin transport (Haarhuis et al., 2014).

1.3.1.3.1 The Prophase Pathway

The removal of cohesin from chromosome arms at prophase depends on Wapl and Pds5 (Gandhi et al 2006; Kueng et al 2006). Phosphorylation of Sororin and SA2 by Cdk1 and polo-like kinase 1 (Plk1), respectively, destabilises cohesin and abolishes the ability of

Sororin to antagonise Wapl (Sumara et al., 2002; Nishiyama et al., 2010). Following further phosphorylation by Aurora B (Nishiyama et al., 2013), Sororin dissociates from chromatin, allowing Wapl to bind Pds5 via the FGF motif, and remove cohesin from the chromosome arms (Chan et al., 2012; Rowland et al., 2009). Wapl may open up the DNA exit gate by directly disengaging Scc1 from Smc3 (Buheitel & Stemmann, 2013; Eichinger et al., 2013).

The Cdk1-mediated inactivation of the Scc2-Scc4 loader complex in mitosis ensures that the cohesin rings removed from chromosome arms by Wapl do not reload until telophase (Gillespie & Hirano, 2004; Watrin et al., 2006). The prophase pathway does not involve Smc3 deacetylation (Beckouet et al., 2010; Borges et al., 2010; Deardorff et al., 2012; Xiong et al., 2010).

1.3.1.3.2 The Spindle Assembly Checkpoint-mediated Pathway

During prophase centromeric cohesin is protected from the Wapl-dependent cohesin removal by Shugoshin (Sgo1) (McGuinness et al., 2005; Salic et al., 2004) which competitively binds to cohesin and inhibits the recruitment of Wapl to SA2/Scc1 (Hara et al., 2014) and recruits protein phosphatase 2A (PP2A) that suppresses the phosphorylation of Sororin and SA2 (Kitajima et al., 2006; Liu et al., 2013b; Nishiyama et al., 2013). The role of centromeric cohesin protection is to confer the cohesion that is required to counteract the pulling forces of spindle microtubules before anaphase. The SAC is constitutively activated as soon as cells enter mitosis and remains so until kinetochores of all chromosomes are attached to microtubules and generate the appropriate bipolar tension and chromosomes are aligned at the metaphase plate (Musacchio & Salmon, 2007). Once bipolar spindle attachment is achieved and the SAC is satisfied, Securin is ubiquitinated by the APC/C and targeted for degradation. This activates Separase which then disrupts the cohesin ring at the centromere by cleaving Scc1, resulting in sister chromatid separation at anaphase (Musacchio & Salmon, 2007; Nasmyth & Haering, 2009; Peters et al., 2008). Cohesins removed from the centromere are recycled by the dephosphorylation of SA2 and deacetylation of Smc3 by HDAC8/Hos1, and can be reloaded onto chromatin in Telophase (Zhang & Pati, 2012).

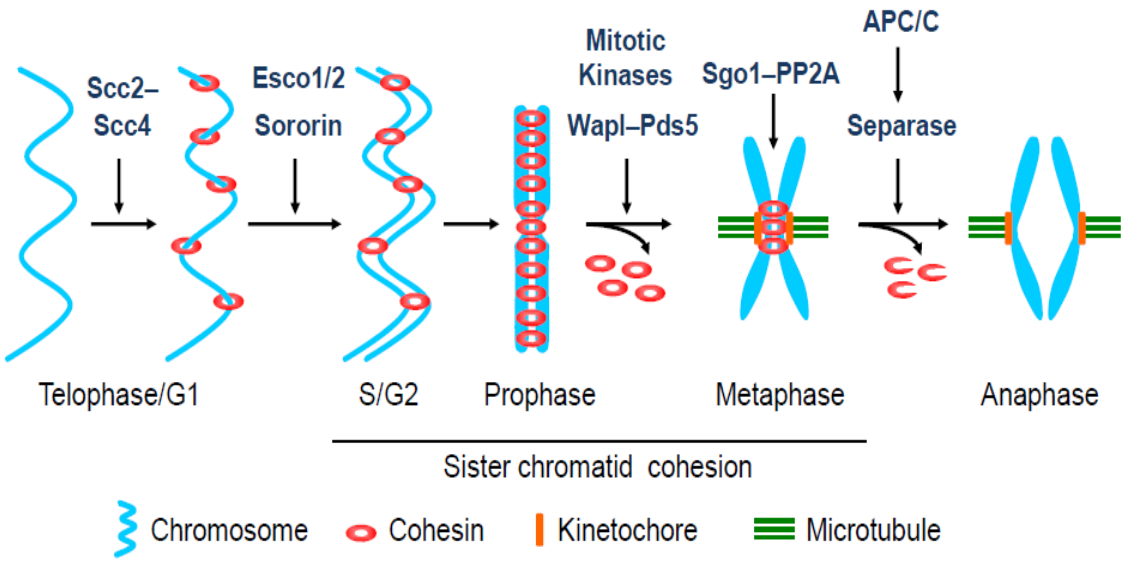

Figure 1.6 Cohesin regulation during the chromosome cycle

The cohesin complex is loaded onto chromatin during telophase and G1 with the aid of loading factors Scc2/Scc4. The cohesin-chromatin association at this stage is dynamic. SCC is established and requires additional factors such as Esco1/2 and Sororin. During prophase, the bulk of cohesin dissociates from chromosome arms via the prophase pathway, involving Plk1, Aurora B and Wapl. However, the centromeric cohesin is protected by the Sgo1-PP2A complex. The centromeric cohesin is removed during metaphase-to-anaphase transition by Separase, following its activation by APC/C which allows the transition to anaphase (Campbell & Cohen-Fix, 2002; Peters et al., 2008; Zheng & Yu, 2015).

1.3.2 Cohesin-related Proteins

As briefly discussed earlier, apart from core subunits Smc1, Smc3, Scc1, and Scc3, the cohesin complex comprises many associated proteins that have been shown to be important for its function. These include establishment of sister chromatid cohesion N-acetyltransferase 1 and 2 (Esco1 and Esco2), precocious dissociation of sisters protein 5 (Pds5), Wings apart-like protein (Wapl), Sororin, and Shugoshin (Sgo1). These proteins are required in various cohesin functions that include establishment, maintenance, and dissolution of sister chromatid cohesion. Pds5 forms a complex with either Sororin or Wapl to mediate cohesion maintenance or dissolution, respectively (Panizza et al., 2000; Gandhi et al., 2006; Nishiyama et al., 2010; Ladurner et al., 2016; Samora et al., 2016). Establishment and maintenance of sister chromatid cohesion depends on Esco1 and Esco2, as well as recruitment of Sororin to chromatin (Rankin et al., 2005; Schmitz et al., 2007; Zhang et al., 2008; Nishiyama et al., 2010). Wapl also requires Scc1 and Scc3 to associate with cohesin (Kueng et al., 2006).

1.3.2.1 Pds5

The precocious dissociation of sisters protein 5 (Pds5) was first identified in a genetic screen for genes important for chromosome structure (Denison et al., 1993), and belongs to a family of highly conserved, HEAT (Huntington, Elongation Factor 3, PR65/A, TOR) repeat-containing proteins (Hartman et al., 2000; Panizza et al., 2000), with homologues in most eukaryotic cells (Table 1.2). HEAT repeats are used as protein interaction domains in other proteins such as Scc2 (Panizza et al., 2000). Vertebrate cells contain two Pds5 homologues, Pds5A and Pds5B (Figure 1.7) (Losada et al., 2005), which are both essential for the establishment and maintenance of sister chromatid cohesion, and co-localize with cohesin during interphase (Hartman et al., 2000).

Pds5 is recruited to chromatin by Scc1 and is required for cohesin's release from chromatin as well as *de novo* Smc3 acetylation (Chan et al., 2013), but is not required for cohesin's recruitment to chromatin (Hu et al., 2011). It has both positive and negative roles in sister chromatid cohesion through the recruitment of positive (such as Eco1/Esco1/Esco2 and Sororin) and negative regulators (such as Wapl) to cohesin (Losada et al., 2005). The Pds5-Wapl sub-complex destabilises the binding of cohesin to

Table 1-2 Pds5 isoform nomenclature and identity

Name	Size (a.a)	Species	Identity (%)	
			Homo sapiens	
			Pds5A (SCC-112)	Pds5B (APRIN, AS3, KIAA0979)
Pds5p	1277	*S. cerevisiae*	19	19
Pds5+	1205	*S. pombe*	23	25
BimD	1506	*A. nidulans*	23	21
Spo76	1596	*S. macrospora*	21	20
Pds5	1218	*D. melanogaster*	37	37
Evl-14	1570	*C. elegans*	20	21
Pds5A	1323	*X. laevis*	86	69
Pds5A	1333	*R. norvegicus*	97	72
Pds5A (SCC112)	1337	*H. sapiens*	-	73
Pds5B	1447	*H. sapiens*	73	-

(Denison et al., 1993).

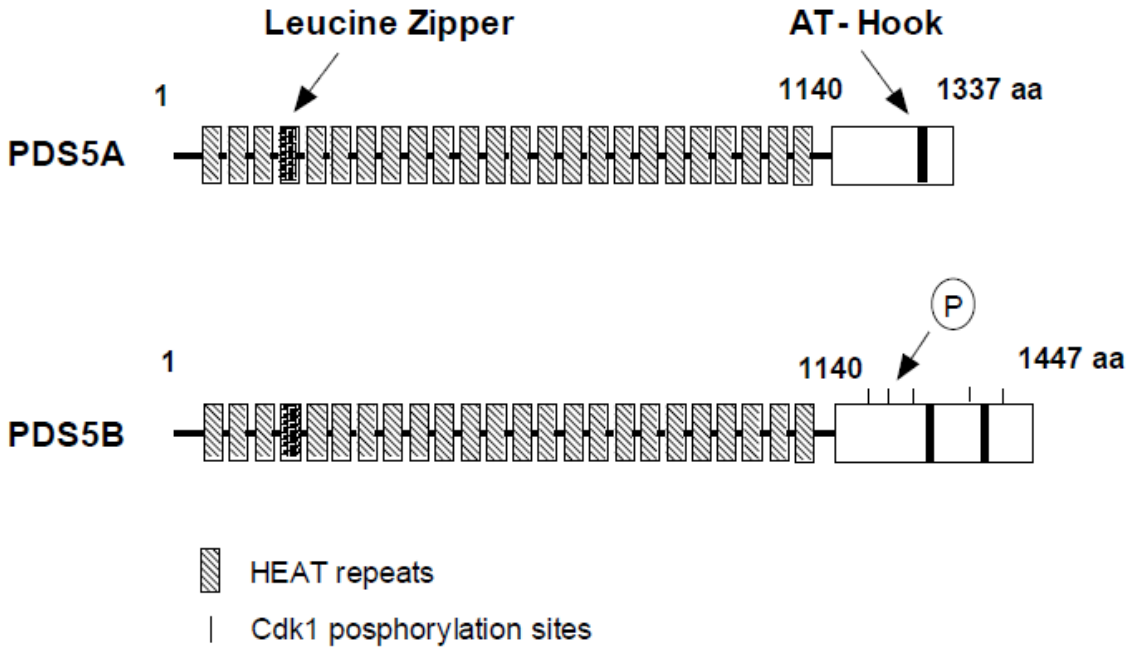

Figure 1.7 Schematic representation of human Pds5A and Pds5B protein sequences

The N-termini of Pds5A and Pds5B are similar, they contain 23 HEAT repeats and one protein-DNA interaction motif (leucine zipper). However, their C- termini differ, whereas Pds5A has one adenine-thymine (AT)-hook domain, Pds5B has two. The AT-hook is thought to bind to the minor groove of AT-rich DNA. There are five possible Cdk1 phosphorylation sites (threonine or serine followed by proline) at the C-terminus of Pds5B (Losada et al., 2005).

chromatin before S-phase and removes cohesin from the chromosome arms during prophase, while the Pds5-Sororin sub-complex establishes and maintains sister chromatid cohesion from S-phase to mitosis (Shintomi & Hirano, 2009; Nishiyama et al., 2010). Both Pds5A and Pds5B can associate with the SA1 and SA2 subunits of cohesin (Sumara et al., 2000; Losada et al., 2005). Since cohesin can only associate with either SA1 or SA2, but not both SA1 and SA2, there are at least four distinct types of cohesins in vertebrate cells (SA1-Pds5A, SA1-Pds5B, SA2-Pds5A, SA2-Pds5B) (Sumara et al., 2000; Losada et al., 2005).

In yeast, loss of Pds5 reduces viability in G2-arrested cells (Tanaka et al., 2001; Wang et al., 2002) and several studies in worms and *Drosophila* have shown that Pds5 is essential for sister chromatid cohesion (Hartman et al., 2000; Panizza et al., 2000; Tanaka et al., 2001; Stead et al., 2003; Wang et al., 2003; Dorsett et al., 2005). In mouse cells, both Pds5A and Pds5B contribute to sister chromatid cohesion (Carretero et al., 2013), although depletion of either Pds5A or Pds5B from vertebrate cells has been found to have minor (Zhang et al., 2007) or no effect on sister chromatid cohesion (Losada et al., 2005). More recent studies have shown that Pds5A- and Pds5B-deficient mice have developmental abnormalities and slow growth of mouse embryonic fibroblasts (MEFs) (Carretero et al., 2013) and that Pds5 recruits Esco1 to chromatin in human cells (Minamino et al., 2015) and is required for *de novo* Smc3 acetylation by Eco1 (Carretero et al., 2013; Chan et al., 2013; Vaur et al., 2012). It is required for sister chromatid resolution in *Xenopus* extracts, and both sister chromatid cohesion and resolution in mice (Carretero et al., 2013; Shintomi & Hirano 2009).

Pds5 is required for cohesin's release from chromatin (Nishiyama et al., 2010; Chan et al., 2013) and prevents Smc3 deacetylation by Hos1 during G2 and M phases, thereby contributing to the maintenance of sister chromatid cohesion (Chan et al., 2013). Contrary to previous studies which suggested that Pds5A and Pds5B are redundant (Zhang et al., 2007, 2009), recent studies reported that while both proteins contribute to telomere and arm cohesion, Pds5B is specifically required for centromeric cohesion (Carretero et al., 2013), suggesting that the two proteins may have non-overlapping functions.

1.3.2.2 Wapl

The wings apart-like protein (Wapl) was first identified in *Drosophila* as a protein required for heterochromatin organization and chromosome segregation (Perimon et al., 1985; Verni et al., 2000; Dobie et al., 2001). It is highly conserved from yeast to man, with high homology in the HEAT repeat-containing C-terminal domain (Kueng et al 2006; Chatterjee et al 2013; Ouyang et al 2013). The Wapl HEAT repeats serve as cohesin binding surfaces (Kueng et al 2006; Chatterjee et al 2013; Ouyang et al 2013). The N-terminal region of Wapl contains three FGF motifs through which it binds Pds5, SA1, and Scc1 (Table 1.3) (Shintomi & Hirano, 2009; Nishiyama et al., 2010; Ouyang et al., 2013). In human cell lysates, Wapl is present in a distinct sub-complex with Pds5A (Kueng et al., 2006; Ladurner et al., 2016; Samora et al., 2016). In mammalian cells, Wapl also binds to cohesin by interacting with SA1 and Scc1 (Kueng et al., 2006; Shintomi & Hirano, 2009).

By binding to Pds5 in interphase, Wapl mediates the dynamic association of cohesin with chromatin before S-phase (Kueng et al., 2006; Nishiyama et al., 2010; Chan et al., 2012). At prophase, Wapl displaces Sororin from Pds5 and removes cohesin from chromosome arms by opening the DNA exit gate at the Smc3–Scc1 interface (Gandhi et al., 2006; Kueng et al., 2006; Nishiyama et al., 2010; Zhang et al., 2011; Chan et al., 2012; Huis et al., 2014). Since the Wapl-orchestrated removal of cohesin from the chromosome arms at prophase is non-proteolytic, the prophase pathway promotes both sister chromatid decatenation and preservation of intact cohesin that can be reloaded onto chromatin in the next cell cycle (Waizenegger et al., 2000; Kueng et al., 2006; Peters et al., 2008; Zhang et al., 2011; Chan et al., 2012; Tedeschi, 2013; Haarhuis et al., 2014).

Wapl is not required for sister chromatid cohesion in vertebrate cells. Studies in several organisms have shown that Wapl inactivation essentially bypasses the requirement for positive cohesion factors such as Eco1, Sororin, or Sgo1 (Kueng et al., 2006; Gandhi et al., 2006; Rowland et al., 2009; Nishiyama et al., 2010), suggesting that Wapl is a negative regulator of cohesin. Overexpression of Wapl leads to precocious separation of sister chromatids (Gandhi et al., 2006).

Previous studies on Wapl have identified 20 putative Plk1 phosphorylation sites matching the consensus sequence (E/D/Q)-x-(S/T) and one matching the consensus sequence (E/D)-x-(S/T)Φ-x-(E/D)Φ, where Φ is a hydrophobic amino acid, suggesting that Wapl is regulated by phosphorylation (Barr et al., 2004; Nakajima et al., 2003).

1.3.2.3 Esco1 and Esco2

The establishment of sister chromatid cohesion N-acetyltransferase 1 and 2 (Esco1 and Esco2) are human orthologs of acetyltransferase Eco1/Ctf7, required in S-phase during establishment of sister chromatid cohesion (Hou & Zou, 2005; Takagi et al., 2008). Eco1 was first identified in *S. cerevisiae* as a sister chromatid cohesion establishment factor (Ivanov et al., 2002; Skibbens et al., 1999; Toth et al., 1999). Apart from Esco1 and Esco2, previous studies have identified several orthologs of Eco1 across species, including Eso1 in fission yeast, Deco in *Drosophila*, and XEco1 and XEco2 in *Xenopus*, all containing an N-terminal C2H2 zinc finger (ZF) and PCNA-interacting Protein (PIP) box domain, as well as a C-terminal acetyltransferase domain (Figure 1.8) (Ivanov et al., 2002; Hou & Zou 2005; Moldovan et al., 2006; Takagi et al., 2008).

While the role of the C2H2 Zinc finger domain remains unknown, the acetyltransferase and PIP domains are required for enzymatic activity and binding to PCNA, respectively (Moldovan et al., 2006; Song et al., 2012). In other proteins, the C2H2 zinc finger domains serve as DNA binding motifs. The Eco1-PCNA interaction is essential in establishing sister chromatid cohesion (Moldovan et al., 2006; Song et al., 2012). The role of Eco1 orthologs in sister chromatid cohesion is highly conserved in several species. Studies in fission yeast have shown that Eso1 is required in S-phase for proper chromosome segregation (Tanaka et al., 2000) while in *Drosophila*, mutations in Deco lead to cohesion defects (Williams et al., 2003). In human cells, depletion of either Esco1 or Esco2 leads to cohesion defects (Brads & Skibbens, 2005; Minamino et al., 2015).

In S-phase, during DNA replication, Eco1 acetylates two lysine residues of Smc3, $K^{115/116}$, while in humans, both Esco1 and Esco2 can acetylate Smc3 on lysine residues $K^{105/106}$ to establish sister chromatid cohesion (Moldovan et al., 2006; Zhang et al., 2008; Song et al., 2012). In humans, acetylation of Smc3 is coupled with the recruitment of Sororin to

Table 1-3 Wapl isoforms

Isoform	Size (a.a)	Name	Interaction	Difference from canonical sequence
1	1190	Wapl	Interacts via FGF motifs with Pds5 and Smc3	Canonical sequence
2	1227	Friend of EBNA2 (FOE)	Interacts with Epstein-Barr virus EBNA2	Extended N-terminal of 43 aa, 510-515 a.a are missing
3*	1275	KIAA0261	Not tested	Extended N-terminal of 85 a.a

*Wapl isoform 3 was determined by a chromosomal mapping of cDNA clones of unidentified human genes from human immature myeloid cell line KG-1. No experimental confirmation is available for this isoform (Oikawa et al., 2004; Kwiatkowski et al., 2004; Nagase et al., 1996).

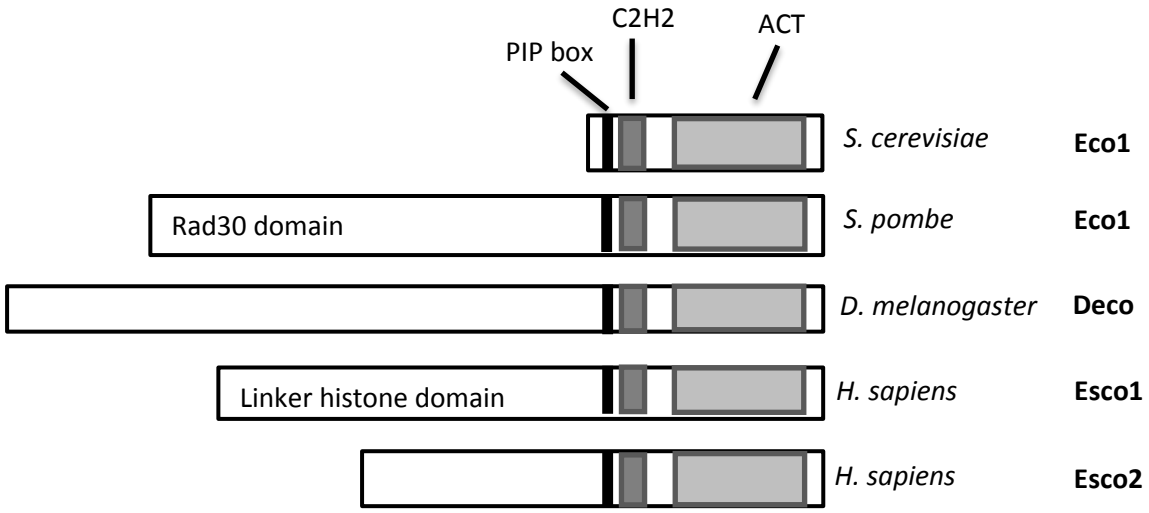

Figure 1.8 The Eco1 acetyltransferase and its homologs

The *S. cerevisiae* Eco1 protein contains PIP box, C2H2 zinc finger, and acetyltransferase domains. Eco1 homologs have been identified in several organisms. Two Eco1 homologs have been identified in *Xenopus* (not shown) and human (Esco1 and Esco2). Each Eco1 homolog has a conserved C terminus containing a PIP box, C2H2 zinc finger, and acetyltransferase domains. The N terminus is divergent. PIP= PCNA-interacting protein box domain; ACT= acetyltransferase domain; C2H2= Cys (2) His (2) zinc finger domain. (Moldovan et al., 2006).

chromatin, which displaces Wapl from Pds5, and establishes sister chromatid cohesion (Lafont et al., 2010; Nishiyama et al., 2010). Acetylation of cohesin has been shown to speed the replication fork (Terret et al., 2009).

Eco1/Ctf7 associates with chromosomes throughout the cell cycle in budding yeast (Skibbens et al., 1999; Toth et al., 1999). However, in human cells, Esco1 and Esco2 differ in the way they associate with chromatin. While Esco1 is expressed throughout the cell cycle, Esco2 is only expressed during S-phase where it has been shown to bind to chromosomes (Hou & Zou , 2005; van der Lelij et al., 2009; Lafont et al., 2010; Song et al., 2012; Whelan et al., 2012). In mitosis, Esco1 is phosphorylated by Cdk1 (Lyons & Morgan, 2011), while Esco2 is degraded by the APC^{Cdh1} (Hou & Zou, 2005; van der Lelij et al., 2009; Song et al., 2012; Whelan et al., 2012).

The Esco1 and Esco2 proteins are not redundant as neither of them can compensate for the loss of the other (Hou & Zou, 2005). Studies in mammalian cells have shown that Esco1 interacts exclusively with Pds5, and that its recruitment to chromatin depends on Pds5 (Minamino et al., 2015). Furthermore, Esco1 is able to acetylate Smc3 independently of DNA replication (Minamino et al., 2015). Acetylation of Smc3's ATPase head domain by the Esco1 and Esco2 cohesin acetyltransferases, with concomitant recruitment and binding of Sororin to Pds5, following the passage of the replication fork, is thought to keep the DNA exit gate locked shut, thereby maintaining sister chromatid cohesion (Buheitel & Stemmann, 2013; Chan et al., 2012; Eichinger et al., 2013).

A number of human diseases have been linked with Eco1 dysregulation. In addition to causing Roberts Syndrome /SC Phocomelia (Brads & Skibbens, 2005; Schule et al., 2005; Vega et al., 2005), Esco2 has been found to be upregulated in aggressive melanoma (Ryu et al., 2007).

1.3.2.4 Sororin

Sororin was initially identified in a genetic screen in *Xenopus laevis* as a substrate of the APC/C, a multi-subunit ubiquitin ligase complex that targets proteins for degradation (Morgan, 1999; Rankin et al., 2005; Reddy et al., 2007; Stegmeier et al., 2007). Although Sororin is conserved in vertebrates, no homolog has been identified in lower eukaryotes (Zhang & Pati, 2012). It has been proposed that the Sororin function is performed by a domain of another cohesin subunit in lower eukaryotes (Chan et al., 2013). Studies in *Drosophila* identified Dalmatian as a homolog of Sororin (Figure 1.9) (Nishiyama et al., 2010). The N-terminus of Sororin contains a KEN box, a Plk1 binding motif and FGF motif (Rankin et al., 2005). Furthermore, the N terminus and middle part of Sororin contain nine consensus sites (S^{21}, S^{75}, T^{48}, S^{79}, T^{111}, T^{115}, T^{159}, S^{181} and S^{209}) for Cdk1/cyclin B1 phosphorylation (Dreier et al., 2011, Zhang et al., 2011). In humans, Sororin is expressed from S to G2-phase and degraded after mitosis in early G1 (Nishiyama et al., 2010; Lafont et al., 2010; Zhang et al., 2011). It is a nuclear protein in interphase cells and dissociates from chromosome arms in prophase, but persists on centromeres until metaphase (Nishiyama et al., 2010; Zhang et al., 2011).

Sororin is a positive regulator of cohesin; it is required for the establishment and maintenance of sister chromatid cohesion (Rankin et al., 2005; Schmitz et al., 2007). Previous studies have shown that siRNA-mediated depletion of Sororin from synchronized HeLa cells at S-phase doubles the distance between chromosome arms (Schmitz et al., 2007; Nishiyama et al., 2010), suggesting that Sororin is required for sister chromatid cohesion.

During S-phase, Sororin is recruited to chromatin by Pds5 in an Smc3 acetylation-dependent manner, and competitively displaces Wapl by causing a conformational rearrangement within cohesin (but Wapl remains associated with Pds5) and binds Pds5 via the FGF motif to establish cohesion (Nishiyama et al., 2010). Mutations in the FGF motif or depletion of Pds5 from *Xenopus* egg extracts decrease the Sororin-Pds5 interaction or association of Sororin with chromatin, respectively (Nishiyama et al., 2010), suggesting that Sororin's FGF motif is important for interaction with Pds5. Depletion of Esco1 and Esco2 from HeLa cells reduced the association of Sororin with

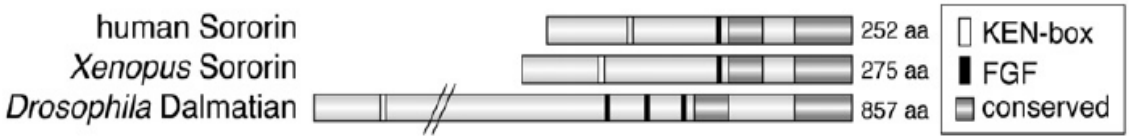

Figure 1.9 Schematic sequence comparison of human and *Xenopus* Sororin and *Drosophila* Dalmatian.

The C-termini of human and *Xenopus* Sororin and *Drosophila* Dalmatian are conserved. Although Dalmatian is bigger than its vertebrate orthologs, these proteins all contain FGF motifs and KEN boxes. While human and *Xenopus* Sororin proteins contain only one FGF motif each, *Drosophila* Dalmatian contains three FGF motifs (Nishiyama et al., 2010).

chromatin (Nishiyama et al., 2010), suggesting that Sororin is recruited to chromatin in a manner that depends on Smc3 acetylation. Recent evidence shows that the C-terminus of Sororin binds to the cohesin core subunit SA2, and can co-IP other cohesin core subunits such as Scc1/Rad21, Smc1, Smc3, and SA1, as well as associated proteins like Pds5A, Pds5B, and Wapl (Zhang & Pati, 2015).

At prophase, Sororin and SA2 are phosphorylated by Cdk1 and polo-like kinase 1 (Plk1), respectively (Sumara et al., 2002; Nishiyama et al., 2010). The phosphorylation of Sororin and SA2 destabilises cohesin and abolishes the ability of Sororin to antagonise Wapl (Sumara et al., 2002; Nishiyama et al., 2010). Following further phosphorylation, Sororin dissociates from chromatin, allowing Wapl to bind Pds5 via the FGF motif, and remove cohesin from the chromosome arms (Chan et al., 2012; Rowland et al., 2009). However, centromere-associated Sororin is removed from chromatin at metaphase. Mutations in all the nine putative Cdk1/cyclin B1 phosphorylation sites blocked the dissociation of Sororin from cohesin (Zhang et al., 2011), indicating that Sororin is regulated by phosphorylation.

1.3.2.5 Shugoshin

Shugoshin (Sgo) was first identified in *Drosophila* (Mei-S332) as a meiotic mutant that resulted in precocious sister centromere separation (Kerrebrock et al., 1995). Genetic screens carried out in fission and budding yeasts later identified Shugoshins (guardian of the genome) as a family of proteins required for protection of meiotic cohesion in these organisms (Marston et al., 2004; Kitajima et al., 2004; Katis et al., 2004; Rabitsch et al., 2004). Shugoshin proteins are neither kinases nor phosphatases; they are relatively divergent proteins except for a conserved C-terminal “SGO” motif and an N-terminal coiled-coil domain (Marston, 2015). Whereas *Drosophila* and budding yeast have only one type of the Shugoshin protein (Sgo1), fission yeast, plants, and mammals have two distinct Shugoshin proteins, Sgo1 and Sgo2, with distinct and overlapping functions (Vanoosthuyse et al., 2007; Kawashima et al., 2007; Gutierrez-Caballero et al., 2012). While depletion of Sgo2 delocalizes PP2A from centromeres (Kitajima et al., 2006) but has little effect on sister chromatid cohesion (Orth et al., 2011), depletion of Sgo1 from human cells results in loss of cohesion without affecting PP2A localization at

centromeres (Kitajima et al., 2006; Tang et al., 2006). Some Shugoshin proteins are only found in meiotic cells while others (such as budding yeast Sgo1 and *Drosophila* Mei-S332) are present in both meiotic and somatic cells (Figure 1.10). Shugoshin 1 (Sgo1) localizes to the centromere in prometaphase of either mitosis or meiosis, and remains bound to centromeric cohesin until segregation of sister chromatids (Moore et al., 1998).

Sgo1 protects centromeric cohesin from the Wapl-mediated prophase pathway removal, thus ensuring centromeric cohesion is maintained until the onset of anaphase (Riedel et al., 2006; Kitajima et al., 2006; Tang et al., 2006; Pouwels et al., 2007). Following its activation by phosphorylation on T346 by Cdk1, Sgo1 binds to pericentromeric cohesin and recruits protein phosphatase 2A (PP2A) that suppresses the phosphorylation of centromeric cohesin, thus protecting centromeric cohesion (Liu et al., 2013).

Previous studies in *Xenopus* and humans have shown that the targeting of Sgo1-PP2A complex to the centromere requires the spindle checkpoint kinase Bub1 (Tang et al., 2004; Kitajima et al., 2005; Tang et al., 2006), while in flies, the localization of Sgo1-PP2A complex to the centromeres requires the Inner centromere protein (INCENP) and Aurora B (Resnick et al., 2006). Dissociation of Sgo1 from chromatin depends on Plk1 (Clarke et al., 2005). When putative phosphorylation sites for Plk1 on Sgo1 were mutated, there was a significant decrease in correct localization and an increase in centriole splitting (Wang et al., 2008; Wang et al., 2006). The Sgo1-PP2A complex contributes to the protection of pericentromeric cohesion by ensuring the concentration of Sororin at centromeres; the complex counteracts Aurora B and Cdk1 to maintain Sororin in the dephosphorylated state, thus preserving its association with Pds5 (Rankin et al., 2005; Nishiyama et al., 2010; Dreier et al., 2011; Nishiyama et al., 2013; Liu et al., 2013a). The Sgo1-PP2A complex also prevents cohesin dissociation through SA2 dephosphorylation (Hauf et al., 2005; Kitajima et al., 2006; McGuinness et al., 2005; Nishiyama et al., 2013) and competitive inhibition of Wapl's association with cohesin, since Sgo1 and Wapl bind the same interface on cohesin (Hara et al., 2014). Non-phosphorylatable Sororin and SA2 mutants have additive effects on slowing cohesin dissociation (Nishiyama et al., 2013).

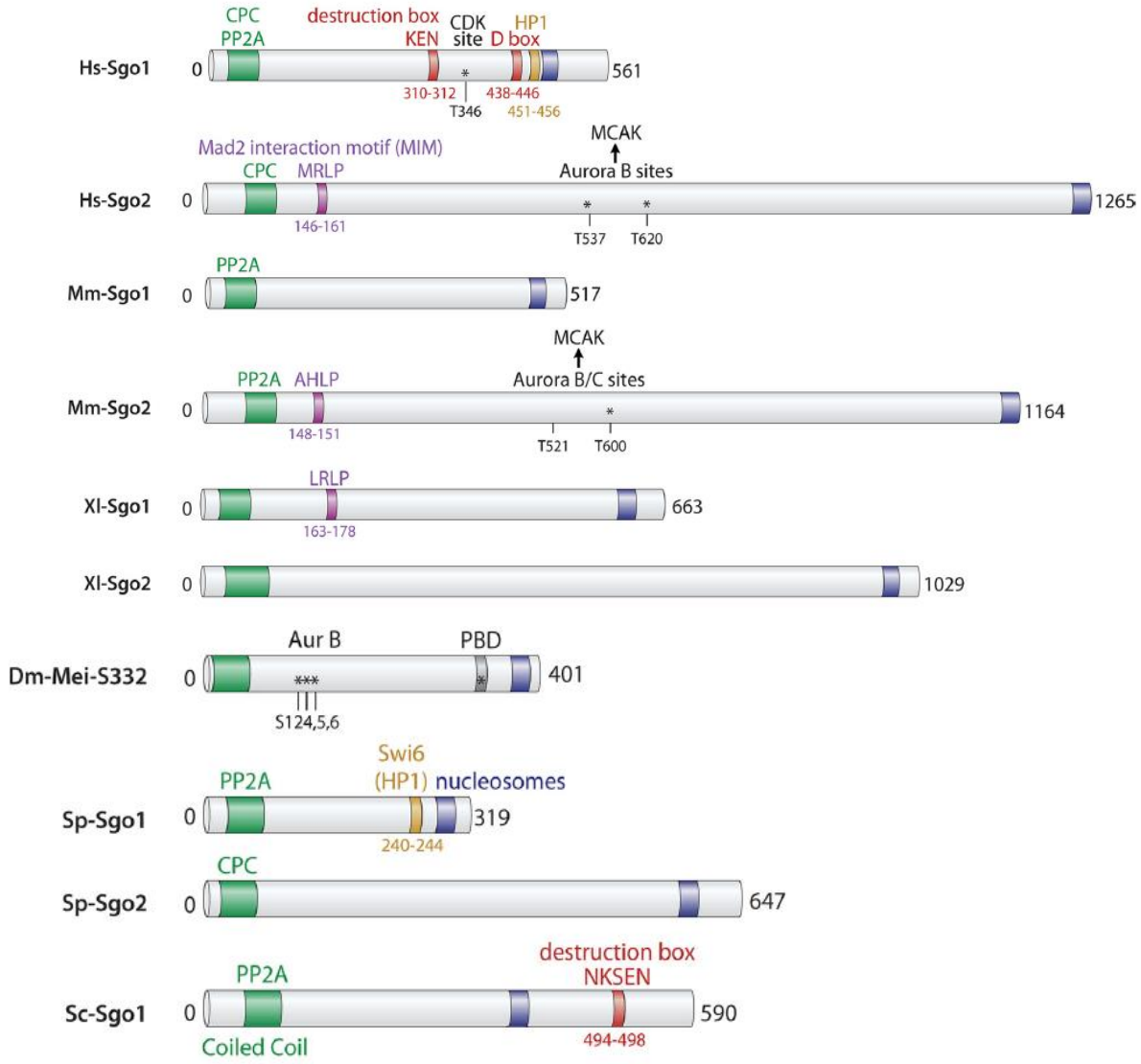

Figure 1.10 Schematic diagram illustrating the key features of Sgo1 homologs

The C-termini of Shugoshin proteins contain a conserved SGO motif (blue). The N-termini also contain a conserved coiled coil (green), which is required for Shugoshin dimerization and association with PP2A and/ or CPC. The SGO motif is required for the interaction with phosphorylated histone H2A. Motifs required for association with Heterochromatin Protein 1 (HP1) or Mad2 (amino acids MRLP, AHLP, and LRLP) or those required for degradation (KEN box, D box, and amino acid sequence NKSEN) are shown. The sites for regulatory phosphorylation events are also shown by asterisks. Hs= *Homo sapiens*; Mm= *Mus musculus*; Xl= *Xenopus laevis*; Dm= *Drosophila melanogaster*; Sp= *Schizosaccharomyces pombe*; Sc= *Saccharomyces cerevisiae* (Marston, 2015).

1.3.3 Additional Functions of Cohesin

1.3.3.1 Cohesin in DNA Damage Repair

In the presence of DNA damage, cohesin assembles around the double strand break (DSB) with the aid of cohesin loading factors Scc2/Scc4 and phosphorylation of histone H2AX by the DNA damage checkpoint kinases Mec1 and Tel1 and the DNA damage sensing complex MRX/N (Mre11/Rad50/Xsr2/Nbs1) (Figure 1.11) (Strom et al., 2004; Unal et al., 2004). The DNA damage checkpoint is activated in response to Mre11 signalling, resulting in phosphorylation of H2AX (called γH2AX) thereby marking the site of DNA damage.

Phosphorylation of H2AX creates a large domain of γH2AX, which is permissive for cohesin binding (Unal et al., 2004). Mre11p enables cohesin binding to the phospho-H2AX domain possibly through a direct interaction or by promoting the formation of single-stranded DNA (ssDNA) (Unal et al., 2004). Eco1/Esco1 acetyltransferase is also activated via DNA damage checkpoint signalling and promotes the establishment of sister chromatid cohesion, which is required for efficient DSB repair.

1.3.3.2 Higher-Order Chromatin Structure

As well as mediating sister chromatid cohesion, the cohesin complex has been shown to regulate cohesion-independent functions such as transcription (Gard et al., 2009) and DNA replication (Guillou et al., 2010) due to its contribution to the topological organisation of the genome (Gibcus & Dekker, 2013; Sofueva et al., 2013; Zuin et al., 2014).

1.3.3.2.1 Cohesin and Transcription

All known cohesin functions rely on its ability to topologically embrace DNA molecules (Nasmyth & Haering, 2009). The observation that in vertebrate cells the binding of cohesin to chromatin does not correlate well with the time during the cell cycle when cohesion exists, and that cohesin expression occurs in a wide range of mammalian cells including post-mitotic neurons that normally do not replicate their DNA and thus cannot establish sister chromatid cohesion, suggested that cohesin's function may not

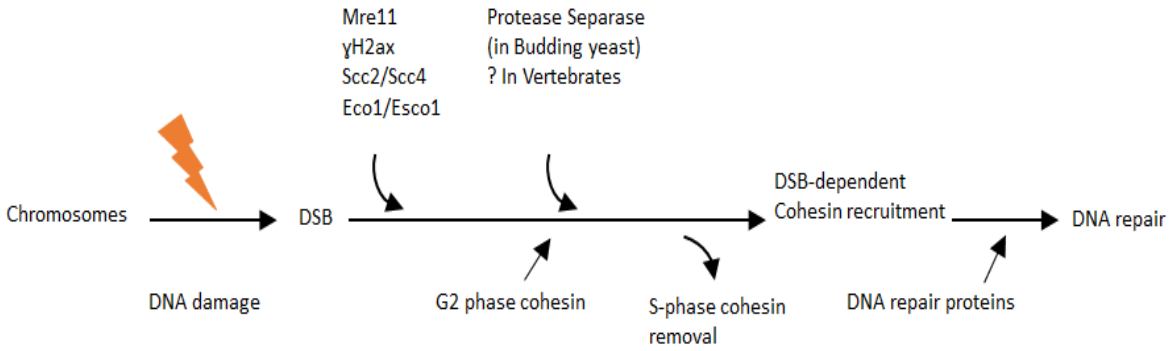

Figure 1.11 Cohesin metabolism during DNA damage repair.

When DNA is damaged, the sensor gene Mre11 promotes signalling pathways that activate DNA damage checkpoints. In budding yeast, DNA damage promotes the dissociation of S-phase-loaded cohesin from chromatin via the separase-mediated pathway. The phosphorylation of H2AX (called γH2AX) marks the site of DNA damage and signals the loading of cohesin around the DSB by the Scc2/Scc4 loader complex. Eco1/Esco1 acetyltransferase is activated via DNA damage checkpoint signalling and promotes the establishment of sister chromatid cohesion, which is required for the efficient DNA repair.

be restricted to sister chromatid cohesin (Losada et al., 1998; Sumara et al., 2000; Gerlich et al., 2006; Wendt et al., 2008).

Cohesin is loaded onto chromatin by the Scc2–Scc4 loader complex (Ciosk et al., 2000; Watrin et al., 2006) but upon loading, it is able to translocate to other genomic sites (Lengronne et al., 2004) such as the ones bound by the chromatin insulator CTCF (CCCTC-binding factor) (Parelho et al., 2008; Wendt et al., 2008). In *Xenopus* cells, loading of cohesin onto chromatin by the Scc-Scc4 heterodimer requires the formation of pre-RCs at origins as a prerequisite (Gillespie & Hirano, 2004; Takahashi et al., 2004), although studies in budding yeast and *Drosophila* have shown that cohesin can associate with chromatin in the absence of pre-RCs (Uhlmann & Nasmyth, 1998; MacAlpine et al., 2010).

The finding that mice lacking cohesin-SA1 have altered gene expression that affects embryonic development (Remeseiro et al., 2012b) consolidated earlier speculations of cohesin's involvement in *Drosophila* and *S. pombe* gene expressions, where it localises with both the loader complex and RNA polymerase II (Misulovin et al., 2008) and acts as a terminator of transcription (Gullerova & Proudfoot, 2008). Incidentally, studies in yeast showed that cohesin accumulates to sites of convergent transcription, but away from actively transcribed genes (Ocampo-Hafalla & Uhlmann 2011), thus contributing to gene regulation by defining the position of genes (Gard et al., 2009).

In conjunction with CTCF, cohesin mediates transcriptional insulation (Parelho et al., 2008; Wendt et al., 2008) by promoting the formation of chromatin loops at several loci such as the β-globin locus and the surrounding olfactory receptor genes (Figure 1.12) (Hadjur et al., 2009; Mishiro et al., 2009; Nativio et al., 2009; Hou et al., 2010; Chien et al., 2011). Cohesin also facilitates DNA looping between enhancers and promoters of genes required for pluripotency maintenance in murine embryonic stem cells (Kagey et al., 2010), independently of CTCF (Kagey et al., 2010; Schmidt et al., 2010). Chromatin loops created by cohesin have various functions, including facilitating enhancer-promoter interactions and regulating expression of genes within clusters by allowing or preventing certain chromatin contacts (Kagey et al., 2010; Monahan et al., 2012).

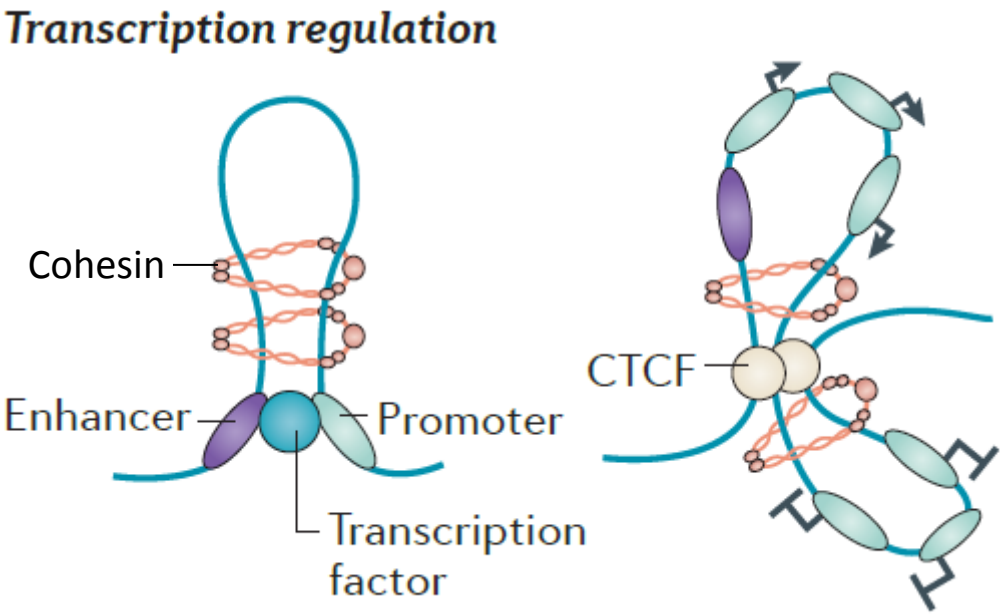

Figure 1.12 The role of cohesin in transcriptional regulation

Cohesin regulates transcription by organizing the genome, which is partitioned into discrete units known as topologically associating domains (TADs) that range from 100 kb to 1 Mb in mammalian cells. Both CTCF (CCCTC-binding factor) and cohesin contribute to this organization through the formation of chromatin loops. TADs confine regulatory activities (e.g. enhancers) to a specific domain. Within a domain, cohesin promotes transcription by facilitating the interaction between an enhancer and a promoter or contribute to the transcriptional regulation of gene clusters. Cohesin has also been proposed to organize chromatin loops at replication factories, thereby facilitating simultaneous firing of the clustered origins (Courbet et al., 2008; Guillou et al., 2010).

1.3.3.2.2 Cohesin and DNA Replication

A proteomics study designed to gain an insight into the regulation of human origins of replication by searching for proteins that interact with the mini-chromosome maintenance (MCM) complex identified all six subunits of MCM (Mcm2–7) and three components of cohesin: Smc1, Smc3, and Rad21; and MCM immunoprecipitated both somatic versions of the SA subunit: SA1 and SA2 at all phases of the cell cycle, suggesting that cohesin interacts with the prereplicative complex (pre-RC) proteins (Guillou et al., 2010). Both MCM and cohesin are loaded onto chromatin at the end of mitosis (Losada et al., 2000; Mendez & Stillman, 2000), but by independent mechanisms, and pre-RC formation is not essential for the recruitment of cohesin to chromatin in human cells (Guillou et al., 2010).

The cohesin-pre-RC components interaction would imply cohesin's participation in DNA replication. Indeed, depletion of cohesin core subunits Rad21 and Smc3 and analysis of DNA replication by FACS showed delayed S-phase (Guillou et al., 2010). However, depletion of Sororin, a cohesin-interacting protein that is essential for cohesion but dispensable for cohesin loading (Schmitz et al., 2007), or Chk1, the main effector kinase activated by ATR in response to DNA damage induced by replicative stress (Smits et al., 2010), had no effect on S-phase, suggesting that the delay in DNA replication caused by depletion of cohesin was independent of cohesion or intra-S-phase checkpoint activation (Guillou et al., 2010).

Further analysis of S-phase delay after cohesin depletion using DNA combing techniques after sequential pulse-labelling of cells with the nucleoside analogs IdU and CldU revealed a three-fold reduction in fork density (number of forks divided by the total length of DNA fibres, normalized by the percentage of cells in S phase), suggesting that the delay was likely caused by a reduced frequency of origin firing, since the levels of most initiator proteins such as ORC, MCM, Cdc45, and GINS (Go, Ichi, Nii, and San; five, one, two, and three in Japanese) (Takayama et al., 2003) subunit did not change after cohesin down-regulation (Guillou et al., 2010).

While the strongest cohesin binding sites (CBSs) are coincidental with the binding sites of the insulator protein CTCF, cohesin also associates with many other positions with lower affinity, including replication origins in human cells, regardless of their timing of replication, and likely contributes to their activation (Guillou et al., 2010). Visualisation of DNA synthesis at replication foci using nucleoside analog 5-ethynyl 2'-deoxyuridine (EdU) labelling showed reduced intensity but not the number of DNA replication foci, suggesting that fewer origins were activated within each replication factory when cohesin was depleted (Guillou et al., 2010).

Cohesin regulates gene expression by stabilizing long-range interactions between distant chromatin sites through the formation of loops (Kagey et al., 2010; Monahan et al., 2012). This suggests that cohesin might contribute to higher-order organization of replication factories by bringing together a group of neighbouring origins and looping out the intervening DNA (Guillou et al., 2010). Estimation of the average length of DNA loops in interphase nuclei depleted of cohesin using fluorescent DNA halo technique (Vogelstein et al., 1980; Buongiorno-Nardelli et al., 1982; Lemaitre et al., 2005; Courbet et al., 2008) showed fewer, longer loops, with increased halo radii, suggesting that cohesin participates in the higher-order organization of replication factories and modulates the size of chromatin loops that likely correspond to replicon units (Figure 1.13) (Guillou et al., 2010).

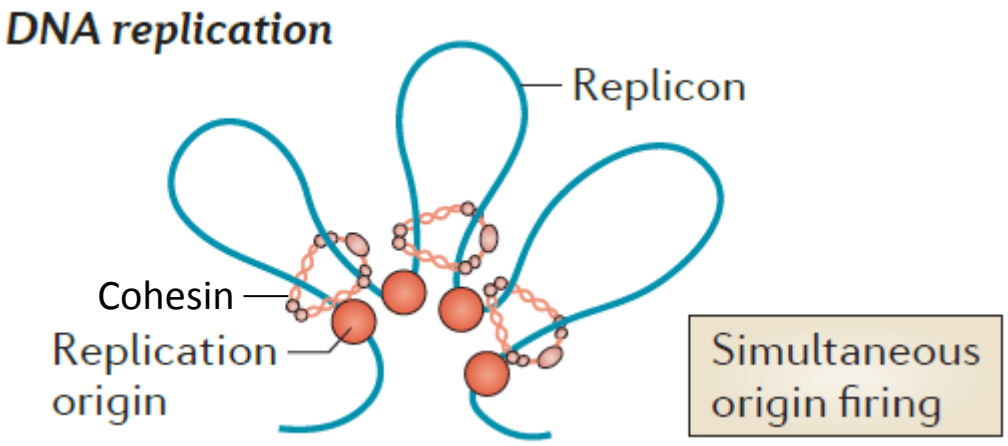

Figure 1.13 The role of cohesin in DNA replication

Cohesin regulates DNA replication by forming and/or stabilizing chromatin loops at replication foci. These long-range intrachromosomal interactions mediated by cohesin are necessary for bringing together a cluster of replication origins, thereby facilitating simultaneous firing of the clustered origins. In chromatin loops, origins of replication are located at the bases of the loops, where they are more prone to fire (Courbet et al., 2008; Guillou et al., 2010).

1.3.4 The Cohesin Complex and Human Disease

1.3.4.1 Cohesin Mutations in Cohesinopathies

Cohesinopathies are a group of human syndromes related to the mutations in protein components of cohesin (McNairn & Gerton, 2008; Remeseiro & Losada, 2013). A number of cohesinopathies have been identified; these include Cornelia de Lange syndrome (CdLS), Roberts syndrome (RBS)/SC Phocomelia, and Warsaw Breakage Syndrome (WABS) (McNairn & Gerton, 2008; van der Lelij et al., 2010; Shen, 2011; Pfau & Amon, 2012; Remeseiro & Losada, 2013).

1.3.4.1.1 Cornelia de Lange Syndrome

CdLS occurs in 1 in 10, 000 live births and is caused by mutations in either Scc2/NIPBL, Smc1A, Smc3, HDAC8, or Rad21 (Krantz et al., 2004; Tonkin et al., 2004; Musio et al., 2006; Deardoff et al., 2007, 2012b; Shen, 2011; Pfau & Amon, 2012); Kaiser et al., 2014). It is a dominantly inherited disorder which is characterised by both physical and mental developmental anomalies, including low birth weight, craniofacial and upper limb abnormalities, and mental retardation (Gillis et al., 2004). CdLS phenotypes range from mild to severe forms (Mannini et al., 2013).

Despite being sensitive to DNA damage, cells from CdLS patients do not have cohesion defects (Dorsett & Strom, 2012). Mice partially deficient for NIPBL recapitulate several features of CdLS, and microarray analysis revealed transcriptional alterations in many genes (Kawauchi et al., 2009). Mice lacking Pds5A and Pds5B die prenatally and show developmental defects that resemble CdLS pathology (Zhang et al., 2009; Zhang et al., 2007). The severity of CdLS depends on the specific cohesin component that is mutated. Mutations in Scc2 have dramatic phenotypes whereas mutations in either Smc1 or Smc3 have milder physical and mental retardation phenotypes (Deardorff et al., 2007).

1.3.4.1.2 Roberts Syndrome/SC Phocomelia

RBS/SC Phocomelia is a rare autosomal recessive disorder caused by mutations in Esco2 and is characterised by pre- and post-natal growth deficiency, long bone abnormalities,

cleft lip, craniofacial abnormalities, mental retardation, and heterochromatic-specific chromatid repulsion, especially in the pericentromeric regions (Vega et al., 2005; Schule et al., 2005; Horsfield et al., 2012). Cells from RBS patients display railroad track-like mitotic chromosome appearance (separated sister chromatids), suggesting cohesion defects (Vega et al., 2005). In mice, Esco2 deficiency results in embryonic lethality (Whelan et al., 2012). Studies in Zebrafish models of RBS in which Esco2 was depleted reported decreased cell proliferation and increased apoptosis during development (Mönnich et al., 2011).

1.3.4.1.3 Warsaw Breakage Syndrome

Warsaw Breakage Syndrome (WABS) is caused by mutations in the gene encoding ChlR1/Ddx1 and has similar cellular and clinical features as RBS, including pre- and post-natal growth deficiency and mental retardation (van der Lelij et al., 2010). ChlR1/Ddx1 is a DNA helicase required for sister chromatid cohesion in yeast and mammalian cells (van der Lelij et al., 2010). WABS cells have defective sister chromatid cohesion, displaying ‘‘railroad tracks’’ conformations (Bharti et al., 2014).

1.3.4.2 Cohesin Mutations in Cancer

Components of the cohesin complex are often mutated in human cancers (Solomon et al., 2014). These mutations occur both in the cohesin core subunits and cohesin regulatory proteins. Heterozygous somatic missense mutations in genes encoding Smc1A, Smc3, Scc2/NIPBL, and SA3/STAG3 have been reported in colon cancer (2-6 %) (Barber et al., 2008). Cells from patients with chronic myelomonocytic leukaemia (CML) and acute myeloid leukaemia (AML) are characterised by individual deletions of Rad21 and STAG2, respectively (Rocquain et al., 2010). STAG1 mutations have also been described in AML. Mutations in STAG2 have also been reported in cell lines and primary tumours from glioblastoma Multiforme (GBM), Ewing Sarcoma, Melanoma, Cervical Carcinoma, and Haematological cancer (15-20 %) (Solomon et al., 2011). Frequent frameshift mutations in Pds5B were reported in microsatellite-unstable gastric and colorectal adenocarcinoma (2 %) (Kim et al., 2013). Esco2 is upregulated in aggressive melanoma (Ryu et al., 2007).

1.4 Aims and Objectives

SCC is mediated by a chromosome-associated protein complex called cohesin, which collaborates with a network of other proteins such as Pds5, Esco1, and Esco2 for the establishment, maintenance, and timely dissolution of cohesion to allow chromosome segregation at anaphase.

Previous work in our lab has implicated Pds5 in DNA replication and studies from other labs have shown that both the Esco1 and Esco2 acetyltransferases are important for the establishment of sister chromatid cohesion after DNA replication through acetylation of Smc3.

Although the manner in which cohesin mediates sister chromatid cohesion has been a subject of intense study, the regulation of this protein complex and the mechanistic consequences of cohesin posttranslational modifications such as acetylation are still poorly understood. The extent to which the loss of Pds5 and Smc3 acetylation affects DNA replication remains unclear.

In this study, my aim was therefore to investigate the control of cohesin's association and dissociation from chromatin during the cell cycle, characterise the Esco1 and Esco2 proteins in the mammalian cell cycle, and investigate the role of Pds5 proteins specifically in DNA replication.

1.4.1 Hypothesis

Previous studies (unpublished) in our lab have implicated Pds5 proteins in DNA replication; siRNA-mediated depletion of either Pds5A or Pds5B in HeLa cells prolonged the time cells completed S-phase. Studies from other labs have also implicated cohesin acetylation in DNA replication in mammalian cells, although in *Xenopus* egg extracts, acetylation has been found to have no effect on DNA replication. Based on the preliminary studies on Pds5 conducted in our lab and studies on Esco1 and Esco2 from other labs, my hypothesis was that Pds5, Esco1, and Esco2 proteins are required for normal DNA replication.

Chapter 2 - Materials and Methods

2.1 Materials

2.1.1 General Chemicals and Reagents

Table 2-1 Chemicals and Reagents

Reagent	Supplier
5-Bromo-2'-deoxyuridine (BrdU)	Calbiochem.
5-Chloro-2'-deoxyuridine (CIdU)	Sigma.
5- Iodo-2'-deoxyuridine (IdU)	Sigma.
Acetic acid	Fisher.
Ammonium persulphate (APS)	Fisher.
Aphidicolin	Sigma.
Bortezomib (PS-341)	Viva Bioscience.
Bovine Serum Albumin (BSA)	Santa Cruz Biotechnology, Inc.
Cell Dissociation Medium (1X)	Sigma.
Citric acid	Fisher.
Colloidal Coomassie Instant Blue stain	Expedeon.
Ethylene Glycol Tetraacetic acid (EGTA)	Fisher.
Ethylenediaminetetraacetic acid (EDTA)	Fisher.
EZ-ECL Chemiluminescence detection kit	Geneflow.
Foetal Bovine Serum (FBS)	Gibco.
Formaldehyde solution	Sigma.
Glycerol	Fisher.
Glycine	Fisher.
HEPES	Fisher.
Hoechst 33342 dye	Sigma.
Hydrochloric acid	Fisher.
Interferin siRNA Transfection Reagent	Polyplus.
Magnesium Chloride	Fisher.
Methanol	Fisher.
Micrococcol Nuclease (from Staphylococcus aureus)	Sigma.
Nitrocellulose Supported Transfer Membrane	Santa Cruz Biotechnology, Inc.
Nocodazole	Sigma.
NP-40	MP Biomedicals.
n-Propyl gallate	Sigma.
Penicillin/Streptomycin (x10)	PAA Laboratories.
Poly-L-Lysine	Sigma.
Potassium Chloride	Fisher.
Potassium Ferricyanide	Acros Organics.

Potassium Ferrocyanide	Acros Organics.
Propidium Iodide	Sigma.
Protease inhibitors (Aprotinin, Leupeptin, Pepstatin)	Sigma.
Protease inhibitors (PMSF)	Bio Basic.
Protein A sepharose Beads	Sigma.
Protogel (30 % acrylamide/ 0.8 % bis-acrylamide)	Geneflow.
Ribonuclease (DNase free)	Sigma.
Ribonuclease A (RNAse A)	Sigma.
siRNA Transfection Medium	Santa Cruz Biotechnology Inc.
Sodium Azide	Sigma.
Sodium Bicarbonate Solution	Gibco.
Sodium Chloride	Fisher.
Sodium deoxycholate	Sigma.
Sodium Dodecyl Sulphate (SDS)	Melford.
Sodium Fluoride	Fisons.
Sodium Orthovanadate	Acros Organics.
Sodium pyrophosphate	Acros Organics.
Spectra Multicolour Broad Range Protein Ladder	ThermoScientific.
Staurosporine	Sigma.
Sucrose	Melford.
Taxol	Sigma.
Tetramethylethylenediamine (TEMED)	Fisher.
Tris-base	Fisher.
Triton X-100	Sigma.
Tween 20	Fisher.
UltraCruz™ Autoradiography (X-ray) films	Santa Cruz Biotechnology, Inc.
Vectorshield Mounting Medium	Vector Laboratories.
β-Glycerophosphate	Sigma.
β-Mercaptoethanol	Acros Organics.

Unless otherwise stated, all other chemicals and reagents were of analytical grade and purchased from either Sigma or Fisher.

2.1.2 Oligonucleotides

2.1.2.1 RNAi Oligonucleotides

The ON-TARGETplus SMARTpool set of four oligonucleotides for Pds5A, Pds5B, Wapl, Esco1, Esco2, and Sororin were purchased from Dharmacon. Sense strand sequences of the siRNA duplexes are shown in Table 2.2.

Table 2-2 siRNA Oligonucleotides

Name	Target sequence
Human Pds5A #1	5’-GAUAAACGGUGGCGAGUAA-3’
Human Pds5A #2	5’-CCAAUAAAGAUGUGCGUCU-3’
Human Pds5A #3	5’-GAACAGCAUUGACGACAAA-3’
Human Pds5A #4	5’-GAGAGAAAUAGCCCGGAAA-3’
Human Pds5B #1	5’-GAAAUAUGCUUUACAGUCA-3’
Human Pds5B #2	5’-UGAUAAAGAUGUUCGCUUA-3’
Human Pds5B #3	5’-GCAUAGUGAUGGAGACUUG-3’
Human Pds5B #4	5’-GGUCAAUGAUCACUUACUU-3’
Human Wapl #1	5’-GGAGUAUAGUGCUCGGAAU-3’
Human Wapl #2	5’-GAGAGAUGUUUACGAGUUU-3’
Human Wapl #3	5’-CAAACAGUGAAUCGAGUAA-3’
Human Wapl #4	5’-CCAAAGAUACACGGGAUUA-3’
Human Esco1 #1	5’-GGAAAGAGCAAACGAGGUA-3’
Human Esco1 #2	5’-GGACAGAAUAGCACGUAAA-3’
Human Esco1 #3	5’-CUAGAAGAGACGAAACGAA-3’
Human Esco1 #4	5’-GGACAAAGCUACAUGAUAG-3’
Human Esco2 #1	5’-CGAGUGAUCUAUAAGCCAA-3’
Human Esco2 #2	5’-GAGAGUAGUUGGGUGUUUA-3’
Human Esco2 #3	5’-GUUGAUACCCUCAGGAAUU-3’
Human Esco2 #4	5’-CAUCGACGCUGGUCAGAAA-3’
Human Sororin #1	5’-UCUAAGAAAGUCAGGCGUU-3’
Human Sororin #2	5’-CCUGAAAUCUGGCCGAAGA-3’
Human Sororin #3	5’-CAGAAAGCCCAUCGUCUUA-3’
Human Sororin #4	5’-CGGAGGUCCCAGCGGAAAU-3’
ON-TARGETplus non-targeting siRNA	5’-UAGCGACUAAACACAUCAA-3’

2.1.3 Antibodies

Table 2-3 Primary Antibodies

Antibody	Catalog No.	Supplier	Dilution used	Technique
Rabbit Anti-Pds5A	A300-089A	Bethyl Laboratories, Inc.	1:5000 1:200	Western Blot. Immunofluorescence.
Rabbit Anti-Pds5B	A300-537A	Bethyl laboratories, Inc.	1:2000 1:200	Western Blot. Immunofluorescence.
Mouse Anti-Wapl	sc-365189	Santa Cruz Biotechnology, Inc.	1:1000 1:200	Western Blot. Immunofluorescence.
Rabbit Anti-Esco1	ab180100	Abcam.	1:1000 1:200	Western Blot. Immunofluorescence.

Rabbit Anti-Esco2	NB100-87021	Novus Biologicals.	1:2000 1:200	Western Blot. Immunofluorescence.
Mouse Anti-Sororin	H00113130-B01P	Abnova.	1:500 1:50	Western Blot. Immunofluorescence.
Mouse Anti-Sgo1	AB58023	Abcam.	1:1000 1:200	Western Blot. Immunofluorescence.
Goat Anti-Smc1	sc-21078	Santa Cruz Biotechnology, Inc.	1:2000	Western Blot.
Rabbit Anti-Smc3	ab128919	Abcam.	1:1000 1:200	Western Blot. Immunofluorescence.
Rabbit Anti-Ac-Smc3	PD040	MBL International Corporation.	1:1000 1:200	Western Blot. Immunofluorescence.
Mouse Anti-Scc1	K0202-3	MBL International Corporation.	1:1000	Western Blot.
Rabbit Anti-p53	sc-6243	Santa Cruz Biotechnology, Inc.	1:1000	Western Blot.
Rabbit Anti-p21	ab109520	Abcam.	1:1000	Western Blot.
Rabbit Anti-p16	ab108349	Abcam.	1:1000	Western Blot.
Mouse Anti-Caspase 3	9668	Cell Signalling	1:1000	Western Blot.
Rabbit Anti-Cleaved Caspase 3	9664	Cell Signalling	1:1000	Western Blot.
Rabbit Anti-Caspase 9	9502	Cell Signalling	1:1000	Western Blot.
Rabbit Anti-Parp	11835238001	Roche Life Science	1:1000	Western Blot.
Rabbit Anti-Cyclin B1	4138	Cell Signalling	1:1000	Western Blot.
Rabbit Anti-Histone H3	4499	Cell Signalling	1:2000	Western Blot.
Rabbit Anti-phospho-Histone H3	9706	Cell Signalling	1:2000	Western Blot.
Mouse Anti-α-Tubulin	sc-23948	Santa Cruz Biotechnology, Inc.	1:2000 1:400	Western Blot. Immunofluorescence.

Rabbit Anti-γ-Tubulin	T3559	Sigma	1:4000 1:500	Western Blot. Immunofluorescence.
Goat Anti-Lamin A+C	6215	Santa Cruz Biotechnology, Inc.	1:5000	Western Blot.
Mouse Anti-BrdU	347580	BD Biosciences	1:100 1:50	BrdU Incorporation. DNA Single Fibre.
Fitc-Rat-anti-BrdU	ab74545	Abcam	1:100	DNA Single Fibre.
Human Anti-Centromere	2786	Cell Signalling	1:200	Immunofluorescence.
Mouse Anti-Cytokeratin 18	12140322001	Roche Life Science	1:10	Immunofluorescence.

Table 2-4 Antibody Binding Sites

Antibody	Clonality	Molecular weight (kDa)	Target Region
Rabbit Anti-Pds5A	Polyclonal	151	Between a.a 1250 and the C-terminus (residue 1297).
Rabbit Anti-Pds5B	Polyclonal	165	Between a.a 1400 and the C-terminus (residue 1447).
Mouse Anti-Wapl	Polyclonal	140	Between a.a 1-300 (N-terminus).
Rabbit Anti-Esco1	Polyclonal	95	Between a.a 661 and 687 (C-terminus).
Rabbit Anti-Esco2	Polyclonal	68	Between a.a 200 and 250.
Mouse Anti-Sororin	Polyclonal	37	Full length.
Mouse Anti-Sgo1	Monoclonal	58	Between a.a 1 and 293.
Goat Anti-Smc1	Polyclonal	α=155 β=150	Near the C-terminus.
Rabbit Anti-Smc3	Monoclonal	141	Between a.a 1163 and 1188 (C-terminus).
Rabbit Anti-Ac-Smc3	Polyclonal	141	Lysine residues ($K^{112/113}$).
Mouse Anti-Scc1	Monoclonal	120	C-terminus fragment (544-631 a.a).
Rabbit Anti-p53	Polyclonal	53	Between a.a 1 and 393 (C-terminus).

Rabbit Anti-p21	Monoclonal	21	Between a.a 1 and 100.
Rabbit Anti-p16	Monoclonal	16	Between a.a 100 and the C-terminus.
Mouse Anti-Caspase 3	Monoclonal	35	Between a.a 28 and 44.
Rabbit Anti-Cleaved Caspase 3	Monoclonal	19	Amino terminal residues adjacent to Asp175.
Rabbit Anti-Caspase 9	Polyclonal	47	Full length.
Rabbit Anti-Parp	Polyclonal	113	Full length.
Rabbit Anti-Cyclin B1	Polyclonal	55	Full length.
Rabbit Anti-Histone H3	Monoclonal	15	C-terminus.
Rabbit Anti-phospho-Histone H3	Monoclonal	15	Phosphorylated Serine residue 10 (Ser10).
Mouse Anti-α-Tubulin	Monoclonal	55	N-terminus.
Rabbit Anti-γ-Tubulin	Monoclonal	48	Between a.a 433 and 451.
Goat Anti-Lamin A+C	Polyclonal	A=69 C=62	N-terminus.
Mouse Anti-BrdU	Monoclonal	-	BrdU incorporated in single stranded DNA, free BrdU, BrdU coupled to a protein carrier, and Iodouridine.
Fitc-Rat-anti-BrdU	Monoclonal	-	BrdU incorporated into single stranded DNA, BrdU attached to a protein carrier, free BrdU, nucleated cells in S-phase which have had BrdU incorporated in their DNA.
Human Anti-Centromere	Polyclonal	135	Full length.
Mouse Anti-Cytokeratin 18	Monoclonal	48	Specific Caspase-cleaved site within Cytokeratin 18.

Table 2-5 Secondary Antibodies

Antibody	Catalog No.	Supplier	Dilution	Technique
HRP-Goat Anti-Rabbit IgG	115-035-144	Jackson ImmunoResearch Laboratories, Inc.	1:5000	Western Blot
HRP-Donkey-Anti-Goat IgG	705-035-147	Jackson ImmunoResearch Laboratories, Inc.	1:5000	Western Blot
HRP-Goat Anti-Mouse IgG	115-035-146	Jackson ImmunoResearch Laboratories, Inc.	1:1000	Western Blot
Goat Anti-Mouse Alexa Fluor 488	A11001	Life Technologies	1:1000	Immunofluorescence
Goat Anti-Mouse Alexa Fluor 594	A11005	Invitrogen	1:1000	Immunofluorescence
Goat Anti-Rabbit Alexa Fluor 488	A11008	Invitrogen	1:1000	Immunofluorescence
Goat Anti-Rabbit Alexa Fluor 594	A11012	Invitrogen	1:1000	Immunofluorescence
Goat Anti-Human Alexa Fluor 594	A11014	Invitrogen	1:1000	Immunofluorescence
Sheep Anti-Mouse Cy3	C2181-1ML	Sigma	1:500	Immunofluorescence

2.1.4 Cell Lines

HeLa (Henrietta Lacks) cells (a human epithelial cell line derived from a cervical carcinoma) were originally purchased from BioWhittaker. EJ p53 cell line (a human bladder carcinoma), with a tetracycline (TET)-regulated p53, was provided by Dr Salvador Macip's lab (University of Leicester). RPE1 (retinal pigment epithelial) cells (a human epithelial cell line derived from the retina) were provided by Professor Andrew Fry's lab (University of Leicester).

2.1.5 Media

Table 2-6 Cell Culture Media

Media	Supplier
Dulbecco's Modified Eagle's Medium (DMEM)	Sigma
Dulbecco's Modified Eagle's Medium/ F-12 +L-Glutamine, + 15 mM HEPES	Gibco
Dulbecco's Phosphate Buffered Saline (1X) without Ca^{2+}/Mg^{2+} (PBS)	Sigma

Table 2-7 Cell Culture Media Recipe per Cell Line

Cell Line	Media Recipe
HeLa Cells	500 ml Dulbecco's Modified Eagle's Medium (DMEM), 10 % v/v Foetal Bovine Serum (FBS), 1 % v/v Penicillin/Streptomycin (Pen/Strep).
RPE1 Cells	500 ml Dulbecco's Modified Eagle's Medium/ F-12 +L-Glutamine, + 15 mM HEPES, 10 % v/v Foetal Bovine Serum (FBS), 1 % v/v Penicillin/Streptomycin (Pen/Strep), 0.25 % v/v $NaHCO_3$.
EJ $p53^+$ Cells	500 ml Dulbecco's Modified Eagle's Medium (DMEM), 10 % v/v Foetal Bovine Serum (FBS), 1 % v/v Penicillin/Streptomycin (Pen/Strep), 1.5 µg/ml Tetracycline.
EJ $p53^-$ Cells	500 ml Dulbecco's Modified Eagle's Medium (DMEM), 10 % v/v Foetal Bovine Serum (FBS), 1 % v/v Penicillin/Streptomycin (Pen/Strep).
All Cell Culture Media were stored at 4 °C and warmed at 37 °C before use.	

2.1.6 Buffers and Solutions

Table 2-8 Cell Lysis Buffers used for Protein Extraction

Buffer	Composition
Radio-Immunoprecipitation Assay (RIPA) Buffer	0.01 M Tris-HCl pH 8.0, 0.15 M NaCl, 2 mM EDTA, 0.1 mM Sodium Orthovanadate, 0.1 % w/v Sodium Dodecyl Sulphate (SDS), 1 % v/v NP-40, 0.5 % w/v Sodium deoxycholate, 50 mM Sodium Fluoride (NaF), 30 mM Sodium pyrophosphate and protease inhibitors (1 mM PMSF, 10 µg/ml Leupeptin, 10 µg/ml Aprotinin, 10 µg/ml Pepstatin).

Lysis Buffer A (LBA)	0.01 M Tris-HCl pH 7.4, 0.05 M NaCl, 5 mM EDTA, 0.1 mM Sodium Orthovanadate, 30 mM Sodium pyrophosphate, 50 mM NaF, 1 % v/v NP-40, 0.1 % w/v BSA and protease inhibitors (1 mM PMSF, 10 µg/ml Leupeptin, 10 µg/ml Aprotinin, 10 µg/ml Pepstatin).
Lysis-Buffer B (LBB)	20 mM Tris-HCl pH 7.5, 100 mM NaCl, 5 mM $MgCl_2$, 0.2 % v/v NP-40, 10 % v/v Glycerol, 1 mM Sodium Fluoride (NaF), 1 mM Sodium Orthovanadate (Na_3VO_4), 20 mM β-Glycerophosphate, 10 mM β-Mercaptoethanol, 1% v/v Triton X-100, and protease inhibitors (1 mM PMSF, 1 µg/ml Leupeptin, 1 µg/ml Aprotinin, 1 µg/ml Pepstatin).
Chromatin Extraction Buffer- Buffer C (LBC)	10 mM Tris-HCl pH7.5, 1 mM $CaCl_2$, 1.5 mM $MgCl_2$, 0.25 M Sucrose, and 0.008 U/µl Micrococcal Nuclease.

Table 2-9 Solutions and Buffers used for Western Blot

Buffer		Gel %					
Resolving Gel (20 ml)	Components (ml)	6	7	8	10	12.5	15
	H_2O	8.23	7.56	6.9	5.6	4.2	2.2
	Protogel	4	4.67	5.34	6.67	8	10
	Tris- HCl pH 8.8	7.5	7.5	7.5	7.5	7.5	7.5
	10 % SDS	0.1	0.1	0.1	0.1	0.1	0.1
	10 % APS	0.150	0.150	0.150	0.150	0.150	0.150
	Temed	0.020	0.020	0.020	0.020	0.020	0.020
Stacking Gel (3 %) (10 ml)	Components	ml					
	H_2O	7.0					
	Protogel	1.6					
	Tris- HCl pH 6.8	1.2					
	10 % SDS	0.1					
	10 % APS	0.075					
	Temed	0.012					
1X SDS PAGE Running Buffer	0.025 M Tris-HCl, 0.192 M Glycine, 1 % w/v SDS.						
SDS-PAGE Transfer Buffer	25 mM Tris-HCl, 192 mM Glycine, 20 % Methanol.						
1X Tris-Saline Tween 20 (TST)	0.01 M Tris-HCl pH 7.4, 0.15 M NaCl, 0.1 % v/v Tween 20.						

Blocking Buffer	5 % w/v Milk (Marvel) in TST Buffer or 5 % w/v BSA/ 0.1 % v/v Tween 20/ sterile Ca^{2+}/Mg^{2+}-free PBS.

Table 2-10 Buffers used for Immunofluorescence

Buffer	Composition
Triton X-100-containing Buffer	0.5 % v/v Triton-X100, 20 mM HEPES pH 7.4, 3 mM $MgCl_2$, 50 mM NaCl, 300 mM Sucrose.
Mounting Medium	Glycerol 9 ml, 1 M Tris-HCl (pH8.0) 1 ml, and n-propyl gallate 0.05 g.

Table 2-11 Solutions used for Fixing Cells for Immunofluorescence

Antibody	Fixative solution (Formaldehyde= 3.7 % v/v, Methanol= 100 %)
Rabbit Anti-Pds5A	Formaldehyde.
Rabbit Anti-Pds5B	Formaldehyde.
Mouse Anti-Wapl	Formaldehyde.
Rabbit Anti-Esco1	Methanol.
Rabbit Anti-Esco2	Methanol.
Mouse Anti-Sororin	Formaldehyde.
Mouse Anti-Sgo1	Formaldehyde.
Rabbit Anti- Smc3	Methanol.
Rabbit Anti-Ac-Smc3	Methanol.
Mouse Anti-BrdU	Methanol.
Mouse Anti-Cytokeratin 18	Methanol.
Human Anti-Centromere	Methanol: Acetic acid (3:1 v/v).
Mouse Anti-α-Tubulin	Methanol.
Rabbit Anti-γ-Tubulin	Methanol.

Table 2-12 Blocking Buffers used for Immunofluorescence Techniques

Technique	Blocking Buffer Composition
Immunofluorescence microscopy	5 % w/v BSA/ sterile Ca^{2+}/Mg^{2+}-free PBS.
BrdU Incorporation Assay	5 % w/v BSA/ 0.1 % (v/v) Tween 20/ sterile Ca^{2+}/Mg^{2+}-free PBS.
DNA Single Fibre Assay	5 % w/v BSA/ sterile Ca^{2+}/Mg^{2+}-free PBS.
Chromosome Spread Preparation	5 % w/v BSA/ 0.1 % (v/v) Tween 20/ sterile Ca^{2+}/Mg^{2+}-free PBS.

Table 2-13 Solution used for Fluorescence-Activated Cell Sorting (FACS)

Solution	Solution Composition
Stain Solution	9.5 ml of 1X PBS, 0.5 ml of 10 µg/ml RNase solution, and 200 µl of 0.02 µg/ml PI solution.

Table 2-14 Solution used for Fixing Chromosome Spreads

Solution	Components
Carnoy's Solution	75 % v/v Methanol 25 % v/v Acetic Acid.

Table 2-15 Solutions used for Senescence-associated Endogenous β-Galactosidase Activity

Solution	Components
X-gal Solution	1 mg/ml X-gal in Dimethylformamide solution, 40 mM Citric acid/Sodium phosphate solution pH 6.0, 5 mM Potassium Ferrocyanide, 5 mM Potassium Ferricyanide, 150 mM Sodium Chloride, 2 mM Magnesium Chloride, and 11.5 ml of Water.

Table 2-16 Solution used for Lysing Cells for DNA Single Fibre Analysis

Solution	Components
DNA Fibre Lysis Solution	50 mM EDTA, 0.5 % w/v SDS, 200 mM Tris-HCl pH 7.5.

Table 2-17 Buffers used for the Comet Assay

Solution	Components
Lysis Buffer	100 mM disodium EDTA, 2.5 M NaCl, 10 mM Tris-HCl pH 10.0, 1 % (v/v) TritonX-100.
Electrophoresis Buffer	300 mM NaOH, 1 mM disodium EDTA pH 13. 0.
Neutralisation Buffer	0.4 M Tris-HCl pH 7.5
PI Solution	50 µl of 1 mg/ml PI and 20 ml ddH_2O
Agarose, Normal Melting Point	1 % Agarose (w/v) in H_2O
Agarose, Low Melting Point	0.6 % Agarose (w/v) in PBS

Table 2-18 Nucleoside Analogs used for Labelling DNA

Analog	Final Concentration
5-Bromo-2'-deoxyuridine (BrdU)	1 µM
5-Chloro-2'-deoxyuridine (CIdU)	250 µM
5- Iodo-2'-deoxyuridine (IdU)	25 µM

2.1.7 Drugs

Table 2-19 Drugs used for Cellular response Induction and Synchronisation

Drug	Final Concentration	Treatment Duration
Aphidicolin	5 µg/ml	24 h
Bortezomib (PS-341)	20 nM	30 min, then 24 h
Cisplatin	10 µM	6 h
Nocodazole	1 µg/ml	24 h
Staurosporine	1 µM	6 h
Taxol	1 µg/ml	24 h

2.1.8 Software

Table 2-20 Specialised Software used for Data Analysis

Software Version	Application
Adobe Photoshop CS5	Immunofluorescence
ImageJ (IJ 1.49)	DNA replication
FlowJo (10.0.6)	Flow Cytometry
GraphPad Prism 6	Statistical data analysis
Komet 5.0	Comet assay

2.2 Methods

2.2.1 Cell Biology Techniques

2.2.1.1 Cell Culture

2.2.1.1.1 Culturing and Passaging HeLa Cells

HeLa cells were cultured in a monolayer in DMEM supplemented with 10 % v/v foetal bovine serum (FBS) and 1% v/v penicillin/ streptomycin solution (100 IU/ml and 100 µg/ml respectively) at 37 °C in a humidified incubator containing 5 % CO_2. Cells were passaged when they were 70-90 % confluent by removing the medium and washing three times with 5 ml of 1X PBS, followed by the addition of 2 ml Cell Dissociation Medium and incubation for 30 min at 37 °C. After incubation, 8 ml complete DMEM was added and the cells dissociated by gently pipetting the cell suspension before 2.5 ml of the cell suspension was added to new tissue culture plates containing 10 ml complete DMEM.

2.2.1.1.2 Culturing and Passaging RPE1 Cells

As described for HeLa cells except DMEM/F-12 supplemented with 0.25 % v/v $NaHCO_3$, 10 % v/v FBS, and 1% v/v penicillin/ streptomycin (100 IU/ml and 100 µg/ml respectively) was used.

2.2.1.1.3 Culturing and Passaging EJ p53 Cells

EJ p53 cells, with a tetracycline (TET)-regulated p53 (provided by Dr Salvador Macip, University of Leicester), were cultured at 37 °C in a humidified incubator containing 5 % CO_2 in monolayer in DMEM containing 10 % v/v FBS and 1% v/v penicillin/ streptomycin solution (100 IU/ml and 100 µg/ml respectively). To repress the expression of p53, the growth medium was supplemented with 1.5 µg/ml tetracycline (EJ $p53^+$). To induce the expression of p53, EJ $p53^+$ cells were washed three times with 5ml of 1X PBS and cultured in medium lacking tetracycline (EJ $p53^-$) for a minimum of seven days. Cells were passaged when they were 70-90 % confluent by removing the medium and washing three times with 5 ml of 1X PBS, followed by the addition of 2 ml Cell

Dissociation Medium and incubation for 30 min at 37 °C. After incubation, 8 ml complete DMEM (with or without tetracycline) was added and the cells dissociated by gently pipetting up and down before 2.5 ml of cell suspension was added to new tissue culture plates containing 10 ml complete DMEM or DMEM supplemented with tetracycline.

2.2.1.1.4 Cell Synchronisation

Cells were synchronised at the G1/S boundary and at M-phase for 24 h by treatment of an asynchronous population of HeLa cells with Aphidicolin (5 µg/ml) and Taxol/Nocodazole (1 µg/ml), respectively. Asynchronous and Aphidicolin-treated cells were collected by washing cells three times with 1X PBS and incubation with 2 ml Cell Dissociation Medium for 30 min while mitotic cells (Taxol/ Nocodazole-treated) were harvested by mitotic shake-off.

2.2.1.1.5 Coverslip Preparation

Coverslips were rinsed three times in deionised water and incubated for 30 min in 1 M HCl. After rinsing in water, the coverslips were washed in 100 % ethanol before they were separated with gloved hands and air-dried at RT. They were sealed in a glass beaker and baked at 250 °C for 30 min and stored in sterile tissue culture plates until required.

2.2.1.1.6 Attaching Cells to Polylysine-coated Coverslips

Coverslips were immersed in polylysine solution (1 mg/ml) in one well of a six-well plate and the plate rocked gently for 30 s. After removing them from the polylysine solution with a pair of forceps, coverslips were rinsed in sterile water and dried with a paper towel before they were put in a new six-well plate. In the tissue culture the cell suspension was titrated onto the polylysine-coated coverslips and incubated for at least 30 min in a CO_2 incubator before cell fixation.

2.2.1.1.7 Cell Treatment with Bortezomib (PS-341)

After synchronising cells for 24 h with Aphidicolin (5 μg/ml), the medium was aspirated and replaced with complete DMEM containing Aphidicolin (5 μg/ml) and Bortezomib (20 nM). Cells were incubated for 30 min in the humidified incubator containing 5 % CO_2 and then washed three times with X1 PBS and released into new complete DMEM containing Bortezomib (20 nM) only. Cells were incubated as before and samples were collected at time points after release from the Aphidicolin (5 μg/ml) block and lysed in RIPA Buffer to prepare total lysates for Western blotting.

2.2.1.1.8 siRNA Transfection (Six-well Plate)

After adding 200 μl of the siRNA Transfection Medium to RNAse-free eppendorf tubes the siRNA oligonucleotides (5-50 nM) were added and immediately vortexed for 10 s, followed by the addition of 8 μl of Interferin. The tubes were vortexed as before. Where a double transfection was used 16 μl of Interferin was used. After incubating the tubes for 30 min in the tissue culture hood the DMEM was removed from the cells and replaced with 2 ml fresh complete DMEM. The siRNA mixture was then added drop-wise to the cells and the tissue culture plate rocked gently, before incubating for 48 h in a CO_2 incubator.

2.2.1.1.9 HeLa Cell Cycle Time Course

HeLa cells were seeded overnight and blocked at G1/S with Aphidicolin (5 μg/ml) for 24 h. After washing three times with 1X PBS, the cells were released into fresh complete DMEM without Aphidicolin (5 μg/ml) and incubated at 37 °C in a CO_2 incubator. Samples were collected at a number of time points after release from the G1/S block and lysed in either RIPA Buffer to prepare total cell lysates, in Cell Lysis Buffer-B (LBB) to prepare soluble and chromatin fractions for Western Blot, or fixed in 70 % ethanol (-20 °C) for FACS analysis.

2.2.1.2 Freezing cells

Cells were seeded in a 10 cm plate for 48 h and when they were 80- 90 % confluent they were washed three times and incubated for 30 min with 2 ml of Cell Dissociation

Medium. After incubation, 5 ml of 1X PBS was added and the cells resuspended gently by pipetting up and down. The cell suspension was centrifuged at 1100 rpm for 5 min at RT. After discarding the supernatant, 1.5 ml of Cell Freezing Medium was added to the pellet and cells gently pipetted up and down. The cell suspension was then transferred to a cryovial and placed on ice for 10 min. The tube was then placed in Isopropanol and left overnight at –80 °C after which it was transferred to liquid nitrogen.

2.2.1.3 Preparation of New Cell Stock from Liquid Nitrogen

To a new stock of frozen cells 1 ml of DMEM without FBS and Pen/Strep was added and cells resuspended in 10 ml of DMEM without FBS and Pen/Strep. After centrifugation, the cell pellet was resuspended in 2 ml of DMEM supplemented with 20 % v/v FBS and 1 % v/v Pen/Strep. The cell suspension was added to 10 ml DMEM containing 20 % v/v FBS and 1 % v/v Pen/Strep and cultured at 37 °C in the tissue culture incubator containing 5 % CO2.

2.2.1.4 Fluorescence-activated Cell Sorting (FACS)

Cells were fixed with ice-cold (- 20 °C) 70 % v/v ethanol and stored at -20 °C. Prior to analysis, the cells were centrifuged at 1100 rpm for 5 min at RT and resuspended in either 1X PBS or Propidium Iodide (PI) (0.02 µg/ml) staining solution and analysed using the NucleoCounter® NC-3000™ (Chemometec) or FACScan (Becton-Dickinson), respectively. Data was analysed using FlowJo (Version 10.0.6).

2.2.1.5 Immunofluorescence

Cells were seeded overnight on sterile glass coverslips in 6-well plates whereas mitotic cells were harvested by shake-off and attached to poly-L-lysine (1 mg/ml) coated coverslips for 30 min at 37 °C in a CO_2 incubator. Cells were fixed with 3.7 % v/v formaldehyde at RT for 20 min followed by permeabilisation with 0.1 % v/v Triton X-100 for 10 min. Alternatively, cells were fixed with ice-cold (-20 °C) methanol for 30 min at -20 °C. For either fixation method, cells were sometimes pre-extracted using 0.5 % v/v Triton X-100 –containing buffer for 10 min at 4 °C before fixation. Cells were blocked with 5 % w/v BSA prior to staining with appropriate primary antibodies and either Alexa

Fluor 488 or 594-labelled secondary antibody. DNA was stained with Hoechst 33342 (0.5 µM) for 5 min at RT. Coverslips were mounted onto glass slides using either n-propyl gallate or Vectorshield Mounting Medium and the edges sealed using clear nail vanish and stored in the dark at 4 °C until examined. Cells were visualised using a Nikon inverted fluorescence microscope (Nikon Eclipse TE 300 semi-automatic Microscope, Tokyo, Japan). Microscopic images were captured using Hamamatsu ORCA-R2 digital camera, 100 × Objective, NA 1.4, or 60 × Objective, NA 1.4, using Volocity software (Improvision) and further processed using Adobe Photoshop (Adobe Photoshop CS5).

2.2.1.6 Preparation of Chromosome Spreads

Cells were seeded overnight in six-well plates and treated with either Sororin, Esco1, or Esco2 siRNAs (50 nM) for 48 h before being blocked in M-phase with Nocodazole (1 µg/ml) for 24 h. Mitotic cells were harvested by shake-off and incubated for 10 min at 37 °C in 100 µl of hypotonic KCl (75 mM) pre-warmed to 37 °C. Cells were centrifuged at 1000 rpm for 10 min and fixed with Carnoy's solution (3:1 v/v Methanol: Acetic acid). After repeating the fixation step the pellet was resuspended in 100 µl of Carnoy's solution and approximately 10 µl of the cell suspension was dropped onto glass slides held at an angle of 45 ° over a 37 °C water bath to allow the suspension to roll across the slides. Slides were dried for 10 min and chromosome spreads blocked in a humidified chamber with 5 % w/v BSA/ 0.1 % v/v Tween 20/ PBS for 1 h prior to staining with a human anti-Centromere antibody and Alexa Fluor 594-labelled Goat anti-Human secondary antibody. DNA was stained with Hoechst 33342 (0.5 µM) for 5 min at RT and coverslips mounted onto glass slides using Vectorshield Mounting Medium. After sealing the edges of the coverslips with clear nail vanish, the chromosome spreads were visualised using a confocal microscope (Leica TCS SP5 Confocal Laser Scanning Microscope) and processed using Adobe Photoshop (Adobe Photoshop CS5), ImageJ (IJ 1.49). Data was quantified using GraphPad Prism 6.

2.2.1.7 BrdU Incorporation Assay

Cells were seeded overnight in six-well plates and treated with either Esco1, Esco2, Pds5A, or Pds5B siRNAs for 48 h before being synchronised at G1/S with Aphidicolin (5

µg/ml) for 24 h. Cells were released from the Aphidicolin (5 µg/ml) block for 30 min and labelled with 5-Bromo-2'-deoxyuridine (BrdU) (1 µM) for 30 min in the tissue culture incubator before they were fixed with ice-cold (-20 °C) methanol for 5 min at -20 °C. Cells were hydrolysed with 2 M HCl/ 0.1 % v/v Tween 20/ PBS for 30 min at RT and blocked with 5 % w/v BSA/ 0.1 % v/v Tween 20/ PBS for 1 h prior to staining with a mouse anti-BrdU antibody and Alexa Fluor 488-labelled goat anti-mouse secondary antibody. DNA was stained with Hoechst 33342 (0.5 µM) for 5 min at RT and the coverslips mounted onto glass slides using Vectorshield Mounting Medium. After sealing the edges of the coverslips with clear nail vanish cells were visualised using a Nikon inverted fluorescence microscope (Nikon Eclipse TE 300 semi-automatic Microscope, Tokyo, Japan) and for every treatment at least 100 cells were counted in randomly selected fields and images captured using Hamamatsu ORCA-R2 digital camera, 100 × Objective, NA 1.4, or 60 × Objective, NA 1.4, using Volocity software (Improvision) and further processed using Adobe Photoshop (Adobe Photoshop CS5). Data was quantified using GraphPad Prism 6.

2.2.1.8 DNA Single Fibre Assay

Cells were seeded overnight in six-well plates and treated with either Esco1, Esco2, Pds5A, or Pds5B siRNAs for 48 h before being blocked at G1/S with Aphidicolin (5 µg/ml) for 24 h. Cells were released from the block and immediately labelled sequentially with Iododeoxyuridine (IdU, 25 µM) and Chlorodeoxyuridine (CldU, 250 µM) for 30 min each. After detaching the labelled cells with Cell Dissociation Medium, the cells were lysed on glass slides for 2 min using DNA Fibre Lysis Buffer. The slides were tilted at an angle of 15 ° to allow the cell suspension to roll to the bottom of the slides. After air-drying glass slides, the DNA fibres were fixed with Carnoy's solution (3:1 v/v Methanol: Acetic acid) for 10 min at RT and washed in distilled water before being hydrolysed with 2.5 M HCl for 80 min. After washing the slides in PBS for 5 min, the DNA fibres were blocked in a humidified chamber with 5 % w/v BSA/PBS for 1 h prior to staining with Fitc-conjugated Rat-anti-BrdU and mouse anti-BrdU antibodies and sheep anti-mouse Cy3 secondary antibody. After washing the slides in PBS for 5 min the coverslips were mounted onto glass slides using Vectorshield Mounting Medium and the edges sealed with clear nail vanish. The DNA fibres were visualised using a Nikon inverted fluorescence microscope

(Nikon Eclipse TE 300 semi-automatic Microscope, Tokyo, Japan) and images captured using Hamamatsu ORCA-R2 digital camera, 100 × Objective, NA 1.4, or 60 × Objective, NA 1.4, using Volocity software (Improvision) and further processed using Adobe Photoshop (Adobe Photoshop CS5). For each treatment, the lengths of 100 DNA fibres were measured using ImageJ (IJ 1.49) from randomly selected fields and data was quantified using GraphPad Prism 6.

2.2.1.9 Senescence-associated Endogenous β-Galactosidase Activity

Cells were washed three times with 1X PBS and fixed for 5 min with 3 % v/v Formaldehyde solution. After fixation, the cells were washed as before prior to staining with the X-Gal solution (Table 2. 15). Stained cells were incubated overnight at 37 °C in an incubator without CO_2 and visualised under a light microscope (Nikon Eclipse TS 100), using NIS-Elements F 3.0 software. For every treatment at least 100 cells were counted in randomly selected fields. Images were processed using Adobe Photoshop (Adobe Photoshop CS5) and data quantified using GraphPad Prism 6.

2.2.2 Biochemical Techniques

2.2.2.1 Preparation of Total Cell Lysates

Asynchronous and Aphidicolin-treated HeLa cells were harvested by washing cells three times with 1X PBS and incubating with 2 ml Cell Dissociation Medium for 30 min. Following incubation, 5 ml of 1x PBS was added and the cells suspension was centrifuged at 1100 rpm for 5 min at room temperature (RT).

Taxol or Nocodazole-arrested cells were harvested by mitotic shake-off and centrifuged at 1100 rpm for 5 min. The pellet was resuspended in 30 ml ice-cold 1x PBS and re-centrifuged as described before. After discarding the supernatant, the cell pellet was resuspended in 500 µl RIPA Buffer and vortexed for 10 s. The lysate was kept on ice for 30 min while vortexing every 10 min. The homogenate was centrifuged at 4 °C for 20 min using the SS-34 Sorval rotor at 20 000 g or the Eppendorf Centrifuge 5417R at 14 000 rpm. The supernatant was collected into pre-cooled eppendorf tubes and proteins stored at either -20 °C or -80 °C.

2.2.2.2 Preparation of Soluble and Chromatin-associated Proteins

Harvested cells were washed with Dulbecco's PBS and resuspended in 500 µl Cell Lysis Buffer B (LBB). The cell suspensions were frozen and thawed three times at -80 °C and clarified by centrifugation (Eppendorf 5417R) at 14 000 rpm at 4 °C for 20 min. The supernatants (soluble protein fractions) were transferred to fresh pre-cooled 1.5 ml Eppendorf tubes and stored at either -20 °C or -80 °C. The pellets were washed three times with 1 ml Chromatin Extraction buffer (LBC) at 14 000 rpm at 4 °C for 20 min and resuspended in 200 µl of LBC containing 5 units of micrococcal nuclease and 0.4 mM $CaCl_2$. The pellet was incubated at 28 °C for 30 min with gentle mixing, then clarified by centrifugation at 14 000 rpm at 4 °C for 20 min and the supernatant was transferred to fresh pre-cooled 1.5 ml Eppendorf tubes (chromatin protein fraction). Both the soluble and chromatin protein fractions were stored at -80 °C until required.

2.2.2.3 Protein Concentration Measurement

Following protein extraction, the concentrations of the cell extracts were determined using the Bradford Assay (Bio-Rad) according to the manufacturer's protocol. Sample absorbance was measured at 595 nm using Novaspec Plus spectrophotometer (Amersham Biosciences). Protein concentrations were normalised by dividing absorbance readings by the lowest reading and diluting the samples by each diluting factor.

2.2.3 Molecular Biology Techniques

2.2.3.1 SDS-PAGE

Sodium dodecyl sulphate polyacrylamide gel electrophoresis (SDS-PAGE) was used for the separation of proteins at 150V (Bio-Rad PowerPac 300). Normalised cell lysates containing 5 to 50 µg protein were combined in a 5: 1 ratio with 5X Laemmli sample buffer, heated at 100 °C for 5 min and then centrifuged for 10 s prior to SDS-PAGE on either 7%, 10% or 12.5% gels, alongside Spectra Multicolour Broad Range Protein Ladder (ThermoScientific).

2.2.3.2 Western Blotting

Following SDS-PAGE the gel was soaked in Transfer Buffer for 15 minutes and placed on a nitrocellulose membrane (Hybond-C Extra) in the TE77 ECL Semi-Dry Transfer Unit (Amersham Biosciences) and the protein transferred by electroblotting at 60 mA/gel at RT for 1 h. The membrane was rinsed in H_2O and incubated with Blocking Buffer for 1 h at RT and then overnight at 4°C with the primary antibody whilst rocking. The membrane was then rinsed six times (10 min each time) with Tris-Saline-Tween (TST), followed by 2 h incubation with the secondary antibody at RT. After washing with TST (x6 for 10 min each), the membrane was incubated in Enhanced Chemiluminescence (ECL) solution for 60 s and immediately exposed to UltraCruz™ Autoradiography (X-ray) Films (Santa Cruz Biotechnology) and developed using an automatic film processor (X-RAY Processor SRX-101A, Konica Minolta, UK). The blots were scanned (CanoScan LiDE 90) and processed using Microsoft PowerPoint.

2.2.3.3 Comet Assay

Control and si-RNA-treated cells were harvested and 170 µl of low melting point agarose was added to each pellet before 80 µl of each mixture was pipetted onto glass slides pre-coated with 1 % (w/v) agarose and allowed to set. Slides were placed in ice-cold lysis buffer containing 1 % (v/v) for 1 h. Slides were washed with ice-cold distilled water and incubated in ice-cold alkali buffer in the dark for 20 min prior to electrophoresis at 30 V, 300 mA for 20 min. Following their 20 min-incubation in neutralising buffer, slides were rinsed in double distilled water and dried overnight at 37 °C. Each slide was rehydrated with double distilled water for 30 min and covered with 1 ml of 2.5 µg/ml PI solution for 20 min at RT in the dark. After washing the PI solution off with double distilled water, slides were oven-dried at 37 °C and stored at RT in the dark until ready for visualisation and comet scoring using a fluorescent microscope fitted with the Komet 5.0 imaging system. Images were processed using Adobe Photoshop (Adobe Photoshop CS5) and data quantified using GraphPad Prism 6.

Chapter 3 - Esco1 and Esco2 are essential for sister chromatid cohesion

3.1 Introduction

Sister chromatid cohesion is mediated by the cohesin complex, which comprises two flexible structural maintenance of chromosomes (Smc) family of ATPases, Smc1/Psm1 (in humans) and Smc3/Psm3 (in humans) and two accessory subunits, the sister chromatid cohesion protein-1 (Scc1/Mcd1/Rad21) and stromal antigens Scc3/Psc3/SA (SA1 and SA2 in vertebrates) (Haering et al., 2002; Gruber et al., 2003b; Nasmyth, 2005). Proper establishment and maintenance of sister chromatid cohesion is essential for faithful chromosome segregation during the metaphase-to-anaphase transition (Nasmyth, 2005; Losada & Hirano, 2005). The cohesin core subunits, Smc1 and Smc3, bind to each other directly via their hinge domains, and their two ATPase head domains are connected by interaction with the C and N-terminal of Scc1/Rad21, respectively, forming a ring-shaped structure that is thought to topologically embrace sister chromatids (see Figure 1.4, page 11) (Nishiyama et al., 2010). The Scc1/Rad21 and SA1/SA2 subunits of the cohesin complex are further associated with several regulatory proteins, including Pds5, Wapl, and Sororin, which enable the establishment, maintenance, and dissolution of sister chromatid cohesion during the cell cycle (see Figures 1.4, page 11, 1.6, page 19, and 5.1, page 157).

Cohesin is loaded onto chromatin by the Scc2-Scc4 complex in telophase (in vertebrates) and dynamically interacts with chromatin before S-phase (Ciosk et al., 2000). Stable binding of cohesin onto chromatin takes place during S-phase, with the aid of replication fork-associated acetyltransferase Eco1/Ctf7 (Esco1 and Esco2 in humans) that catalyses the acetylation of Smc3 on two lysine residues ($K^{105/106}$) once the replication fork passes through the cohesin ring (Skibbens et al., 1999; Toth et al., 1999; Ivanov et al., 2002; Unal et al., 2007; Juraj et al., 2008; Zhang et al., 2008). In humans, both Esco1 and Esco2 have been shown to acetylate Smc3 during DNA replication (Nasmyth, 2005). In higher organisms, Smc3 acetylation is coupled with the recruitment of Sororin which binds to cohesin-associated Pds5 (Pds5A/Pds5B) and increases the stability of cohesin's association with chromatin (Nishiyama et al., 2010).

Chapter 3: Esco1 and Esco2 are essential for sister chromatid cohesion

In yeast, Eco1 physically interacts with PCNA during DNA replication (Moldovan et al., 2006). The Eco1-PCNA interaction enables Eco1 to transiently bind to chromosomes and acetylate Smc3, thereby establishing cohesion (Lengronne et al., 2006). Sister chromatid cohesion, established in S-phase, is maintained until mitosis when sister chromatids separate. In higher eukaryotes, two distinct pathways, the prophase pathway and the spindle assembly checkpoint (SAC)-mediated pathway, are responsible for the two-stage dissociation of cohesin from chromosomes (Nishiyama et al., 2010).

Even though both Esco1 and Esco2 can acetylate Smc3 at lysine residues ($K^{105/106}$) in mammalian cells, the two proteins are regulated differently. While Esco1 is expressed throughout the cell cycle, Esco2 is only expressed during S-phase where it has been shown to bind to chromosomes (Hou & Zou, 2005; van der Lelij et al., 2009; Song et al., 2012; Whelan et al., 2012; Lafont et al., 2010). Neither of the two proteins is able to compensate for the loss of the other, suggesting that they are not redundant (Hou & Zou, 2005). Studies in mammalian cells have shown that Esco1 interacts exclusively with Pds5 proteins, and that its recruitment to chromatin depends on Pds5 (Minamino et al., 2015). Furthermore, Esco1 is able to acetylate Smc3 independently of DNA replication (Minamino et al., 2015). Acetylation of cohesin has been shown to speed the replication fork (Terret et al., 2009). In eukaryotes, cohesin acetylation appears to be the glue that locks the cohesin subunits together and facilitates the recruitment of other regulatory factors such as Sororin that maintain sister chromatid cohesion from S-phase to mitosis.

Although the manner in which Esco1 and Esco2 regulate cohesin function has been a subject of intense investigation, the mechanistic consequences of cohesin acetylation are still poorly understood. In this study, I have used an siRNA approach to characterise the role of acetyltransferases Esco1 and Esco2 proteins in mammalian cells. My results show that depletion of either Esco1 or Esco2 slows down DNA replication, results in precocious chromosome separation and apoptosis or senescence depending on the cell type. These results led me to conclude that DNA replication-coupled Smc3 acetylation stabilises replication forks, a condition that may be required for normal fork progression, and that failure to establish sister chromatid cohesion results in aneuploidy and either apoptosis or senescence.

3.2 Results

3.2.1 Characterisation of antibodies

To test the specificity of the commercial antibodies raised against Esco1, Esco2, and Sororin, I transfected asynchronously growing HeLa cells with a pool of four small interfering RNAs (siRNAs) each against Esco1, Esco2, or Sororin mRNAs, and immunoblotted the total lysates with either anti-Esco1, anti-Esco2, anti-Sororin, or anti-α-Tubulin antibody (Figure 3.1). The Esco1 (Figure 3.1A) and Sororin (Figure 3.1C) bands disappeared with increasing amount of siRNA, indicating that these were the Esco1 and Sororin proteins, respectively. The Esco2 immunoblot (Figure 3.1B) produced a doublet, with the upper band disappearing with increasing amount of siRNA, suggesting that the upper band was the Esco2 protein. The lower band could possibly be a degradation product, since Esco2 undergoes an APC/Cyclosome-mediated degradation (Hou & Zou 2005), or non-specific (Nishiyama et al., 2010). To further check the specificity of the Esco1, Esco2, and Sororin antibodies, I transfected asynchronous HeLa cells with a pool of four siRNAs each against Esco1, Esco2, and Sororin proteins, and fixed the cells as described in Materials and Methods and stained them with either anti-Esco1, anti-Esco2, or anti-Sororin antibody (Figure 3.2). The Esco1 siRNA decreased Esco1 nuclear localisation (Figure 3.2A) by 60 % (Figure 3.2D), while the Esco2 nuclear localisation (Figure 3.2B) was reduced by 95 % (Figure 3.2E) by the Esco2 siRNA. The Sororin siRNA decreased Sororin nuclear localisation (Figure 3.2C) by 92 % (Figure 3.2F). These results suggested that my siRNAs were targeting the right mRNAs. Taken together, this data showed that my antibodies were specific and targeting proteins with the right molecular weights (kDa), hence they could be used for further studies.

3.2.2 Intracellular localisation of Esco1 and Esco2 is cell cycle regulated

The fact that Esco1 is expressed throughout the cell cycle while Esco2 is only expressed during S-phase (Hou & Zou, 2005; van der Lelij et al., 2009; Song et al., 2012; Whelan et al., 2012; Lafont et al., 2010) suggests that the two proteins regulate sister chromatid cohesion in different ways and may have non-overlapping functions.

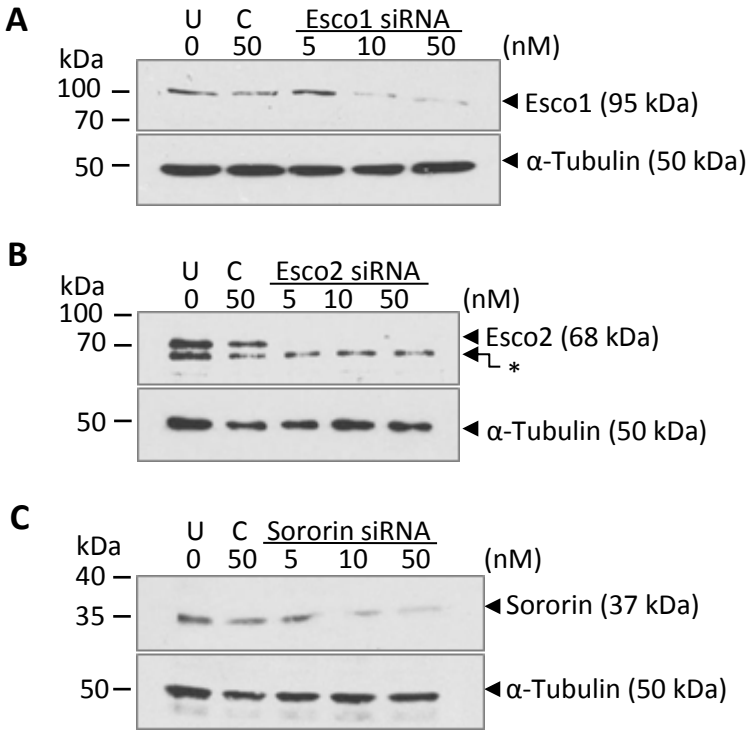

Figure 3.1 The specificity of the Esco1, Esco2, and Sororin antibodies

(**A**-**C**) Western blots of HeLa cell lysates following a 48-h treatment with either control (50 nM), Esco1, Esco2, or Sororin siRNAs (5-50 nM). Cells were lysed in RIPA buffer prior to Western blotting with either anti-Esco1, anti-Esco2, anti-Sororin, or anti-α-Tubulin antibody. U= untreated, and C= control siRNA. *= Non-specific binding. This figure is representative of three independent experiments.

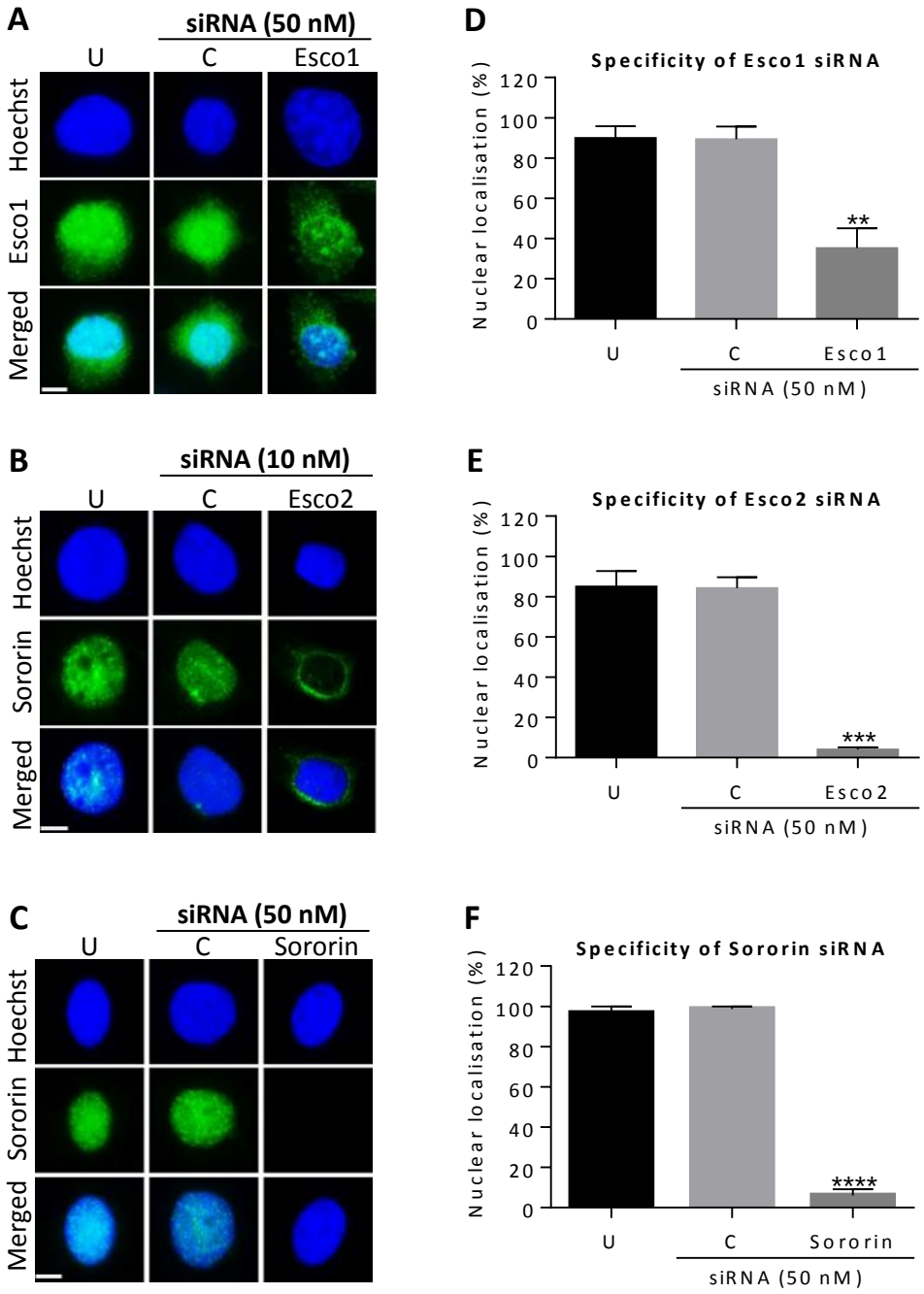

Figure 3.2 The specificity of the Esco1, Esco2, and Sororin antibodies

(**A**-**C**) Immunofluorescence images of asynchronous HeLa cells following a 48-h treatment with 50 nM of either control, Esco1, Esco2, or Sororin siRNAs. Cells were fixed in either Methanol or Formaldehyde (3.7 % v/v) and permeabilised with Triton X-100 (0.1 % v/v) before being blocked with BSA (5 % w/v) and stained with either anti-Esco1, anti-Esco2, or anti-Sororin antibody (green). DNA was stained with Hoechst 33342 (blue). Merged images are shown in the bottom panels in A-C. Scale bar: 10 μm. (**D**-**F**) Histograms showing quantitation of data in (**A**-**C**), respectively. The mean+s.e.m of at least 100 cells counted in randomly selected fields is shown. **P < 0.01, ***P < 0.001, ****P< 0.0001. P values were calculated using a two-tailed Student t-test. U= untreated, and C= control. This figure is representative of three independent experiments.

Chapter 3: Esco1 and Esco2 are essential for sister chromatid cohesion

To study the intracellular localisation of acetyltransferases Esco1 and Esco2 during the cell cycle, I fixed asynchronous HeLa cells as described in Materials and Methods and stained them with antibodies raised against the Esco1 and Esco2 proteins. I also stained for Sgo1 as a positive control, since it is known to bind centromeric cohesin from interphase to the end of mitosis (Kitajima et al., 2006). Both Esco1 (Figure 3.3A) and Esco2 (Figure 3.3B) proteins localised to chromatin during interphase but as cells entered mitosis they dissociated from chromatin at anaphase. However, Esco2 localised to both the nucleus and around the nuclear periphery during interphase (Figure 3.3B), suggesting a short-lived association with chromatin. As expected, Sgo1 localised to chromatin during interphase (Figure 3.4). At prophase, it displayed punctate localisation on chromatin, suggesting centromeric loci along condensed chromosomes. Sgo1 protein localised to chromatin until anaphase.

If Esco2 has a nuclear-specific function during interphase and displayed brief localisation to chromatin as observed (Figure 3.3B), it is likely that its localisation is regulated by either shuttling it out of the nucleus or degradation at mitosis. In this sense, chromatin-bound Esco2 levels should decrease from S-phase to mitosis. To test this, I initially fixed mitotically-arrested HeLa cells as described in Materials and Methods and stained them with antibodies raised against Esco1, Esco2, or Sgo1 as a marker which localises to chromatin from interphase to anaphase (Figure 3.4) and analysed the relative abundance of Esco1 and Esco2 on chromatin during mitosis (Figure 3.5). At either prophase (Figures 3.5A and D), metaphase (Figures 3.5B and E), or anaphase (Figures 3.5C and F) there was more chromatin-bound Sgo1 than Esco1 or Esco2. Both Esco1 and Esco2 proteins dissociated from chromatin at anaphase (Figures 3.5C and F). This data showed that during mitosis, there is reduced Esco2 staining on chromatin compared to Sgo1. I next analysed the total levels of endogenous Esco1 and Esco2 proteins at specific stages of the cell cycle by arresting exponentially growing HeLa cells at G1/S or M-phase (Figure 3.6A-C), and preparing total cell lysates as described in Materials and Methods for Western blotting with antibodies raised against the Esco1, Esco2, α-Tubulin, or ɣ-Tubulin proteins (Figures 3.6D and E). I also blotted for Sgo1 as a marker (Figure 3.6F). There was no change observed in the protein levels of

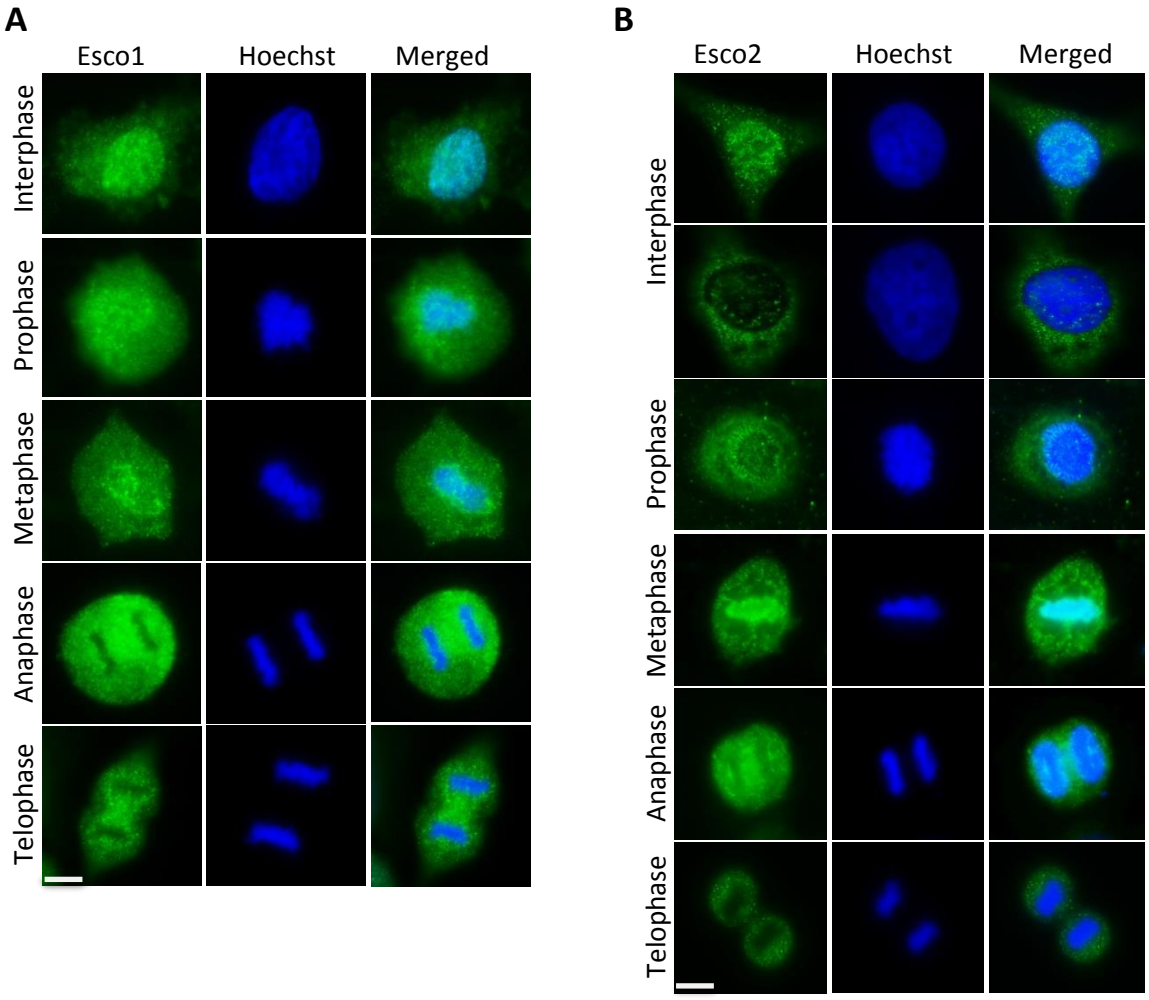

Figure 3.3 Esco1 and Esco2 are DNA-associated proteins but dissociate from chromatin during mitosis

(**A** and **B**) Immunofluorescence images of asynchronous HeLa cells showing the intracellular localisation of Esco1 and Esco2, respectively. Cells were fixed in Methanol before being blocked with BSA (5 % w/v) and stained with either anti-Esco1 or anti-Esco2 antibody (green). DNA was stained with Hoechst 33342 (blue). Merged images are shown in the last panels in A and B. Scale bar: 10 μm. This figure is representative of three independent experiments.

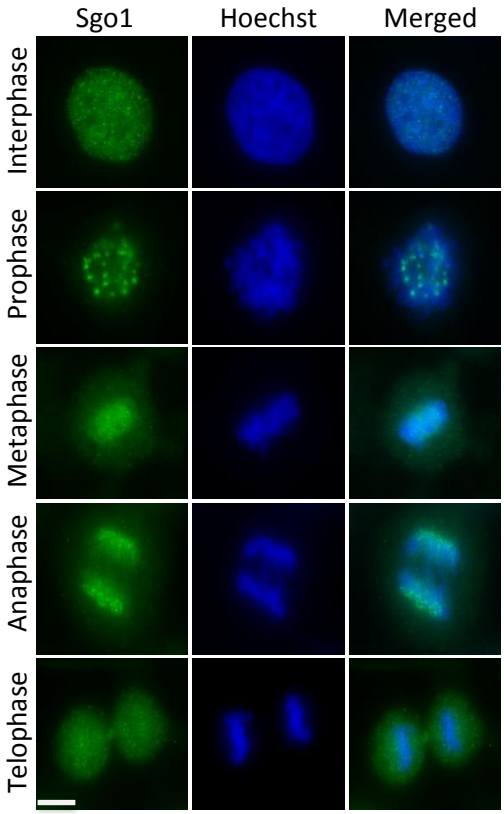

Figure 3.4 Sgo1 is associated with chromatin at mitosis

Immunofluorescence images of asynchronous HeLa cells showing the intracellular localisation of Sgo1. Cells were fixed in Formaldehyde (3.7 % v/v) and permeabilised with Triton X-100 (0.1 % v/v) before being blocked with BSA (5 % w/v) and stained with a Sgo1 antibody (green). DNA was stained with Hoechst 33342 (blue). Merged images are shown in the last panel. Scale bar: 10 μm. This figure is representative of three independent experiments.

Esco1 in interphase and at mitosis (Figure 3.6D). The Esco2 immunoblot produced doublet bands in asynchronous and G1/S-blocked lysates, as earlier observed (Figure 3.1B), and a single faster-migrating band in mitotically arrested lysates (Figure 3.6E).

The Esco2 upper band in G1/S-arrested lysates was stronger than the band detected in asynchronous lysates, suggesting that endogenous Esco2 expression is higher in G1/S-arrested cells. The fact that my Esco2 siRNA is only targeting the mRNA corresponding to the slower migrating protein (Figure 3.1B) shows that the faster migrating band detected in asynchronous, G1/S, and mitotically-arrested lysates (Figure 3.6E) represents either a degradation product of Esco2 or a non-specific protein. This has been reported in previous studies (Nishiyama et al., 2010; Hou & Zou, 2005). There was no change observed in the protein levels of Sgo1 in interphase and at mitosis (Figure 3.6F), suggesting that Sgo1 total protein levels do not change before the end of mitosis. Accumulation of the Esco2 protein in G1/S-arrested lysates is consistent with studies which report that Esco2 is only expressed during S-phase (Hou F & Zou H, 2005).

I then investigated the differential localisation of Esco2 observed in interphase cells (Figure 3.3B) and further analysed the difference in the expression of endogenous Esco1 and Esco2 proteins (Figure 3.6) by both Immunofluorescence microscopy and Western blot in a synchronised populations of HeLa cells. I investigated the differential localisation of Esco1 and Esco2 at intervals after releasing the cells from a G1/S-phase arrest. Cells were fixed in methanol and stained with either the Esco1 or Esco2 antibody. Alternatively, cells were lysed in RIPA buffer and the blots probed with either the Esco1, Esco2, Cyclin B1, or α-Tubulin antibodies (Figure 3.7E).

The Esco1 immunofluorescence data showed primarily homogeneous nuclear localisation in both asynchronous and G1/S-arrested cells (Figure 3.7A). The Esco1 protein remained in the nucleus and cytoplasm from 0 to 3 h. From 6 to 9 h, Esco1 nuclear localisation became more distinct. Quantification of the relative abundance of nuclear and cytoplasmic Esco1 showed increased nuclear staining of the protein as cells progressed from S-phase to G2 (Figure 3.7C), suggesting that endogenous Esco1 expression continues from S-phase to G2.

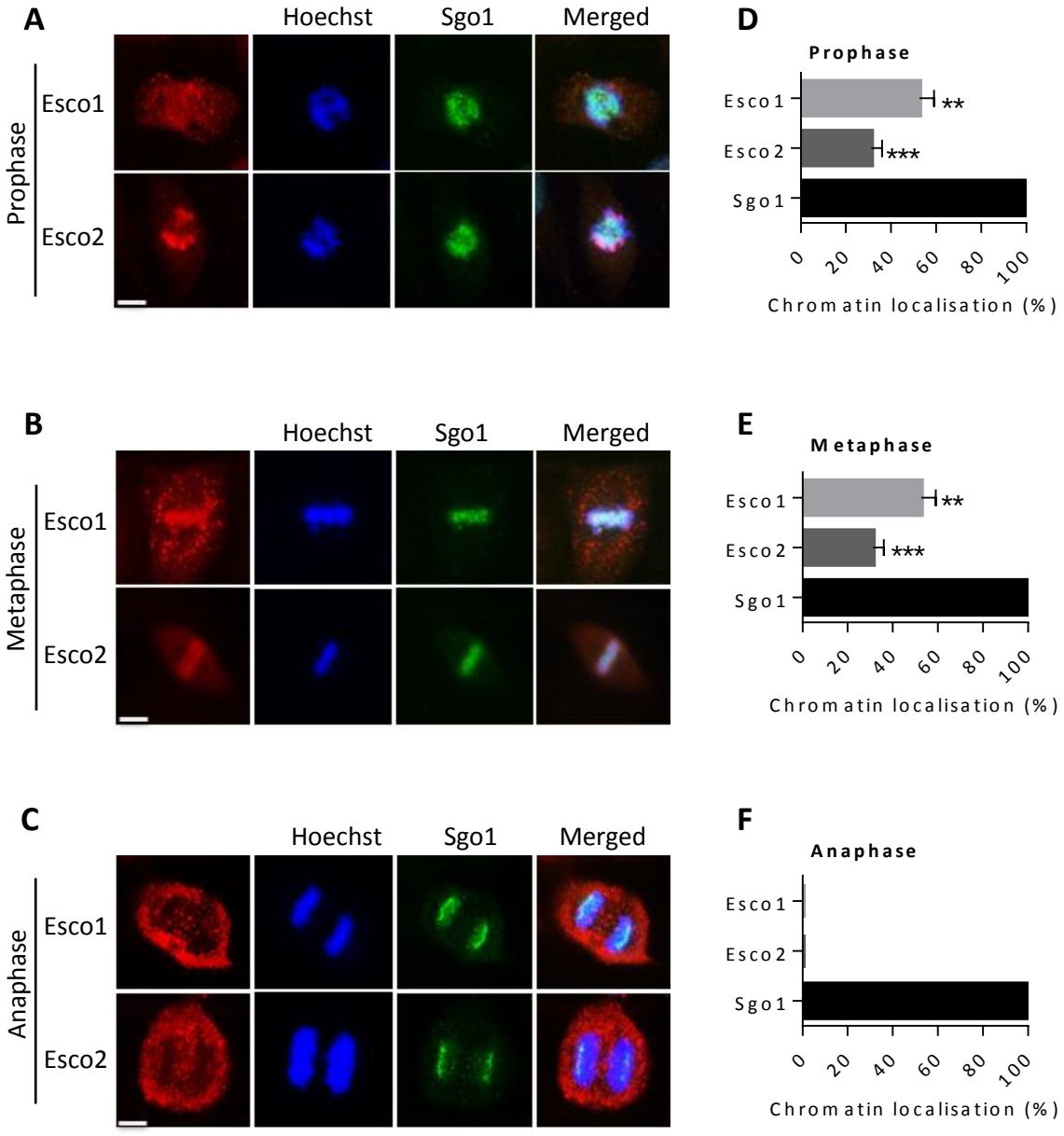

Figure 3.5 Dissociation of Esco1 and Esco2 from chromatin at mitosis

(**A-C**) Immunofluorescence images of mitotic HeLa cells showing the intracellular localisation of Esco1, Esco2, and Sgo1 during mitosis. Cells were fixed in either Methanol or Formaldehyde (3.7 % v/v) and permeabilised with Triton X-100 (0.1 % v/v) before being blocked with BSA (5 % w/v) and stained with either anti-Esco1 (red), anti-Esco2 (red), or anti-Sgo1 antibody (green). DNA was stained with Hoechst 33342 (blue). Merged images are shown in the right panels in A-C. Scale bar: 10 μm. (**D**-**F**) Histograms showing quantitation of data in (**A-C**), respectively. This figure is representative of three independent experiments.

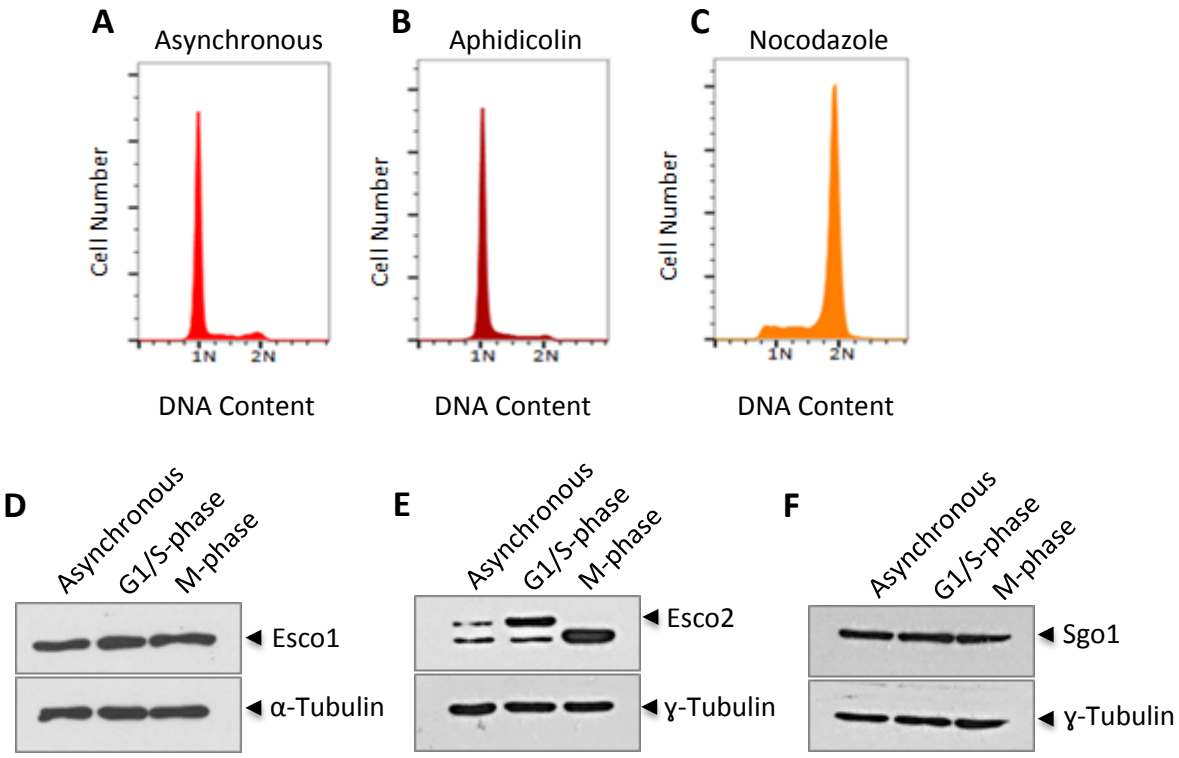

Figure 3.6 Esco1 and Esco2 proteins are differentially regulated in interphase and at mitosis

(**A**-**C**) FACS profile of asynchronous, Aphidicolin (5 μg/ml), and Nocodazole (1 μg/ml)-arrested HeLa cells. Cells were fixed in Ethanol (70 % v/v) and stained with Propidium Iodide (0.02 μg/ml) before FACS with the NucleoCounter® NC-3000™. (**D**-**F**) Western blots of HeLa cell lysates synchronised as described in (**A**-**C**). Cells were lysed in RIPA buffer prior to Western blotting with either anti-Esco1, anti-Esco2, anti-Sgo1, anti-α-Tubulin, or anti-γ-Tubulin antibody. This figure is representative of three independent experiments.

The Esco2 immunofluorescence data showed punctate nuclear localisation in cells blocked at the G1/S boundary, indicative of nuclear foci where the protein might possibly be aggregated in response to the Aphidicolin block (Figure 3.7B and F). The nuclear distribution became more homogeneous between 1 and 3 h after release from the Aphidicolin block. At 6 h, Esco1 localised towards the nuclear periphery. Quantification of the relative abundance of nuclear and cytoplasmic Esco2 showed an increase in number of cells showing nuclear localisation at 1 h after release from the Aphidicolin block, followed by a steady decrease in nuclear localisation from 3 to 9 h (Figure 3.7D). This result suggests that in interphase cells the majority of Esco2 is nuclear, but as cells exit S-phase and enter G2, the Esco2 protein becomes cytoplasmic or localises to the nuclear periphery, indicating that endogenous Esco2 expression decreases from S-phase to G2 (see Figure 4.6, page 124). Since Esco2 only binds chromatin during S-phase (Hou F & Zou H, 2005) and that both Esco1 and Esco2 can acetylate Smc3 during DNA replication (Nasmyth, 2005; Zhang et al., 2008), the brief association of Esco2 with chromatin observed in this study may be specifically targeted for Smc3 acetylation during DNA replication.

My immunoblot data (Figure 3.7E) showed that while endogenous Esco1 protein levels did not change from 0 to 9 h, the protein levels of Esco2 only increased slightly from 0 to 3 h, and steadily declined thereafter, further suggesting that the expression of endogenous Esco2 protein decreases as cells get to G2, consistent with my earlier observation of reduced Esco2 staining on chromatin at mitosis (Figure 3.5).

I next examined the levels of endogenous Esco1 and Esco2 proteins during the cell cycle using a synchronised population of HeLa cells (Figure 3.8A). My immunoblot results showed that while the level of total Esco1 protein was constant, total Esco2 levels gradually decreased as cells entered mitosis (Figure 3.8B), suggesting that the two proteins have different modes of regulation and that Esco2 may be degraded after S-phase. These results are consistent with a study which reports that Esco1 is continuously expressed during the cell cycle while Esco2 is degraded at mitosis (Hou F & Zou H, 2005).

To confirm that Esco2 is degraded after S-phase, I treated a synchronised population of HeLa cells with the proteasome inhibitor, Bortezomib (PS-341), which blocks cell cycle progression at the G2/M phase (Ling et al., 2002), and monitored their progression through the cell cycle for 24 h (Figure 3.9A). I also treated asynchronous HeLa cells with the proteosome inhibitor for the same length of time (Figure 3.9B). My immunoblots showed that Esco2 was stabilised in the presence of the inhibitor and the level of total Esco1 was also constant, as observed earlier (Figure 3.9B). A check on the Esco2 protein sequence revealed a KEN box (Figure 3.9C), the general degradation targeting signal for APC^{Cdh1} (Pfleger & Kirschner, 2000). This data suggests that the Esco2 function may be more restricted to S-phase and that as cells enter mitosis, the protein is degraded via ubiquitination, as has been reported earlier (Lafont et al., 2010). These results are consistent with my western blot data (see Figure 4.6, page 124).

Taken together, my data indicates that the Esco1 and Esco2 proteins are nuclear and chromatin-bound during interphase, and that their chromatin association decreases as cells progress through mitosis, a pattern similar to the localisation of cohesin and Pds5 proteins (Chapter 4, Figures 4.1 and 4.3) and published data that report a temporal association of cohesin with chromatin in interphase and dissociation during mitosis (Nishiyama et al., 2010; Zhang et al., 2011). In mitosis, the Esco1 and Esco2 proteins are regulated differently; while total Esco1 levels remain constant and phosphorylated (Hou & Zou, 2005; van der Lelij et al., 2009; Song et al., 2012; Whelan et al., 2012), Esco2 is degraded (Hou & Zou, 2005; Lafont et al., 2010).

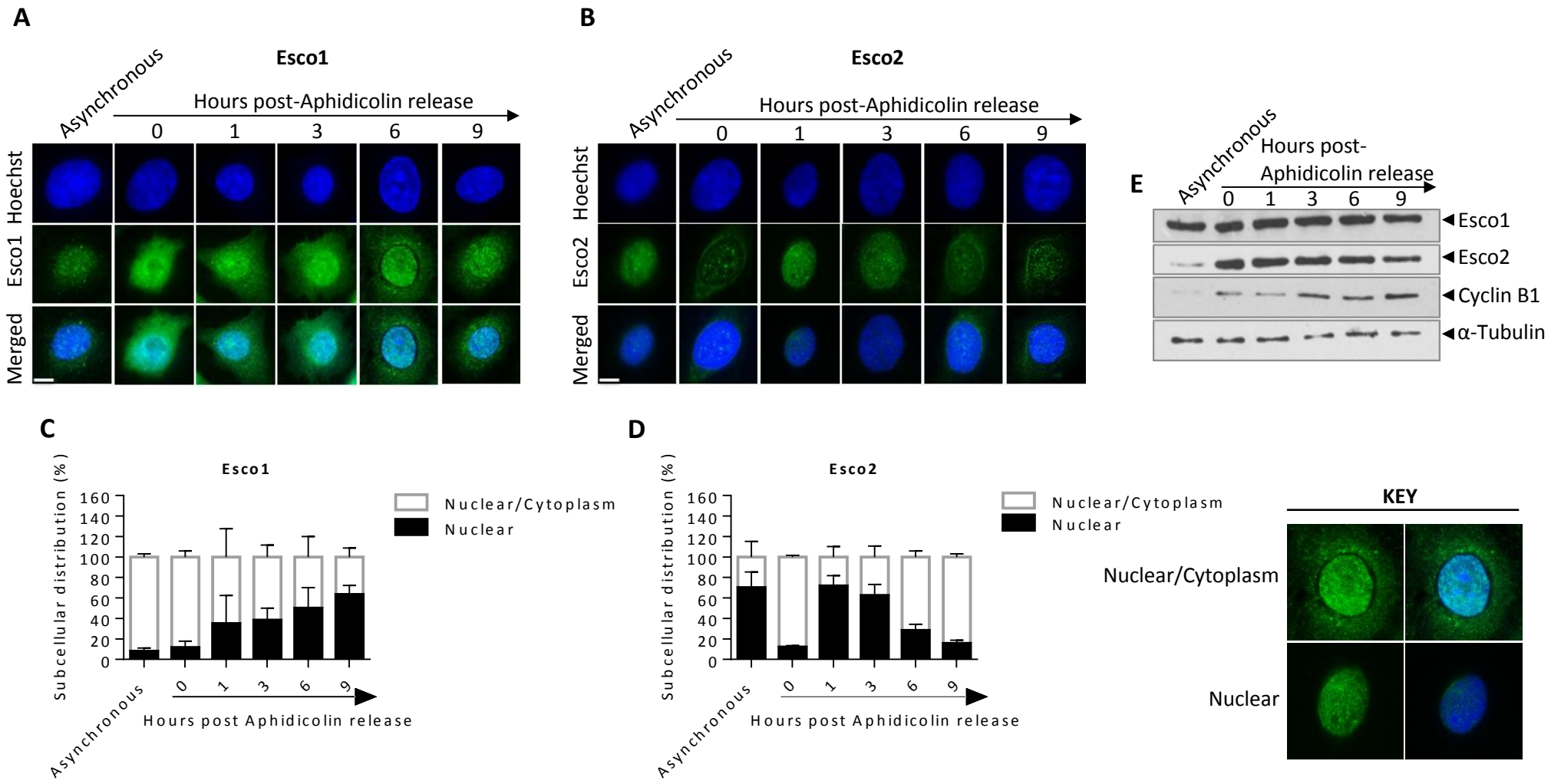
A
Esco1
Asynchronous
Hours post-Aphidicolin release
0
1
3
6
9
Hoechst
Esco1
Merged
B
Esco2
Asynchronous
Hours post-Aphidicolin release
0
1
3
6
9
Hoechst
Esco2
Merged
E
Asynchronous
Hours post-Aphidicolin release
0
1
3
6
9
Esco1
Esco2
Cyclin B1
α-Tubulin
C
Esco1
Subcellular distribution (%)
160
140
120
100
80
60
40
20
0
Nuclear/Cytoplasm
Nuclear
Asynchronous
0
1
3
6
9
Hours post Aphidicolin release
D
Esco2
Subcellular distribution (%)
160
140
120
100
80
60
40
20
0
Nuclear/Cytoplasm
Nuclear
Asynchronous
0
1
3
6
9
Hours post Aphidicolin release
KEY
Nuclear/Cytoplasm
Nuclear

F

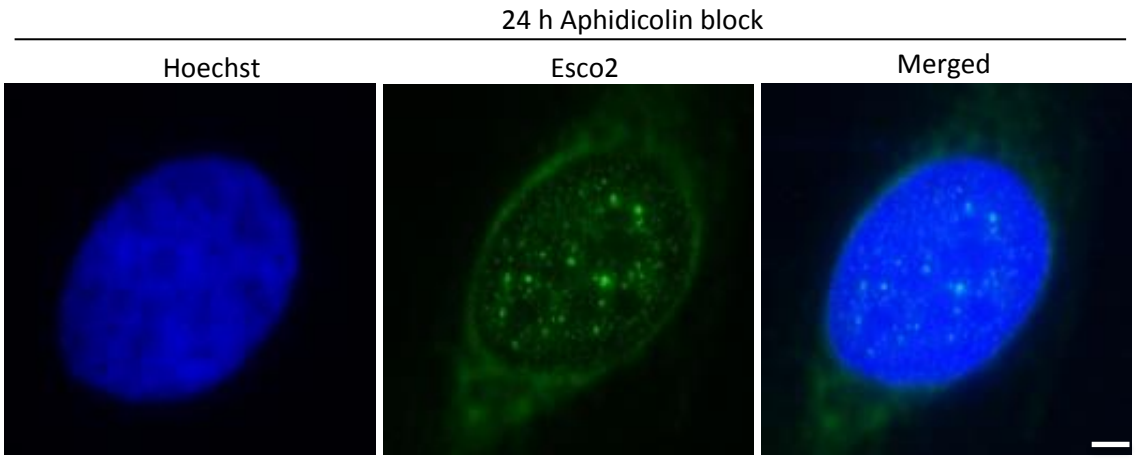

Figure 3.7 Differential localisation of Esco1 and Esco2 during S-phase

(**A** and **B**) Immunofluorescence images of HeLa cells showing the intracellular localisation of Esco1 and Esco2, respectively, following release from a 24 h-Aphidicolin (5 μg/ml) block. Cells were fixed in Methanol before being blocked with BSA (5 % w/v) and stained with either anti-Esco1 or anti-Esco2 antibody (green). DNA was stained with Hoechst 33342 (blue). Merged images are shown in the bottom panels in A and B. Scale bar: 10 μm. (**C** and **D**) Histograms showing quantitation of data in (**A** and **B**), respectively. A total of 100 cells were counted in randomly selected fields. (**E**) Western blot of HeLa cell lysates after release from a 24 h-Aphidicolin (5 μg/ml) block. Cells were lysed in RIPA buffer prior to Western blotting with either anti-Esco1, anti-Esco2, anti-Cyclin B1, or anti-α-Tubulin antibody. (**F**) An enlarged immunofluorescence image of HeLa cells in (**B**) showing the punctate localisation of Esco2 following a 24 h Aphidicolin (5 μg/ml) block. This figure is representative of three independent experiments.

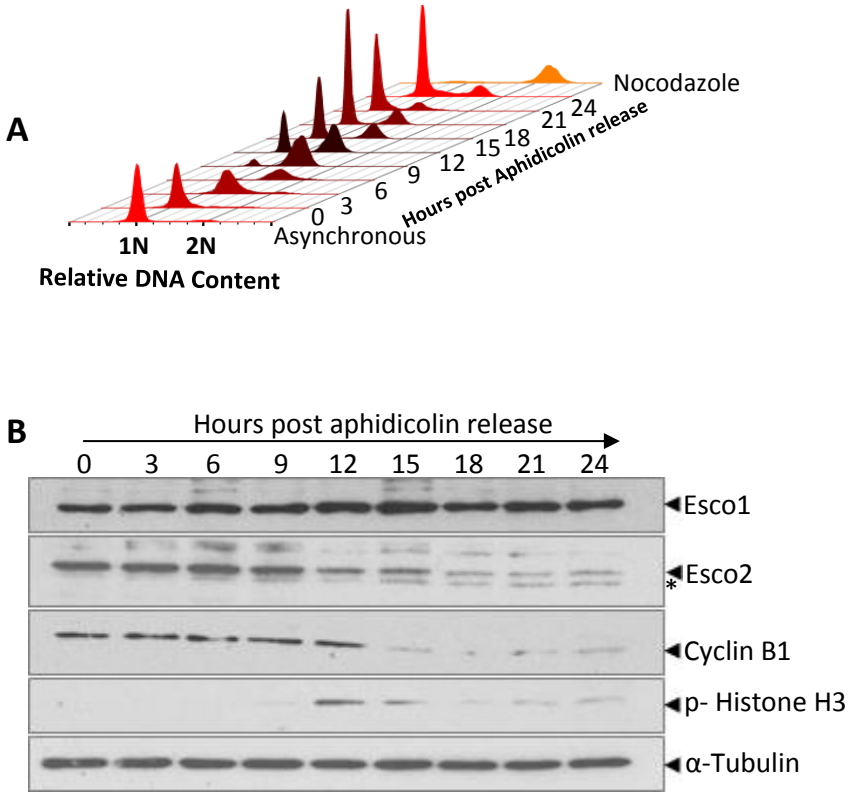

Figure 3.8 Esco1 and Esco2 protein levels during the HeLa cell cycle

(**A**) FACS profile of HeLa cells following release from a 24 h-Aphidicolin (5 μg/ml) block. Asynchronous and Nocodazole (1 μg/ml)-arrested cells were also profiled. Cells were fixed in Ethanol (70 % v/v) and stained with Propidium Iodide (0.02 μg/ml) before FACS with the NucleoCounter® NC-3000™. (**B**) Western blot of HeLa cell lysates after release from a 24 h-Aphidicolin (5 μg/ml) block. Cells were lysed in RIPA buffer prior to Western blotting with either anti-Esco1, anti-Esco2, anti-Cyclin B1, anti-p-Histone H3, or anti-α-Tubulin antibody. *= Non-specific binding. This figure is representative of three independent experiments.

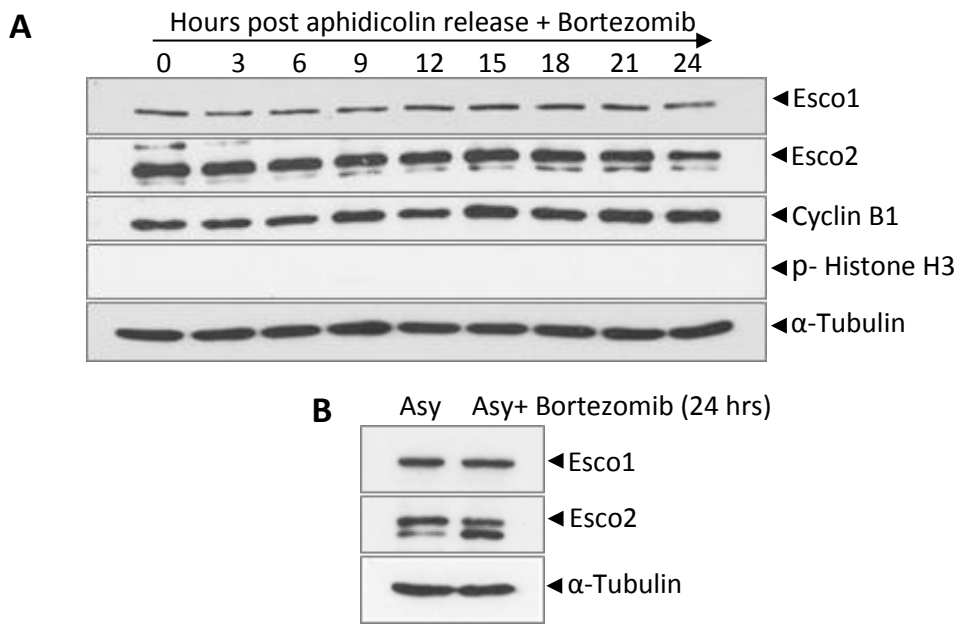

C

Esco2 Sequence

MAALTPRKRKQDSLKCDSLLHFTENLFPSPNKKHCFYQNSDKNEENLHCSQQEHFVLSAL

KTTEINRLPSANQGSPFKSALSTVSFYNQNKWYLNPLERKLIKESRSTCLKTNDEDKSFP

IVTEKMQGKPVCSKKNNKKPQKSLTAKYQPKYRHIKPVSRNSRNSKQNRVIYKPIVEKEN

NCHSAENNSNAPRVLSQKIKPQVTLQGGAAFFVRKKSSLRKSSLENEPSLGRTQKSKSEV

IEDSDVETVSEKKTFATRQVPKCLVLEEKLKIGLLSASSKNKEKLIKDSSDDRVSSKEHK

VDKNEAFSSEDSLGENKTISPKSTVYPIFSASSVNSKRSLGEEQFSVGSVNFMKQTNIQK

NTNTRDTSKKTKDQLIIDAGQKHFGATVCKSCGMIYTASNPEDEMQHVQHHHRFLEGIKY

VGWKKERVVAEFWDGKIVLVLPHDPSFAIKKVEDVQELVDNELGFQQVVPKCPNKIKTFL

FISDEKRVVGCLIAEPIKQAFRVLSEPIGPESPSSTECPRAWQCSDVPEPAVCGISRIWV

FRLKRRKRIARRLVDTLRNCFMFGCFLSTDEIAFSDPTPDGKLFATKYCNTPNFLVYNFN

S

Figure 3.9 Endogenous Esco2 protein levels are stabilised in the presence of proteosome inhibitor

(**A** and **B**) Western blots of HeLa cell lysates following a 24 h-treatment with Bortezomib (PS-341, 20 nM) and Aphidicolin (5 μg/ml) and release from the block. Cells were lysed in RIPA buffer prior to Western blotting with either anti-Esco1, anti-Esco2, anti-Cyclin B1, anti-p-Histone H3, or anti-α-Tubulin antibody. (**C**) Esco2 protein sequence showing the KEN BOX (highlighted in yellow). This figure is representative of two independent experiments.

3.2.3 Depletion of Esco1 and Esco2 delays DNA replication

During S-phase, the Esco1 and Esco2 acetyltransferases acetylate Smc3 on two residues ($K^{105/106}$) in mammalian cells (Nasmyth, 2005; Zhang et al., 2008). Not only has cohesin acetylation been shown to be important in establishing sister chromatid cohesion (Nishiyama et al., 2010; Minamino M et al., 2015; Ladurner et al., 2016), but also speed the replication fork (Terret et al., 2009). To confirm whether Smc3 acetylation is required for DNA replication, I depleted Esco1 and Esco2 using a pool of four siRNAs, either individually or in combination. My immunoblot data showed successful depletion of both proteins at siRNA concentration of 50 nM (Figure 3.10). Furthermore, my data also showed that depletion of both Esco1 and Esco2 proteins inhibits Smc3 acetylation, and that of the two proteins, depletion of Esco1 reduced Smc3 acetylation more than depletion of Esco2 (Figure 3.10), suggesting that Smc3 is acetylated primarily by Esco1.

I then analysed DNA replication in either asynchronous or synchronised population of HeLa cells depleted of either Esco1, Esco2, or both Esco1 and Esco2 proteins by labelling them with the Thymidine analog, 5'-Bromo-2'-deoxyuridine (BrdU) (Figures 3.11A and B). Quantification of Immunofluorescence data of asynchronous cells labelled with BrdU revealed no significant difference in the number of control and Esco1 and Esco2-depleted cells that incorporated BrdU (Figure 3.11C). However, in a synchronised population of HeLa cells, there was a significant reduction in BrdU incorporation in Esco1 and Esco2-depleted cells compared to control siRNA-treated cells (Figure 3.11D), suggesting that acetyltransferases Esco1 and Esco2 proteins are required for DNA replication. To further test the requirement for Esco1 and Esco2 proteins in S-phase, I analysed DNA replication at a single molecule level using the DNA single fibre technique to monitor replication fork movements in a synchronised population of HeLa cells depleted of either Esco1, Esco2, or both Esco1 and Esco2 proteins. I sequentially labelled cells depleted of either Esco1, Esco2, or both Esco1 and Esco2 proteins with halogenated nucleosides Iododeoxyuridine (IdU) and Chlorodeoxyuridine (CIdU) for 30 min each following release from Aphidicolin block (Figure 3.12A), after which I extracted genomic DNA and stretched it on glass slides, before labelling with IdU- and CIdU-specific antibodies.

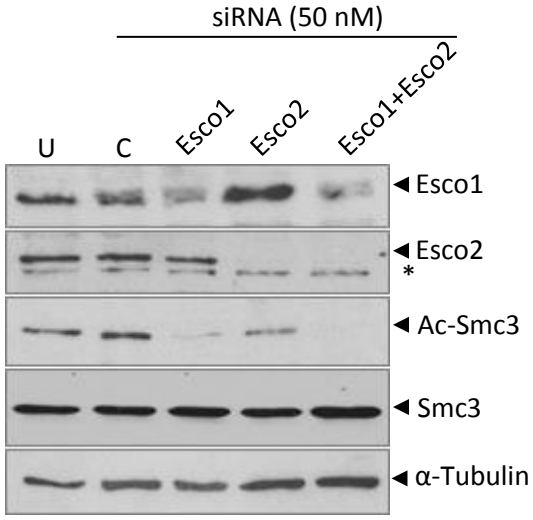

Figure 3.10 Depletion of Esco1 and Esco2 proteins prevents Smc3 acetylation

Western blot of HeLa cell lysates following a 48 h-transfection with 50 nM of either control, Esco1, Esco2, or a mixture of both Esco1 and Esco2 siRNAs. Cells were lysed in RIPA buffer and Western blot was carried out using either anti-Esco1, anti-Esco2, anti-Ac-Smc3, anti-Smc3, or anti-α-Tubulin antibody. U = Untreated, and C = control. This figure is representative of three independent experiments.

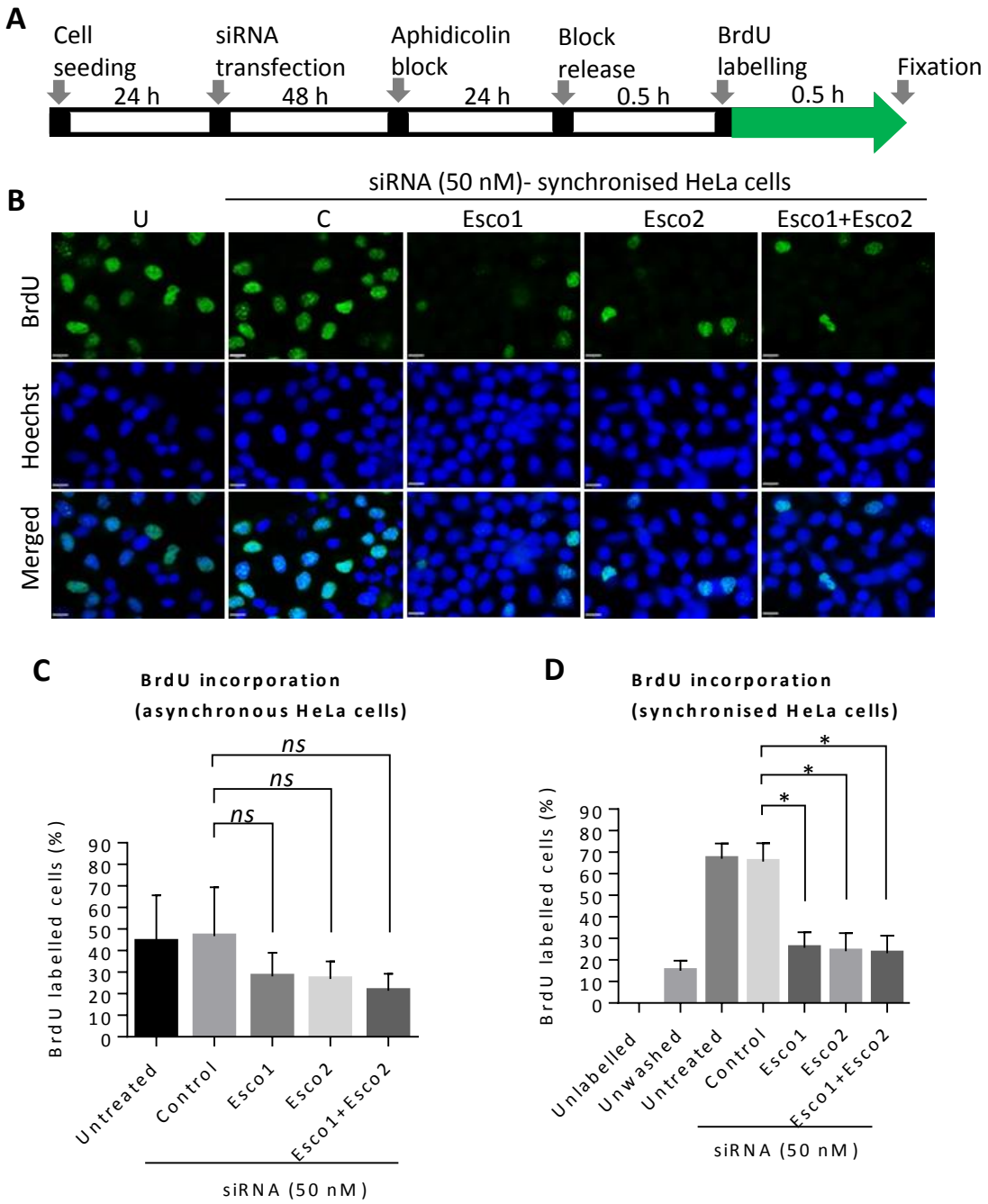

Figure 3.11 Depletion of Esco1 and Esco2 proteins impedes DNA replication

(**A**) Schematic representation of BrdU (1 µM) incorporation assay in a synchronised population of HeLa cells depleted of Esco1 and Esco2 proteins. (**B**) Immunofluorescence images of BrdU (1 µM)-labelled HeLa cells following a 48 h-treatment with 50 nM of either control, Esco1, Esco2, or both Esco1 and Esco2 siRNAs and 24 h-treatment with Aphidicolin (5 µg/ml). Cells were fixed in Methanol before being blocked with BSA (5 % w/v) and stained with anti-BrdU antibody (green). DNA was stained with Hoechst 33342 (blue). Scale bar: 10 µm. (**C** and **D**) Histograms showing quantitation of data in (**B**). The mean+s.e.m of at least 100 cells counted in randomly selected fields is shown. $^{ns}P > 0.05$, $*P < 0.05$; P values were calculated using a two-tailed Student t-test. This figure is representative of three independent experiments.

Single fibre analysis showed four major differences between control and Esco1, Esco2, or both Esco1 and Esco2-depleted cells (Figure 3.12B). Compared to control cells (Figure 3.12B i-iii), Esco1, Esco2, or both Esco1 and Esco2-depleted cells were characterised by short labelled DNA fibres (Figure 3.12B iv, vii, viii, and x) and (Figure 3.12C), an indication of slow-moving replication forks. Calculation of the replication fork velocity showed a significant reduction from 0.58 kb/min in the control cells to 0.49 kb/min, 0.48 kb/min, and 0.47 kb/min in the synchronised population of Esco1, Esco2, or both Esco1 and Esco2-depleted cells, respectively (Figure 3.12D). Furthermore, there was a significant increase in the number of stalled replication forks in cells depleted of both Esco1 and Esco2 proteins, compared to control cells (Figure 3.12B v and xi) and (Figure 3.12E), suggesting that the absence of Esco1 and Esco2 proteins inhibits replication fork progression. There were also numerous intermittent gaps in the labelled DNA fibres derived from cells depleted of either Esco1, Esco2, or both Esco1 and Esco2 proteins (Figure 3.12B vi, ix, and xii), suggesting an increase in firing of latent origins after fork stalling in the absence of Esco1 and Esco2 proteins. Additionally, there was a significant reduction in the number of interspaced fibres (Figure 3.12B iii) for labelled DNA derived from either Esco1 or both Esco1 and Esco2-depleted cells, compared to control cells (Figure 3.12F), suggesting slowed DNA replication. Collectively, this data showed that Esco1 and Esco2 proteins are required during S-phase for replication fork progression, consistent with published data which reported that acetylation is required for normal fork progression (Terret et al., 2009).

3.2.4 Depletion of Esco1 and Esco2 causes precocious chromosome separation and is characterised by chromatin deformities and aneuploidy

Acetylation of cohesin is important for the establishment and maintenance of sister chromatid cohesion. Recently, it has been shown that depletion of Esco1 and Esco2 proteins leads to untimely separation of chromosomes (Minamino et al., 2015). To confirm this, I prepared chromosome spreads as described in Materials and Methods using HeLa cells treated for 48 h with either control, Esco1, Esco2, or both Esco1 and Esco2 siRNAs. I also prepared chromosome spreads using cells depleted of Sororin, a known cohesion establishment factor that has been shown to keep sister chromatids together (Nishiyama et al., 2010) and whose depletion is characterised by metaphase

abnormalities (see Figure A2, page 207). Immunofluorescence analysis of chromosome spreads (Figure 3.13A) and measurements of distances between kinetochore pairs showed a significant increase from 3.0 µm in the control cells to 12.4 µm, 12.8 µm, and 15.5 µm in the Esco1, Esco2, or both Esco1 and Esco2-depleted cells, respectively (Figure 3.13B). As expected, depletion of Sororin also resulted in an increase in kinetochore pair distances (11.0 µm) (Figure 3.13B). This data showed that depletion of Esco1 and Esco2 proteins causes precocious separation of sister chromatids.

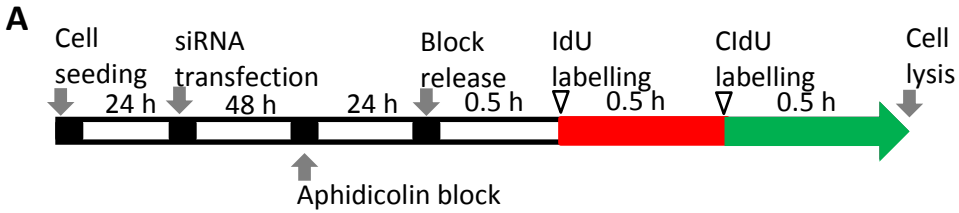
A
Cell seeding
24 h
siRNA transfection
48 h
24 h
Block release
0.5 h
IdU labelling
0.5 h
CldU labelling
0.5 h
Cell lysis
Aphidicolin block

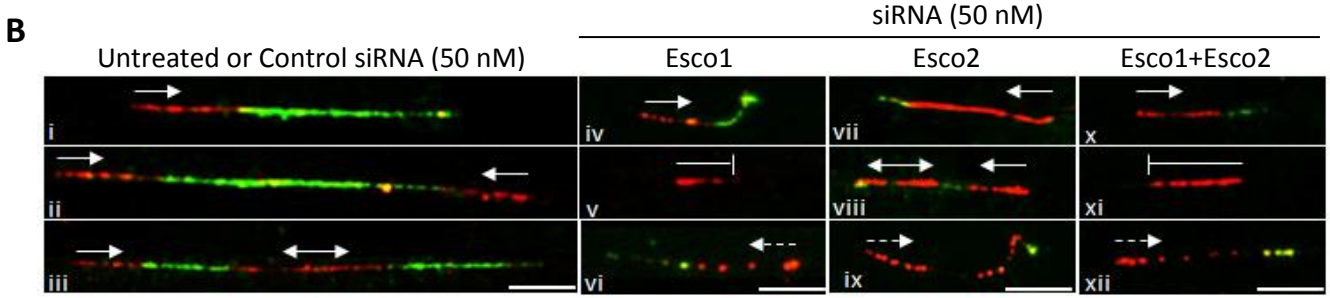
B
siRNA (50 nM)
Untreated or Control siRNA (50 nM)
Esco1
Esco2
Esco1+Esco2
i
ii
iii
iv
v
vi
vii
viii
ix
x
xi
xii

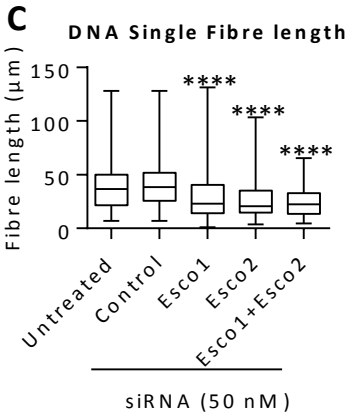
C
DNA Single Fibre length
Fibre length (µm)
150
100
50
0
****
****
****
Untreated
Control
Esco1
Esco2
Esco1+Esco2
siRNA (50 nM)

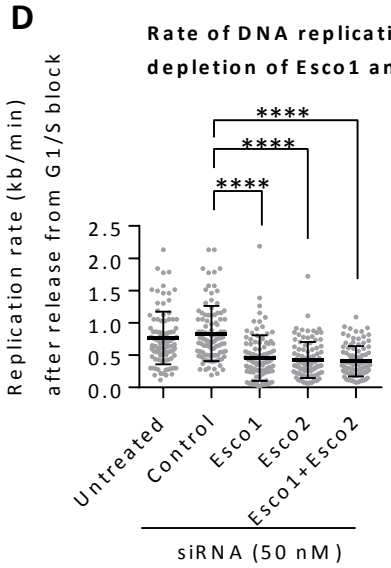
D
Rate of DNA replication after depletion of Esco1 and Esco2
Replication rate (kb/min) after release from G1/S block
2.5
2.0
1.5
1.0
0.5
0.0
****
****
****
Untreated
Control
Esco1
Esco2
Esco1+Esco2
siRNA (50 nM)

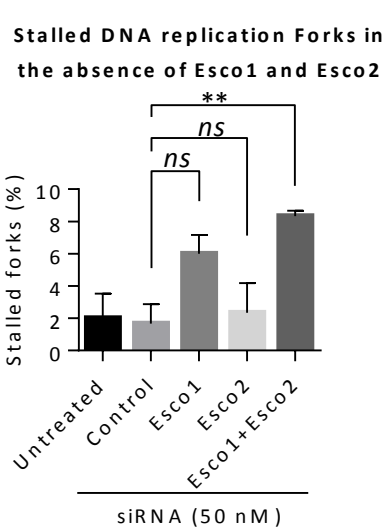
E
Stalled DNA replication Forks in the absence of Esco1 and Esco2
Stalled forks (%)
10
8
6
4
2
0
**
ns
ns
Untreated
Control
Esco1
Esco2
Esco1+Esco2
siRNA (50 nM)

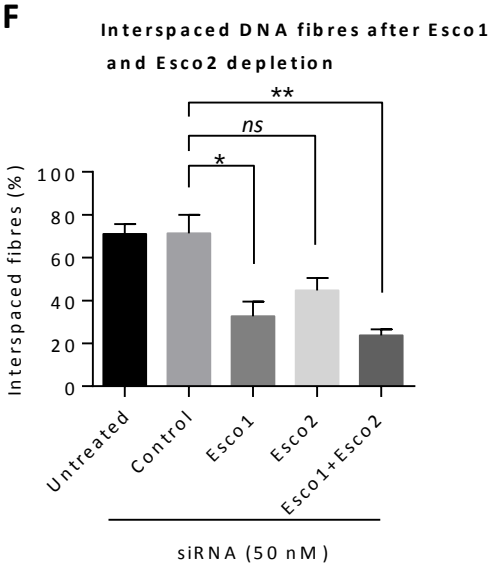
F
Interspaced DNA fibres after Esco1 and Esco2 depletion
Interspaced fibres (%)
100
80
60
40
20
0
**
ns
*
Untreated
Control
Esco1
Esco2
Esco1+Esco2
siRNA (50 nM)

Figure 3.12 Cells depleted of Esco1 and Esco2 proteins are characterised by defective DNA strands and stalled replication forks

(**A**) Schematic representation of DNA single fibre assay in a synchronised population of Esco1 and Esco2-depleted HeLa cells. (**B**) Immunofluorescence images of DNA replication forks (red = IdU, 25 μM and green = CIdU, 250 μM) observed in HeLa cells following a 48 h-treatment with 50 nM of either control, Esco1, Esco2, or both Esco1 and Esco2 siRNAs and release from Aphidicolin (5 μg/ml) block. Cells were lysed in DNA Fibre Lysis Buffer, fixed with Carnoy's solution (3:1 v/v Methanol: Acetic acid), and hydrolysed in HCl (2.5 M) before being blocked with BSA (5 % w/v) and stained with either Fitc-conjugated-anti-BrdU (green) or anti-BrdU antibody (red). White arrows indicate direction of fork movement. Scale bar: 20 μm. Panels i, iv, vii, and x represent elongating forks; panels ii and viii represent termination points; panels v and xi represent stalled forks; panel iii represents interspaced fibres; and panels vi, ix, and xii represent intermittent gaps. (**C**) Box plot showing a reduction in DNA fibre lengths in Esco1 and Esco2-depleted cells. (**D**) Dot plot showing a reduction in replication fork velocities in Esco1 and Esco2-depleted cells. (**E**) Histogram showing an increase in the number of stalled replication forks in Esco1 and Esco2-depleted cells. (**F**) Histogram showing a reduction in the number of interspaced DNA fibres in Esco1 and Esco2-depleted cells. For the data set C-F, the mean ± s.e.m of at least 100 DNA fibre tracts counted in randomly selected fields is shown. $^{ns}P > 0.05$, *P < 0.05, **P < 0.01, ****P < 0.0001. P values were calculated using a two-tailed Student t-test. This figure is representative of three independent experiments.

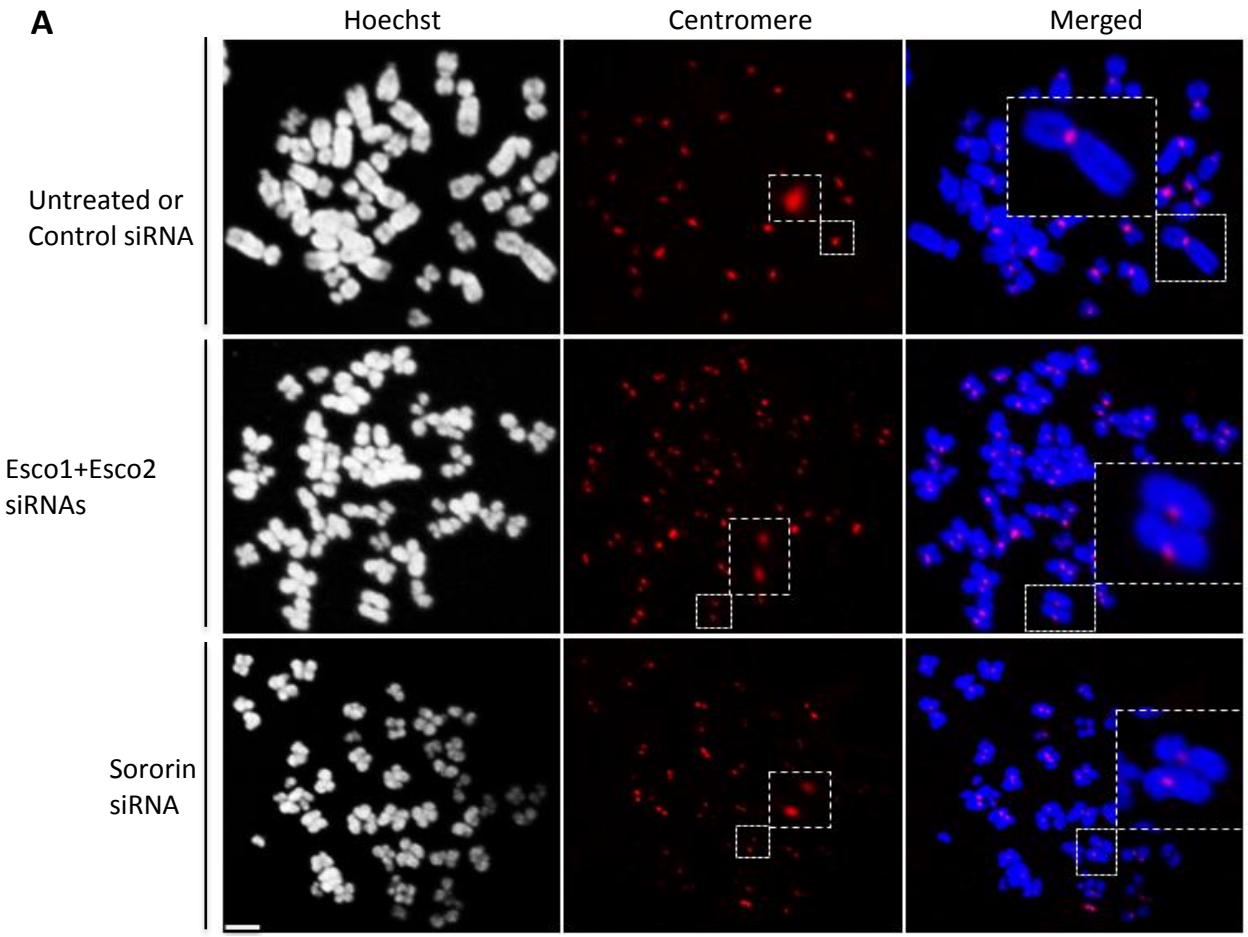
A
Hoechst
Centromere
Merged
Untreated or
Control siRNA
Esco1+Esco2
siRNAs
Sororin
siRNA

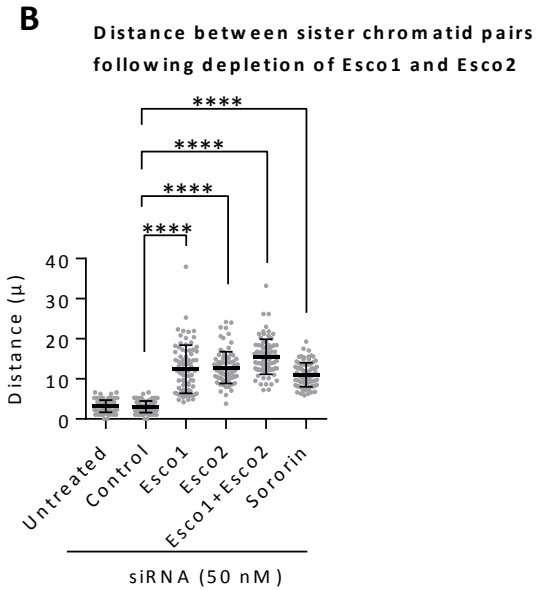
B
Distance between sister chromatid pairs
following depletion of Esco1 and Esco2
****
****
****
****
Distance (μ)
40
30
20
10
0
Untreated
Control
Esco1
Esco2
Esco1+Esco2
Sororin
siRNA (50 nM)

Figure 3.13 Depletion of Esco1 and Esco2 proteins causes precocious sister chromatid separation

(**A**) Immunofluorescence images of chromosome spreads following a 48-h treatment with 50 nM of either control, Esco1, Esco2, or Sororin antibody, and a 24 h-Nocodazole (1 μg/ml) block. Mitotic shake-off cells were swelled in hypotonic KCl (75 mM) before being fixed with Carnoy's solution (3:1 v/v Methanol: Acetic acid), lysed by dropping from a distance of 30 cm, and blocked with 5 % w/v BSA/ 0.1 % v/v Tween 20/ PBS, prior to staining with anti-Centromere antibody (red). DNA was stained with Hoechst 33342 (white). Merged images are shown in the last panels in A and squares indicate enlarged images of kinetochore pairs. Scale bar: 10 μm. (**B**) Dot plot quantitation of data in (**A**) showing distances between chromosomes in Esco1, Esco2, and Sororin-depleted cells. Each dot represents a pair of sister kinetochores. ****P < 0.0001. P values were calculated using a two-tailed Student t-test. This figure is representative of three independent experiments.

To further investigate the consequences of loss of Esco1 and Esco2 on chromatin structure, I transfected asynchronous HeLa cells with the control, Esco1, Esco2, or both Esco1 and Esco2 siRNAs and fixed the cells as described in Materials and Methods before staining them with either anti-α-Tubulin or anti-ɣ-Tubulin antibody. My Immunofluorescence data revealed a number of chromatin abnormalities in cells depleted of Esco1 and Esco2. Apart from multilobed nuclei (Figure 3.14A and B; see also Figure A1, page 206), cells depleted of Esco1 and Esco2 were also characterised by multiple spindle poles (Figure 3.15A and B), chromosomal bridges (Figure 3.16A and B), and micronuclei (Figure 3.17A and B). This data suggests that in the absence of Esco1 and Esco2 proteins, cells are unable to maintain sister chromatid cohesion, resulting in precocious separation of sister chromatids, failure to align chromosomes at the metaphase plate, and uneven distribution of chromosomes resulting in phenotypes reminiscent of aneuploidy.

3.2.5 Depletion of Esco1 and Esco2 proteins in HeLa cells induces apoptosis

Cohesin acetylation is the glue that helps hold sister chromatids together to ensure accurate chromosome segregation at mitosis. Loss of acetylation has many consequences during mitosis, including precocious chromosome separation (Figure 3.13) and defects in chromosome segregation (Figure 3.15). To maintain genome integrity, cells have evolved a number of mechanisms that ensure that defective DNA is not propagated and passed on to new daughter cells. Depletion of either Esco1, Esco2, or both Esco1 and Esco2 proteins from HeLa cells resulted in a third of cells detaching from tissue culture plates at 48 h after treatment with the siRNAs and appeared to be dying, as they could not incorporate BrdU (Figure A3, page 208). Surprisingly, depletion of Esco1, Esco2, or both Esco1 and Esco2 proteins from a primary cell line, retinal pigment epithelial (RPE1) cells, did not lead to cell detachment from tissue culture plates.

It is unclear how depletion of Esco1 and Esco2 proteins results in different observable phenotypes in HeLa and RPE1 cells. One possibility is that HeLa cells arrest in mitosis with activated SAC and undergo apoptosis after Esco1 and Esco2 depletion due to lack of functional p53 (Scheffner, 1998; Hietanen, 2000). To test if cells depleted of Esco1

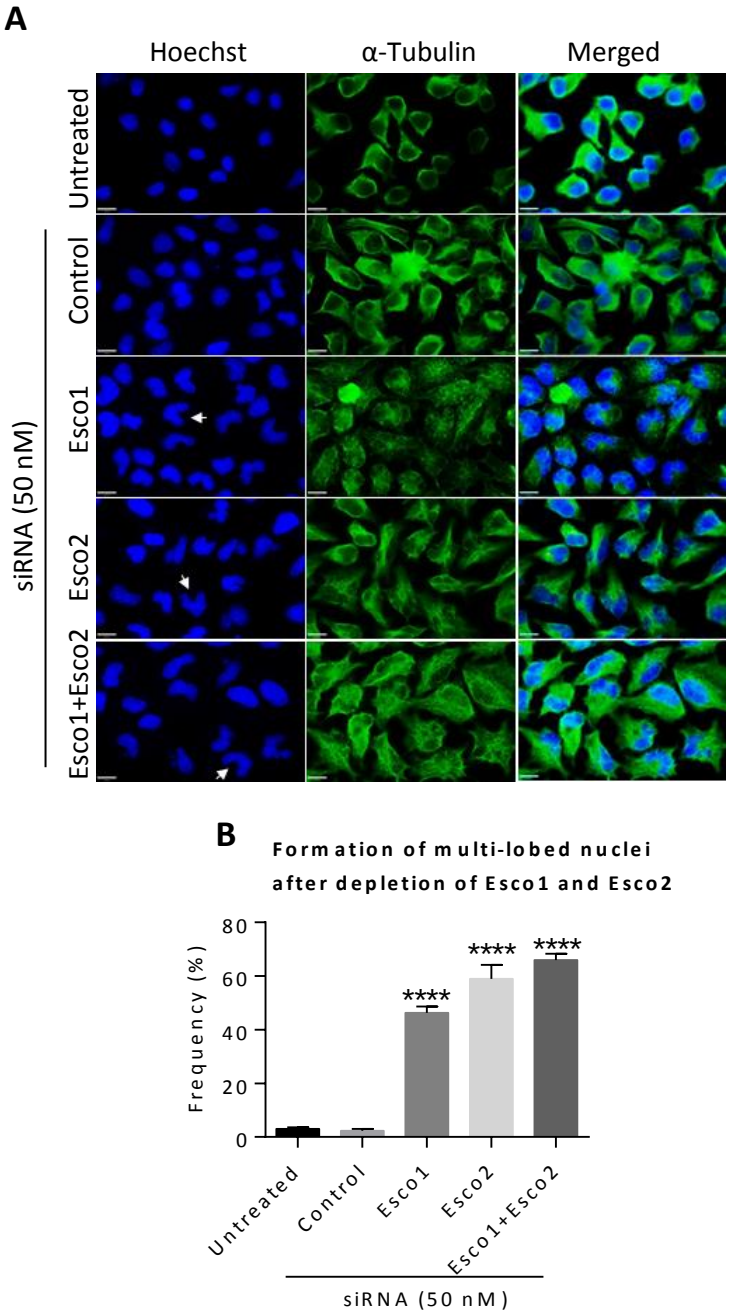

Figure 3.14 Depletion of Esco1 and Esco2 induces the formation of multilobed nuclei

(**A**) Immunofluorescence images of asynchronous HeLa cells following a 48 h-treatment with 50 nM of either control, Esco1, Esco2, or both Esco1 and Esco2 antibodies. Cells were fixed in Methanol before being blocked with BSA (5 % w/v) and stained with anti-α-Tubulin antibody (green). DNA was stained with Hoechst 33342 (blue). Merged images are shown in the last panels in A. Scale bar: 10 μm. White arrows indicate examples of lobed nuclei. (**B**) Histogram showing quantitation of data in (**A**). The mean+s.e.m of at least 100 cells counted in randomly selected fields is shown. ****P < 0.0001. P values were calculated using a two-tailed Student t-test. This figure is representative of three independent experiments.

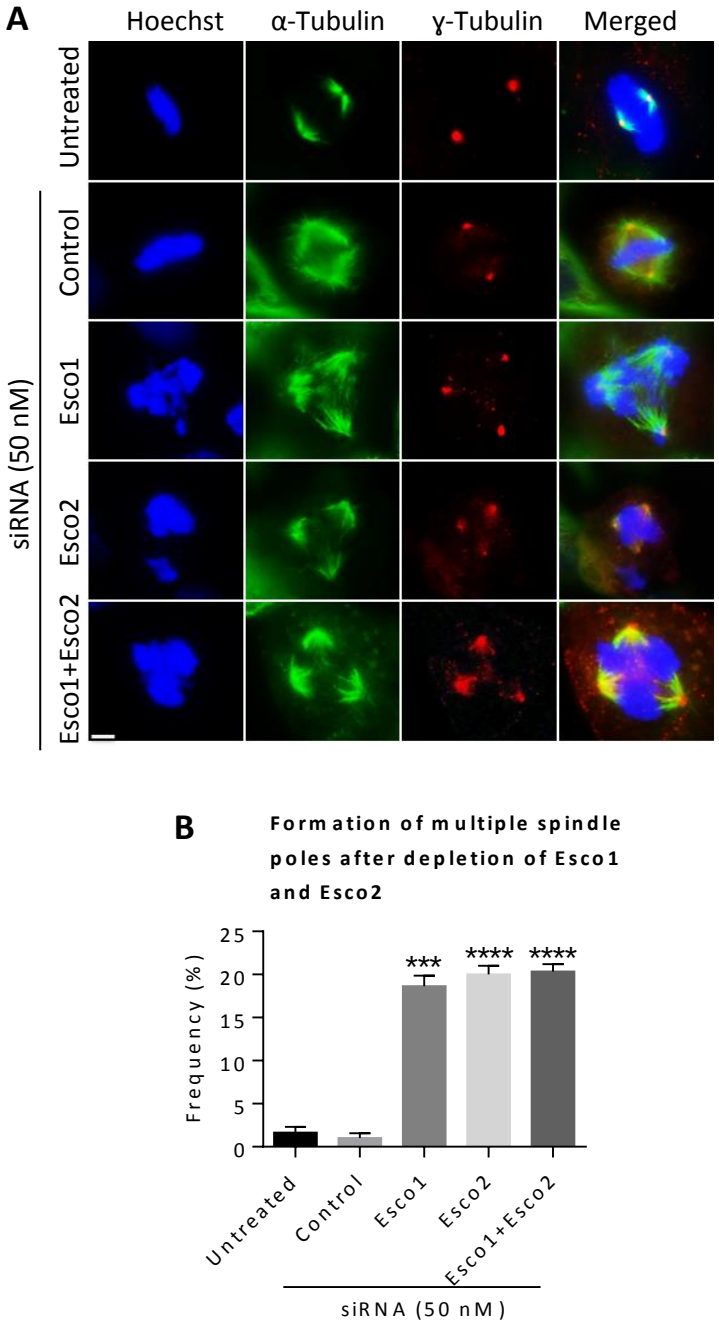

Figure 3.15 Depletion of Esco1 and Esco2 proteins induces the formation of multiple spindle poles

(**A**) Immunofluorescence images of mitotic HeLa cells following a 48 h-treatment with 50 nM of either control, Esco1, Esco2, or both Esco1 and Esco2 antibodies. Cells were fixed in Methanol before being blocked with BSA (5 % w/v) and stained with either anti-α-Tubulin antibody (green) or anti-γ-Tubulin antibody (red). DNA was stained with Hoechst 33342 (blue). Merged images are shown in the last panels in A. Scale bar: 10 μm. (**B**) Histogram showing quantitation of data in (**A**). The mean+s.e.m of at least 100 cells counted in randomly selected fields is shown. ***P $<$ 0.001, ****P < 0.0001. P values were calculated using a two-tailed Student t-test. This figure is representative of three independent experiments.

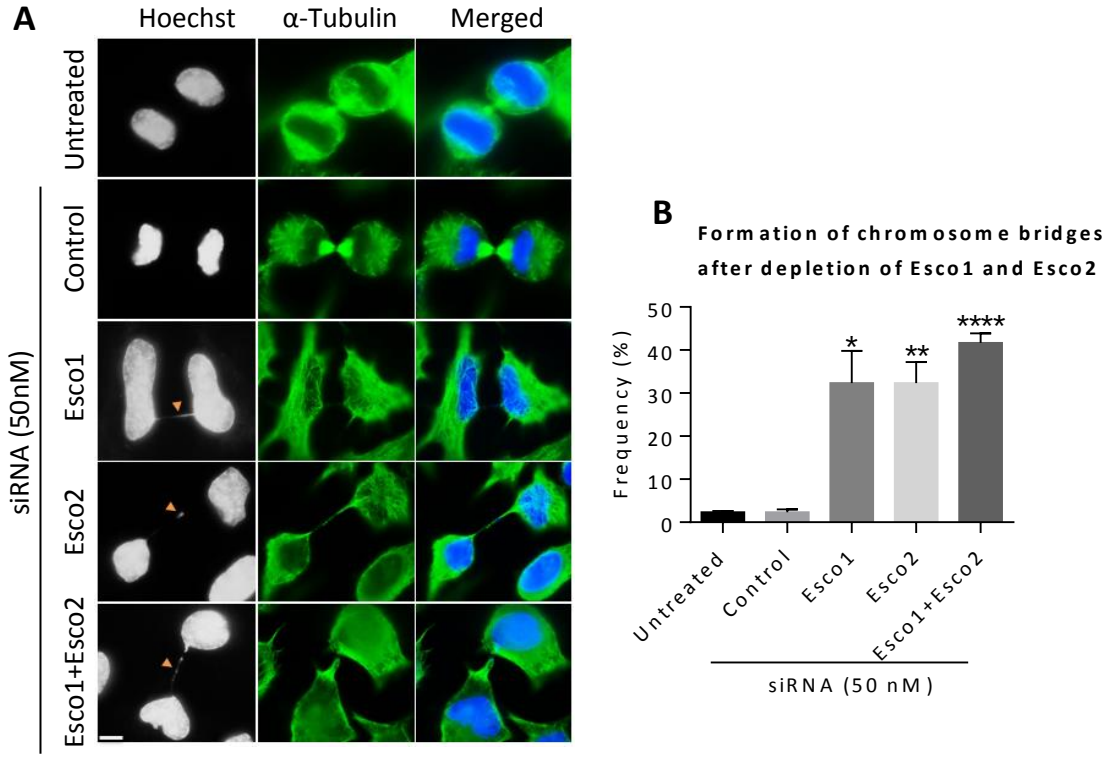

Figure 3.16 Depletion of Esco1 and Esco2 proteins induces the formation of chromosomal bridges

(**A**) Immunofluorescence images of mitotic HeLa cells following a 48 h-treatment with 50 nM of either control, Esco1, Esco2, or both Esco1 and Esco2 antibodies. Cells were fixed in Methanol before being blocked with BSA (5 % w/v) and stained with anti-α-Tubulin antibody (green). DNA was stained with Hoechst 33342 (white). Merged images are shown in the last panels in A. Scale bar: 10 μm. Orange arrows indicate chromosomal bridges. (**B**) Histogram showing quantitation of data in (**A**). The mean+s.e.m of at least 100 cells counted in randomly selected fields is shown. *P < 0.05, **P < 0.01, ****P < 0.0001. P values were calculated using a two-tailed Student t-test. This figure is representative of three independent experiments.

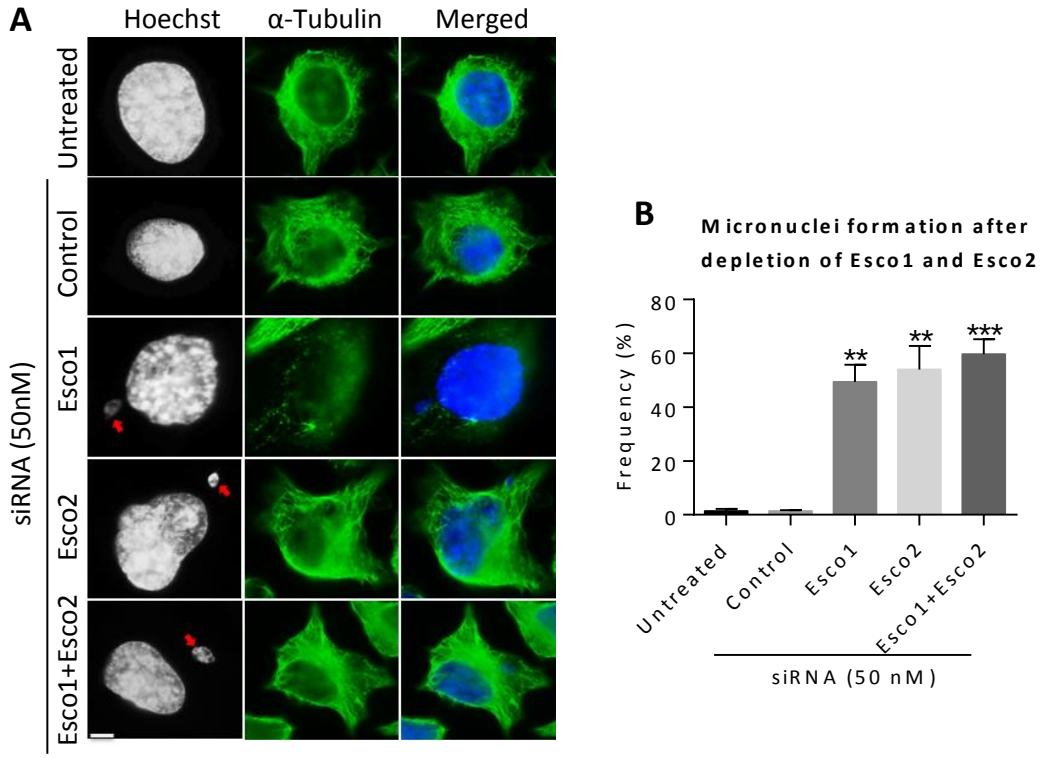

Figure 3.17 Depletion of Esco1 and Esco2 proteins induces the formation of micronuclei

(**A**) Immunofluorescence images of asynchronous HeLa cells following a 48 h-treatment with 50 nM of either control, Esco1, Esco2, or both Esco1 and Esco2 antibodies. Cells were fixed in Methanol before being blocked with BSA (5 % w/v) and stained with anti-α-Tubulin antibody (green). DNA was stained with Hoechst 33342 (white). Merged images are shown in the last panels in A. Scale bar: 10 μm. Red arrows indicate micronuclei. (**B**) Histogram showing quantitation of data in (**A**). The mean+s.e.m of at least 100 cells counted in randomly selected fields is shown. **P < 0.01, ***P < 0.001. P values were calculated using a two-tailed Student t-test. This figure is representative of three independent experiments.

and Esco2 proteins undergo apoptosis, I stained both the RPE1 and HeLa detached cells with the Cytokeratin 18 antibody following siRNA treatment (Figures 3.18A and B). The Cytokeratin 18 antibody detects caspase 3-cleaved cytokeratin 18 (Caulin et al., 1997). My data showed that HeLa cells depleted of Esco1, Esco2, or both Esco1 and Esco2 stained positively for cleaved cytokeratin 18 while depletion of Esco1 and Esco2 in RPE1 cells did not have any effect (Figures 3.18A and B).

To confirm the activation of apoptotic response observed (Figure 3.18A), I depleted Esco1, Esco2, or both Esco1 and Esco2 proteins from HeLa cells and prepared total cell lysates as described in Materials and Methods. Protein samples were resolved by SDS-PAGE and immunoblotted with antibodies raised against Esco1, Esco2, Caspase 9, Caspase 3, Cleaved Caspase 3, and α-Tubulin (Figure 3.18C). My immunoblot data showed cleavage of Caspase 3 and disappearance of Pro-Caspase 9 in cells depleted of both Esco1 and Esco2 (Figure 3.18C). Furthermore, HeLa cells were characterised by reduced growth in the absence of Esco1 and Esco2 proteins (Figure 3.19B), possibly because HeLa cells depleted of Esco1 and Esco2 detach from tissue culture plates (see Figure A3, page 208). Collectively, this data shows that depletion of Esco1 and Esco2 proteins causes HeLa cells to undergo apoptosis. This is a novel result; it is the first time loss of Esco1 and Esco2 has been shown to result in apoptosis.

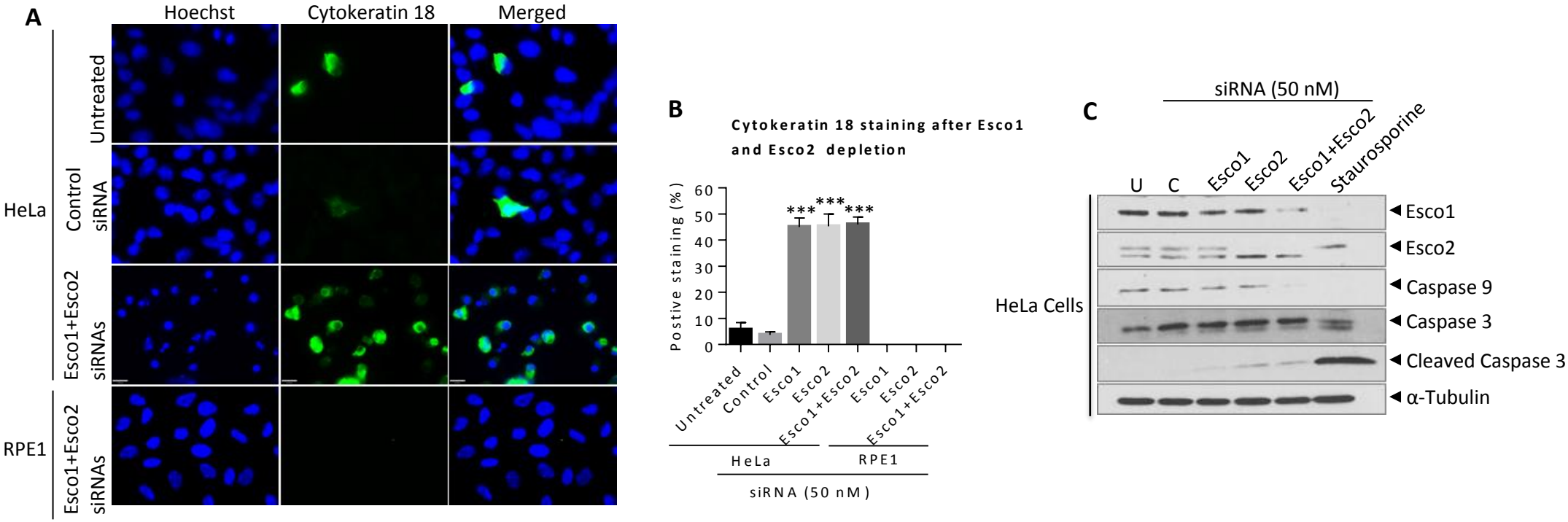

Figure 3.18 Depletion of Esco1 and Esco2 in HeLa cells induces apoptosis

(**A**) Immunofluorescence images of HeLa mitotic shake-off and RPE1 cells following a 48 h-treatment with 50 nM of either control, Esco1, Esco2, or both Esco1 and Esco2 siRNA. Cells were fixed in Methanol before being blocked with BSA (5 % w/v) and stained with anti-Cytokeratin 18 antibody (green). DNA was stained with Hoechst 33342 (white). Merged images are shown in the last panels in A. Scale bar: 10 μm. (**B**) Histogram showing quantitation of data in (**A**). The mean+s.e.m of at least 100 cells counted in randomly selected fields is shown. ***$P < 0.001$. P values were calculated using a two-tailed Student t-test. (**C**) Western blot of HeLa cell lysates following a 48 h-treatment with 50 nM of either control, Esco1, Esco2, or both Esco1 and Esco2 siRNAs, or 6 h-treatment with Staurosporine (1 μM). Cells were lysed in RIPA buffer prior to Western blotting with either anti-Esco1, anti-Esco2, anti-Caspase 9, anti-Caspase 3, anti-cleaved Caspase 3, or anti-α-Tubulin antibody. U = Untreated, and C = control. This figure is representative of three independent experiments.

3.2.6 Depletion of Esco1 and Esco2 proteins induces cellular senescence in primary (RPE1) cells

Unlike HeLa cells (Scheffner, 1998; Hietanen, 2000), primary cells such as RPE1 have functional p53 (Bodnar et al., 1998; Jiang et al., 1999; Liu et al., 2006) hence they are able to initiate other cellular responses after depletion of Esco1 and Esco2, such as senescence, to prevent the propagation of a defective genome. This could be the reason why they did not undergo apoptosis after depletion of Esco1 and Esco2 (Figure 3.18A and B). To test whether depletion of Esco1 and Esco2 proteins activates senescence in primary cells, I first examined the growth of RPE1 cells in the absence of Esco1 and Esco2 proteins (Figure 3.19). My data showed that depletion of Esco1 and Esco2 proteins slowed down the growth of RPE1 cells, suggesting that Esco1 and Esco2 proteins are factors required for the division of RPE1 cells.

I then treated the RPE1 cells with either control, Esco1, Esco2, or both Esco1 and Esco2 siRNAs for 48 h or 96 h and fixed them as described in Materials and Methods before staining with the X-Gal solution to test for senescence-associated endogenous β-galactosidase activity (Figure 3.20A). I also stained the EJ $p21^{+}$ and EJ $p21^{-}$ cells with the X-Gal solution, as negative and positive control, respectively (Figure 3.20B). My data showed that depletion of Esco1 and Esco2 proteins from RPE1 cells caused a significant increase in β-galactosidase activity (Figure 3.20C), suggesting that loss of Esco1 and Esco2 proteins from primary cells (RPE1) initiates senescence. To confirm this result, I treated RPE1 cells with either control, Esco1, Esco2, or both Esco1 and Esco2 siRNAs for 48 h or 96 h before preparing total cell lysates as described in Materials and Methods. I also lysed the EJ $p53^{+}$ and EJ $p53^{-}$ cells in RIPA buffer and prepared total lysates, as negative and positive control, respectively. I resolved protein samples by SDS-PAGE and immunoblotted with either Esco1, Esco2, p53, p21, p16, or α-Tubulin antibody (Figure 3.20D). My immunoblot data showed an increase in the senescence-associated factors, p53, p21, and p16 (Macip et al., 2002; Althubiti et al., 2014) in cells depleted of either Esco1, Esco2, or both Esco1 and Esco2 proteins, suggesting activation of senescence in the absence of Esco1 and Esco2 proteins. Collectively, this data suggests that loss of Esco1 and Esco2 may cause non-transformed cells to undergo senescence. This is a

novel result; it is the first time that loss of Esco1 and Esco2 has been shown to cause cell senescence.

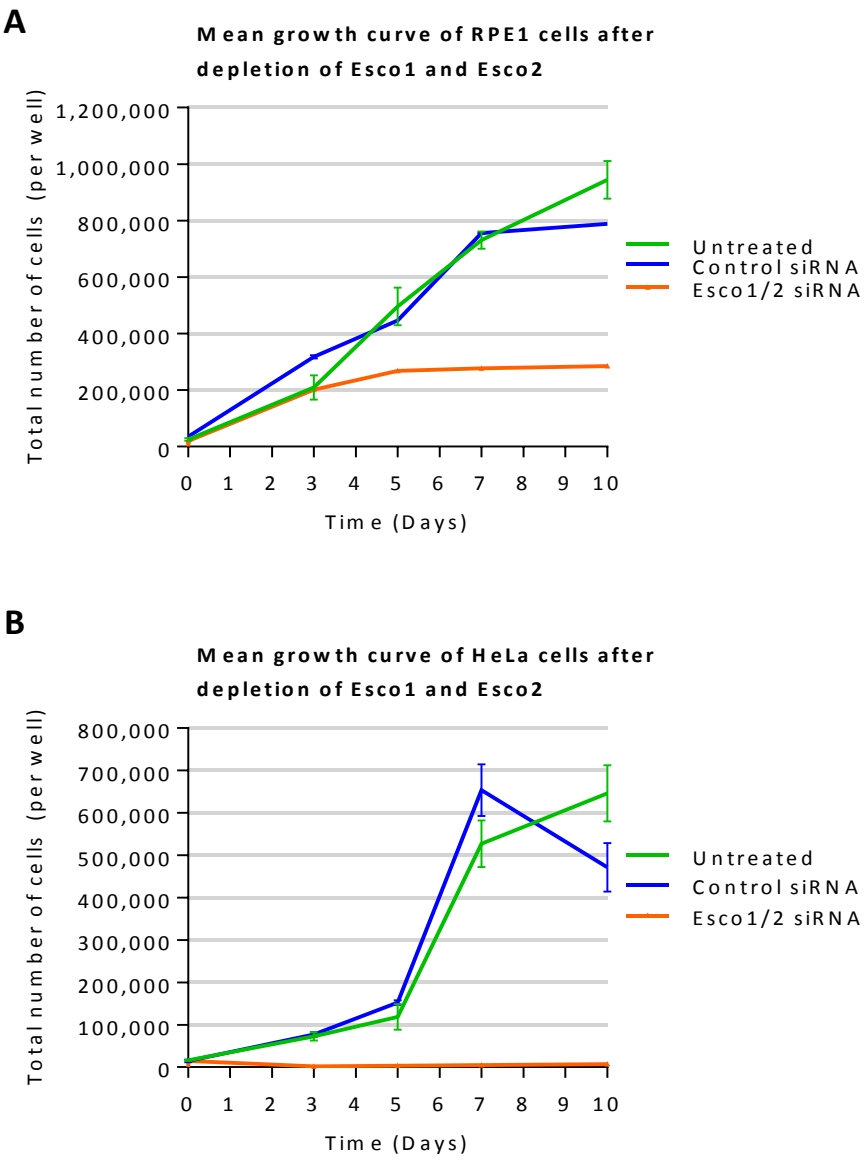

Figure 3.19 Depletion of Esco1 and Esco2 proteins slows the growth of RPE1 cells

(**A** and **B**) Mean growth curves of RPE1 and HeLa cells, respectively, following transfection with 50 nM of either control, Esco1, Esco2, or a mixture of both Esco1 and Esco2 siRNAs. Cells were cultured over a period of 10 days and scored on a daily basis using a Haemocytometer. This figure is representative of three independent experiments.

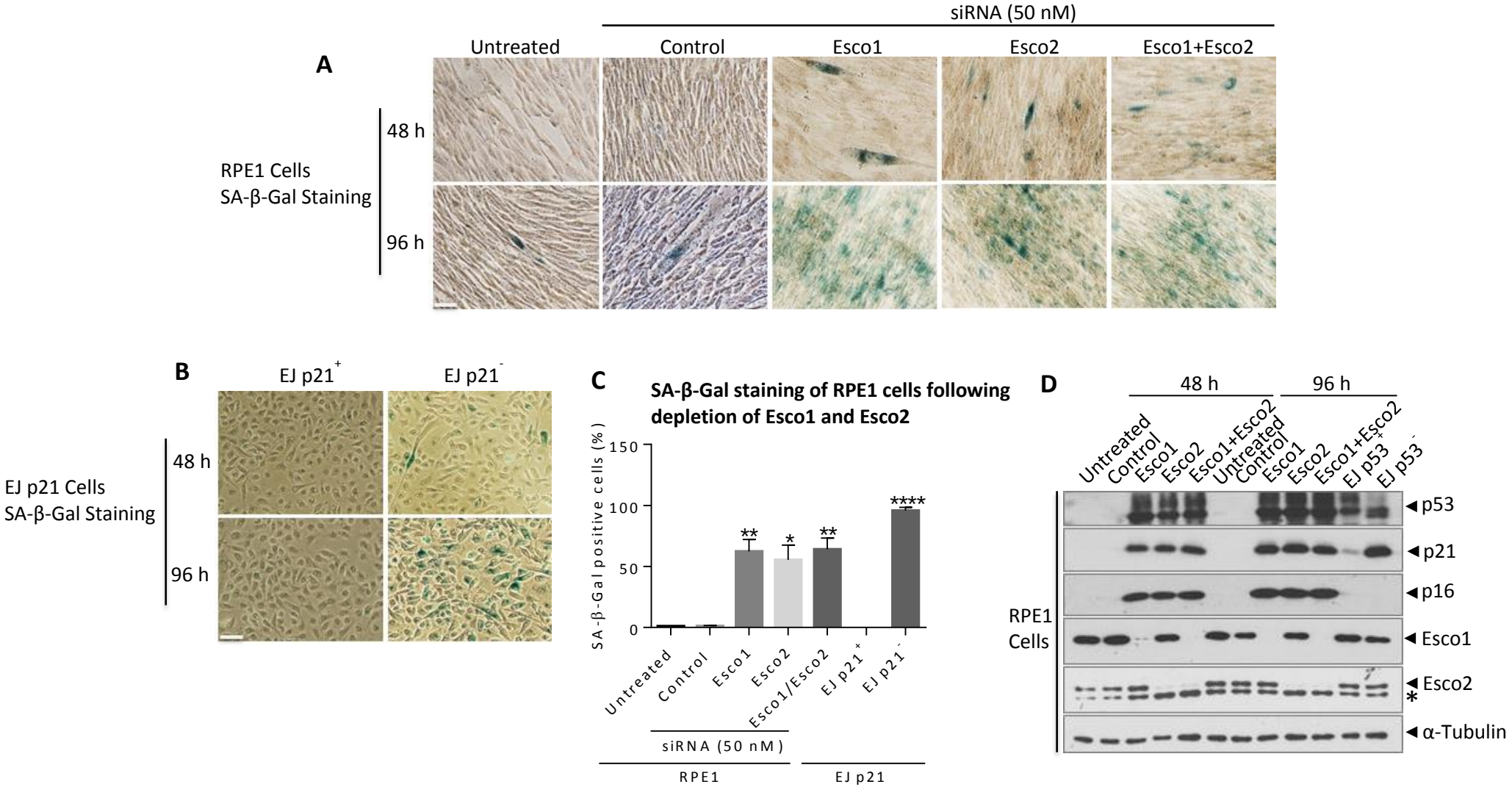
A
siRNA (50 nM)
Untreated
Control
Esco1
Esco2
Esco1+Esco2
RPE1 Cells
SA-β-Gal Staining
48 h
96 h
B
EJ p21+
EJ p21-
EJ p21 Cells
SA-β-Gal Staining
48 h
96 h
C
SA-β-Gal staining of RPE1 cells following depletion of Esco1 and Esco2
SA-β-Gal positive cells (%)
150
100
50
0
**
*
**
****
Untreated
Control
Esco1
Esco2
Esco1/Esco2
EJ p21+
EJ p21-
siRNA (50 nM)
RPE1
EJ p21
D
48 h
96 h
Untreated
Control
Esco1
Esco2
Esco1+Esco2
Untreated
Control
Esco1
Esco2
Esco1+Esco2
EJ p53+
EJ p53-
RPE1 Cells
p53
p21
p16
Esco1
Esco2
*
α-Tubulin

Figure 3.20 Depletion of Esco1 and Esco2 proteins from RPE1 cells induces senescence

(**A** and **B**) Representative images of senescence-associated endogenous β-galactosidase activity in RPE1 and EJp21 cells following a 48 or 96 h-treatment with 50 nM of either control, Esco1, Esco2, or both Esco1 and Esco2 antibodies. Cells were fixed with 3 % (v/v) Formaldehyde solution prior to staining with the X-Gal solution. Scale bar: 10 μm. (**C**) Histogram showing quantitation of data in (**A** and **B**). The mean+s.e.m of at least 100 cells counted in randomly selected fields is shown. *P < 0.05, **P < 0.01, ****P < 0.0001. P values were calculated using a two-tailed Student t-test. (**D**) Western blot of RPE1 cell lysates following a 48 or 96 h-treatment with 50 nM of either control, Esco1, Esco2, or both Esco1 and Esco2 siRNAs. Cells were lysed in RIPA buffer prior to Western blotting with either anti-Esco1, anti-Esco2, anti-p53, anti-p21, anti-p16, or anti-α-Tubulin antibody. *= non-specific binding. This figure is representative of three independent experiments.

3.2.7 Discussion

Cohesin acetylation is required for the establishment of sister chromatid cohesion. Proper establishment and maintenance of sister chromatid cohesion is important in safeguarding genome integrity. Errors in sister chromatid cohesion have been implicated in congenital birth defects (Shen, 2011; Pfau & Amon, 2012) and cancer (Thol et al., 2014; Thota et al., 2014). In this study I characterised the role of cohesin acetyltransferases Esco1 and Esco2 in the mammalian cell cycle. I report the requirement for Esco1 and Esco2 in DNA replication and the prevention of aneuploidy, apoptosis, and senescence.

In mammalian cells, both Esco1 and Esco2 acetylate Smc3 on two Lysine residues ($K^{105/106}$) during DNA replication (Nasmyth, 2005; Zhang et al., 2008). In higher eukaryotes cohesin acetylation is coupled with Sororin recruitment to chromatin, which establishes and maintains sister chromatid cohesion from S-phase to mitosis (Zhang & Pati, 2012). Consistent with this notion, my data shows that Esco1 and Esco2 proteins localise to chromatin during interphase and dissociate from chromatin at mitosis (Figure 3.3), a localisation similar to that of Sgo1 which protects centromeric cohesin until the end of mitosis (Figure 3.4).

In yeast, Eco1 has been found to be phosphorylated by Cdk1 and degraded after S-phase (Lyons & Morgan, 2011). In humans, it has been shown that Esco1 is expressed throughout the cell cycle (Song et al., 2012; Whelan et al., 2012) while Esco2 is only expressed during S-phase (Hou F & Zou H, 2005; van der Lelij et al., 2009; Song et al., 2012; Whelan et al., 2012). This might explain the difference in the abundance of these proteins at mitosis (Figure 3.5) and the fact that endogenous Esco1 protein levels do not change greatly in interphase and at mitosis (Figure 3.6D) while Esco2 exhibits a rapid degradation at mitosis (Figure 3.6E). Accumulation of Esco2 in G1/S-blocked lysates and its disappearance from lysates blocked in M-phase (Figure 3.6E) coupled with its transient interphase localisation (Figure 3.3B) suggests that Esco2 function may be restricted to interphase only.

In S-phase, Esco1 accumulates in the nucleus (Figure 3.7A), and its levels steadily increase throughout G2 (Figure 3.7C). This is in stark contrast to Esco2 which only localises to the nucleus during S-phase (Figure 3.7B). As cells progress to G2, Esco2 gradually disperses from the nucleus (Figure 3.7D). The fact that Esco2 forms punctate structures in cells blocked at the G1/S boundary (Figure 3.7B and F) and that its endogenous levels only steadily increase for 3 h after release from Aphidicolin block (Figure 3.7E) shows that the protein is only required during S-phase and may be important in DNA replication. Our previous results in the lab (unpublished) have shown that both Esco1 and Esco2 bind to chromatin after treatment of HeLa cells with Cisplatin. As cells exit S-phase, Esco2 may be degraded.

My cell cycle profile data (Figure 3.8A) showed that while total Esco1 protein levels remain constant throughout the cell cycle, Esco2 protein levels are greatly reduced as cells enter mitosis (Figure 3.8B). Furthermore, my data showed that the Esco2 protein is stabilised in the presence of the proteosome inhibitor (Figures 3.9A and B). An inspection of the protein sequence revealed that Esco2 possesses a KEN BOX (Figure 3.9C). This data shows that Esco2 is only required during S-phase and that the protein is ubiquitinated (by APC^{Cdh1}) and degraded when cells enter mitosis, consistent with previous studies (Lafont et al., 2010).

It has recently been shown that Esco1 acetylates cohesin via a mechanism different from that of Esco2, in that depletion of Pds5 abolishes the Esco1-dependent cohesion pathway whereas the Esco2 function is not affected by Pds5 depletion (Minamino et al., 2015). My data shows that Smc3 acetylation is largely carried out by Esco1, although depletion of both Esco1 and Esco2 has a bigger effect on prevention of acetylation than depletion of either protein (Figure 3.10). While Smc3 was acetylated as early as telophase when cells come out of mitosis (see Figure 4.3B, page 118), both Esco1 and Esco2 were seen to localise on chromatin only during interphase (Figure 3.3). It may be that as the nuclear envelope divides into two new daughter cells at the end of mitosis, de novo acetylation of the newly loaded chromatin-bound cohesin (Smc3) is carried out by Esco1, which is expressed throughout the cell cycle in vertebrates (Song et al., 2012; Whelan et al., 2012). The possible reason why Esco1 could not be detected by Immunofluorescence at telophase (Figure 3.3A) could be due to epitope masking upon

phosphorylation (Hou & Zou, 2005; Lyons & Morgan, 2011) and protein conformational change at mitosis. The Esco2 function may be more restricted to S-phase, where the protein seems to accumulate during the time that marks the period of DNA replication (see Figures 3.7, page 79, and 3.8, page 80), consistent with the finding that the protein is only expressed during S-phase (Hou F & Zou H, 2005; van der Lelij et al., 2009; Song et al., 2012; Whelan et al., 2012).

Acetylation of Smc3 renders cohesin resistant to removal by Wapl, and hence locks the DNA exit gate (Rolef Ben-Shahar et al., 2008; Rowland et al., 2009; Sutani et al., 2009; Unal et al., 2008; Zhang et al., 2008). In mitosis, Smc3 is deacetylated by HDAC8/Hos1, following the removal of cohesin from chromatin (Beckouët et al., 2010). The establishment and maintenance of sister chromatid cohesion by Smc3 acetylation coupled with Sororin recruitment is important in ensuring bi-polar spindle attachment to kinetochores and prevention of precocious separation of chromosomes (Minamino M et al., 2015).

Esco1 is recruited to chromatin by Pds5 (Minamino M et al., 2015). In yeast, Eco1/Ctf7 (Esco1/Esco2 in humans) physically interacts with PCNA during DNA replication (Moldovan et al., 2006). The Eco1-PCNA interaction enables Eco1 to transiently bind to chromosomes and acetylate Smc3, thereby establishing cohesion (Lengronne et al., 2006). In this sense, loss of acetyltransferases Esco1 and Esco2 should inhibit DNA replication.

Interestingly, cohesin acetylation has been shown to speed the replication fork in mammalian cells (Terret et al., 2009). However, studies in *Xenopus* egg extracts showed that acetylation does not affect DNA replication (Lafont et al., 2010). My data shows that depletion of Esco1 and Esco2 proteins significantly reduces BrdU incorporation (Figure 3.11B) by a synchronised population of HeLa cells (Figure 3.11D), suggesting that loss of Esco1 and Esco2 proteins hinders DNA replication in mammalian cells. However, depletions of these proteins from asynchronous cells did not have any significant effect on BrdU incorporation (Figure 3.11C).

Further analysis of DNA replication in HeLa cells depleted of Esco1 and Esco2 proteins using DNA single fibre techniques showed a number of deformities in newly replicated DNA strands, including short labelled DNA fibres (Figure 3.12B iv, vii, and x) and (Figure 3.12C) suggesting slow-moving replication forks, significant reduction in fork velocity (Figure 3.12D), significant increase in the number of stalled replication forks (Figure 3.12B v and xi) and (Figure 3.12E) suggesting inhibition of fork progression, numerous intermittent gaps (Figure 3.12B vi, ix, and xii) indicating an increase in the number of stalled replication forks, and significant reduction in the number of interspaced fibres (Figure 3.12F) suggesting slowed DNA replication.

The fact that DNA is labelled, although with numerous abnormalities such as stalled replication forks, reduced fork velocity, short labelled fibres, and intermittent gaps in the DNA fibres, shows that the origins of replication can still fire in the absence of Esco1 and Esco2 proteins, indicating that these proteins are not required for initiation but progression of replication forks. Interestingly, depletion of Esco1 reduced Smc3 acetylation more than depletion of Esco2 (Figure 3.10) despite that depletion of either protein reduced BrdU incorporation (Figure 3.11D) and slowed DNA replication (Figure 3.12). The fact that depletion of Esco2 does not completely inhibit Smc3 acetylation (Figure 3.10) but reduces BrdU incorporation (Figure 3.11D) and delays DNA replication (Figure 3.12) shows that acetylation does not have an effect on DNA replication.

The importance of cohesin acetylation to DNA replication (Terret et al., 2009) likely depends on the fact that it is coupled to the recruitment of cohesion establishment factors such as Sororin (Nishiyama et al., 2010; Ladurner et al., 2016). Crucially, Sororin's recruitment to chromatin depends on Esco2 (Lafont et al., 2010) and cohesin has been shown to be present at replication origins and participates in DNA replication by regulating higher-order organisation of replication factories and modulating the size of chromatin loops that likely correspond to replicon units (Figure 1.13) (Guillou et al., 2010).

Given that the recruitment of Sororin depends on Esco2 (Lafont et al., 2010), and that Sororin is a cohesion establishment factor (Nishiyama et al., 2010), it is plausible to think that the depletion of Esco2 may have inhibited Sororin's recruitment to chromatin and

establishment of sister chromatid cohesion, resulting in cohesin's inability to regulate higher-order organisation of replication factories. This eventually resulted in fewer, longer chromatin loops, which ultimately slowed down DNA replication. Taken together, my data suggests that cohesin acetylation by Esco1 and Esco2 may be required but not essential for replication fork progression in mammalian cells. This result is in contrast to reports that cohesin acetylation speeds the replication forks (Terret et al., 2009).

Failure to establish sister chromatid cohesion in S-phase results in poorly attached sister chromatids which can have consequences ranging from precocious chromosome separation to lagging chromosomes at anaphase. In the face of aberrant chromosome alignment at the metaphase plate, cells can activate the spindle assembly checkpoint and arrest in mitosis. This may be the reason why depletion of Esco1 and Esco2 from HeLa cells resulted 33 % of cells detaching from tissue culture plates (Figure 3.19B), whose immunofluorescence after BrdU labelling revealed no BrdU incorporation (see Figure A3, page 208). My data show that depletion of either Esco1, Esco2, or both Esco1 and Esco2 results in precocious separation of sister chromatids (Figure 3.13A); this is consistent with results that were reported while my study was underway (Minamino M et al., 2015). The precocious chromosome separation observed is a result of failure of sister chromatid cohesion establishment, most likely due to loss of acetylation, as sister kinetochores from Esco1, Esco2, or both Esco1 and Esco2-depleted cells significantly drifted away from each other (Figures 3.13A and B).

A check on chromatin organisation following depletion of Esco1 and Esco2 proteins revealed numerous chromatin abnormalities, including multilobed nuclei (Figure 3.14), multiple spindle poles (Figure 3.15), chromosomal bridges (Figure 3.16), and micronuclei (Figure 3.17), suggesting that in the absence of these proteins, chromatin organisation and chromosome segregation are impaired, resulting in phenotypes suggestive of aneuploidy (gain or loss of chromosomes). Aneuploidy is one of the most common hallmarks of cancer that has been documented in most malignancies. My data shows that acetyltransferases Esco1 and Esco2 are required for prevention of precocious sister chromatid separation and abnormal chromosome segregation

Chapter 3: Esco1 and Esco2 are essential for sister chromatid cohesion

To maintain genome integrity, cells have evolved a number of mechanisms that ensure that defective DNA is not propagated and passed on to new daughter cells. The fatal consequences of loosely attached sister chromatids should therefore be dealt with before the onset of anaphase. Staining of HeLa mitotic shake-off cells with the Cytokeratin 18 antibody following siRNA treatment showed that depletion of either Esco1, Esco2, or both Esco1 and Esco2 proteins from HeLa cells activates the apoptotic response (Figures 3.18A and B). This was confirmed by cleavage of Caspase 3 (Figure 3.18C). These results show that Esco1 and Esco2 are required for prevention of apoptosis.

Surprisingly, depletion of either Esco1, Esco2, or both Esco1 and Esco2 proteins from primary cells, RPE1, did not cause cells to undergo apoptosis (Figure 3.18A, bottom panels). It is possible that in primary cells like RPE1, loss of Esco1 and Esco2 may initiate other cellular responses such as senescence, since these cells contain functional p53 (Bodnar et al., 1998; Jiang et al., 1999; Liu et al., 2006) and are viable. My analysis of cell growth after depletion of Esco1 and Esco2 from RPE1 cells showed reduced growth in the absence of both proteins (Figure 3.19), suggesting that loss of acetylation inhibits cell proliferation. Staining for Senescence-Associated-β-Galactosidase activity following depletion of Esco1 and Esco2 from RPE1 cells showed that loss of these proteins activates senescence (Figure 3.20A, B, and C). Immunoblotting for senescence-associated factors, p53, p21, and p16 (Macip et al., 2002; Althubiti et al., 2014), revealed higher expression of these proteins (Figure 3.20D), suggesting that depletion of Esco1 and Esco2 from primary cells initiates senescence.

Characterisation of Esco1 and Esco2 in the mammalian cell cycle has shed more light on the mechanistic consequences of cohesin acetylation. With contradictory reports emerging in the recent past regarding the extent to which loss of Smc3 acetylation affects normal cellular processes such as DNA replication (Lafont et al., 2010; Terret et al., 2009), this study provides further evidence about the relevance of Esco1 and Esco2 in chromosome biology. Through this study, I have confirmed, as previously reported (Terret et al., 2009; Minamino et al., 2015), that Esco1 and Esco2 are required for DNA replication and prevention of precocious chromosome separation. Crucially, I have

demonstrated, for the first time, that not only are Esco1 and Esco2 proteins important for prevention of precocious sister chromatid separation, but also apoptosis and senescence. Overall, data from this study suggests that depletion of Esco1 and Esco2 prevents Smc3 acetylation, which results in failure to establish sister chromatid cohesion; loosely attached sister chromatids may lead to either senescence (in primary cells) or apoptosis (in transformed cells). Cells that manage to evade the mitotic cell cycle arrest fail to align their chromosomes at the metaphase plate, resulting in precocious separation and aneuploidy.

The disparity in cell fate observed after depletion of Esco1 and Esco2 has interesting implications. Recently, it was reported that there is a strong correlation between Esco1 expression and bladder cancer (Zhang et al., 2016), and that Esco2 is one of the proteins that are highly upregulated in aggressive melanoma (Ryu et al., 2007). Since both primary (RPE1) and transformed (HeLa) cells employ normal cellular responses (apoptosis and senescence) to depletion of Esco1 and Esco2 to halt propagation of defective chromosomes, unwanted signalling mishaps can be selectively eliminated by targeting these proteins. For example, therapeutics aimed at alleviating tumour growth can exploit the fate of transformed (cancerous) cells following depletion of Esco1 and Esco2. Having Esco1 and Esco2 as cancer drug targets would only eliminate affected cells by targeting them for normal cell death (apoptosis). Of note, however, is the detrimental effects of Esco1 and Esco2 knockdown on normal development (Shen, 2011; Pfau & Amon, 2012). Targeting and mitigating overly expressed Esco1 and Esco2 mRNAs in malignancy to tolerable levels could be an exciting intervention.

Future experiments should seek to explore protein localisation and cellular fate after mutating the phosphorylation sites of Esco1 and the KEN box of Esco2. Identifying the binding partners of Esco1 and Esco2 will help clarify how loss of acetylation results in apoptosis or senescence. Whether these cellular responses are merely a consequence of loosely attached sister chromatids remains speculative at the minute. It will also be important to determine if the delay in DNA replication observed after depletion of Esco1 and Esco2 can be reversed by over expression of these proteins. Determining if loss of acetylation gives rise to DNA damage and whether or not in the face of damaged DNA cells lacking Esco1 and Esco2 can repair their DNA will be key to understanding whether

the delay in DNA replication observed after depletion of Esco1 and Esco2 only came as a result of failure to establish sister chromatid cohesion.

Main conclusions from this Chapter:

- The data in this chapter has shown that depletion of either Esco1 or Esco2 prevents Smc3 acetylation, although by only a smaller fraction in Esco2-depleted cells, and results in a delay in DNA replication.

- Depletion of either Esco1 or Esco2 results in precocious separation of sister chromatids, chromosome missegregation, and either apoptosis or senescence.

Chapter 4 - Pds5A and Pds5B are required for DNA Replication

4.1 Introduction

Sister chromatid cohesion, mediated by the cohesin complex, is important for the maintenance of genome integrity (Shen, 2011). Without correct establishment and maintenance of sister chromatid cohesion, cells fail to correctly segregate their chromosomes during mitosis, resulting in aneuploidy (a hallmark of cancer) and congenital birth defects, collectively termed cohesinopathies (Shen, 2011; Pfau & Amon, 2012). The cohesin complex consists of four core subunits; these are Smc1, Smc3 (members of the structural maintenance of chromosomes family of ATPases), the kleisin subunit Scc1/Rad 21 (sister chromatid cohesion 1), and stromal antigens Scc3/Psc3 (SA1 or SA2 in humans) (Haering et al., 2002; Gruber et al., 2003). Additional proteins regulate the functions of cohesin; these include Pds5 (Pds5A and Pds5B in vertebrates), Wapl, Sororin, Sgo1, and Eco1 (Esco1 and Esco2 in humans).

De novo association of cohesin with chromatin is mediated by the loader complex, Scc2-Scc4, which loads cohesin onto chromatin during telophase (in vertebrates) or early G1 (in budding yeast) (Gillespie & Hirano, 2004; Takahashi et al., 2004; Guacci et al., 1997; Michaelis et al., 1997). Before S-phase, the anti-establishment activity of Wapl, bound to Pds5, keeps cohesin in a dynamic state and prevents its stable association with chromatin (Nishiyama et al., 2010). Stable association of cohesin with chromatin and establishment of sister chromatid cohesion occurs following the acetylation of Smc3 by Esco1/Esco2 coupled with the recruitment of Sororin to chromatin once the replication fork passes through the cohesin ring (Nishiyama et al., 2010). Sororin binds to Pds5 and displaces Wapl, thereby establishing sister chromatid cohesion, which is maintained until mitosis (Nishiyama et al., 2010).

In higher eukaryotes, two distinct pathways, the prophase pathway and the spindle assembly checkpoint (SAC)-mediated pathway, are responsible for the two-stage dissociation of cohesin from chromosomes (Nishiyama et al., 2010). In prophase, SA2 and Sororin are phosphorylated by Polo-like kinase 1 (Plk1) and Cdk1, respectively

(Zhang et al., 2011). The phosphorylation of Sororin inhibits its ability to bind to Pds5 and antagonise Wapl. This allows Wapl to bind to Pds5 and displace Sororin and remove cohesin from the chromosome arms. However, at the centromere, cohesin is protected from the prophase pathway by Shugoshin 1 (Sgo1), which recruits a serine/threonine protein phosphatase 2A (PP2A) that suppresses the phosphorylation of cohesin. During the metaphase-to-anaphase transition, following bipolar spindle attachment to sister kinetochores, ubiquitination of Securin by the anaphase promoting complex (APC)/Cyclosome frees Separase, which then cleaves the Scc1 subunit of centromeric cohesin, thereby triggering the segregation of chromosomes (Nishiyama et al., 2010).

Although recent studies have increased our understanding of the molecular mechanisms that regulate sister chromatid cohesion and separation, the role of Pds5 in sister chromatid cohesion is only partially understood. Not only has Pds5 been implicated in establishing and maintaining sister chromatid cohesion (in yeast) but also in the release of cohesin from chromatin (Muir et al., 2016). In mammals, cohesin is dysfunctional in the absence of Pds5 (Carretero et al., 2013). Furthermore, mice deficient for either Pds5A or Pds5B fail to complete embryonic development and cells from Pds5B-null mice are characterised by aneuploidy and an impaired spindle assembly checkpoint (Carretero et al., 2013). Cohesin has a separate DNA entry and exit gate (Chan et al., 2012; Murayama & Uhlmann, 2015) and mediates DNA replication (Guillou et al., 2010). Upon recruitment to chromatin, Pds5 binds tightly to Scc1 and in close proximity to the Scc1-Smc3 interface. The disengagement of the Scc1-Smc3 interface is thought to be required for the release of DNA from cohesin (Chan et al., 2012; Buheitel & Stemmann, 2013; Chan et al., 2013; Eichinger et al., 2013). It is possible that Pds5 may regulate cohesin function by controlling the opening and closure of the Scc1-Smc3 interface. In both cases, modulation of ATP hydrolysis by the Smc1 and Smc3 head domains, acetylation of Smc3, and recruitment of Wapl may be required (Shintomi & Hirano, 2009; Chan et al., 2013).

Overall, Pds5 seems to be an important point of convergence for diverse cohesin functions. Previous work (unpublished) in our lab has implicated Pds5 in DNA replication. In the current study, I have used an siRNA approach to analyse the role of Pds5 proteins in DNA replication in mammalian cells. My results show that depletion of

either Pds5A or Pds5B results in DNA damage which activates the intra-S-phase DNA damage checkpoint and slow down DNA replication. Depletion of both Pds5A and Wapl rescues the defect in DNA replication observed when Pds5A is depleted alone. These results led me to conclude that during DNA replication, Pds5, bound to Wapl, is required for the disengagement of the DNA exit gate, the interface between Scc1 and Smc3 (Buheitel & Stemmann, 2013), and normal cohesin conformational change upon Smc3 acetylation, thereby facilitating the passage of the replication fork through the cohesin ring and establishment of sister chromatid cohesion.

4.2 Results

4.2.1 The Intracellular localisation and chromatin association of Pds5 is cell cycle regulated

Pds5 has been shown to regulate the establishment, maintenance, and removal of cohesin from chromatin (Panizza et al., 2000; Chan et al., 2013). In this sense it should associate with DNA during the time when cohesin is bound to chromatin and regulate cohesin function. On chromatin, Pds5 occurs as a complex with either Wapl or Sororin, in close proximity to the Scc1-Smc3 interface (Buheitel & Stemmann, 2013). Scc1, one of Pds5's known binding partners on cohesin, has been shown to undergo proteolytic cleavage and dissociation from chromatin during mitosis (Nishiyama et al., 2010). If Scc1, which recruits Pds5 to chromatin and provides a binding platform for Pds5 on cohesin, undergoes proteolytic cleavage at the end of mitosis, a similar mechanism should mediate Pds5's interaction with chromatin during the cell cycle.

To confirm whether Pds5 has the same intracellular localisation pattern as cohesin during the cell cycle, I fixed asynchronous HeLa cells as described in Materials and Methods and stained them with antibodies raised against Pds5A, Pds5B, Wapl, Smc3, and acetylated Smc3 (Ac-Smc3). These commercial antibodies were previously validated in our lab and were found to be specific. Wapl and Smc3 were stained for because they occur as a complex with Pds5 (Kueng et al., 2006a; Nishiyama et al., 2010), and Ac-Smc3 was stained for because Pds5 recruits Esco1 (Minamino et al., 2015) to chromatin which acetylates Smc3 during S-phase (Minamino et al., 2015). Both Pds5A and Pds5B localised to chromatin during interphase but as cells entered mitosis they dissociated from chromatin at either prophase (Pds5A) or anaphase (Pds5B) and re-associated with chromatin at telophase (Figure 4.1).

Surprisingly, of the two Pds5 orthologs, Pds5A had a shorter chromatin residence time; it dissociated from chromatin at prophase (Figure 4.1A) whereas Pds5B localised to chromatin until metaphase (Figure 4.1B). This disparity in localisation displayed by the

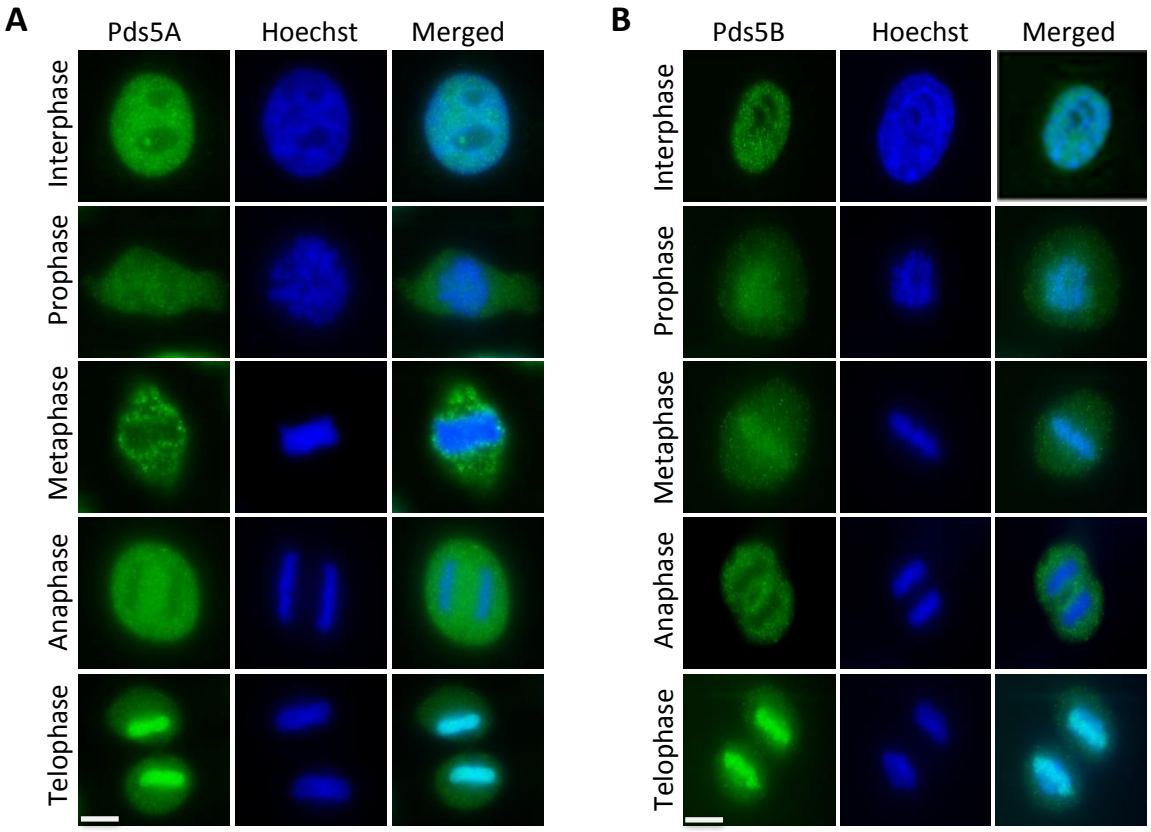

Figure 4.1 Pds5 dissociates from chromatin during mitosis

(**A** and **B**) Immunofluorescence images of asynchronous HeLa cells showing the intracellular localisation of Pds5A and Pds5B, respectively. Cells were fixed in Formaldehyde (3.7 % v/v) and permeabilised with Triton X-100 (0.1 % v/v) before being blocked with BSA (5 % w/v) and stained with either anti-Pds5A or anti-Pds5B antibody (green). DNA was stained with Hoechst 33342 (blue). Merged images are shown in the last panel in A and B. Scale bar: 10 μm. This figure is representative of three independent experiments.

Pds5 paralogs may imply differential cohesin regulation or spatial distribution of the two proteins.

As expected, Wapl dissociated from chromatin at metaphase (Figure 4.2), before re-associating with chromatin at telophase, like Pds5A (Figure 4.1). Smc3 dissociated from chromatin at prophase (Figure 4.3A) while Ac-Smc3 persisted on chromatin until metaphase (Figure 4.3B). This may represent centromeric cohesin which remains bound to chromatin after prophase to enable bi-polar spindle attachment to kinetochores in metaphase (McGuinness et al., 2005).

My data indicates that Pds5 proteins are nuclear during interphase and that their chromatin association decreases as cells progress through mitosis. This is similar to published data that report the temporal association of cohesin with chromatin in interphase and dissociation during mitosis (Nishiyama et al., 2010; Zhang et al., 2011). The distribution of Pds5A and Pds5B also suggests that the two proteins may not be redundant; although not confirmed, it is possible that Pds5A may be more abundant on the chromosome arms while Pds5B may be mostly associated with centromeric cohesin. Indeed, while this study was underway another lab reported the specific requirement of Pds5B for centromeric cohesion (Carretero M et al., 2013). Together, my results show that the intracellular localisation of Pds5 proteins is cell cycle regulated.

To further confirm the association and dissociation of the Pds5 proteins from chromatin I first analysed the endogenous levels of Pds5 proteins during the cell cycle by arresting exponentially growing HeLa cells at specific stages of the cell, G1/S or M-phase (Figure 4.4 A-C). Protein samples were resolved by SDS-PAGE and immuno-blotted with antibodies raised against Pds5A, Pds5B, Wapl, Sororin, Smc1, Smc3, Scc1, Ac-Smc3, and ɣ-Tubulin (Figure 4.4 D-K). There was no change observed in protein levels of Pds5A, Pds5B, and Wapl in interphase and at mitosis (Figure 4.4 D-F). There was also no change in protein levels of the cohesin core subunits, Smc1 and Smc3, in interphase and at mitosis (Figure 4.4 H and I). Sororin protein levels increased in S-phase, and the protein exhibited a mobility shift at mitosis (Figure 4.4 G). This could be due to protein phosphorylation during mitosis as has been reported (Dreier et al., 2011). Consistent with previous reports, Scc1

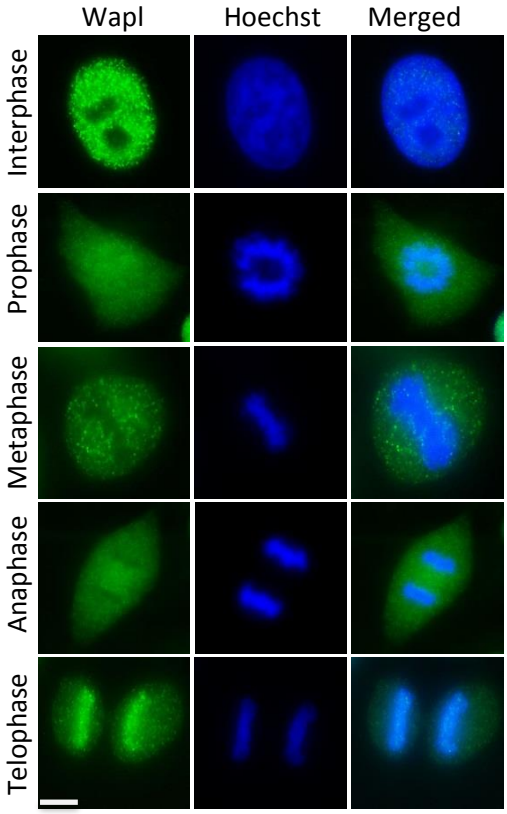

Figure 4.2 Wapl dissociates from chromatin during mitosis

Immunofluorescence images of asynchronous HeLa cells showing the intracellular localisation of Wapl. Cells were fixed in Formaldehyde (3.7 % v/v) and permeabilised with Triton X-100 (0.1 % v/v) before being blocked with BSA (5 % w/v) and stained with a Wapl antibody (green). DNA was stained with Hoechst 33342 (blue). Merged images are shown in the last panel. Scale bar: 10 μm. This figure is representative of three independent experiments.

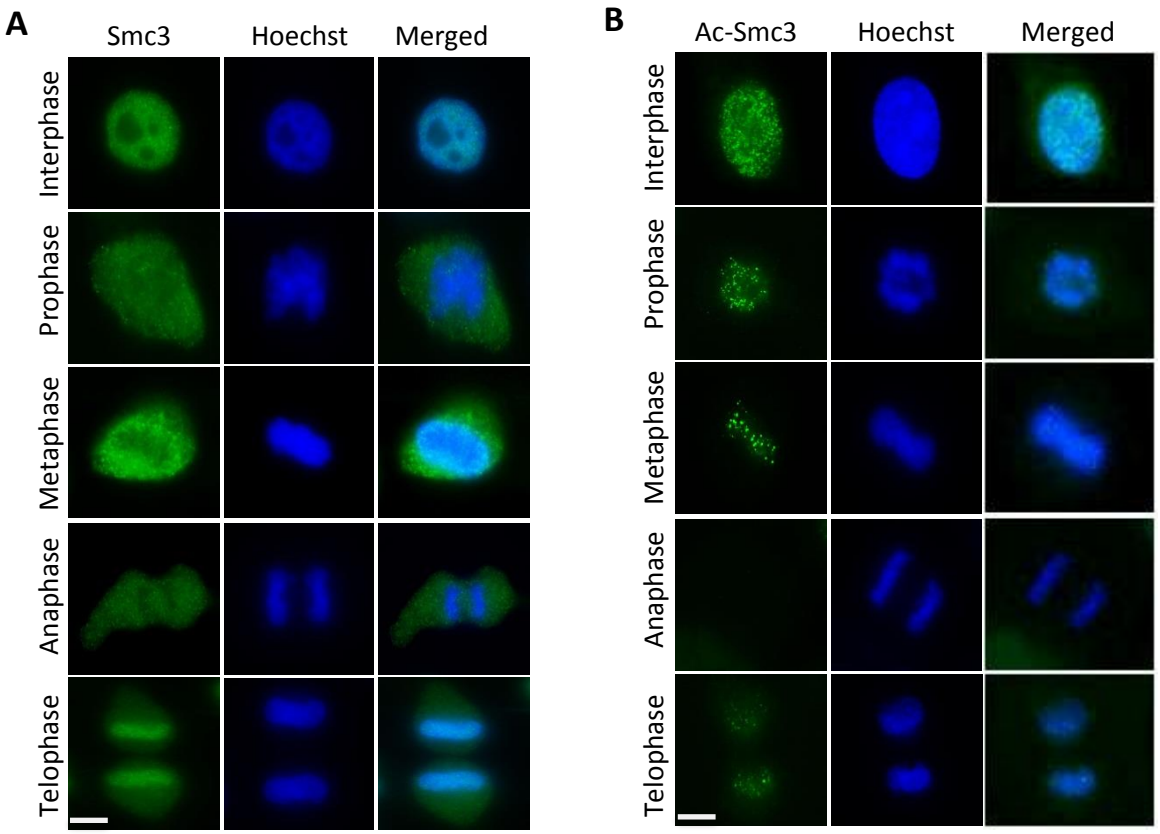

Figure 4.3 Smc3 dissociates from chromatin and gets deacetylated during mitosis

(**A** and **B**) Immunofluorescence images of asynchronous HeLa cells showing the intracellular localisation of Smc3 and acetylated Smc3 (Ac-Smc3), respectively. Cells were fixed in Methanol before being blocked with BSA (5 % w/v) and stained with either anti-Smc3 or anti-Ac-Smc3 antibody (green). DNA was stained with Hoechst 33342 (blue). Merged images are shown in the last panel in A and B. Scale bar: 10 μm. This figure is representative of three independent experiments.

protein levels decreased in mitotically arrested cells (Figure 4.4 J), an indication that the protein is regulated by proteolytic degradation at mitosis (Peters et al., 2008; Onn et al., 2008). As expected, Smc3 was deacetylated during mitosis (Figure 4.4 K), the time when HDAC1/Hos1 recycles cohesin via deacetylation of Smc3 in readiness for the next cell cycle (Zhang & Pati, 2012). This data showed that, like the cohesin core subunits Smc1 and Smc3 (Peters et al., 2008; Onn et al., 2008), Pds5A and Pds5B total protein levels remain unchanged in interphase and at mitosis. To specifically demonstrate this, I arrested asynchronous HeLa cells at the G1/S boundary and monitored their progression at intervals during the cell cycle for 24 h after release from the block (Figure 4.5A). Mitosis occurred at 12 h after release from Aphidicolin block as indicated by the phosphorylation of Histone H3 (p-Histone H3) and exit from mitosis occurred at 15 h as indicated by cyclin B degradation. My immunoblot data revealed uniform levels of Pds5A and Pds5B throughout the cell cycle, like the cohesin core subunits Smc1 and Smc3 (Figure 4.5B). The Scc1 protein levels decreased in mitosis (12 h), an indication of proteolytic cleavage, possibly by caspases (Chen et al., 2002; Uhlmann et al., 1999). (Chen F et al., 2002). These results showed that Pds5 proteins are not degraded during the cell cycle even as cohesin is removed from chromatin, an indication that cohesin function is not regulated by changes in expression levels of the Pds5 proteins.

Next, I optimised the protocol for preparing soluble and chromatin fractions and checked the purity of the two normalised protein fractions by immuno-blotting with anti-α-Tubulin and anti-Histone H3 antibodies (Figure 4.6A). The α-Tubulin immunoblot data indicated that the HeLa soluble proteins had been successfully separated from chromatin associated proteins, while the Histone H3 result indicated that the chromatin-bound proteins had been successfully extracted and were free of contaminating cytoplasmic proteins. Taken together, these results showed that fractionation of soluble and chromatin associated proteins had been successful. I then synchronised and released HeLa cells from the G1/S block and monitored their progression through the cell cycle by FACS (Figure 4.6B). Cell lysates were fractionated and the soluble and chromatin fractions immuno-blotted with antibodies raised against Pds5A, Pds5B, cohesin (Smc1, Smc3, Scc1, and Ac-Smc3), and some of the cohesin associated proteins (Wapl, Sororin, Esco1, and Esco2) (Figure 4.6C).

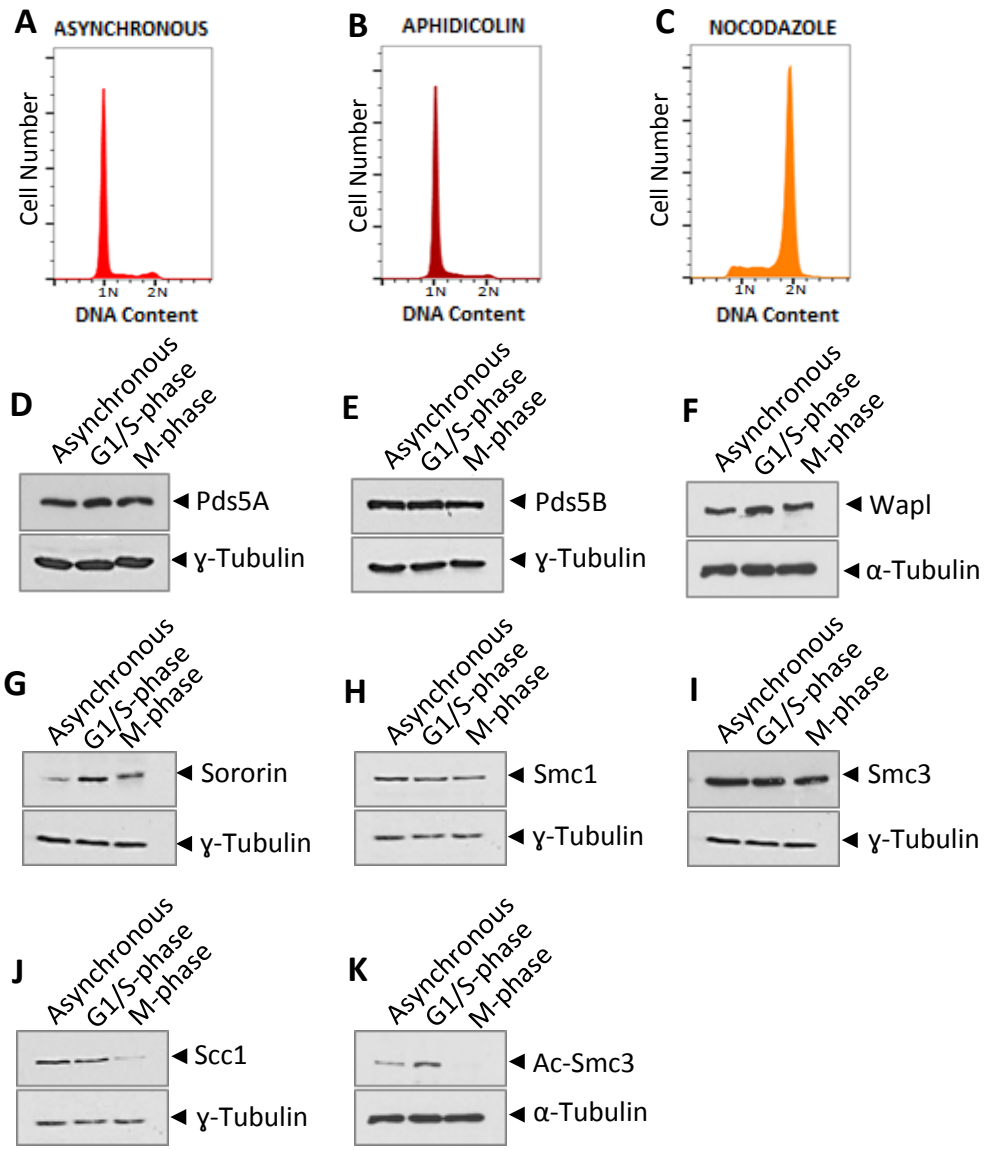

Figure 4.4 Endogenous Pds5 protein levels are identical in interphase and at mitosis

(**A**-**C**) FACS profile of asynchronous, Aphidicolin (5 μg/ml), and Nocodazole (1 μg/ml)-arrested HeLa cells. Cells were fixed in Ethanol (70 % v/v) and stained with Propidium Iodide before FACS with the NucleoCounter® NC-3000™. (**D**-**K**) Western blot of HeLa cell lysates synchronised as described in (**A**-**C**). Cells were lysed in RIPA buffer prior to Western blotting with either anti-Pds5A, anti-Pds5B, anti-Wapl, anti-Sororin, anti-Smc1, anti-Smc3, anti-Scc1, anti-Ac-Smc3, anti-α-Tubulin, or anti-γ-Tubulin antibody. This figure is representative of four independent experiments.

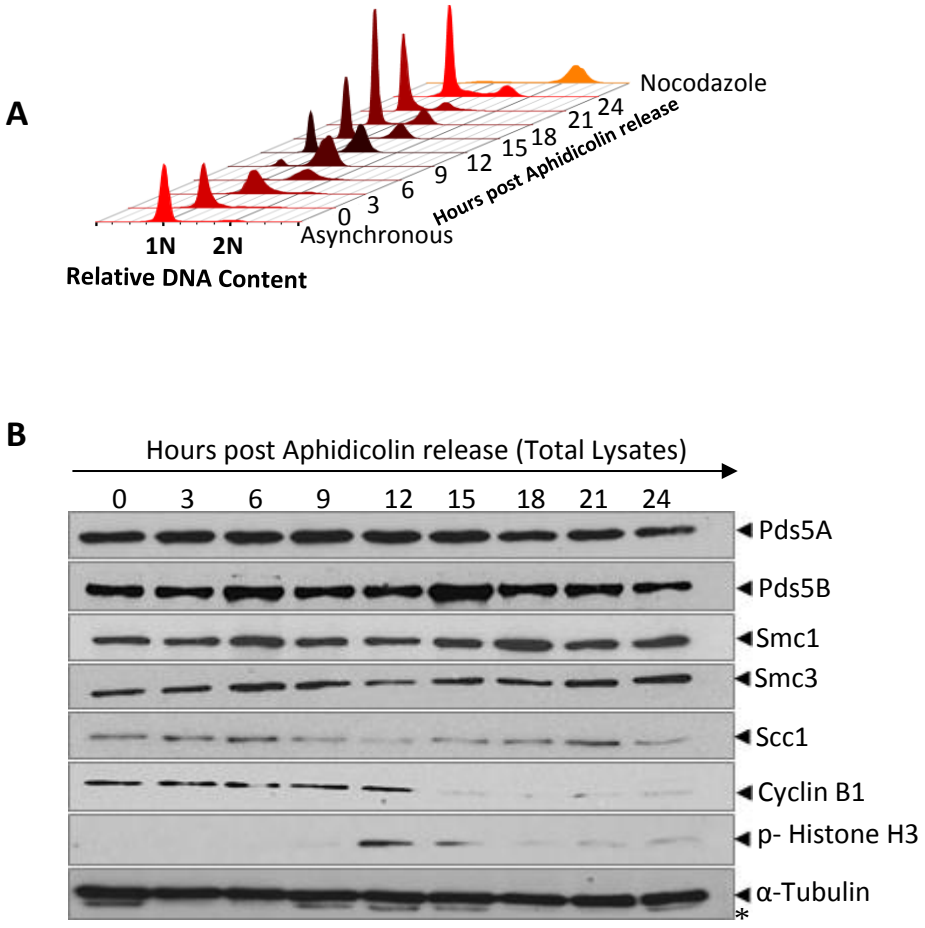

Figure 4.5 Endogenous Pds5 protein levels are constant during the cell cycle

(**A**) FACS profile of HeLa cells following release from a 24 h-Aphidicolin (5 μg/ml) block. Asynchronous and Nocodazole (1 μg/ml)-arrested cells were also profiled. Cells were fixed in Ethanol (70 % v/v) and stained with Propidium Iodide before FACS with the NucleoCounter® NC-3000™. (**B**) Western blot of HeLa cell lysates after release from a 24 h-Aphidicolin (5 μg/ml) block. Cells were lysed in RIPA buffer prior to Western blotting with either anti-Pds5A, anti-Pds5B, anti-Smc1, anti-Smc3, anti-Scc1, anti-Cyclin B1, anti-phospho-Histone H3, or anti-α-Tubulin antibody. *= non-specific binding. This figure is representative of two independent experiments.

Like the cohesin core subunits (Smc1, Smc3, and Scc1), Pds5A and Pds5B protein levels on chromatin decreased as cells entered mitosis (12 h), before reappearing on chromatin as cells exited mitosis (15 h). This pattern was also observed for cohesion establishment factors Sororin and Esco1. However, the Wapl, Esco2, and Ac-Smc3 protein levels, which increased from 0-6 h after release from the block, declined steadily as cells progressed through the cell cycle, with Esco2 exhibiting doublet bands (studied further in Chapter 3) on chromatin at the end of mitosis. The Wapl result is consistent with studies that show that the protein dissociates from chromatin from prophase until telophase (Kueng et al., 2006a).

These results indicate that Pds5, the cohesin core complex, as well as other cohesin regulatory proteins dissociate from chromatin during mitosis. Smc3 acetylation could be one of the many mechanisms by which cells distinguish which cohesin heterodimers associate with chromatin. My Pds5, cohesin core complex (Smc1, Smc3, and Scc1), and cohesin regulatory protein (Wapl, Sororin, Esco1, and Esco2) results are consistent with published data that propose a complete separation of cohesin from chromatin during mitosis (Nasmyth, 2005; Alberts, 2008; Peters et al., 2008; Nishiyama et al., 2010). The Pds5, Wapl, Smc3 and Ac-Smc3 immunoblot results are also consistent with my immunofluorescence data (Figures 4.1, 4.2, and 4.3) that suggest a complete separation of these proteins from chromatin during mitosis. Collectively, my results show that the association and dissociation of Pds5 proteins from chromatin is cell cycle regulated.

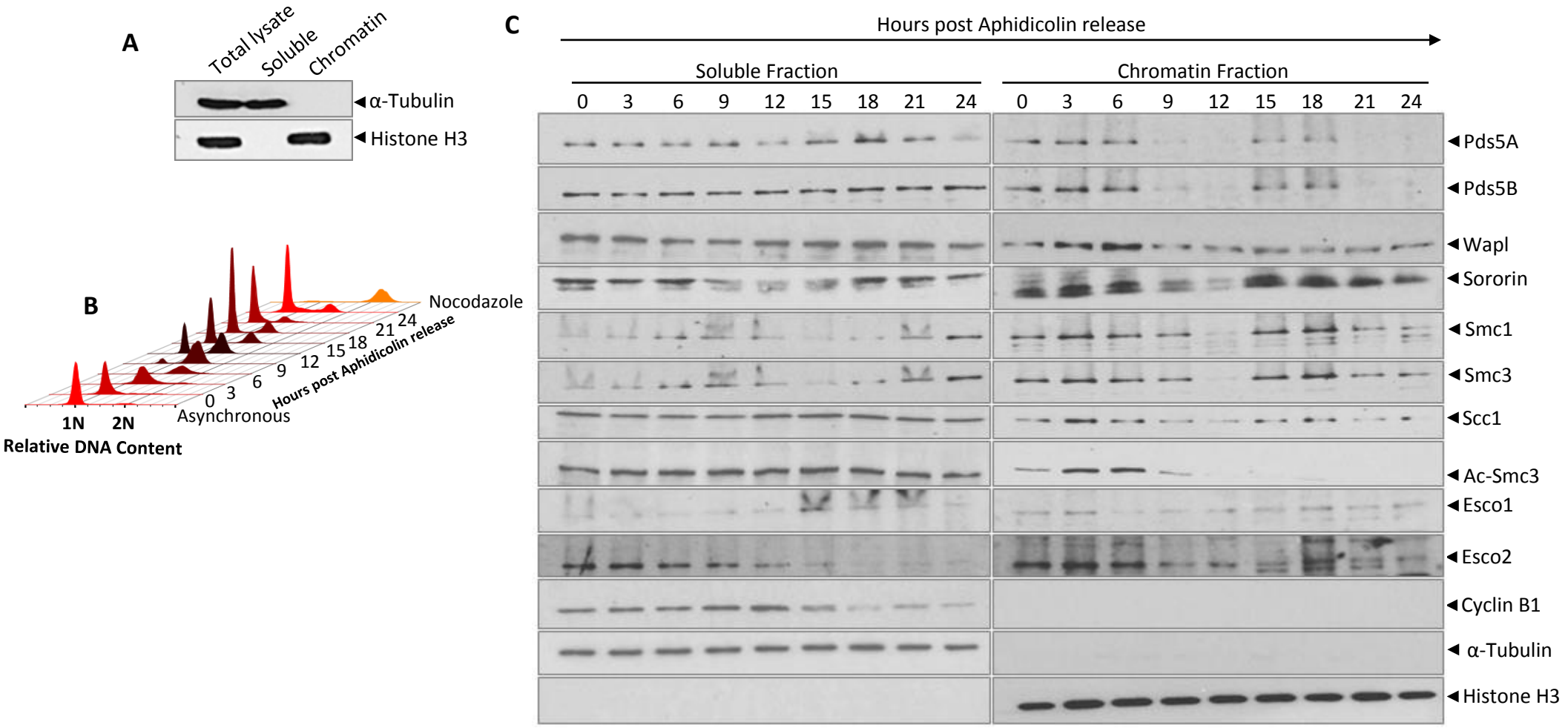
A
Total lysate
Soluble
Chromatin
α-Tubulin
Histone H3
B
Nocodazole
0
3
6
9
12
15
18
21
24
Hours post Aphidicolin release
Asynchronous
1N
2N
Relative DNA Content
C
Hours post Aphidicolin release
Soluble Fraction
Chromatin Fraction
0 3 6 9 12 15 18 21 24
0 3 6 9 12 15 18 21 24
Pds5A
Pds5B
Wapl
Sororin
Smc1
Smc3
Scc1
Ac-Smc3
Esco1
Esco2
Cyclin B1
α-Tubulin
Histone H3

Figure 4.6 Pds5 proteins have low chromatin affinity at mitosis

(**A**) Western blot of HeLa cell lysates following optimisation of fractionation of soluble and chromatin proteins. Asynchronous HeLa cells were lysed in RIPA buffer, Cell Lysis Buffer-B (LBB), or Chromatin Extraction Buffer-C (LBC) to prepare total lysates, soluble, or chromatin fractions, respectively. The purity of the soluble and chromatin fractions was analysed using the α-Tubulin and Histone H3 antibodies. (**B**) FACS profile of HeLa cells following release from a 24 h-Aphidicolin (5 μg/ml) block. Asynchronous and Nocodazole (1 μg/ml)-arrested cells were also profiled. Cells were fixed in Ethanol (70 % v/v) and stained with Propidium Iodide before FACS with the NucleoCounter® NC-3000™. (**C**) Western blot of HeLa cell lysates after release from a 24 h-Aphidicolin (5 μg/ml) block. Cells were lysed in Cell Lysis Buffer-B (LBB) to prepare soluble fractions or resuspended in Chromatin Extraction Buffer-C (LBC) to prepare chromatin fractions. Protein levels in both soluble and chromatin fractions during the time-course were analysed using antibodies raised against cohesin and cohesin associated proteins, as shown. This figure is representative of two independent experiments.

4.2.2 Depletion of Pds5 delays DNA replication

Pds5 is an essential component of the cohesin complex; it is necessary for sister chromatid cohesion establishment, maintenance, and resolution (Panizza et al., 2000). Cohesin has been shown to be necessary for efficient DNA replication during S-phase (Guillou et al., 2010; Sherwood et al., 2010). It is unclear whether important cohesin regulatory proteins such as Pds5A and Pds5B are required for DNA replication. Previous work (unpublished) in our lab showed that siRNA-mediated depletion of either Pds5A or Pds5B in HeLa cells prolonged S-phase.

To test whether Pds5A and Pds5B proteins have a role in DNA replication, I depleted Pds5A and Pds5B individually or both together using a pool of four small interfering RNAs (siRNAs). My immunoblot data showed successful depletion of both Pds5A and Pds5B proteins (Figure 4.7). I then analysed DNA replication in either an asynchronous or synchronised population of HeLa cells depleted of Pds5 proteins by labelling them with the thymidine analog 5'-Bromo-2'-deoxyuridine (BrdU) (Figures 4.8A and B). For both asynchronous (Figure 4.8C) and synchronised HeLa cells (Figure 4.8D) there was a significant reduction in BrdU incorporation in Pds5 depleted cells compared to control siRNA-treated cells. This data suggested that the absence of Pds5 proteins inhibited DNA replication.

To further test the requirement for Pds5 proteins in S-phase, I blocked both the control and Pds5-depleted HeLa cells at the G1/S boundary before labelling them with BrdU and monitoring the progression of the labelled cells in S-phase for 2 h following release from the block (Figure 4.9A and B). My data showed that 90 % of control cells completed S-phase in 1 h, compared to 25 % and 20 % of Pds5A and Pds5B-depleted cells, respectively, that completed S-phase within that interval (Figure 4.9C). These data showed that in the absence of Pds5 proteins, DNA replication is slow. To determine whether the reduction in BrdU incorporation observed after depletion of Pds5 resulted from the inhibition of origin firing or the slow movement of replication forks, I employed DNA single fibre analysis for synchronised population of HeLa cells depleted of Pds5A and Pds5B proteins. I sequentially labelled Pds5-depleted cells with Iododeoxyuridine (IdU) and Chlorodeoxyuridine (CIdU) for 30 min each following release from Aphidicolin

block (Figure 4.10A). I extracted and stretched the DNA before labelling it with antibodies raised against IdU and CIdU. Single fibre analysis revealed four major differences between control and Pds5-depleted cells (Figure 4.10B). Compared to control cells (Figure 4.10B i-iii), Pds5-depleted cells were characterised by short labelled DNA fibres (Figure 4.10B iv and vii) and (Figure 4.10C), indicating slow-moving replication forks. Calculation of the replication fork velocity showed a significant reduction from 0.59 kb/min in the control cells to 0.39 kb/min and 0.36 kb/min in the synchronised population of Pds5A and Pds5B-depleted cells, respectively (Figure 4.10D).

Furthermore, there was a significant increase in the number of stalled replication forks (single labelled) in the Pds5A and Pds5B-depleted cells compared to control cells (Figure 4.10B v and viii) and (Figure 4.10E), suggesting that the absence of Pds5 proteins does not inhibit origin firing but fork progression. Labelled DNA fibres derived from Pds5-depleted cells were also characterised by numerous intermittent gaps (Figure 4.10B vi and ix), indicating an increase in the number of stalled replication forks and firing of other origins.

Additionally, there was a significant reduction in the number of interspaced fibres for labelled DNA derived from the Pds5-depleted cells, compared to control siRNA-treated cells (Figure 4.10F), suggesting slowed DNA replication. Together, these results showed that Pds5 proteins are required for DNA replication; the absence of Pds5 proteins does not inhibit origin of replication firing but efficient fork progression.

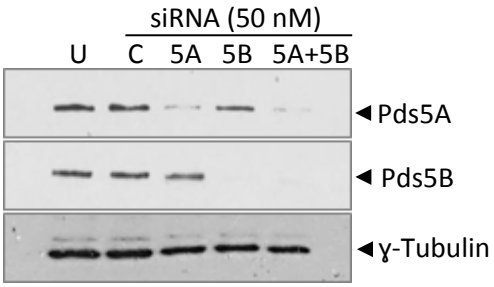

Figure 4.7 siRNA-mediated depletion of Pds5 proteins

Western blot of HeLa cell lysates following a 48 h-transfection with 50 nM of either control, Pds5A, Pds5B, or a mixture of both Pds5A and Pds5B siRNAs. Cells were lysed in RIPA buffer and a Western blot performed using either anti-Pds5A, anti-Pds5B, or anti-γ-Tubulin antibody. U = Untreated, C = control, 5A = Pds5A, and 5B = Pds5B. This figure is representative of three independent experiments.

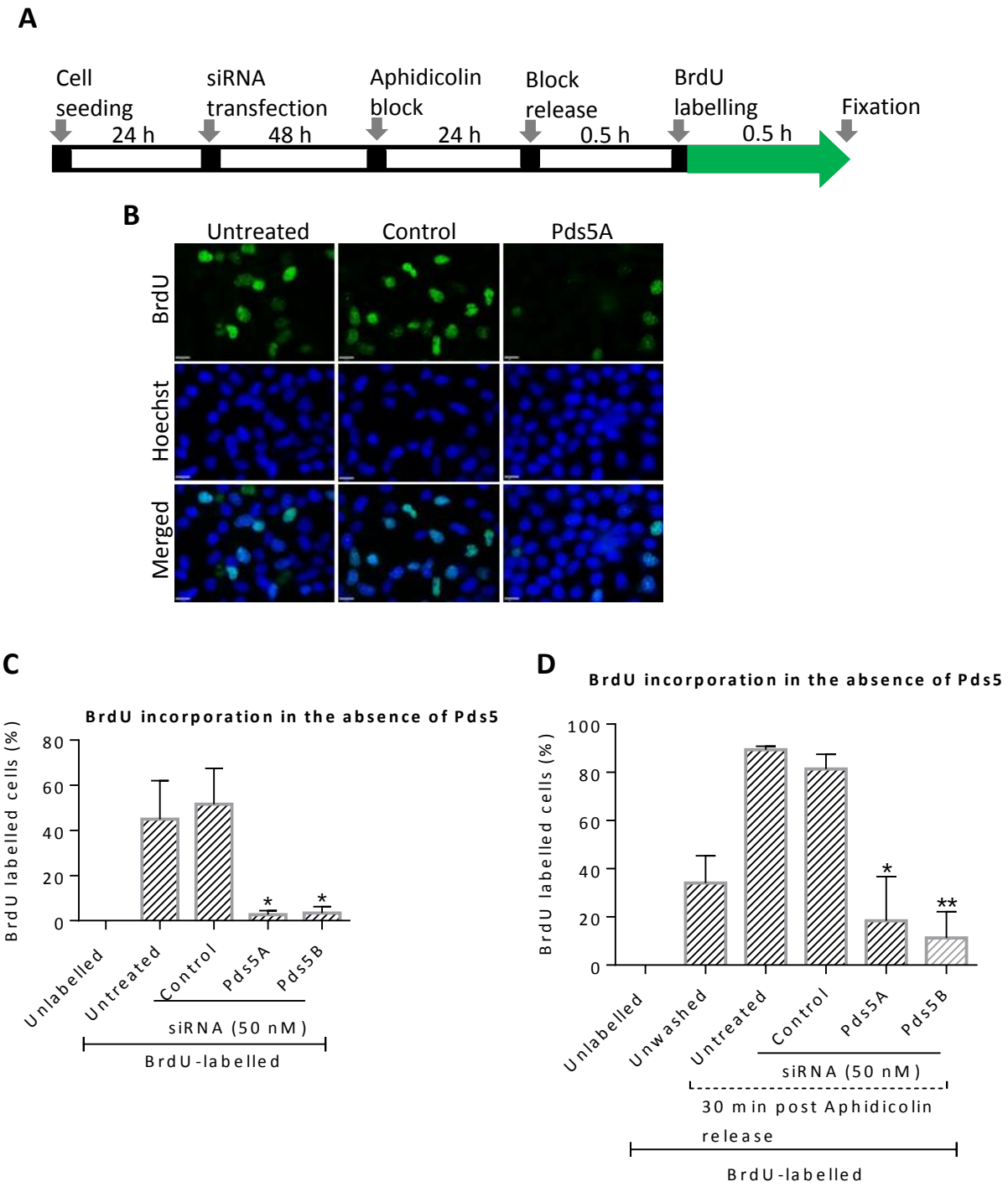

Figure 4.8 Depletion of Pds5 proteins affects DNA replication

(**A**) Schematic representation of BrdU (1 µM) incorporation assay in a synchronised population of HeLa cells depleted of Pds5 proteins. (**B**) Immunofluorescence images of BrdU (1 µM)-labelled HeLa cells following a 48 h treatment with 50 nM of either control or Pds5A siRNAs. Similar results as shown in the last panel were obtained with Pds5B siRNA treatment. Cells were fixed in Methanol and stained with anti-BrdU antibody (green). DNA was stained with Hoechst 33342 (blue). Scale bar: 10 µm. (**C** and **D**) Histograms showing quantitation of data in (**B**). The mean+s.e.m of at least 100 cells counted in randomly selected fields is shown. *P < 0.05, **P < 0.01 compared to control siRNA-treated cells; P values were calculated using a two-tailed Student t-test. This figure is representative of three independent experiments.

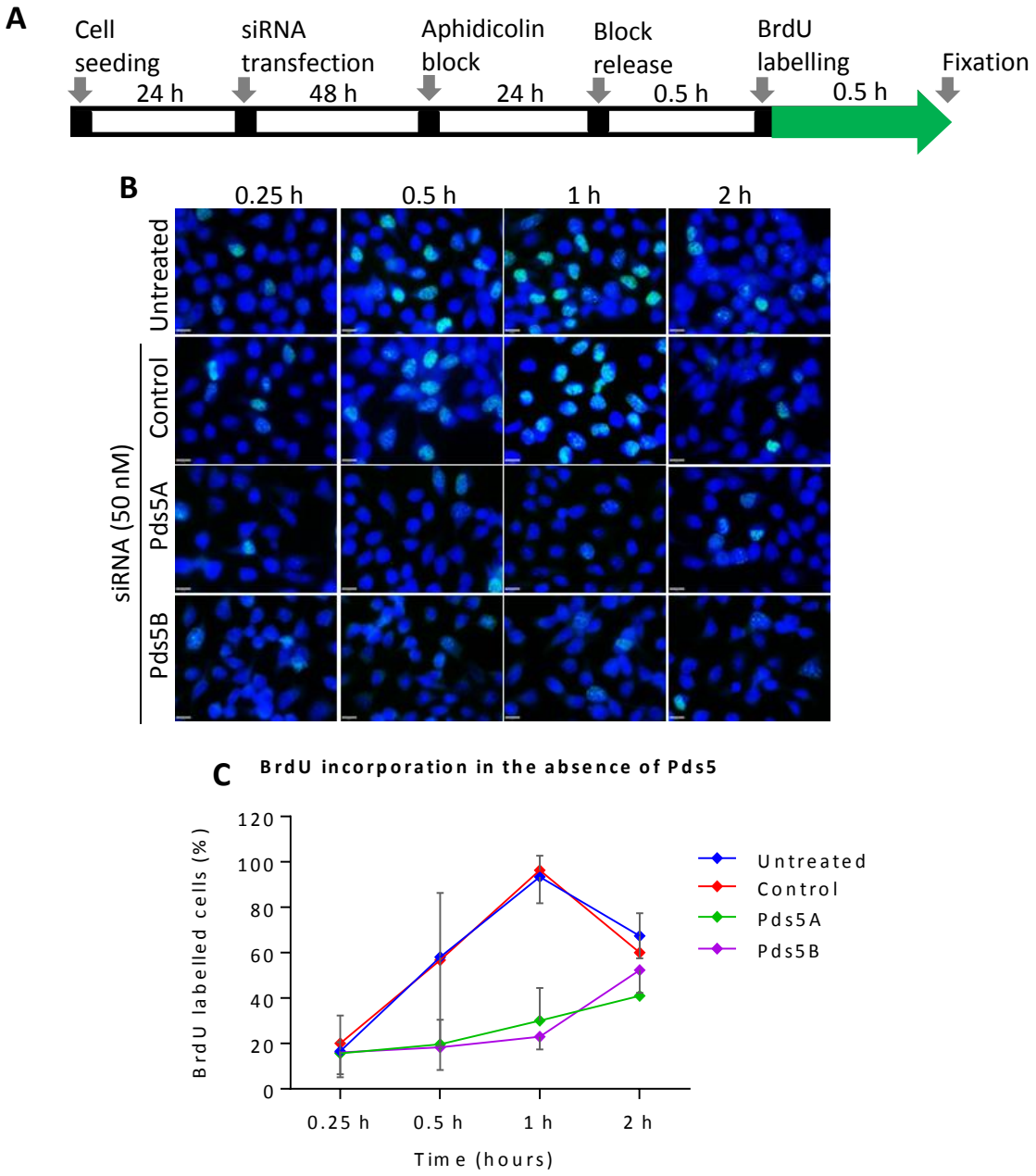

Figure 4.9 Depletion of Pds5 proteins delays DNA replication

(**A**) Schematic representation of BrdU (1 μM) incorporation assay in a synchronised population of HeLa cells depleted of Pds5 proteins. (**B**) Merged immunofluorescence images of BrdU (1 μM)-labelled, Pds5-depleted HeLa cells at the indicated times after release from Aphidicolin (5 μg/ml) block. Cells were fixed in Methanol and stained with anti-BrdU antibody (green). DNA was stained with Hoechst 33342 (blue). Scale bar: 10 μm. (**C**) Graph showing quantitation of data in (**B**). At least 100 cells were counted in randomly selected fields. Each point represents the mean ± s.e.m of three independent experiments.

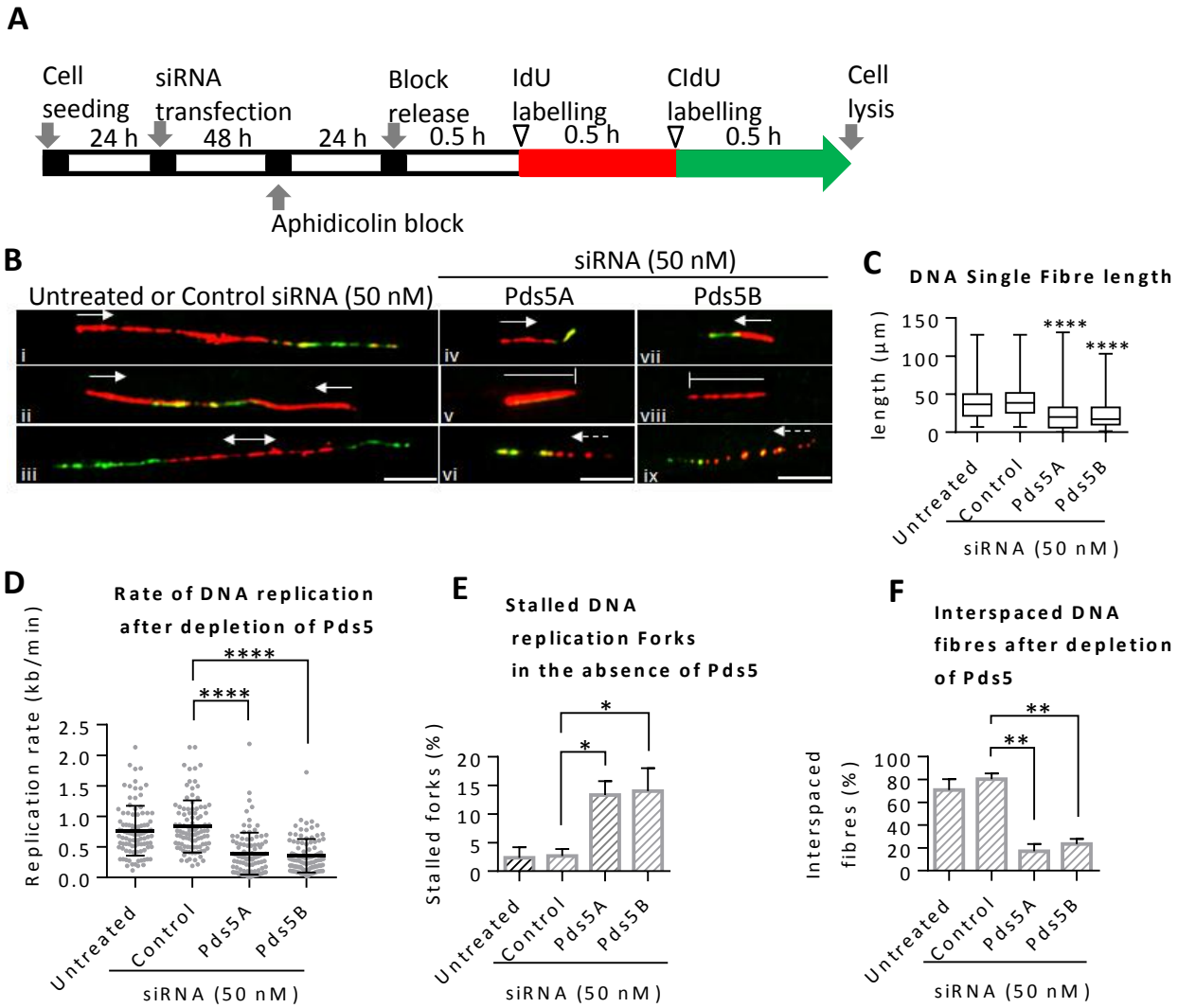

Figure 4.10 Cells depleted of Pds5 proteins are characterised by defective DNA strands and reduced rate of replication

(**A**) Schematic representation of DNA single fibre assay in a synchronised population of Pds5-depleted HeLa cells. (**B**) Immunofluorescence images of DNA replication forks (red = IdU, 25 µM and green = CIdU, 250 µM) observed in HeLa cells following a 48 h-treatment with 50 nM of either control, Pds5A, or Pds5B siRNAs and release from Aphidicolin (5 µg/ml) block, showing (i) elongating fork, (ii) fork termination, and (iii) interspaced fibre. Cells were lysed in DNA Fibre Lysis Buffer, fixed in Carnoy's solution (3:1 v/v Methanol: Acetic acid), and hydrolysed in HCl (2.5 M) before being blocked with BSA (5 % w/v) and stained with either Fitc-conjugated-anti-BrdU (green) or anti-BrdU antibody (red). White arrows indicate direction of fork movement. Scale bar: 20 µm. (**C**) Box plot showing a reduction in DNA fibre lengths in Pds5-depleted cells. (**D**) Dot plot showing a reduction in replication fork velocities in Pds5-depleted cells. (**E**) Histogram showing an increase in the number of stalled replication forks in Pds5-depleted cells. (**F**) Histogram showing a reduction in the number of interspaced DNA fibres in Pds5-depleted cells. For the data set C-F, the mean ± s.e.m of at least 100 DNA fibre tracts counted in randomly selected fields is shown. *P < 0.05, **P < 0.01, ****P < 0.0001 compared to control siRNA-treated cells. P values were calculated using a two-tailed Student t-test. This figure is representative of three independent experiments.

4.2.3 Depletion of Wapl rescues the delay in DNA replication observed after depletion of Pds5A.

Pds5 proteins form a complex with Wapl which destabilises the binding of cohesin to chromatin before DNA replication (Gandhi et al., 2006; Kueng et al., 2006a). The Pds5-Wapl complex also actively removes cohesin from the chromosome arms during prophase (Gandhi et al., 2006; Kueng et al., 2006a). However, recent studies in yeast have shown that the Pds5-Wapl complex facilitates cohesin loading, and that individually, the two proteins have opposing effects on cohesin-chromatin interaction (Murayama & Uhlmann, 2015). Pds5 competes with the Scc2-Scc4 complex for cohesin binding and inhibits the loading of cohesin onto chromatin, although it does not form a stable complex with cohesin (Murayama & Uhlmann, 2015). Wapl compensates for Pds5's inhibitory cohesin loading effect and restores cohesin loading (Murayama & Uhlmann, 2015). Recently, it has been found that Wapl inactivation speeds up DNA replication in both yeast and human cells (Lopez-Serra et al., 2013; Manning et al., 2014).

How Wapl's absence from chromatin supports DNA replication remains unclear, given that it facilitates cohesin loading onto chromatin (Murayama & Uhlmann, 2015). One possibility is that inactivation of Wapl allows stable binding of cohesin to chromatin by negating its cohesin removal activity in complex with Pds5 before S-phase (Nishiyama et al., 2010). Whether inactivating both Pds5 and Wapl reverses the effects of depleting Pds5 alone is unknown. To test this, I initially depleted Wapl and Pds5A separately and both together from HeLa cells using a pool of four siRNAs. After a 24 h-block with Aphidicolin, I released the cells from the block and monitored their progression through S-phase for 8 h before lysing them to prepare soluble and chromatin fractions for Western blotting (Figure 4.11).

Analysis of factors bound to chromatin revealed that cells depleted of Pds5A alone recruited more Esco1 to chromatin, compared to cells depleted of either Wapl or both Wapl and Pds5A (previous studies in the lab, unpublished data). There was also more Esco2 recruitment to chromatin in cells depleted of both Pds5A and Wapl than in cells depleted of Wapl alone. Cells depleted of Wapl and both Pds5A and Wapl recruited less

cohesin (Scc1 and Smc3) to chromatin compared to control cells. However, cells depleted of Wapl alone had more Scc1 at 8 h compared to cells where both Pds5A and Wapl were depleted, indicating that cohesin still stably associated with chromatin in mitosis. Furthermore, cells depleted of Pds5A or Wapl alone displayed persistent Smc3 acetylation from 0 to 8 h, and Ac-Smc3 showed transient association with chromatin when Wapl was depleted together with Pds5A. More Sororin was recruited to chromatin when Wapl and Pds5A were depleted together. The fact that less Scc1 and Smc3 were recruited to chromatin but persisted for a longer period in Wapl-depleted cells compared to control siRNA-treated cells shows that Wapl depletion allows cohesin stabilisation on chromatin, possibly due to failure to disengage the DNA exit gate by cells lacking Wapl.

I then analysed DNA replication by BrdU incorporation assay after depletion of Pds5 and Wapl. Following depletion of Wapl from asynchronous population of HeLa cells, I resolved the protein samples by SDS-PAGE before immuno-blotting with antibodies raised against Wapl and α-Tubulin. My immunoblot (Figure 4.12A) data showed successful depletion of Wapl. I analysed DNA replication by BrdU labelling (Figure 4.12B) of either asynchronous or synchronised population of HeLa cells depleted of Wapl. There was no significant difference in BrdU incorporation for both asynchronous (Figure 4.12C) and synchronised (Figure 4.12D) population of HeLa cells depleted of Wapl, compared to control siRNA-treated cells, suggesting that Wapl depletion has no effect on DNA replication. I next depleted Pds5A and Wapl individually and both together from an asynchronous population of HeLa cells before labelling them with BrdU. My immunoblot (Figure 4.13A) results showed successful depletion of both Pds5A and Wapl proteins. Analysis of BrdU incorporation (Figure 4.13B) following depletion of Pds5A and Wapl showed an increase in the number of cells taking up BrdU when both Pds5A and Wapl are depleted together, compared to when Pds5A is depleted alone (Figure 4.13C). While there was a significant difference in BrdU incorporation between control siRNA and Pds5A-depleted cells, no significant difference in BrdU incorporation between control siRNA-treated cells and cells depleted of both Pds5A and Wapl was observed. This result showed that the delay in DNA replication observed after depleting Pds5A alone was rescued by the depletion of both Wapl and Pds5A together.

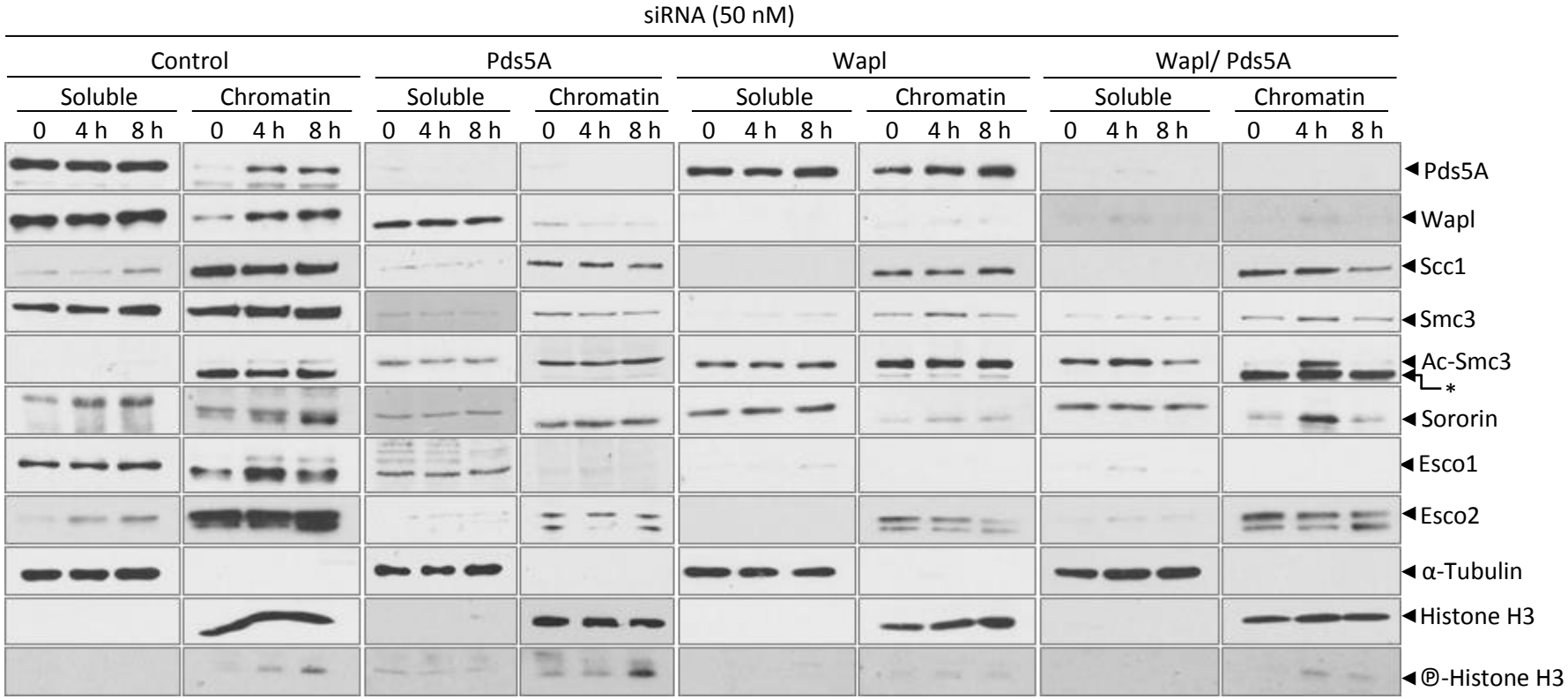

Figure 4.11 Depletion of both Pds5A and Wapl promotes Smc3 deacetylation

Western blot of HeLa cell lysates after release from a 24 h-Aphidicolin (5 μg/ml) block. Cells were lysed in Cell Lysis Buffer-B (LBB) to prepare soluble fractions or resuspended in Chromatin Extraction Buffer-C (LBC) to prepare chromatin fractions. Protein levels in both soluble and chromatin fractions during the time-course were analysed using antibodies raised against cohesin and cohesin associated proteins, as shown. *= non-specific binding. This figure is representative of one experiment.

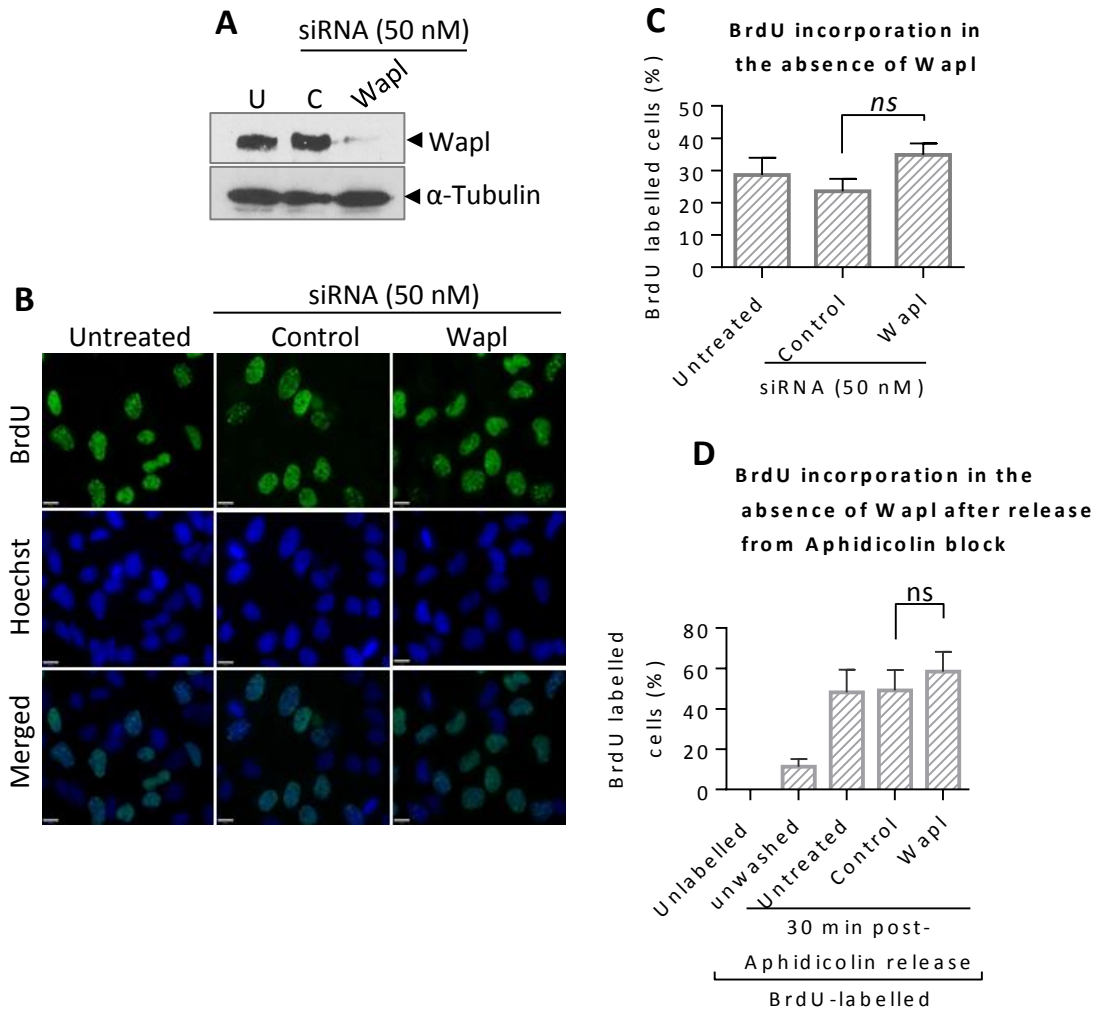

Figure 4.12 Depletion of Wapl does not inhibit DNA replication

(**A**) Western blot of HeLa cell lysates following a 48 h-transfection with 50 nM of either control or Wapl siRNAs. Cells were lysed in RIPA buffer and Western blot was carried out using either anti-Wapl or anti-α-Tubulin antibody. (**B**) Immunofluorescence images of BrdU (1 μM)-labelled HeLa cells following a 48 h-treatment with 50 nM of either control or Wapl siRNAs. Cells were fixed in Methanol and stained with anti-BrdU antibody (green). DNA was stained with Hoechst 33342 (blue). Scale bar: 10 μm. (**C** and **D**) Histograms showing quantitation of data in (**B**). The mean+s.e.m of at least 100 cells counted in randomly selected fields is shown. $^{ns}P > 0.05$; P values were calculated using a two-tailed Student t-test. U = Untreated, and C = control. This figure is representative of three independent experiments.

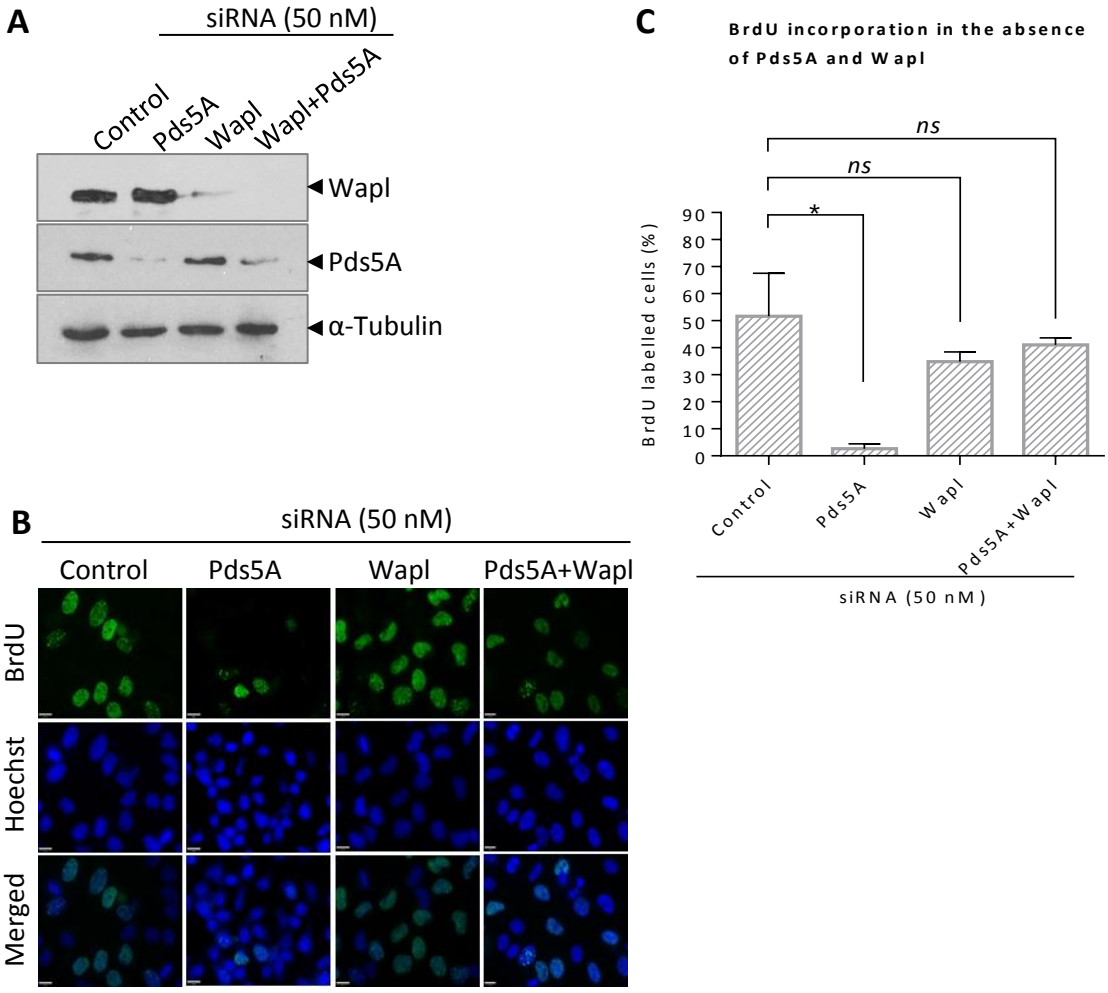

Figure 4.13 Depletion of Wapl rescues the DNA replication inhibition observed after depletion of Pds5A

(**A**) Western blot of HeLa cell lysates following a 48 h-transfection with 50 nM of either control, Pds5A, Wapl, or both Pds5A and Wapl siRNAs. Cells were lysed in RIPA buffer and Western blot was carried out using either anti-Wapl, anti-Pds5A, or anti-α-Tubulin antibody. (**B**) Immunofluorescence images of BrdU (1 μM)-labelled HeLa cells following a 48 h-treatment with 50 nM of either control, Pds5A, Wapl, or both Pds5A and Wapl siRNAs. Cells were fixed in Methanol and stained with anti-BrdU antibody (green). DNA was stained with Hoechst 33342 (blue). Scale bar: 10 μm. (**C**) Histogram showing quantitation of data in (**B**). The mean+s.e.m of at least 100 cells counted in randomly selected fields is shown. *P < 0.05, ^{ns}P > 0.05 compared to control siRNA-treated cells; P values were calculated using a two-tailed Student t-test. This figure is representative of three independent experiments.

4.2.4 Depletion of Pds5 induces the DNA damage response and is characterised by DNA single strand breaks

Pds5 proteins are crucial in cohesin regulation; they have both establishment (when bound to Sororin) and anti-establishment (when bound to Wapl) roles in sister chromatid cohesion. Cohesin loading is required for the integrity of the DNA damage checkpoints (Lightfoot et al., 2011). However, it is unclear whether sister chromatid cohesion is essential for replication fork stability. Given the significance of Pds5's role in the establishment of sister chromatid cohesion during S-phase, it is plausible to think that the delay in DNA replication observed earlier (Figures 4.8, 4.9, and 4.10) resulted from altered cohesin structures and unstable replication forks that might have possibly activated the intra-S-phase DNA damage checkpoint response. Unstable replication forks are a prime source of DNA damage in both prokaryotes and eukaryotes (Heller & Marians, 2006).

In the presence of stalled replication forks or DNA damage, eukaryotic cells maintain the stability of the genome by activation of the intra S-phase checkpoint that suppresses the firing of origins and stabilises stalled forks (Errico & Costanzo, 2012). Key components of this checkpoint include the DNA damage-sensing kinase ATR and its downstream effector kinase Chk1 (Gonzalez Besteiro & Gottifredi, 2015). To check for the presence of DNA damage after depletion of Pds5 proteins, I prepared total protein lysates for Western blotting with a phospho-specific antibody that recognizes Chk1, a kinase activated by ATR in response to DNA damage (Smith et al., 2010; Gonzalez & Gottifredi, 2015). My immunoblot data showed that Chk1 was phosphorylated in Pds5-depleted cells (Figure 4.14A). This indicates that the absence of Pds5 proteins may cause DNA replication stress or other types of DNA damage, possibly due to defective DNA replication, which then activates the DNA damage checkpoint response.

To determine the kind of DNA damage that results from the loss of Pds5 proteins, I subjected asynchronous HeLa cells depleted of Pds5A and Pds5B proteins to Single Cell Gel Electrophoresis (Comet Assay) under alkaline conditions as described in Materials and Methods. My results showed that cells depleted of Pds5A and Pds5B proteins had

longer migration smears (comet tails) compared to control siRNA-treated cells (Figure 4.14B), indicating that loss of Pds5 proteins generated a faster migrating form of DNA.

Further analysis revealed a significant amount of DNA content in comet tails of Pds5A and Pds5B-depleted cells compared to control siRNA-treated cells (Figure 4.14C; see also Figure A4, page 209), implying accumulation of faster migrating form of DNA in the comet tails of Pds5-depleted cells. This data showed that depletion of Pds5A and Pds5B proteins results in DNA damage (single strand breaks). An ongoing study in our lab (unpublished) has also shown that Histone H2AX is phosphorylated upon depletion of Pds5 proteins, indicating that loss of Pds5 proteins also induces DNA double strand breaks. Taken together, my results suggest that depletion of Pds5 proteins generated DNA strand breaks which then activated the intra S-phase DNA damage checkpoint that slowed DNA replication. This result is novel; it is the first time I am demonstrating the requirement for Pds5 proteins for the maintenance of chromatin integrity and consequently DNA replication progression.

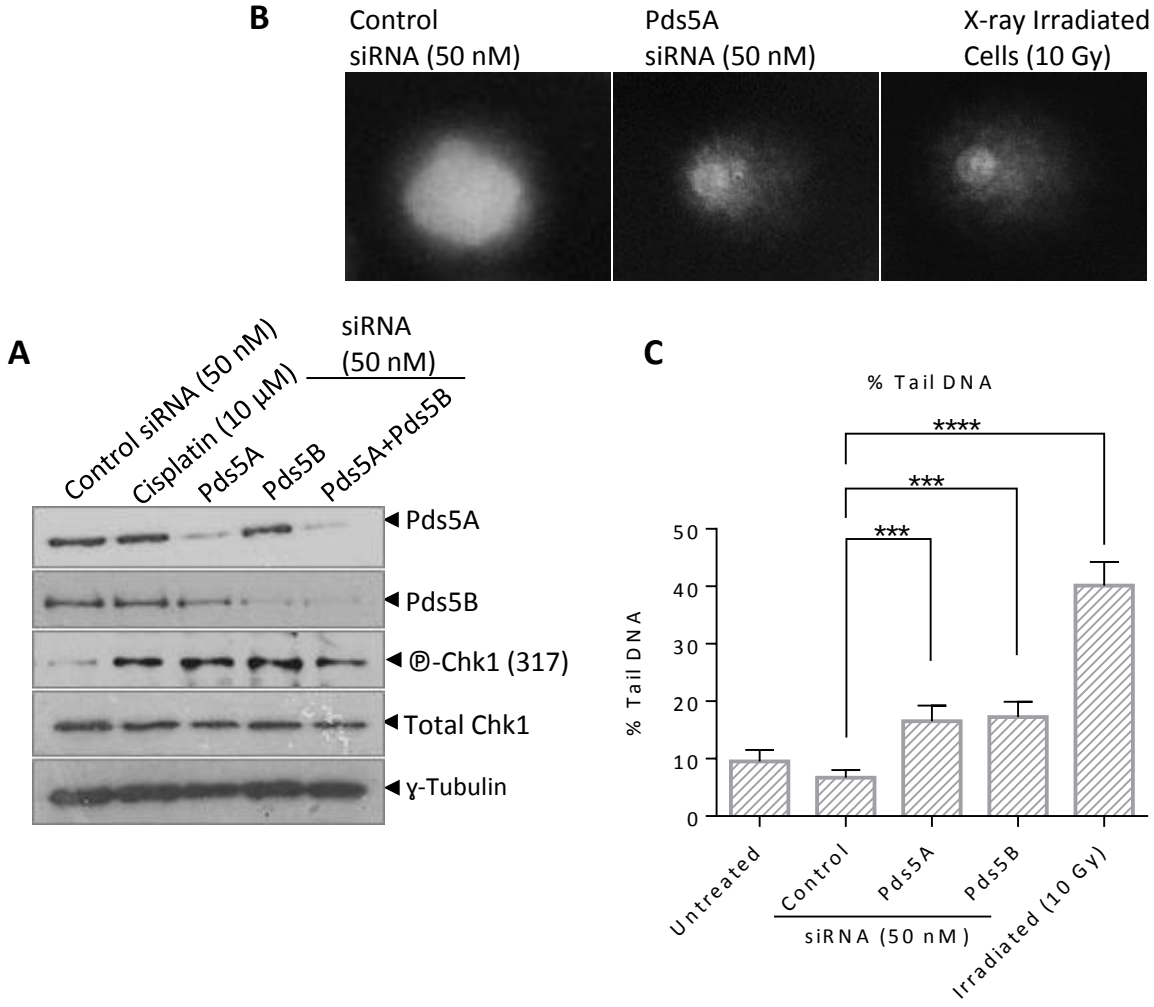

Figure 4.14 Depletion of Pds5 proteins induces DNA damage

(**A**) Western blot of HeLa cell lysates following a 48 h-transfection with 50 nM of either control, Pds5A, or Pds5B siRNAs. Cells were lysed in RIPA buffer and Western blot was carried out using either anti-Pds5A, anti-Pds5B, anti-P-Chk1, anti-Chk1, or anti-α-Tubulin antibody. (**B**) Comet images of Propidium Iodide (1 mg/ml)-labelled HeLa cells following a 48 h-treatment with 50 nM of either control or Pds5A siRNAs. Similar results were obtained with cells depleted of the Pds5B protein. Cells were mixed with low melting point agarose prior to electrophoresis in ice-cold alkali buffer at 30V, 300mA for 20 min. Control cells were also X-Ray irradiated (10 Gy). Scale bar: 10 μm. (**C**) Histogram showing quantitation of data in (**B**). The mean+s.e.m of at least 100 cells scored in randomly selected fields is shown. **P < 0.01, ***P < 0.001 ****P < 0.0001. P values were calculated using a two-tailed Student t-test. This figure is representative of one experiment.

4.2.5 Discussion

Pds5 is a highly conserved cohesin subunit whose role in the regulation of sister chromatid cohesion is still poorly understood. Studies so far have shown that it is involved in regulating a number of cohesin functions ranging from sister chromatid cohesion establishment to maintenance and resolution (Panizza et al., 2000). Cohesin dysregulation has not only been shown to cause congenital birth defects (Shen, 2011; Pfau & Amon, 2012), but also cancerous phenotypes (Thol F et al., 2014; Thota S et al., 2014). Previous work (unpublished) in our lab showed that depletion of Pds5 proteins in HeLa cells prolonged S-phase. In this study I sought to investigate the role of Pds5 proteins in DNA replication. The role of Pds5 proteins in DNA replication has not been clearly investigated before. I report the requirement for Pds5 proteins in DNA replication in mammalian cells.

4.2.5.1 Dynamics of cohesin regulatory proteins during the cell cycle.

The cohesin core subunits are loaded onto chromatin in telophase in mammalian cells (see Figures 1.6, page 19, and 5.1, page 157). However, the cohesin regulatory proteins are loaded onto chromatin at different stages of the cell cycle and their maintenance and removal follow a pattern that ensures fidelity of the sister chromatid cohesion (Zhang & Pati, 2012). Consistent with this notion, my data shows that in mammalian cells Pds5 proteins are loaded onto chromatin during telophase; they localise to chromatin during interphase and dissociate from chromatin as cells enter mitosis (Figure 4.1).

Although both Pds5 orthologs localise to chromatin during interphase, Pds5A (Figure 4.1A) has a shorter chromatin residence time compared to Pds5B (Figure 4.1B). The disparity in Pds5A and Pds5B dissociation from chromatin suggests differential cohesin regulation or spatial distribution of the two proteins. While both proteins contribute to chromosomal arm cohesion, Pds5B has been reported to be specifically required for centromeric cohesion (Carretero M et al., 2013). Wapl is known to form a complex with Pds5 proteins that destabilises the binding of cohesin to chromatin before DNA replication (Ouyang et al., 2013). Like Pds5 proteins, Wapl is loaded onto chromatin during telophase and remains associated with chromatin during interphase before it

dissociates from chromatin in mitosis (Figure 4.2). Even though both Pds5 proteins can interact with Wapl, it is Pds5A that has been shown to form a sub-complex with Wapl (Kueng et al., 2006b). My data suggests that Pds5A and Pds5B proteins do not have redundant functions in chromosome biology; Pds5A may be more involved with arm-cohesin regulation during the prophase pathway in complex with Wapl, while Pds5B may be associated with centromeric cohesin complexes and mediate important chromosome dynamics such as bipolar spindle attachment. Consistent with this notion, Pds5B's localisation (Figure 4.1B) is similar to that of Sgo1 in that it is still associated with chromatin at metaphase (Chapter 3, Figure 3.4). Sgo1's role in centromeric cohesin regulation is already established (McGuinness et al., 2005). Whether Pds5B's centromeric cohesin affinity relies on Sgo1 function requires further investigation.

The intracellular localisation of Pds5 and Wapl proteins is similar to that of cohesin (Smc3) (Figure 4.3A). Deacetylation of Smc3 is thought to take place upon entry into mitosis, following the removal of cohesin from the chromosome arms (Nishiyama et al., 2010; Zhang et al., 2011). As cohesin (Smc3) is removed from chromatin in mitosis (Figure 4.3A), deacetylase, HDAC8, recycles them via deacetylation, and they can be reloaded onto chromatin in the next cycle (Beckouët et al., 2010). This may account for the disappearance of Ac-Smc3 at anaphase (Figure 4.3B).

The chromatin-associated Ac-Smc3 observed from prophase to metaphase (Figure 4.3B) may represent the centromeric cohesin which is protected from the prophase pathway by Sgo1, which recruits PP2A to the centromere and keep cohesin in a hypophosphorylated form to achieve bi-polar spindle attachment to the kinetochores and prevent precocious dissociation of sister chromatids (McGuinness et al., 2005). The fact that Pds5B has been found to be specifically required for centromeric cohesion (Carretero M et al., 2013) and persists on chromatin until metaphase (Figure 4.1B), a localisation similar to that of Sgo1 (Chapter 3, Figure 3.4) suggests that Ac-Smc3 observed from prophase to metaphase (Figure 4.3B) represents centromeric cohesin.

Dissociation of cohesin from chromatin is a two-stage process that starts in prophase via the non-proteolytic action of Wapl complexed with Pds5 and ends with the cleavage of centromeric cohesin (Scc1) by the APC/Cyclosome-activated Separase during the

metaphase-to-anaphase transition in mitosis (Onn et al., 2008). My data shows that the endogenous levels of Pds5 proteins, like Wapl, Smc1, and Smc3, do not change in interphase and at mitosis (Figure 4.4D and E). The Sororin result (Figure 4.4G) indicates that the Sororin protein level is higher in G1/S-arrested cells than in asynchronous or M-phase-arrested cells. It has been speculated that cohesin pre-occupancy on chromatin is required but not sufficient for Sororin to associate with chromatin, but that the phosphorylation of the protein is necessary for its dissociation from Pds5 (Zhang et al., 2011). The higher protein levels observed in G1/S-arrested cells shows that Sororin is mostly expressed at S-phase, the time when it is recruited to chromatin-bound cohesin to establish sister chromatid cohesion (Zhang & Pati, 2012). The mobility shift observed in the mitotic total lysates may be a result of changes in the phosphorylation status of Sororin. The phosphorylated form of Sororin is reported to be ubiquitinated and targeted for degradation by the APC^{cdh1} (Zhang et al., 2011) while non-phosphorylated Sororin is bound to chromatin (Figure 4.6).

Since Nocodazole prevents anaphase (Figure 4.4C), the reduction in Scc1 protein levels observed in lysates derived from M-phase-arrested cells (Figure 4.4J) cannot be attributed to the function of Separase, neither can it be due to Wapl because the Wapl-orchestrated prophase pathway is non-proteolytic (Losada et al., 1998; Sumara et al., 2002; Waizenegger et al., 2000). Interestingly, Scc1 has been found to be preferentially cleaved at Asp279 by caspases-3 and -7 *in vitro* in cells undergoing apoptosis in response to diverse stimuli (Chen F et al., 2002). It is plausible to think that caspase proteolysis of the chromosome-dissociated cohesin subunit was responsible for the reduction in Scc1 protein level in M-phase-arrested cells.

Ac-Smc3 protein levels were higher in G1/S-arrested cells (Figure 4.4K). Accumulation of Ac-Smc3 in G1/S-arrested cells coincides with the time when Esco1 is recruited to chromatin by Pds5 (Minamino et al., 2015 where it physically interacts with PCNA (Moldovan et al., 2006) and the time when Esco2 endogenous protein levels are higher (Chapter 3, Figure 3.6E). This shows that Smc3 is mostly acetylated during S-phase, the time when concomitant DNA replication-coupled cohesin acetylation and Sororin recruitment to chromatin have been shown to establish cohesion (Skibbens et al., 1999; Toth et al., 1999; Ivanov et al., 2002; Unal et al., 2007). Consistent with my

immunofluorescence data (Figure 4.3B), Ac-Smc3 was undetectable in lysates derived from M-phase-arrested cells (Figure 4.4K), an indication of HDAC8 activity in mitosis as cohesins are removed from chromatin and recycled via deacetylation (Beckouët et al., 2010).

Further analysis of endogenous protein levels using lysates from synchronised HeLa cells (Figure 4.5A) shows that Pds5 total protein levels are constant throughout the cell cycle, a result similar to that of cohesin core subunits Smc1 and Smc3 (Figure 4.5B). The Scc1 immunoblot shows a reduction in Scc1 protein levels as cells enter mitosis (12 h). This is an indication of the Separase enzymatic activity, which is activated during the metaphase-to-anaphase transition to enable chromosome disjunction (Onn et al., 2008). This data shows that cohesin function is not regulated by changes in the expression levels of Pds5 proteins.

The currently accepted model (see Figures 1.4, page 11, and 5.1, page 157) of cohesin-chromatin interaction postulated by many studies depicts a tripartite cohesin ring structure that completely dissociates from chromosome arms during the prophase pathway and from the centromere upon cleavage of the Scc1 subunit of the cohesin complex during the metaphase-to-anaphase transition (Alberts, 2008; Peters et al., 2008; Nishiyama et al., 2010). Consistent with this model (see Figure 5.1, page 157), my data shows that Pds5 proteins dissociate from chromatin as cells get to mitosis (12 h), before re-associating with chromatin at the end of mitosis (15 h) (Figure 4.6C). This pattern was also similar to that of cohesin core subunits Smc1, Smc3, and Scc1, as well as cohesion establishment factors Sororin and Esco1 (Figure 4.6C). Furthermore, I noted that the acetylation levels of Smc3 (Ac-Smc3) declined on chromatin as cells entered mitosis, and indication of HDAC8 deacetylase activity in mitosis (Beckouët et al., 2010). These results show that the association and dissociation of Pds5 proteins from chromatin is cell cycle regulated.

Wapl is known to bind Pds5 during prophase and remove cohesin from chromosome arms. The function of Wapl at this stage undermines the stability of its binding platform on chromatin and it is expected that as cohesin is removed from chromatin, Wapl's levels on chromatin should decrease. This could account for the steady decline of Wapl

on chromatin observed during mitosis (Figure 4.6C), consistent with reports that the protein dissociates from chromatin from prophase until telophase (Kueng et al., 2006a). The Smc3-Scc1 interface is thought to house DNA's exit gate, whose function is partly modulated by Pds5 and Eco1 (Esco1 and Esco2 in humans). Acetylation of Smc3's ATPase head domain by the Esco1 and Esco2 cohesin acetyltransferases (Chan et al., 2013), with concomitant recruitment and binding of Sororin to Pds5 (Nishiyama et al., 2010; Ladurner et al., 2016), following the passage of the replication fork, is thought to keep the DNA exit gate locked shut, thereby maintaining sister chromatid cohesion (Buheitel & Stemmann, 2013; Chan et al., 2012; Eichinger et al., 2013). Disengagement of the exit gate via phosphorylation of Sororin and SA2 in prophase, by Plk1 and Cdk1, respectively, allows the removal of cohesin from chromosome arms in prophase (Zhang & Pati, 2012). Consistent with previous studies that report an S-phase-specific Esco2-chromatin interaction (Hou F & Zou H, 2005), my data shows that the Esco2 protein levels on chromatin are higher during the time coinciding with the period of DNA replication (0-6 h), before they steadily decrease as cells get to mitosis; and that in both soluble and chromatin fractions, the protein is only significantly expressed before entry into mitosis (0-6 h). This result suggests that the role of Esco2 is restricted to S-phase.

4.2.5.2 Pds5 and DNA replication

Cohesin is required for efficient DNA replication during S-phase (Sherwood et al., 2010; Guillou et al., 2010). Pds5 is an integral member of the cohesin complex and regulates important functions including cohesion establishment, maintenance, and resolution (Panizza et al., 2000). Cohesin is acetylated by Esco1 and Esco2 as the new strands emerge from the replisome during DNA replication. Recruitment of Esco1 to chromatin depends on Pds5 (Minamino et al., 2015). Cohesin acetylation has been shown to speed the replication fork (Terret et al., 2009). This is because acetylation promotes the recruitment of Sororin to chromatin by Pds5 to establish cohesion (Nishiyama et al., 2010). However, in *Xenopus*, acetylation is reported to have no effect on DNA replication (Lafont et al., 2010).

In light of the foregoing, loss of either Pds5 or acetyltransferases Esco1 and Esco2 should impede the process of DNA replication. My data shows that depletion (Figure 4.7) of

Pds5 proteins significantly reduces BrdU incorporation (Figures 4.8B) by either asynchronous (Figure 4.8C) or synchronised (Figure 4.8D) population of HeLa cells, suggesting that loss of Pds5 hampers DNA replication. Further analysis of BrdU incorporation (Figure 4.9B) by HeLa cells showed that cells depleted of Pds5 proteins take longer to complete S-phase (Figure 4.9C). This result shows that the absence of Pds5 proteins delays DNA replication.

A closer analysis of DNA replication in the absence of Pds5 proteins using DNA single fibre techniques revealed four altered parameters: short labelled DNA fibres (Figure 4.10B iv and vii) and (Figure 4.10C) suggesting slow-moving replication forks, significant reduction in fork velocity (Figure 4.10D), and significant increase in the number of stalled replication forks (Figure 4.10B v and viii) and (Figure 4.10E) suggesting inhibition of fork progression. Furthermore, there were numerous intermittent gaps (Figure 4.10B vi and ix) indicating an increase in the number of stalled replication forks, and significant reduction in the number of interspaced fibres (Figure 4.10F) suggesting slowed DNA replication.

The fact that origins of replication can still fire in the absence of Pds5 proteins suggests that Pds5 proteins are not required for initiation of DNA replication. However, numerous stalled replication forks, reduced fork velocity, short labelled fibres, and intermittent gaps in the DNA fibres show that it is the progression of replication forks which is inhibited by the absence of Pds5 proteins. Collectively, my data shows that Pds5 proteins are required for efficient replication fork progression during DNA replication. The finding that loss of Pds5 proteins delays DNA replication in mammalian cells is novel; this observation has not been reported before.

What remains enigmatic, however, is the mechanism by which Pds5 proteins regulate DNA replication. Before DNA replication, Pds5 proteins form a complex with Wapl; the Pds5-Wapl complex keeps cohesin in a dynamic state, destabilising its binding to chromatin (Gerlich et al., 2006). More recently, it has been shown that the Pds5-Wapl complex is required for cohesin loading onto chromatin in yeast (Murayama &Uhlmann, 2016). During DNA replication, displacement of Wapl by Sororin from Pds5, coupled with Smc3 acetylation by Esco1 and Esco2, establishes sister chromatid cohesion

(Nishiyama et al., 2010). Given that cohesin is required for efficient DNA replication during S-phase (Guillou et al., 2010; Sherwood et al., 2010) and that Pds5 proteins play many roles in cohesin regulation, it is possible that the delay in DNA replication observed after depletion of Pds5 proteins (Figures 4.8, 4.9, and 4.10) resulted from altered cohesin structures on chromatin, giving rise to unstable replication forks.

My data shows increased Smc3 acetylation and a reduction in the levels of chromatin-bound Wapl after depletion of Pds5A (Figure 4.11). Increased Smc3 acetylation would be expected to enhance DNA replication, as previously reported (Terret et al., 2009). Meanwhile, a reduction in Wapl levels on chromatin is expected to lead to the stabilisation of cohesin on chromatin, since cohesin is no longer in a dynamic state, thereby impeding the passage of the replication fork, and delaying DNA replication. However, recent reports show that although Wapl is required for cohesin loading onto chromatin (Murayama & Uhlmann, 2015), its inactivation speeds up DNA replication in both yeast and human cells (Lopez-Serra et al., 2013b; Manning et al., 2014), suggesting that the absence of Wapl from chromatin does not hinder the passage of the replication fork.

My data further shows that depletion of both Esco1 and Esco2 prevents Smc3 acetylation and delays DNA replication (Chapter 3, Figures 3.9, 3.10, and 3.11) while depletion of Wapl causes more Smc3 acetylation (Figure 4.11) without inhibiting BrdU incorporation (Figure 4.12). This data suggests that neither the increase in Smc3 acetylation nor the reduction in chromatin-bound Wapl in the absence of Pds5A accounted for the delay in DNA replication observed.

Surprisingly, depletion of both Wapl and Pds5A was characterised by transient association of Ac-Smc3 and Sororin with chromatin, as well as accumulation of Esco2 on chromatin (Figure 4.11), suggesting that cells successfully complete S-phase and enter mitosis, where Ac-Smc3 and Sororin are removed from chromatin via deacetylation and phosphorylation, respectively. Consistent with this notion, depletion of both Wapl and Pds5A (Figure 4.13A) significantly increases BrdU incorporation (Figures 4.13B) by asynchronous HeLa cells (Figure 4.13C), suggesting that the defect in DNA replication observed after depletion of Pds5 alone can be rescued by depleting both Pds5 and

Wapl. This result is novel; for the first time, my data indicates a requirement for Pds5 proteins in DNA replication and that the replication defect encountered due to loss of Pds5 can be rescued by depletion of Wapl.

How Wapl's absence from chromatin supports DNA replication is unclear. Given that Wapl is a cohesin destabilising factor when bound to Pds5, it is conceivable that Wapl depletion supports DNA replication by allowing stable binding of cohesin to chromatin. Chromatin accumulation of Scc1 at 8 h and increased Smc3 acetylation (Figure 4.11) after Wapl depletion supports this notion. Consistent with previous reports which show the requirement for cohesin in DNA replication (Guillou et al., 2010; Sherwood et al., 2010), removal of the anti-establishment complex (Wapl-Pds5) should therefore allow more cohesin to associate with chromatin, resulting in enhanced DNA replication (Figure 4.13). However, depletion of the Wapl-Pds5 complex resulted in less cohesin (Scc1 and Smc3) recruited to chromatin compared to control siRNA-treated cells (Figure 4.11).

The fact that depletion of Pds5A alone is characterised by persistent acetylation of Smc3 from 0 to 8 h (Figure 4.11) shows that the delay in DNA replication observed in Pds5-depleted cells is not due to a failure to recruit cohesin complexes to chromatin. Importantly, it has been shown that the phosphorylation of Scc1 by Chk1 promotes Eco1 activity only in response to DNA damage (Unal et al., 2007; Heidinger-Pauli et al., 2009), suggesting that persistent Smc3 acetylation observed after depletion of Pds5A (Figure 4.11) could be due DNA damage. Since cohesin is required for DNA replication (Guillou et al., 2010; Sherwood et al., 2010), it is conceivable that the absence of a versatile cohesin regulatory protein such as Pds5 destabilises the replication forks by preventing the establishment of sister chromatid cohesion, resulting in the activation of the DNA damage checkpoint response. Unstable replication forks have been shown to be prime sources of DNA damage in both prokaryotes and eukaryotes (Heller & Marians, 2006).

Indeed, depletion of either Pds5A or Pds5B led to the phosphorylation of Chk1 on ser317 (Figure 4.14A), indicating that loss of Pds5 proteins activates the DNA damage checkpoint response. An ongoing study (unpublished) in our lab that examined whether the protein kinase activity of Chk1 was responsible for inhibiting fork progression upon

Pds5 depletion has shown that co-depletion of Chk1 with Pds5A results in a partial rescue of the S-phase delay. This effect was not observed when both Pds5B and Chk1 were depleted. The rescue of DNA replication in the absence of Pds5A and Chk1 was confirmed in whole cell BrdU-labelling experiments of synchronised HeLa cells; 71% of the Chk1 and Pds5A-depleted cells incorporated BrdU 1 hr after release from the Aphidicolin block compared to 10.3% when only Pds5A was depleted. The rescue of the S-phase delay in the absence of Pds5B and Chk1 was less efficient with only 20% of cells staining positively for BrdU at 1 hr post Aphidicolin release. This study has also shown that depletion of Pds5 proteins results in phosphorylation of Histone H2AX, suggesting the presence of double strand breaks. Further analysis using the comet assay of the nature of DNA damage caused by depletion of Pds5 proteins also revealed single strand breaks in both Pds5A and Pds5B-depleted cells (Figures 4.14B and C).

4.2.5.3 The putative mechanism by which Wapl rescues replication delay in Pds5A-depleted cells

Putatively, Wapl rescues the delay in DNA replication observed when Pds5A is depleted alone by allowing normal chromatin conformational change that decreases the level of DNA damage. This notion needs further testing by comparing the level of DNA damage in Pds5A and Pds5A-Wapl depleted cells, given that cells depleted of both Pds5 and Wapl are characterised by cohesion defects (Tong & Skibbens, 2015). Suffice to say that in Pds5A depleted cells, cohesin is loaded normally, since Wapl has no counter effect on cohesin loading when unbound to Pds5 (Murayama & Uhlmann, 2015). My data shows less Wapl recruited to chromatin in cells depleted of Pds5A, possibly due to the fact that Wapl preferentially forms a complex with Pds5A on chromatin (Kueng et al., 2006b). The DNA exit gate (Beckouët et al., 2016; Buheitel & Stemmann, 2013; Chan et al., 2012) is expected to remain closed, since Pds5, which is required for gate disengagement, is absent. The absence of Pds5 further results in failure to establish sister chromatid cohesion, resulting in cohesion defects. Anomalous Chromatin conformational change in the absence of Pds5 leads to single and double strand breaks which cannot be repaired since Pds5 which is required to establish cohesion is absent. This results in persistent cohesin acetylation (Figure 4.11) due to DNA damage (Figure 4.14), which slows DNA replication (Figures 4.8, 4.9, and 4.10).

In Wapl-depleted cells, Pds5 competes with the Scc2-Scc4 complex for cohesin binding (Murayama & Uhlmann, 2015), resulting in less cohesin (Scc1 and Smc3) recruited to chromatin (Figure 4.11). Once loaded, cohesin is protected by Pds5 from spontaneous removal (Murayama & Uhlmann, 2015). The DNA exit gate (Beckouët et al., 2016; Buheitel & Stemmann, 2013; Chan et al., 2012) remains closed since Wapl is absent, resulting in hypercohesed sister chromatids that cannot resolve their arms (our previous studies in the lab, unpublished data) and persistent cohesin at mitosis (Figure 4.11). DNA replication proceeds as normal, since Pds5 and Sororin form a cohesion establishment complex and stabilise cohesin on chromatin. Normal Chromatin conformation upon acetylation and Sororin recruitment facilitates fork progression. However, since sister chromatids cannot resolve their arms, cohesin remains acetylated at mitosis (Figure 4.11).

In Wapl and Pds5A- depleted cells, cohesin is loaded by the Scc2-Scc4 complex, but lack of compensatory loading by the Pds5-Wapl complex (Murayama & Uhlmann, 2015) results in less cohesin recruited to chromatin (Figure 4.11). Establishment of sister chromatid cohesion is not achieved, since Sororin requires to bind Pds5 and displace Wapl to establish cohesion (Nishiyama et al., 2010), resulting in cohesion defects in cells lacking both Pds5 and Wapl (Tong & Skibbens, 2015). In these cells, the DNA exit gate (Beckouët et al., 2016; Buheitel & Stemmann, 2013; Chan et al., 2012) is expected to remain open, leading to transient interaction of cohesin with chromatin (Figure 4.11). However, the absence of both Pds5A and Wapl allows normal chromatin conformational change upon acetylation, resulting in progression of the replication forks.

Since this is only a putative mechanism by which Wapl supposedly rescues the defect in DNA replication when Pds5A is depleted alone, it will be important to test some of these assertions in future. Testing whether depletion of both Wapl and Pds5B reverses the effect of Pds5B depletion will be important. Furthermore, it will also be interesting to assess the level of chromatin loop formation in both Pds5A and Pds5A-Wapl depleted cells, as this may give a clue to chromatin conformation and organisation upon Pds5 depletion.

Taken together, my data suggests that the delay in DNA replication observed after depletion of Pds5 proteins (Figures 4.8, 4.9, and 4.10) resulted from failure to repair damaged DNA that occurred due abnormal cohesin conformational change. The absence of Pds5 proteins during DNA replication causes DNA single strand breaks, leading to double strand breaks. However, cohesin loading and cohesion establishment, which is required for the integrity of the DNA damage checkpoints (Lightfoot et al., 2011), cannot be established, since Pds5 proteins are lacking, thus compromising the DNA damage repair mechanism and destabilising the replication forks. Unrepaired DNA activates the DNA damage checkpoint response, which eventually slows down DNA replication. This result is novel, no study has previously shown that loss of Pds5 proteins causes DNA single strand breaks and consequently DNA damage checkpoint activation and DNA replication delay.

This study has produced a number of important clues into the role of Pds5 proteins in chromosome biology. Pds5, whose role in DNA replication has previously been unknown, is an integral cohesin regulatory protein required for both establishment and dissolution of sister chromatid cohesion. Through this study, I have shown that the two Pds5 orthologs, whose intracellular localisation is cell cycle regulated, are not redundant, and that their association and dissociation from chromatin is similar to that of cohesin core subunits, Smc1 and Smc3. Importantly, I have demonstrated, for the first time, that Pds5 proteins are required for efficient fork progression during DNA replication, and that depletion of Pds5 proteins induces DNA damage which in turn activates the intra S-phase DNA damage checkpoint that slows DNA replication. I have further shown that the delay in DNA replication observed after depleting Pds5 can be rescued by depleting both Wapl and Pds5 proteins.

In future, it will be important to investigate how the absence of Pds5 proteins triggers DNA damage. Whether this results from cohesin's anomalous conformational change upon acetylation and binding of Sororin to SA1/2 only in the absence of Pds5, causing strain and breaks in entrapped DNA strands, is not yet known. If this is the case, it may help explain why Wapl inactivation supports DNA replication. Since Wapl is a cohesin destabilising factor, its depletion should allow efficient binding of Sororin to Pds5 and

SA1/2, resulting in normal conformational change of the cohesin complex that allows progression of DNA replication.

Main conclusions from this chapter:

- The data in this chapter has shown that depletion of Pds5 proteins causes both single and double strand breaks which ultimately activate the DNA damage checkpoint and delay DNA replication.

- The delay in DNA replication observed when Pds5A is depleted alone can be rescued by depleting the anti-establishment complex, Pds5A and Wapl.

Chapter 5 - General Discussion

5.1 Main Findings

- This study has shown that depletion of either Esco1 or Esco2 prevents Smc3 acetylation, although by only a smaller fraction in Esco2-depleted cells, and results in a delay in DNA replication.

- Esco1 and Esco2 may have non-overlapping functions and are differentially regulated. The fact that Esco2 depletion prevents acetylation only by a smaller fraction but cells still fail to replicate their DNA shows that acetylation may not be sufficient for DNA replication.

- Depletion of either Esco1 or Esco2 results in precocious separation of sister chromatids, chromosome missegregation, and either apoptosis or senescence.

- Depletion of Pds5 proteins causes both single and double strand breaks which ultimately activate the DNA damage checkpoint and delay DNA replication.

- The delay in DNA replication observed when Pds5A is depleted alone can be rescued by depleting the anti-establishment complex, Pds5A and Wapl.

5.2 Overview

The cohesin complex is a multi-subunit protein complex whose role in sister chromatid cohesion is regulated by associated proteins that include, among others, Pds5 and the acetyltransferases Esco1 and Esco2. Sister chromatid cohesion, once established in S-phase after the passage of the replication fork and Smc3 acetylation-coupled recruitment of Sororin to chromatin, is maintained until the onset of anaphase. Proper establishment and maintenance of sister chromatid cohesion is important in safeguarding genome integrity. Errors in sister chromatid cohesion have been implicated in congenital birth defects (Shen, 2011; Pfau & Amon, 2012) and cancer (Thol F et al., 2014; Thota S et al., 2014). Pds5 recruits Esco1 chromatin (Minamino et al., 2015), which together with Esco2, acetylate Smc3 on lysine residues K^{105} and K^{106} in vertebrates to establish sister chromatid cohesion. Sororin's recruitment to chromatin

depends on Esco2 (Lafont et al., 2010); it stably associates with chromatin and maintains cohesion by binding to Pds5 via the FGF motif and displacing Wapl (Nishiyama et al., 2010).

Cohesin has been shown to participate in DNA replication by regulating higher-order organisation of replication factories and modulating the size of chromatin loops that likely correspond to replicon units (Guillou et al., 2010). Furthermore, cohesin acetylation reportedly speeds replication forks in human somatic cells (Terret et al., 2009), although these results are disputed in *Xenopus* egg extracts (Lafont et al., 2010). Recently, proteins involved in DNA replication, including Ctf4 (chromosome transmission fidelity 4) and Chl1/ChlR1 (chromosome loss 1), have been shown to be important in sister chromatid cohesion establishment (Samora et al., 2016).

Despite recent advances in our quest to understand cohesin regulation and its roles in chromosome biology, information on mechanistic consequences of cohesin posttranslational modifications such as acetylation remains scanty and contradictory. While Pds5's role in sister chromatid cohesion maintenance and resolution has been explored, no study to date has reported its participation in DNA replication. Pilot studies (unpublished) in our lab have implicated Pds5 in DNA replication.

In light of the foregoing, the work presented in this thesis was conducted with the aim of further characterising the role of acetyltransferases Esco1 and Esco2 and Pds5 in the mammalian cell cycle and specifically their role in DNA replication. To achieve these aims, siRNA-mediated depletion and DNA combing techniques were employed. Initially, the intracellular localisations of Esco1, Esco2, and Pds5 proteins were analysed by immunofluorescence and the temporal association and dissociation of cohesin from chromatin during the cell cycle was analysed by Western blotting. This was followed by depletion of Esco1, Esco2, and Pds5 using siRNA for each protein and analysing DNA replication by BrdU labelling and the Single fibre technique. Cell apoptosis and senescence, due to loss of Esco1 and Esco2, was analysed by a combination of immunostaining, Western blotting, and SA-β-Galactosidase staining.

On commencing the study, my hypothesis was that Esco1, Esco2, and Pds5 proteins are required for normal DNA replication. The data collected in this study not only agrees with my hypothesis, but also presents new insights into the regulation of cohesin and the role of cohesin regulatory proteins Esco1, Esco2, and Pds5 in chromosome biology.

5.3 The cell cycle-dependent dynamic localisation of Esco1, Esco2, and Pds5 proteins

The Immunofluorescence data presented in Chapter 3 and Chapter 4 show that the intracellular localisation of Esco1, Esco2, Pds5A, and Pds5B proteins is cell cycle regulated. This data further highlights the important differences in the functions and regulations of these homolog pairs. Although both Esco1 and Esco2 proteins localise to chromatin during interphase (Figure 3.3), Esco2 is only expressed during S-phase (Hou & Zou, 2005) where it accumulates during the time that marks the period of DNA replication (Figures 3.6E, 3.7B and D, 3.8B, and 4.6) and gets degraded at mitosis (Hou & Zou, 2005). In contrast, Esco1 is expressed throughout the cell cycle (Figures 3.6E, 3.7B and D, 3.8B, and 4.6) and only undergoes phosphorylation (Lyons & Morgan, 2011) at mitosis in vertebrates. The fact that Esco1 is only phosphorylated while Esco2 is degraded in vertebrates could account for the higher abundance of Esco1 on chromatin than Esco2 that was observed in this study (Figure 3.5). These results are consistent with previous reports which demonstrated the functional differences between these two proteins (Hou & Zou, 2005; van der Lelij et al., 2009; Lyons & Morgan, 2011; Song et al., 2012; Whelan et al., 2012).

Recently, it was demonstrated that Esco1 acetylates cohesin via a different mechanism from that of Esco2 (Minamino et al., 2015) and that Esco1 is recruited to chromatin by Pds5 (Minamino et al., 2015) while Esco2's recruitment to chromatin depends on Sororin (Lafont et al., 2010). There is currently no evidence as to why there are two Eco1 orthologs in vertebrates while lower organisms have only one ortholog, and why these two proteins (Esco1 and Esco2) have different mechanisms by which they are recruited to chromatin in vertebrates. Interestingly, depletion of either Esco1 or Esco2 from HeLa cells results in cohesion failure (Figure 3.13), suggesting a non-redundant function (Lafont et al., 2010).

In budding yeast, Eco1/Ctf7 has different cohesin subunit substrates; it acetylates both Smc3 and Scc1/Mcd1 (Heidinger-Pauli et al., 2009), suggesting that in vertebrates, the Eco1 functions may have diverged to two separate proteins during the course of evolution. However, both Esco1 and Esco2 proteins can acetylate Smc3 on two lysine residues ($K^{105/106}$) during DNA replication (Nasmyth, 2005; Zhang et al., 2008), although acetylation is largely carried out by Esco1 in mammalian cells (Figure 3.10). This suggests that Esco1 and Esco2 may have retained some overlapping functions that ensure stable sister chromatid cohesion is maintained throughout a relatively extended G2 period in vertebrates.

Furthermore, Sororin and Esco2 have been shown to be co-regulated by APC^{Cdh1} (Lafont et al., 2010), suggesting that these two proteins, but not Esco1, comprise a regulatory module that helps prevent ectopic (such as intrachromatid or interchromosomal) cohesion events particularly in G1, reserving them for S-phase when there are two sister chromatids that can be tied together. These results demonstrate similar but independent roles of Esco1 and Esco2 proteins in cohesin regulation.

Like cohesin (see Figure 4.3A, page 118), Pds5 proteins are loaded onto chromatin during telophase; they localise to chromatin during interphase and dissociate from chromatin at mitosis (Figure 4.1). Although my immunoblot data did not show any changes in the levels of total Pds5 proteins throughout the HeLa cell cycle (Figures 4.4D and E, and 4.5), there were significant differences in the intracellular localisation of Pds5A and Pds5B. Pds5A (Figure 4.1A) was typified by a shorter chromatin residence time compared to Pds5B (Figure 4.1B). Notably, Pds5A has one AT-hook-type high mobility group (HMG) box motif while Pds5B has two (Figure 1.7) (Zhang et al., 2009a). The difference in Pds5A and Pds5B dissociation from chromatin may be a consequence of Pds5B's higher binding affinity for chromatin or perhaps the two proteins regulate different pools of cohesin on chromatin.

Differential regulation and spatial distribution of Pds5A and Pds5B could also account for the disparity in localisation observed (Figure 4.1), as Pds5B has been reported to be specifically required for centromeric cohesion (Carretero et al., 2013) while Pds5A preferentially forms a sub-complex with Wapl (Kueng et al., 2006b). Interestingly, Smc3

remains acetylated until metaphase (Figure 4.3B), suggesting residual centromeric cohesin that persists on chromatin until bi-polar spindle attachment is achieved. The localisation of Pds5A and Pds5B suggests that Pds5A may be more involved with arm-cohesin regulation during the prophase pathway in complex with Wapl while Pds5B may be important in the regulation of chromosome dynamics such as bipolar spindle attachment. Consistent with this notion, Pds5A's localisation (Figure 4.1A) is similar to that of Wapl (Figure 4.2) while Pds5B's gross localisation (Figure 4.1B) is similar to that of Sgo1 during the cell cycle (Chapter 3, Figure 3.4). It is plausible to think that the fraction of Pds5B protein that remains associated with chromatin from prophase to metaphase is probably not associated with Wapl, because Wapl, like Pds5A, has already dissociated from chromosomes by metaphase.

Contrary to previous reports that Pds5A and Pds5B proteins are redundant (Zhang et al., 2007, 2009), my localisation data suggests that Pds5A and Pds5B proteins may have different roles in mitosis, consistent with recent studies in mammalian cells (Minamino et al., 2015). Whether Pds5B's centromeric cohesin affinity relies on Sgo1 function requires further investigation. Co-staining mitotic spreads with the anti-centromere antibody will be important in confirming the spatial distribution of Pds5A and Pds5B on chromosomes. Taken together, this data shows that the intracellular localisation of Esco1, Esco2, and Pds5 proteins is cell cycle regulated.

5.4 Linking sister chromatid cohesion with DNA replication: novel roles of Pds5 and acetyltransferases Esco1 and Esco2 proteins in DNA replication

Previous studies have shown that cohesin complexes are assembled prior to their recruitment to DNA (Losada et al., 1998; Waizenegger et al., 2000) and loaded onto chromatin by the Scc2-Scc4 heterodimers (also known as the Kollerin complex, or Nipbl and Mau2, respectively) in telophase in vertebrates, or late G1 in yeast (Ciosk et al., 2000) (Figure 5.1). The difference in timing between vertebrate and yeast cohesin's recruitment to chromatin is the continued destruction of Scc1 by Separase through G1 in yeast (Uhlmann et al., 1999). Cohesin rings transiently open up to allow the entry of DNA, via the DNA entry gate, the hinge interface that connects Smc1 to Smc3 (Gruber

et al., 2006; Buheitel & Stemmann, 2013). The Scc2/Scc4 complex is thought to regulate the opening and closing of the hinge interface in a manner that requires the ATPase activity of the Smc1 and Smc3 head domains (Arumugam et al., 2003; Hu et al., 2011; Murayama & Uhlmann, 2014).

Loading of the Scc2-Scc4 complex itself onto chromatin depends on pre-RCs, at least in *Xenopus* (Gillespie & Hirano, 2004; Takahashi et al., 2004), which are formed by sequential assembly of origin recognition complex (ORC), Cdc6, and Cdt1 at replication origins (Bell & Dutta, 2002). pre-RCs are required for loading the inactive Mcm2–7 helicase onto DNA (Randell et al., 2006; Evrin et al., 2009; Remus et al., 2009), which is subsequently activated at the G1/S transition through phosphorylation by the S-phase kinase Cdc7 (Masai et al., 2006; Sheu & Stillman, 2006) and interaction with Cdc45 and GINS (Gambus et al., 2006; Moyer et al., 2006; Pacek et al., 2006; Aparicio et al., 2009; Ilves et al., 2010).

In *Xenopus* egg extracts, Cdc7 also interacts with Scc2-Scc4 heterodimers, and its kinase activity is required for loading the Scc2-Scc4 complexes onto chromatin (Takahashi et al., 2008). The fact that Cdc7 interacts with Scc2-Scc4 complexes and associates with pre-RCs in G1 phase and activates them at the G1/S transition suggests that its involvement might target cohesin to sites of imminent replisome assembly, thereby facilitating cohesin's subsequent interaction with fork-associated regulators.

Before S-phase, the cohesin loaded onto chromatin in telophase or late G1 is highly dynamic (Gerlich et al., 2006), as the HEAT repeat-containing proteins, Pds5 and Wapl, which form a sub-complex by Pds5 interacting via the FGF motif of Wapl, continuously remove cohesin from chromatin in a reaction that requires opening of the cohesin's DNA exit gate, the interface between Smc3 and Scc1 (Beckouët et al., 2016; Buheitel & Stemmann, 2013; Chan et al., 2012; Gandhi et al., 2006; Gligoris et al., 2014; Huis in 't Veld et al., 2014; Kueng et al., 2006; Murayama & Uhlmann, 2015; Rowland et al., 2009).

Like cohesin (Figure 4.3A), Pds5 (Figure 4.1) and Wapl (Figure 4.2) are loaded onto chromatin during telophase. The importance of the Wapl-Pds5-orchestrated destabilisation of cohesin on chromatin before S-phase is a subject of ongoing debate.

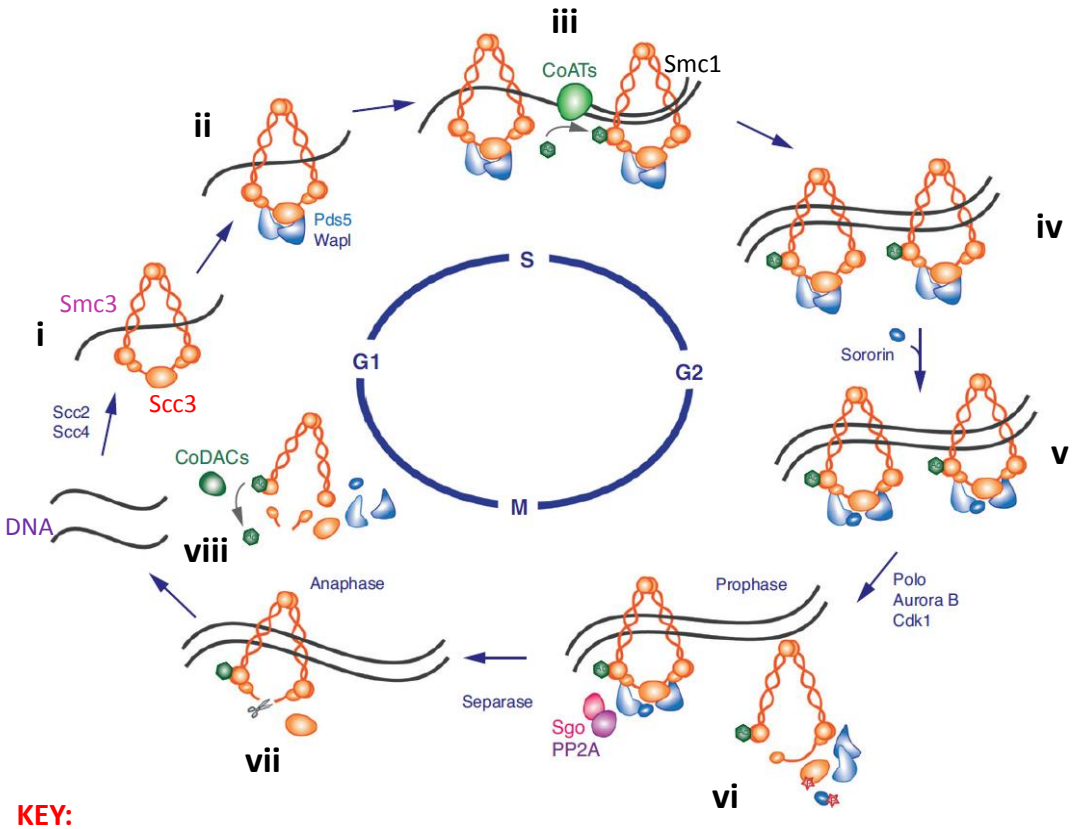

KEY:
CoDACs = HDAC8/Hos1
CoATs = Eco1 (Esco1/Esco2)

Figure 5.1 A model of cohesin regulation during the cell cycle

(i) Cohesin is loaded onto chromatin via the Smc1-Smc3 hinge domain in telophase in vertebrates or G1 in yeast. **(ii)** Before S-phase the Wapl-Pds5 complex destabilises the binding of cohesin on chromatin, keeping it in a dynamic state. **(iii)** During DNA replication in S-phase, the replication fork is thought to pass through the cohesin ring. Following the passage of the replication fork, Smc3 is acetylated by Esco1 and Esco2. This is coupled with the recruitment of Sororin **(iv)** to chromatin. The cohesin-releasing activity of the Wapl-Pds5 complex is blocked after Wapl is displaced from the central binding site of Pds5 by Sororin, which establishes sister chromatid cohesion. **(v)** Sister chromatid cohesion is maintained throughout G2. **(vi)** At prophase, Sororin is phosphorylated by Cdk1/cyclin B, which facilitates Plk1 to bind to Sororin and phosphorylates SA2. Phosphorylation of SA2 destabilizes cohesin complexes. Sororin dissociates from chromatin after it is further phosphorylated, which provides an opportunity for Wapl to bind back to Pds5 and restore its cohesin-releasing activity in complex with Pds5. At this stage the Wapl-Pds5 complex only removes cohesin from the chromosome arms; centromeric cohesin is protected by the Sgo1-PP2A complex. After cohesins are removed by Wapl-Pds5 complex, the arms of the sister chromatid are resolved. **(vii)** Following bi-polar spindle attachment at the metaphase plate, the APC/Cyclosome-mediated degradation of Securin allows the activation of Separase, which cleaves the Scc1 subunit of cohesin, allowing the separation of sister chromatids at anaphase. **(viii)** The released cohesins are regenerated by deacetylation of Smc3 and dephosphorylation of SA2, which can be reused in telophase/G1. CoDAC= cohesin deacetylase; CoAT= cohesin acetyltransferase. (Losada & Remeseiro, 2013; Zhang & Pati, 2012).

Interestingly, it has been shown that loading of cohesin onto chromatin is essential but not sufficient to establish sister chromatid cohesion, and that establishment of sister chromatid cohesion occurs concomitantly with DNA replication, following the passage of the replication fork and acetylation of Smc3 on lysine residues K^{105} and K^{106} by Esco1 and Esco2 in metazoans (Chan et al., 2012; Nishiyama et al., 2010; Rankin, 2005; Rolef Ben- Shahar et al., 2008; Rowland et al., 2009; Sherwood et al., 2010; Unal et al., 2008). In vertebrates, acetylation of Smc3 is coupled with the recruitment of Sororin to chromatin, which competes with Wapl for binding to Pds5 (Nishiyama et al., 2010).

Importantly, the displacement of Wapl from Pds5 by Sororin brings to an end the Wapl-Pds5-dependent cohesin releasing activity, and acetylation locks the cohesin ring by preventing DNA from triggering ATP hydrolysis, thereby stabilising cohesin on chromatin (Uhlmann, 2016). These findings have further heightened the debate on the role of the Wapl-Pds5 sub-complex before DNA replication, resulting in two hypotheses of how DNA replication-coupled sister chromatid cohesion establishment occurs.

One possibility is that the replication fork passes through the cohesin ring during DNA replication (Figure 5.2A). In this case, cohesin would efficiently capture sister chromatids, since they are already encircled, and acetylation during or just after the passage of the replication forks would result in cohesion establishment, as no renewed DNA entry reactions are required during cohesion establishment. This model is supported by the finding that cohesion establishment is insensitive to mutations in the cohesin ATPase that slow down DNA entry, and that the Scc2-Scc4 cohesin loader is no longer essential during DNA replication (Lengronne et al., 2006). The Wapl-Pds5 cohesin removal activity in this case would be a futile reaction to DNA replication, other than limiting a pool of cohesins on chromatin before the passage of the replication forks.

The alternative model proposes that if the replication fork cannot pass through the cohesin ring, the cohesin ring must open up to allow the passage of the replication fork, and acetylation and establishment of sister chromatid cohesion happens behind the replication forks as new strand emerge from the replisome (Figure 5.2B). In this case, cohesin acts as a lockable structure that establishes sister chromatid cohesion by stochastic co-entrapment of replication products behind replication forks. In this model,

the role of the Wapl-Pds5 sub-complex upstream of replication forks would be to keep cohesin in a dynamic state, allowing the passage of the replication forks by disengaging the Scc1-Smc3 interface, in a similar mechanism as the one mediated by the Scc2-Scc4 complex.

Acetylation of Smc3, following the passage of the replication fork, renders cohesin resistant to Wapl, and hence locks the DNA exit gate (Rolef Ben-Shahar *et al.*, 2008; Rowland *et al.*, 2009; Sutani *et al.*, 2009; Unal *et al.*, 2008; Zhang *et al.*, 2008). The establishment and maintenance of sister chromatid cohesion by Smc3 acetylation coupled with Sororin recruitment is important in ensuring bi-polar spindle attachment to kinetochores and prevention of precocious separation of chromosomes (Minamino et al., 2015).

Contradictory reports have emerged in the recent past regarding the role of cohesin acetylation in DNA replication in vertebrates. A study in mammalian cells reported that cohesin acetylation speeds replication forks (Terret *et al.*, 2009) while studies in *Xenopus* egg extracts showed that acetylation does not affect DNA replication (Lafont *et al.*, 2010). My data suggests that loss of acetylation, by depletion of Esco1 and Esco2, slows replication fork progression, but not origin firing, in a synchronised population of HeLa cells (Figures 3.11 and 3.12). Furthermore, depletion of either Esco1 or Esco2 results in precocious separation of sister chromatids (Figure 3.13).

Of the two proteins, Esco1 appeared to have more effect on cohesin acetylation than Esco2, although depletion of Esco2 still manifested consequences of loosely attached sister chromatids (Figure 3.13) as well as defective DNA replication (Figure 3.11). The fact that cells still fail to replicate their DNA efficiently (Figure 3.11) even with the slightest reduction in Smc3 acetylation (Figure 3.10) shows that acetylation per se may not have a significant effect on DNA replication; but the property that cohesin acquires upon Smc3 acetylation could be the determinant factor that makes cohesin more competent to regulate DNA replication. The known cohesion establishment factor whose recruitment to chromatin is coupled with Smc3 acetylation is Sororin, which competes with Wapl to bind Pds5 via the FGF motif and establish sister chromatin cohesion in S-phase (Nishiyama et al., 2010; Ladurner et al., 2016).

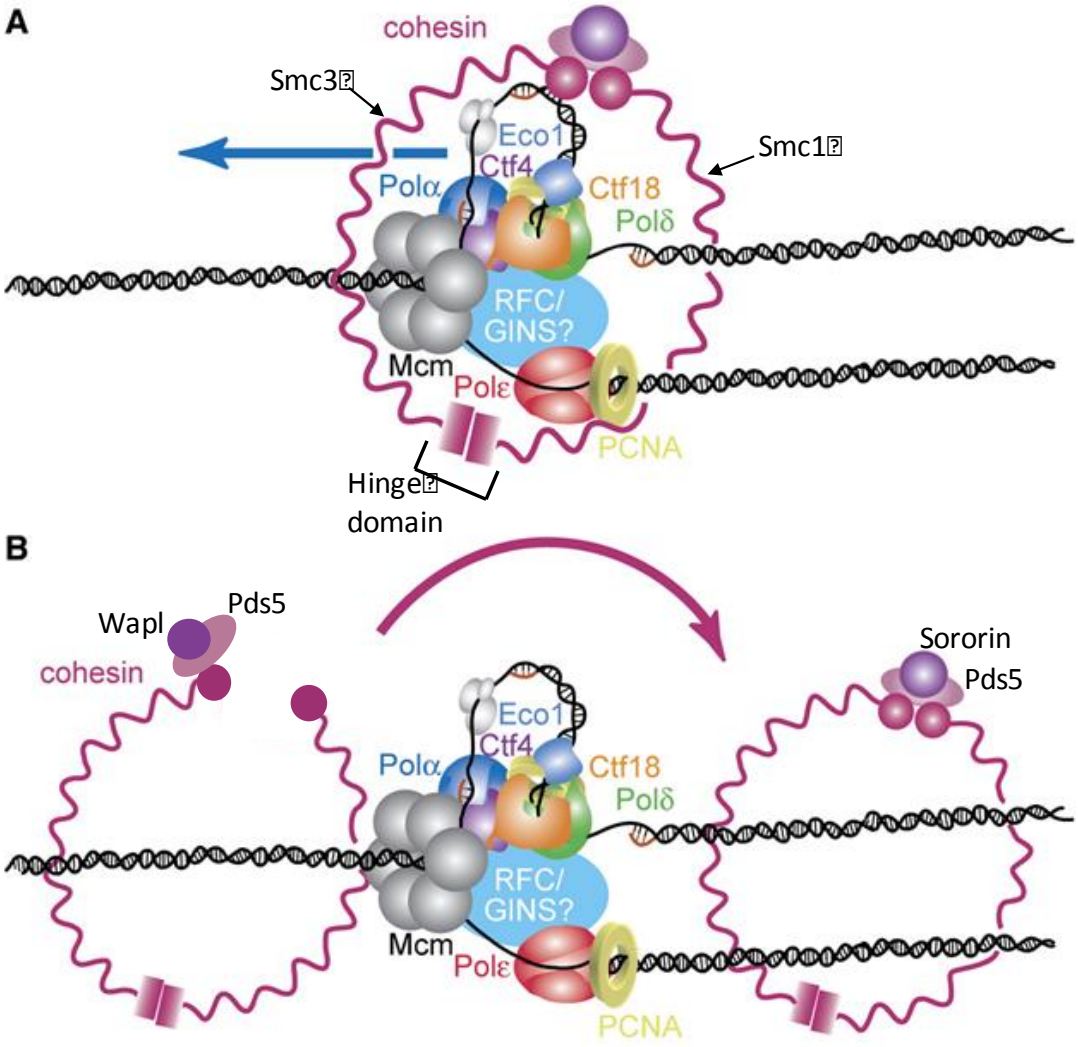

Figure 5.2 Models of sister chromatid cohesion establishment during replication fork passage

(**A**) The replication fork passes through the cohesin ring during DNA replication. Additional proteins such as Mcm10, Cdc45, Sld2, Sld3, Dpb11, Tof1, Mrc1, and Csm3 are thought to associate with the eukaryotic replication fork. In this case, cohesin would efficiently capture sister chromatids, since they are already encircled, and acetylation during or just after the passage of the replication forks would result in cohesion establishment. (**B**) Alternatively, if the replication fork together with the associated proteins cannot pass through the cohesin ring, the ring loses its topological contact with DNA by opening up to allow the passage of the replication fork. Smc3 acetylation and sister chromatid cohesion establishment happens behind the replication forks (adapted, with modifications, from Lengronne et al., 2006).

Recent studies have shown that Sororin's recruitment to chromatin also depends on Esco2 (Lafont et al., 2010). It is conceivable that failure to recruit Sororin to chromatin upon loss of Esco2 would have led to impaired sister chromatid cohesion, resulting in a delay in DNA replication. However, depletion of Sororin alone does not delay DNA replication (Guillou et al., 2010), suggesting that the delay in DNA replication observed after depletion of Esco2 is independent of the loss of sister chromatid cohesion. Importantly, cohesin has been shown to be present at replication origins and participates in DNA replication by regulating higher-order organisation of replication factories and modulating the size of chromatin loops that likely correspond to replicon units (Figure 1.13) (Guillou et al., 2010).

Given that the recruitment of Sororin also depends on Esco2 (Lafont et al., 2010), and that Sororin is a cohesion establishment factor (Nishiyama et al., 2010), it is plausible to think that depletion of Esco2 may have led to cohesin's inability to regulate higher-order organisation of replication factories, resulting in fewer, longer chromatin loops which ultimately slowed down DNA replication. In future, it will be important to test if Esco2 is important in the regulation of the length of chromatin loops, using the Fluorescence DNA halo technique (Vogelstein et al., 1980) to estimate the average length of DNA loops in interphase cells upon depletion of Esco2. Briefly, this requires permeabilising cells with detergents and depleting soluble proteins by extraction with high salt buffers; supercoiled DNA loops then unwind and form a halo around an insoluble scaffold that can be visualised by fluorescence staining (Vogelstein et al., 1980).

The fact that acetylation occurs after the passage of the replication forks (Figure 5.2B) further suggests that its impairment, by depletion of Esco1 or both Esco1 and Esco2, would not necessarily block fork progression. Interestingly, studies in yeast have shown that Eco1/Ctf7 physically interacts with PCNA during DNA replication (Moldovan *et al.*, 2006) and that this interaction enables Eco1 to transiently bind to chromosomes and acetylate Smc3, thereby establishing cohesion (Lengronne *et al.*, 2006). Given that PCNA tethers many other replication proteins and DNA polymerases, the delay in DNA replication observed after depletion of Esco1 could have resulted from a number of factors besides loosely attached sister chromatids, including, possibly, reduced PCNA versatility and failure of cohesin to regulate higher-order organisation of replication

factories. It is also plausible to think that since Sororin recruitment to chromatin is coupled with Smc3 acetylation and requires Esco2, and that Sororin competes with Wapl for binding to Pds5 (Nishiyama et al., 2010), loss of acetylation should lead to reduced Sororin recruitment to chromatin, thereby enabling Wapl to continue binding to Pds5 and preventing sister chromatid cohesion establishment.

Recently, it was shown that Ctf4 and Chl1 (Kouprina et al., 1992) physically interact and that this interaction is required for Chl1 function in sister chromatid cohesion (Samora et al., 2016). Chl1 is recruited to the budding yeast DNA replication fork via a conserved Ctf4-interaction peptide (CIP box) motif (Samora et al., 2016). By this interaction, Ctf4 links DNA replication with sister chromatid cohesion establishment (Samora et al., 2016). Originally identified as a DNA polymerase α-interacting factor important for chromosome stability, Ctf4 serves as a structural component of the replisome, linking the MCM helicase via GINS to the DNA polymerase α-primase complex (Kouprina et al., 1992; Miles and Formosa, 1992; Hanna et al., 2001; Gambus et al., 2006, 2009; Lengronne et al., 2006; Tanaka et al., 2009a). In vertebrates, Ctf4 is known as And1, where its role in sister chromatid cohesion is highly conserved (Errico et al., 2009). Ctf4 is a homotrimer to which GINS and DNA polymerase α bind via a shared interaction motif (Simon et al., 2014). Chl1/ChIR1 is a DNA helicase (Gerring et al., 1990) that progresses along single-stranded DNA in the 5'-3' direction (Farina et al., 2008; Hirota and Lahti, 2000) whose ATPase is required in preventing chromosome loss in both yeast and mice (L Holloway, 2000; Inoue et al., 2007). Chl1/ChIR1 promotes sister chromatid cohesion in yeast and humans (Farina et al., 2008; Mayer et al., 2004; Parish et al., 2006; Skibbens, 2004). The finding that deletion of Ctf4 or ChI1 causes synthetic growth defects in the absence of Eco1 (Borges et al., 2013) suggests that Ctf4 and Chl1 support cohesin acetylation by acting in parallel to Eco1 (Esco1/2). Molecularly, it is not yet known how Ctf4 and ChI1 achieve this.

Future experiments should seek to test whether Sororin is recruited to chromatin in the absence of Esco1 and Esco2, e.g. by nuclear fractionation and immunoblotting, using G1/S-synchronised lysates, following depletion of Esco1 and Esco2. My data suggests that while cohesin acetylation may be required for efficient replication fork progression

in mammalian cells, as reported before (Terret *et al.*, 2009), it is the property acquired by cohesin upon acetylation that makes it more competent to regulate DNA replication.

While Wapl is a negative regulator of cohesin (Kueng et al., 2006), Pds5 plays both positive and negative roles in regulating cohesin. Inactivation of either protein has different effects, depending on the organism. *Xenopus* egg extracts depleted of either Wapl or Pds5, or human cells depleted of Wapl, have hypercohesed sister chromatids which fail to resolve at mitosis (Gandhi et al. 2006; Kueng et al. 2006; Shintomi & Hirano 2009). However, *Drosophila* Wapl mutant embryos or yeast Wpl1 and Pds5 mutants have less cohesin on chromatin which results in loosely attached sister chromatids (Panizza et al., 2000; Tanaka et al., 2001; Stead et al., 2003; Rowland et al., 2009; Sutani et al., 2009; Verni et al. 2000).

Loosely attached sister chromatids have also been reported after depletion of Pds5A or Pds5B in human cells (Losada et al., 2005), although previous studies (unpublished) in our lab showed that depletion of either Pds5 or Wapl from HeLa cells results in hypercohesed sister chromatids which cannot resolve at mitosis. Given that the Wapl-Pds5 sub-complex regulates cohesin via a similar mechanism as the Scc2-Scc4 complex, stepwise opening and closing of the cohesin ring, it is plausible to think that the effect of Wapl and Pds5 inactivation in a given organism depends on whether it is the ring opening or ring closing reaction that is affected, hence resulting in varied depletion phenotypes across species.

Cohesin is required for efficient DNA replication during S-phase (Sherwood et al., 2010) because it modulates the size of chromatin loops that likely correspond to replicon units (Guillou et al., 2010). Recent studies have reported that DNA replication and sister chromatid cohesion are linked processes (Samora et al., 2016). Given that Pds5 is an integral member of the cohesin complex and regulates important functions including cohesion establishment, maintenance, and resolution (Panizza et al., 2000), and that recruitment of Esco1 to chromatin, which partly acetylates cohesin to speed replication forks (Terret *et al.*, 2009), depends on Pds5 (Minamino et al., 2015), it is conceivable that loss of Pds5 should inhibits DNA replication.

Preliminary studies (unpublished) in our lab demonstrated that depletion of either Pds5A or Pds5B from HeLa cells increased the amount of time cells spent in S-phase. My data shows that depletion of Pds5 proteins significantly reduces BrdU incorporation (Figures 4.8B) by either asynchronous (Figure 4.8C) or synchronised (Figure 4.8D) population of HeLa cells, and that cells depleted of Pds5 proteins take longer to complete S-phase (Figure 4.9C), as earlier observed in our preliminary studies (unpublished). This data suggests that loss of Pds5 delays DNA replication. Further analysis of DNA replication using DNA combing techniques revealed that cells depleted of Pds5 proteins have reduced fork velocity (Figure 4.10D) and increased number of stalled replication forks (Figure 4.10B v and viii), among other defects, suggesting that Pds5 proteins are required for efficient replication fork progression during DNA replication.

It is still not yet clear how Pds5 regulates DNA replication. Among the many functions of Pds5 is to destabilise cohesin on chromatin, in complex with Wapl, before DNA replication (Gerlich et al., 2006; Nishiyama et al., 2010). According to one of the models of cohesion establishment (Figure 5.2B), the cohesin ring must open up to allow the passage of the replication fork, and the Wapl-Pds5 sub-complex upstream of replication forks allows the passage of the replication forks by disengaging the Scc1-Smc3 interface. According to this model, it is conceivable that depletion of Pds5 proteins should compromise cohesin structures on chromatin, possibly by locking cohesin on chromatin, thereby blocking the passage of replication forks or slowing down the rate at which forks pass through the cohesin rings, resulting in unstable replication forks that cannot replicate DNA efficiently (Figures 4.8, 4.9, and 4.10). My data supports the model of cohesion establishment shown in Figure 5.2B.

Recent studies have reported that Wapl inactivation speeds up DNA replication in both yeast and human cells (Lopez-Serra et al., 2013b; Manning et al., 2014), suggesting that the absence of Wapl from chromatin does not hinder the passage of the replication fork. However, my data shows that depletion of Wapl has no effect on DNA replication (Figure 4.12), although it dispels speculation that Wapl depletion may have similar effects as Pds5 depletion (locking cohesin on chromatin: see data in text above).

Given that Wapl is a cohesin destabilising factor when bound to Pds5, it is possible that its depletion supports DNA replication (Lopez-Serra et al., 2013b; Manning et al., 2014) by allowing stable binding of cohesin to chromatin. Chromatin accumulation of Scc1 at 8 h after release from Aphidicolin block and increased Smc3 acetylation (Figure 4.11) after Wapl depletion supports this notion. Consistent with previous reports which show the requirement for cohesin in DNA replication (Guillou *et al.*, 2010; Sherwood *et al.*, 2010), removal of the anti-establishment complex (Wapl-Pds5) resulted in reconstitution of DNA replication in cells depleted of both Pds5 and Wapl (Figure 4.13), suggesting that more cohesin was stabilised on chromatin (behind the forks) and that the defect in DNA replication observed after depletion of Pds5 alone can be rescued by depleting both Pds5 and Wapl. However, depletion of Wapl and Pds5 resulted in less cohesin (Scc1 and Smc3) recruited to chromatin (Figure 4.11), suggesting that it is not the amount but the state of cohesin on chromatin that determines fork progression. This data suggests that depletion of Pds5 alone abolishes the dynamic state of cohesin upstream of the replication forks, possibly locking it on chromatin, and consequently deterring the passage of the replication forks. This data is in support of the model that proposes that the cohesin ring must open up during DNA replication to allow the passage of the replication forks (see Figure 5.2B, page 160). However, the finding that Wapl-depleted cells replicate their DNA normally (Figures 4.12 and 4.13) but are characterised by hypercohesed sister chromatids (unpublished data in the lab) and persistent cohesin at mitosis (Figure 4.11) shows that exit gate (Beckouët et al., 2016; Buheitel & Stemmann, 2013; Chan et al., 2012) disengagement is not essential for DNA replication. This data supports the model shown in Figure 5.2A, that the replisome passes through the cohesin ring.

Surprisingly, depletion of Esco1 and Esco2 prevents Smc3 acetylation and delays DNA replication (Chapter 3, Figures 3.9, 3.10, and 3.11). This is contrary to my other results that show that depletion of Wapl causes more Smc3 acetylation (Figure 4.11) without slowing down DNA replication (Figure 4.12). This data implies that the delay in DNA replication observed after depletion of Pds5 (Figures 4.8, 4.9, and 4.10) was neither a consequence of Smc3 acetylation nor the reduction in chromatin-bound Wapl. Interestingly, a number of proteins important in sister chromatid cohesion

establishment have been identified using genetic screens in yeast. These include PCNA, Ctf4, and Chl1/ChIR1 (Mayer et al., 2001; Hanna et al., 2001; Skibbens, 2004).

Although these proteins are not part of the cohesin complex, they contribute to the establishment of sister chromatid cohesion, as inactivation of their pairwise combinations results in additive sister chromatid cohesion defects and lethality (Xu et al., 2007). Depletion of any of these proteins reduces cohesin acetylation during S phase, suggesting that they all act at least in part by facilitating the acetylation reaction (Borges et al., 2013). Deletion of Ctf4 or Chl1 causes a marked synthetic growth defect in the absence of Eco1, suggesting that Ctf4 and Chl1 support cohesin acetylation by acting in parallel to Eco1 (Borges et al., 2013).

PCNA is a homotrimeric sliding clamp that tethers DNA polymerases and other replication proteins, including Eco1, to replication forks (Moldovan et al., 2007). Recently, it was shown that Esco1's recruitment to chromatin requires Pds5 (Minamino et al., 2015). Consistent with this finding, my data shows that depletion of either Wapl or Pds5A and Wapl blocks the recruitment of Esco1, but not Esco2, to chromatin (Figure 4.11).

Recently, it was shown that Ctf4 and Chl1 physically interact and that this interaction is required for Chl1 function in sister chromatid cohesion (Samora et al., 2016). The Ctf4-Chl1 interaction suggests a structural role for Chl1 in cohesion establishment that might involve a direct interaction with cohesin at replication forks, and that Ctf4 forms an interaction hub within the replisome that links replication fork progression to sister chromatid cohesion establishment (Samora et al., 2016). This data and other previous studies (Guillou et al., 2010; Sherwood et al., 2010) suggests that the absence of a versatile cohesion establishment factor such as Pds5 should destabilise the replication forks due to failure to establish sister chromatid cohesion. This might consequently lead to activation of the DNA damage checkpoint response, as unstable replication forks have been shown to be prime sources of DNA damage in both prokaryotes and eukaryotes (Heller & Marians, 2006). Consistent with this notion, depletion of either Pds5A or Pds5B led to the phosphorylation of Chk1 on ser317 (Figure 4.14A), suggesting that loss of Pds5 proteins activates the DNA damage checkpoint response. Furthermore,

my data revealed single and double strand breaks in both Pds5A and Pds5B-depleted cells (Figures 4.14B and C).

Taken together, my data suggests that the delay in DNA replication observed after depletion of Pds5 proteins (Figures 4.8, 4.9, and 4.10) resulted from failure to establish sister chromatid cohesion behind the replication forks and loss of the Wapl-Pds5 sub-complex's ability to keep cohesin in a dynamic state upstream of the replication forks, resulting in DNA strand breaks (both single and double) due to cohesin's anomalous conformational change upon acetylation and binding of Sororin to SA1/2 only (in the absence of Pds5). The resultant DNA damage would further delay replication as sister chromatid cohesion which is required for the integrity of the DNA damage checkpoints (Lightfoot *et al.*, 2011) cannot be established, since Pds5 proteins are lacking, thereby compromising the DNA damage repair mechanism and destabilising the replication forks, which results in constitutively activated DNA damage checkpoint response which delays DNA replication.

5.5 The importance of cohesin acetylation in sister chromatid cohesion

The data presented in Chapter 3 shows that depletion of acetyltransferases Esco1 and Esco2 results in precocious sister chromatid separation (Figure 3.13), consistent with previous reports (Minamino et al., 2015). This data suggests that during S-phase cells failed to establish sister chromatid cohesion, possibly due to loss of acetylation and failure to recruit Sororin upon Esco1 and Esco2 depletion (Figure 3.10). Loosely attached sister chromatids cannot align at the metaphase plate and separate precociously, leading to chromosome missegregation.

In normal cells, missegregation is usually prevented by the spindle assembly checkpoint, which is activated in the face of aberrant regulation such as unattached kinetochores (see Figure 1.3, page 9) (Bharadwaj & Yu, 2004; Barbosa et al., 2011). Depletion of Esco1 and Esco2 in HeLa cells resulted in detachment of cells from tissue culture plates (see Figures 3.19, page 100, and A3, page 208). These floating cells could not incorporate BrdU, suggesting that they had already exited S-phase and were most likely arrested in mitosis due to loosely attached sister chromatids. To be able to definitively say that

depletion of Esco1 and Esco2 activates the spindle assembly checkpoint, future experiments must seek to stain for markers such as Mad2, which localise to unattached kinetochores.

Failure to establish sister chromatid cohesion has many adverse consequences for chromosome segregation, including multilobed nuclei (Figure 3.14), multiple spindle poles (Figure 3.15), chromosomal bridges (Figure 3.16), and micronuclei (Figure 3.17). This data suggests that loss of acetylation upon depletion of Esco1 and Esco2 results in loosely attached sister chromatids, which eventually impairs chromatin organisation and leads to chromosome missegregation. This set of data was generated using transformed cells (HeLa) that have inactive p53 (Scheffner, 1998; Hietanen, 2000) and it is not surprising to note that some cells evaded the spindle assembly checkpoint and proceeded to telophase, carrying with them numerous abnormalities such as chromosomal bridges (Figure 3.16) and phenotypes suggestive of aneuploidy, micronuclei (3.17) and multiple spindle poles (Figure 3.15).

Cells have evolved mechanisms such as apoptosis and senescence by which they maintain genome integrity and ensure that defective DNA is not propagated and passed on to new daughter cells. My data shows that HeLa cells depleted of Esco1 and Esco2 undergo apoptosis (Figures 3.18A and B). This was confirmed by cleavage of Caspase 3 (Figure 3.18C), suggesting that Esco1 and Esco2 are required for prevention of apoptosis. Surprisingly, depletion of either Esco1, Esco2, or both Esco1 and Esco2 proteins from RPE1 cells did not induce apoptosis (Figure 3.18A, bottom panels) but was characterised by low cell growth (Figure 3.19) and senescence (Figure 3.20A, B, and C). Primary cells like RPE1 contain functional p53 (Bodnar et al., 1998; Jiang et al., 1999; Liu et al., 2006) and are therefore able to induce senescence in the face of aberrant regulation such as loosely attached sister chromatids. This data showed that loss of acetylation inhibits cell proliferation, induces apoptosis in transformed cells, and initiates senescence in primary cells. Collectively, my data shows that cohesin acetylation is vital for the establishment of sister chromatid cohesion, failure of which inhibits cellular proliferation and induces different cellular fates, depending on cell type.

A recent study has reported that there is a strong correlation between Esco1 expression and bladder cancer (Zhang et al., 2016). Esco2 is reported to be one of the proteins that are highly upregulated in aggressive melanoma (Ryu et al., 2007). The disparity in cell fate observed upon depletion of Esco1 and Esco2 has interesting implications that can be exploited by therapeutics aimed at alleviating tumour growths by selectively targeting these proteins. Transformed (cancerous) cells can be selectively eliminated by having cancer drugs that target Esco1 and Esco2, since both primary (RPE1) and transformed (HeLa) cells employ normal cellular responses (senescence and apoptosis) to depletion of Esco1 and Esco2 to halt propagation of defective chromosomes. These interventions could be aimed at only mitigating overly expressed Esco1 and Esco2 mRNAs in malignancy to tolerable levels, to avoid detrimental effects of Esco1 and Esco2 complete knockdown. Esco1 and Esco2 are potential targets for cancer therapy.

5.6 Concluding remarks

In recent years, major advances have been made in the quest to elucidate molecular mechanisms of cohesin regulation. Cohesin is an evolutionarily conserved multi-subunit protein complex that mediates sister chromatid cohesion. All known functions of cohesin appear to involve its capacity to embrace DNA molecules within its ring-shaped structure. Cohesin comprises many associated proteins that have been shown to be important for its normal functions. These include Pds5 and acetyltransferases Esco1 and Esco2. Pds5 has two homologs, Pds5A and Pds5B. In prophase and telophase or G1, Pds5 proteins form a complex with another cohesin regulatory protein, Wapl, and destabilize the interaction of cohesin with chromatin. In S-phase, Pds5 proteins are important in the establishment of sister chromatid cohesion, upon acetylation of the cohesin core-subunit Smc3 by both Esco1 and Esco2, following the passage of the replication fork. Recent studies have posted conflicting results on the role of cohesin acetylation in regulating DNA replication. Although Pds5 has been studied extensively with regard to its participation in regulating sister chromatid cohesion, its role in regulating DNA replication was unknown, until now.

The work presented in this thesis has fulfilled the overall aim of the study, which was to characterise the Esco1 and Esco2 proteins in the mammalian cell cycle and investigate

the role of Pds5 proteins specifically in DNA replication. The data presented here indicate that Pds5 and acetyltransferases Esco1 and Esco2 are functionally important in DNA replication. Although both Esco1 and Esco2 localise to chromatin in interphase, these proteins are differentially regulated in mitosis; Esco1 is phosphorylated while Esco2 is degraded. Depletion of either Esco1 or Esco2 prevents Smc3 acetylation, albeit by only a smaller fraction in Esco2-depleted cells. However, depletion of either Esco1 or Esco2 results in precocious separation of sister chromatids, delay in DNA replication, apoptosis or senescence, and chromosome missegregation.

Pds5A has a shorter chromatin residence time in mitosis compared to Pds5B. The total protein levels of both Pds5A and Pds5B remain constant throughout the cell cycle. Like cohesin, Pds5 proteins are loaded onto chromatin in telophase and dissociate from chromatin at mitosis. Depletion of Pds5 proteins is characterised by both single and double strand break and ultimately activation of the DNA damage checkpoint. Depletion of either Pds5A or Pds5B delays DNA replication. Depletion of the anti-establishment complex Pds5A and Wapl rescues the defect in DNA replication observed when Pds5A is depleted alone. Pds5 seems to regulate DNA replication by facilitating chromatin organization and recruitment of cohesin regulatory proteins to chromatin.

This work has uncovered a number of novel insights into the roles of Pds5 proteins and acetyltransferases Esco1 and Esco2 and adds substantially to our current understanding of cohesin regulation. I have demonstrated, for the first time, that Pds5 proteins are required for efficient fork progression during DNA replication, and that depletion of Pds5 proteins induces DNA damage which in turn activates the intra S-phase DNA damage checkpoint that slows DNA replication. I have further shown that the delay in DNA replication observed after depleting Pds5A can be rescued by depleting the anti-establishment sub-complex, Wapl and Pds5A. I have also shown, for the first time, that not only are Esco1 and Esco2 proteins important for prevention of aneuploidy, but also apoptosis and senescence. Importantly, I have demonstrated that acetylation on its own may not determine the rate of DNA replication; my data is suggestive of the property that cohesin acquires in S-phase that makes it more competent to regulate DNA replication.

This research has thrown up many questions in need of further investigation. What is now needed is a study exploring protein localisation and cellular fate after mutating the phosphorylation sites of Esco1 and the KEN box of Esco2. Identifying the binding partners of Esco1 and Esco2 will help clarify how loss of acetylation results in apoptosis or senescence. Whether these cellular responses are merely a consequence of loosely attached sister chromatids is unknown at the moment.

Further research should also investigate whether cohesion establishment factors such as Sororin are recruited to chromatin in the absence of Esco1 and Esco2. It will also be important to test if Pds5 proteins and acetyltransferases Esco1 and Esco2 are important in the regulation of the length of chromatin loops that house replicon units. Investigating how the absence of Pds5 proteins triggers DNA damage will also be key to unlocking the mechanism behind the delay in DNA replication upon Pds5 depletion. Whether this results from cohesin's anomalous conformational change upon acetylation and binding of Sororin to SA1/2 only in the absence of Pds5, causing strain and breaks in entrapped DNA strands, remains speculative.

Chapter 6 - REFERENCES

Alberts, B., 2008. *Molecular biology of the cell* 5th edition ed. New York: Garland Science.

Altan-Bonnet, N., 2007. Imaging the Golgi apparatus in living mitotic cells. *Methods in Molecular Biology.* **390,** 309-328.

Althubiti, M., Lezina, L., Carrera, S., Jukes-Jones, R., Giblett, S.M., Antonov, A., Barlev, N., Saldanha, G.S., Pritchard, C.A., Cain, K., Macip, S., 2014. Characterization of novel markers of senescence and their prognostic potential in cancer. *Cell Death & Disease.* **5,** e1528.

Banfalvi, G., 2011. Overview of cell synchronization. *Methods in Molecular Biology.* **761,** 1-23.

Barber, T.D., McManus, K., Yuen, K.W.Y., Reis, M., Parmigiani, G., Shen, D., Barrett, I., Nouhi, Y., Spencer, F., Markowitz, S., Velculescu, V.E., Kinzler, K.W., Vogelstein, B., Lengauer, C., Hieter, P., 2008. Chromatid cohesion defects may underlie chromosome instability in human colorectal cancers. *Proceedings of the National Academy of Sciences of the United States of America.* **105,** 3443-3448.

Barbosa, J., Nascimento, A.V., Faria, J., Silva, P., Bousbaa, H., 2011. The spindle assembly checkpoint: Perspectives in tumorigenesis and cancer therapy. *Frontiers in Biology.* **6,** 147-155.

Barr, F.A., Sillje, H.H., Nigg, E.A., 2004. Polo-like kinases and the orchestration of cell division. *Nature Reviews Molecular Cell Biology.* **5,** 429-440.

Bartek, J. & Lukas, J., 2003. Chk1 and Chk2 kinases in checkpoint control and cancer. *Cancer Cell.* **3,** 421-429.

Baumann, K., 2013. CHROMOSOMES Architectural cohesin. *Nature Reviews Molecular Cell Biology.* **14,** 607-607.

Beckouët, F., Hu, B., Roig, M.B., Sutani, T., Komata, M., Uluocak, P., Katis, V.L., Shirahige, K., Nasmyth, K., 2010. An Smc3 Acetylation Cycle Is Essential for Establishment of Sister Chromatid Cohesion. *Molecular Cell.* **39,** 689-699.

Beisswanger, S., Stephan, W., De Lorenzo, D., 2006. Evidence for a selective sweep in the wapl region of Drosophila melanogaster. *Genetics.* **172,** 265-274.

Ben-Shahar, T.R., Heeger, S., Lehane, C., East, P., Flynn, H., Skehel, M., Uhlmann, F., 2008. Eco1-dependent cohesin acetylation during establishment of sister chromatid cohesion. *Science.* **321,** 563-566.

Bertoli, C., Skotheim, J.M., de Bruin, R.A.M., 2013. Control of cell cycle transcription during G1 and S phases. *Nature Reviews Molecular Cell Biology.* **14,** 518-528.

Bharadwaj, R. & Yu, H., 2004. The spindle checkpoint, aneuploidy, and cancer. *Oncogene.* **23,** 2016-2027.

Bharti, S.K., Khan, I., Banerjee, T., Sommers, J.A., Wu, Y., Brosh, R.M.J., 2014. Molecular functions and cellular roles of the ChlR1 (DDX11) helicase defective in the rare cohesinopathy Warsaw breakage syndrome. *Cellular & Molecular Life Sciences.* **71,** 2625-2639.

Birkenbihl, R.P. & Subramani, S., 1992. Cloning and characterization of rad21 an essential gene of Schizosaccharomyces pombe involved in DNA double-strand-break repair. *Nucleic Acids Research.* **20,** 6605-6611.

Blat, Y. & Kleckner, N., 1999. Cohesins bind to preferential sites along yeast chromosome III, with differential regulation along arms versus the centric region. *Cell.* **98,** 249-259.

Bodnar, A.G., Ouellette, M., Frolkis, M., Holt, S.E., Chiu, C.P., Morin, G.B., Harley, C.B., Shay, J.W., Lichtsteiner, S., Wright, W.E., 1998. Extension of life-span by introduction of telomerase into normal human cells. *Science.* **279,** 349-352.

Borges, V., Lehane, C., Lopez-Serra, L., Flynn, H., Skehel, M., Rolef Ben-Shahar, T., Uhlmann, F., 2010. Hos1 deacetylates Smc3 to close the cohesin acetylation cycle. *Molecular Cell.* **39,** 677-688.

Borges, V., Smith, D.J., Whitehouse, I., Uhlmann, F., 2013. An Eco1-independent sister chromatid cohesion establishment pathway in S. cerevisiae. *Chromosoma.* **122,** 121-134.

Brands, A. & Skibbens, R.V., 2005. Ctf7p/Eco1p exhibits acetyltransferase activity--but does it matter?. *Current Biology.* **15,** R50-1.

Buheitel, J. & Stemmann, O., 2013. Prophase pathway-dependent removal of cohesin from human chromosomes requires opening of the Smc3-Scc1 gate. *EMBO Journal.* **32,** 666-676.

Buongiorno-Nardelli, M., Micheli, G., Carri, M.T., Marilley, M., 1982. A relationship between replicon size and supercoiled loop domains in the eukaryotic genome. *Nature.* **298,** 100-102.

Campbell, J.L. & Cohen-Fix, O., 2002. Chromosome cohesion: ring around the sisters? *Trends in Biochemical Sciences.* **27,** 492-495.

Carretero M, Ruiz-Torres M, Rodriguez-Corsino M, Barthelemy I, Losada A, 2013. Pds5B is required for cohesion establishment and Aurora B accumulation at centromeres. *EMBO Journal.* **32,** 2938-2949.

Caulin, C., Salvesen, G.S., Oshima, R.G., 1997. Caspase cleavage of keratin 18 and reorganization of intermediate filaments during epithelial cell apoptosis. *Journal of Cell Biology.* **138,** 1379-1394.

Chambon, J., Touati, S.A., Berneau, S., Cladiere, D., Hebras, C., Groeme, R., McDougall, A., Wassmann, K., 2013. The PP2A Inhibitor I2PP2A Is Essential for Sister Chromatid Segregation in Oocyte Meiosis II. *Current Biology.* **23,** 485-490.

Chan, K.-., Gligoris, T., Upcher, W., Kato, Y., Shirahige, K., Nasmyth, K., Beckouët, F., 2013. Pds5 promotes and protects cohesin acetylation. *Proceedings of the National Academy of Sciences of the United States of America.* **110,** 13020-13025.

Chan, K., Roig, M.B., Hu, B., Beckouet, F., Metson, J., Nasmyth, K., 2012. Cohesin's DNA Exit Gate Is Distinct from Its Entrance Gate and Is Regulated by Acetylation. *Cell.* **150,** 961-974.

Chatterjee, A., Zakian, S., Hu, X.-., Singleton, M.R., 2013. Structural insights into the regulation of cohesion establishment by Wpl1. *EMBO Journal.* **32,** 677-687.

Cheeseman, I.M. & Desai, A., 2008. Molecular architecture of the kinetochore-microtubule interface. *Nature Reviews Molecular Cell Biology.* **9,** 33-46.

Chen F, Kamradt M, Mulcahy M, Byun Y, Xu H, McKay MJ, Cryns VL, 2002. Caspase proteolysis of the cohesin component RAD21 promotes apoptosis. *Journal of Biological Chemistry.* **277,** 16775-16781.

Chen, M., Ryan, C.E., Piwnica-Worms, H., 2003. Chk1 kinase negatively regulates mitotic function of Cdc25A phosphatase through 14-3-3 binding. *Molecular & Cellular Biology.* **23,** 7488-7497.

Chien, R., Zeng, W., Kawauchi, S., Bender, M.A., Santos, R., Gregson, H.C., Schmiesing, J.A., Newkirk, D.A., Kong, X., Ball, A.R.J., Calof, A.L., Lander, A.D., Groudine, M.T., Yokomori, K., 2011. Cohesin mediates chromatin interactions that regulate mammalian beta-globin expression. *Journal of Biological Chemistry.* **286,** 17870-17878.

Ciosk, R., Shirayama, M., Shevchenko, A., Tanaka, T., Toth, A., Shevchenko, A., Nasmyth, K., 2000. Cohesin's binding to chromosomes depends on a separate complex consisting of Scc2 and Scc4 proteins. *Molecular Cell.* **5,** 243-254.

Clarke, A.S., Tang, T.T., Ooi, D.L., Orr-Weaver, T.L., 2005. POLO kinase regulates the Drosophila centromere cohesion protein MEI-S332. *Developmental Cell.* **8,** 53-64.

Clarke, A. & Orr-Weaver, T.L., 2006. Sister chromatid cohesion at the centromere: Confrontation between kinases and phosphatases? *Developmental Cell.* **10,** 544-547.

Clift, D. & Marston, A.L., 2011. The role of shugoshin in meiotic chromosome segregation. *Cytogenetic & Genome Research.* **133,** 234-242.

Cohen-Fix, O., 2001. The making and breaking of sister chromatid cohesion. *Cell.* **106,** 137-140.

Collin, P., Nashchekina, O., Walker, R., Pines, J., 2013. The spindle assembly checkpoint works like a rheostat rather than a toggle switch. *Nature Cell Biology.* **15,** 1378-1385.

Coudreuse, D. & Nurse, P., 2010. Driving the cell cycle with a minimal CDK control network. *Nature.* **468,** 1074-U474.

Courbet, S., Gay, S., Arnoult, N., Wronka, G., Anglana, M., Brison, O., Debatisse, M., 2008. Replication fork movement sets chromatin loop size and origin choice in mammalian cells. *Nature.* **455,** 557-560.

Cuadrado, A., Remeseiro, S., Gomez-Lopez, G., Pisano, D.G., Losada, A., 2012. The specific contributions of cohesin-SA1 to cohesion and gene expression Implications for cancer and development. *Cell Cycle.* **11,** 2233-2238.

Cunningham, M.D., Gause, M., Cheng, Y., Noyes, A., Dorsett, D., Kennison, J.A., Kassis, J.A., 2012. Wapl antagonizes cohesin binding and promotes Polycomb-group silencing in Drosophila. *Development.* **139,** 4172-4179.

Dai, W., 2009. Suppression of genomic instabilities caused by chromosome mis-segregation: a perspective from studying BubR1 and Sgo1. *Journal of the Formosan Medical Association.* **108,** 904-911.

Deardorff, M.A., Kaur, M., Yaeger, D., Rampuria, A., Korolev, S., Pie, J., Gil-Rodríguez, C., Arnedo, M., Loeys, B., Kline, A.D., Wilson, M., Lillquist, K., Siu, V., Ramos, F.J., Musio, A., Jackson, L.S., Dorsett, D., Krantz, I.D., 2007. Mutations in cohesin complex members SMC3 and SMC1A cause a mild variant of Cornelia de Lange syndrome with predominant mental retardation. *American Journal of Human Genetics.* **80,** 485-494.

Deardorff, M.A., Bando, M., Nakato, R., Watrin, E., Itoh, T., Minamino, M., Saitoh, K., Komata, M., Katou, Y., Clark, D., Cole, K.E., De Baere, E., Decroos, C., Di Donato, N., Ernst, S., Francey, L.J., Gyftodimou, Y., Hirashima, K., Hullings, M., Ishikawa, Y., Jaulin, C., Kaur, M., Kiyono, T., Lombardi, P.M., Magnaghi-Jaulin, L., Mortier, G.R., Nozaki, N., Petersen, M.B., Seimiya, H., Siu, V.M., Suzuki, Y., Takagaki, K., Wilde, J.J., Willems, P.J., Prigent, C., Gillessen-Kaesbach, G., Christianson, D.W., Kaiser, F.J., Jackson, L.G., Hirota, T., Krantz, I.D., Shirahige, K., 2012. HDAC8 mutations in Cornelia de Lange syndrome affect the cohesin acetylation cycle. *Nature.* **489,** 313-317.

Denison, S.H., Kafer, E., May, G.S., 1993. Mutation in the bimD gene of Aspergillus nidulans confers a conditional mitotic block and sensitivity to DNA damaging agents. *Genetics.* **134,** 1085-1096.

Diaz-Martinez, L.A. & Clarke, D.J., 2009. Chromosome cohesion and the spindle checkpoint. *Cell Cycle.* **8,** 2733-2740.

Diaz-Martinez, L.A., Gimenez-Abian, J.F., Clarke, D.J., 2008. Chromosome cohesion - rings, knots, orcs and fellowship. *Journal of Cell Science.* **121,** 2107-2114.

Diaz-Martinez, L.A., Gimenez-Abian, J.F., Clarke, D.J., 2007. Regulation of centromeric cohesion by sororin independently of the APC/C. *Cell Cycle.* **6,** 714-724.

Dobie, K.W., Kennedy, C.D., Velasco, V.M., McGrath, T.L., Weko, J., Patterson, R.W., Karpen, G.H., 2001. Identification of chromosome inheritance modifiers in Drosophila melanogaster. *Genetics.* **157,** 1623-1637.

Dong, Q. & Han, F., 2012. Phosphorylation of histone H2A is associated with centromere function and maintenance in meiosis. *Plant Journal.* **71,** 800-809.

Dorsett, D., 2007. Roles of the sister chromatid cohesion apparatus in gene expression, development, and human syndromes. *Chromosoma.* **116,** 1-13.

Dorsett, D., Eissenberg, J.C., Misulovin, Z., Martens, A., Redding, B., McKim, K., 2005. Effects of sister chromatid cohesion proteins on cut gene expression during wing development in Drosophila. *Development.* **132,** 4743-4753.

Dorsett, D. & Strom, L., 2012. The ancient and evolving roles of cohesin in gene expression and DNA repair. *Current Biology.* **22,** R240-50.

Dreier, M.R., Bekier,Michael E.,,II, Taylor, W.R., 2011. Regulation of sororin by Cdk1-mediated phosphorylation. *Journal of Cell Science.* **124,** 2976-2987.

Dudas, A., Ahmad, S., Gregan, J., 2011. Sgo1 is required for co-segregation of sister chromatids during achiasmate meiosis I. *Cell Cycle.* **10,** 951-955.

Earnshaw, W.C. & Mackay, A.M., 1994. Role of nonhistone proteins in the chromosomal events of mitosis. *FASEB Journal.* **8,** 947-956.

Eichinger, C.S., Kurze, A., Oliveira, R.A., Nasmyth, K., 2013. Disengaging the Smc3/kleisin interface releases cohesin from Drosophila chromosomes during interphase and mitosis. *EMBO Journal.* **32,** 656-665.

Errico, A., Cosentino, C., Rivera, T., Losada, A., Schwob, E., Hunt, T., Costanzo, V., 2009. Tipin/Tim1/And1 protein complex promotes Pol alpha chromatin binding and sister chromatid cohesion. *EMBO Journal.* **28,** 3681-3692.

Errico, A. & Costanzo, V., 2012. Mechanisms of replication fork protection: a safeguard for genome stability. *Critical Reviews in Biochemistry & Molecular Biology.* **47,** 222-235.

Farina, A., Shin, J.-., Kim, D.-., Bermudez, V.P., Kelman, Z., Seo, Y.-., Hurwitz, J., 2008. Studies with the human cohesin establishment factor, ChlR1: Association of ChlR1 with Ctf18-RFC and Fen1. *Journal of Biological Chemistry.* **283,** 20925-20936.

Furnari, B., Rhind, N., Russell, P., 1997. Cdc25 mitotic inducer targeted by chk1 DNA damage checkpoint kinase. *Science.* **277,** 1495-1497.

Gambus, A., Jones, R.C., Sanchez-Diaz, A., Kanemaki, M., van Deursen, F., Edmondson, R.D., Labib, K., 2006. GINS maintains association of Cdc45 with MCM in replisome progression complexes at eukaryotic DNA replication forks. *Nature Cell Biology.* **8,** 358-366.

Gandhi, R., Gillespie, P.J., Hirano, T., 2006. Human Wapl is a cohesin-binding protein that promotes sister-chromatid resolution in mitotic prophase. *Current Biology.* **16,** 2406-2417.

Gard, S., Light, W., Xiong, B., Bose, T., McNairn, A.J., Harris, B., Fleharty, B., Seidel, C., Brickner, J.H., Gerton, J.L., 2009. Cohesinopathy mutations disrupt the subnuclear organization of chromatin. *Journal of Cell Biology.* **187,** 455-462.

Gause, M., Misulovin, Z., Bilyeu, A., Dorsett, D., 2010. Dosage-Sensitive Regulation of Cohesin Chromosome Binding and Dynamics by Nipped-B, Pds5, and Wapl. *Molecular and Cellular Biology.* **30,** 4940-4951.

Gerlich, D., Koch, B., Dupeux, F., Peters, J.-., Ellenberg, J., 2006. Live-Cell Imaging Reveals a Stable Cohesin-Chromatin Interaction after but Not before DNA Replication. *Current Biology.* **16,** 1571-1578.

Gerring, S.L., Spencer, F., Hieter, P., 1990. The CHL1(CTF1) gene product of Saccharomyces cerevisiae is important for chromosome transmission and normal cell cycle progression in G2/M. *EMBO Journal.* **9,** 4347-4358.

Gerton, J., 2005. Chromosome cohesion: A cycle of holding together and falling apart. *PLoS Biology.* **3,** 0371-0374.

Gibcus, J.H. & Dekker, J., 2013. The hierarchy of the 3D genome. *Molecular Cell.* **49,** 773-782.

Giet, R. & Glover, D.M., 2001. Drosophila aurora B kinase is required for histone H3 phosphorylation and condensin recruitment during chromosome condensation and to organize the central spindle during cytokinesis. *Journal of Cell Biology.* **152,** 669-682.

Gillespie, P.J. & Hirano, T., 2004. Scc2 couples replication licensing to sister chromatid cohesion in Xenopus egg extracts. *Current Biology.* **14,** 1598-1603.

Gillis, L.A., McCallum, J., Kaur, M., DeScipio, C., Yaeger, D., Mariani, A., Kline, A.D., Li, H., Devoto, M., Jackson, L.G., Krantz, I.D., 2004. NIPBL mutational analysis in 120 individuals with Cornelia de Lange syndrome and evaluation of genotype-phenotype correlations. *American Journal of Human Genetics.* **75,** 610-623.

Gligoris, T.G., Scheinost, J.C., Burmann, F., Petela, N., Chan, K., Uluocak, P., Beckouet, F., Gruber, S., Nasmyth, K., Lowe, J., 2014. Closing the cohesin ring: structure and function of its Smc3-kleisin interface. *Science.* **346,** 963-967.

Gonzalez Besteiro, M.A. & Gottifredi, V., 2015. The fork and the kinase: a DNA replication tale from a CHK1 perspective. *Mutation Research-Reviews in Mutation Research.* **763,** 168-180.

Goto, H., Yasui, Y., Nigg, E.A., Inagaki, M., 2002. Aurora-B phosphorylates Histone H3 at serine28 with regard to the mitotic chromosome condensation. *Genes to Cells.* **7,** 11-17.

Goulding, S.E. & Earnshaw, W.C., 2005. Shugoshin: a centromeric guardian senses tension. *Bioessays.* **27,** 588-591.

Gregan, J., Spirek, M., Rumpf, C., 2008. Solving the shugoshin puzzle. *Trends in Genetics.* **24,** 205-207.

Griffith, J.D., Lindsey-Boltz, L.A., Sancar, A., 2002. Structures of the human Rad17-replication factor C and checkpoint Rad 9-1-1 complexes visualized by glycerol spray/low voltage microscopy. *Journal of Biological Chemistry.* **277,** 15233-15236.

Gruber, S., Haering, C.H., Nasmyth, K., 2003. Chromosomal cohesin forms a ring. *Cell.* **112,** 765-777.

Gruber, S., Arumugam, P., Katou, Y., Kuglitsch, D., Helmhart, W., Shirahige, K., Nasmyth, K., 2006. Evidence that loading of cohesin onto chromosomes involves opening of its SMC hinge. *Cell.* **127,** 523-537.

Guacci, V., Koshland, D., Strunnikov, A., 1997. A direct link between sister chromatid cohesion and chromosome condensation revealed through the analysis of MCD1 in S. cerevisiae. *Cell.* **91,** 47-57.

Guillou, E., Ibarra, A., Coulon, V., Casado-Vela, J., Rico, D., Casal, I., Schwob, E., Losada, A., Mendez, J., 2010. Cohesin organizes chromatin loops at DNA replication factories. *Genes & Development.* **24,** 2812-2822.

Gullerova, M. & Proudfoot, N.J., 2008. Cohesin complex promotes transcriptional termination between convergent genes in S. pombe. *Cell.* **132,** 983-995.

Gutierrez-Caballero, C., Cebollero, L.R., Pendas, A.M., 2012. Shugoshins: from protectors of cohesion to versatile adaptors at the centromere. *Trends in Genetics.* **28,** 351-360.

Gutierrez-Caballero, C., Herran, Y., Sanchez-Martin, M., Angel Suja, J., Luis Barbero, J., Llano, E., Pendas, A.M., 2011. Identification and molecular characterization of the mammalian alpha-kleisin RAD21L. *Cell Cycle.* **10,** 1477-1487.

Haarhuis, J.H.I., Elbatsh, A.M.O., Rowland, B.D., 2014. Cohesin and its regulation: On the logic of X-shaped chromosomes. *Developmental Cell.* **31,** 7-18.

Haarhuis, J.H.I., Elbatsh, A.M.O., van den Broek, B., Camps, D., Erkan, H., Jalink, K., Medema, R.H., Rowland, B.D., 2013. WAPL-mediated removal of cohesin protects against segregation errors and aneuploidy. *Current Biology.* **23,** 2071-2077.

Hadjur, S., Williams, L.M., Ryan, N.K., Cobb, B.S., Sexton, T., Fraser, P., Fisher, A.G., Merkenschlager, M., 2009. Cohesins form chromosomal cis-interactions at the developmentally regulated IFNG locus. *Nature.* **460,** 410-413.

Haering, C.H., Lowe, J., Hochwagen, A., Nasmyth, K., 2002. Molecular architecture of SMC proteins and the yeast cohesin complex. *Molecular Cell.* **9,** 773-788.

Haering, C.H., Farcas, A., Arumugam, P., Metson, J., Nasmyth, K., 2008. The cohesin ring concatenates sister DNA molecules. *Nature.* **454,** 297-301.

Haering, C.H. & Jessberger, R., 2012. Cohesin in determining chromosome architecture. *Experimental Cell Research.* **318,** 1386-1393.

Haering, C.H., Schoffnegger, D., Nishino, T., Helmhart, W., Nasmyth, K., Lowe, J., 2004. Structure and stability of cohesin's Smc1-kleisin interaction. *Molecular Cell.* **15,** 951-964.

Hagemann, C., Weigelin, B., Schommer, S., Schulze, M., Al-Jomah, N., Anacker, J., Gerngras, S., Kuehnel, S., Kessler, A.F., Polat, B., Ernestus, R., Patel, R., Vince, G.H., 2011. The cohesin-interacting protein, precocious dissociation of sisters 5A/sister chromatid cohesion protein 112, is up-regulated in human astrocytic tumors. *International Journal of Molecular Medicine.* **27,** 39-51.

Hanna, J.S., Kroll, E.S., Lundblad, V., Spencer, F.A., 2001. Saccharomyces cerevisiae CTF18 and CTF4 are required for sister chromatid cohesion. *Molecular & Cellular Biology.* **21,** 3144-3158.

Hara, K., Zheng, G., Qu, Q., Liu, H., Ouyang, Z., Chen, Z., Tomchick, D.R., Yu, H., 2014. Structure of cohesin subcomplex pinpoints direct shugoshin-Wapl antagonism in centromeric cohesion. *Nature Structural & Molecular Biology.* **21,** 864-870.

Harashima, H., Dissmeyer, N., Schnittger, A., 2013. Cell cycle control across the eukaryotic kingdom. *Trends in Cell Biology.* **23,** 345-356.

Hartman, T., Stead, K., Koshland, D., Guacci, V., 2000. Pds5p is an essential chromosomal protein required for both sister chromatid cohesion and condensation in Saccharomyces cerevisiae. *Journal of Cell Biology.* **151,** 613-626.

Hauf, S., Roitinger, E., Koch, B., Dittrich, C.M., Mechtler, K., Peters, J., 2005. Dissociation of cohesin from chromosome arms and loss of arm cohesion during early mitosis depends on phosphorylation of SA2. *Plos Biology.* **3,** e69.

Hegarat, N., Smith, E., Nayak, G., Takeda, S., Eyers, P.A., Hochegger, H., 2011. Aurora A and Aurora B jointly coordinate chromosome segregation and anaphase microtubule dynamics. *Journal of Cell Biology.* **195,** 1103-1113.

Heidinger-Pauli, J.M., Unal, E., Koshland, D., 2009. Distinct targets of the Eco1 acetyltransferase modulate cohesion in S phase and in response to DNA damage. *Molecular Cell.* **34,** 311-321.

Heller, R.C. & Marians, K.J., 2006. Replisome assembly and the direct restart of stalled replication forks. *Nature Reviews Molecular Cell Biology.* **7,** 932-943.

Heo, S.J., Tatebayashi, K., Ikeda, H., 1999. The budding yeast cohesin gene SCC1/MCD1/RHC21 genetically interacts with PKA, CDK and APC. *Current Genetics.* **36,** 329-338.

Hietanen, S., Lain, S., Krausz, E., Blattner, C., Lane, D.P., 2000. Activation of p53 in cervical carcinoma cells by small molecules. *Proceedings of the National Academy of Sciences of the United States of America.* **97,** 8501-8506.

Higashi, T.L., Ikeda, M., Tanaka, H., Nakagawa, T., Bando, M., Shirahige, K., Kubota, Y., Takisawa, H., Masukata, H., Takahashi, T.S., 2012. The prereplication complex recruits XEco2 to chromatin to promote cohesin acetylation in Xenopus egg extracts. *Current Biology.* **22,** 977-988.

Higgins, J.M.G., 2013. Chromosome segregation: Learning to let go. *Current Biology.* **23,** R883-R885.

Higgins, J.M.G. & Herbert, M., 2013. Nucleosome Assembly Proteins Get SET to Defeat the Guardian of Chromosome Cohesion. *Plos Genetics.* **9,** e1003829.

Hill, V.K., Kim, J., Waldman, T., 2016. Cohesin mutations in human cancer. *Biochimica Et Biophysica Acta.* **1866,** 1-11.

Hinds, P.W., Mittnacht, S., Dulic, V., Arnold, A., Reed, S.I., Weinberg, R.A., 1992. Regulation of retinoblastoma protein functions by ectopic expression of human cyclins. *Cell.* **70,** 993-1006.

Hirano, T., 2005. Condensins: organizing and segregating the genome. *Current Biology.* **15,** R265-75.

Hirano, T., 2005. SMC proteins and chromosome mechanics: from bacteria to humans. *Philosophical Transactions of the Royal Society of London - Series B: Biological Sciences.* **360,** 507-514.

Hirano, T., 2000. Chromosome cohesion, condensation, and separation. *Annual Review of Biochemistry.* **69,** 115-144.

Hirota, Y. & Lahti, J.M., 2000. Characterization of the enzymatic activity of hChlR1, a novel human DNA helicase. *Nucleic Acids Research.* **28,** 917-924.

Hochegger, H., Takeda, S., Hunt, T., 2008. Cyclin-dependent kinases and cell-cycle transitions: does one fit all?. *Nature Reviews Molecular Cell Biology.* **9,** 910-916.

Hoffmann, I., 2006. Protein kinases involved in mitotic spindle checkpoint regulation.

Hopfner, K.P., 2003. Chromosome cohesion: closing time. *Current Biology.* **13,** R866-8.

Horsfield, J.A., Print, C.G., Monnich, M., 2012. Diverse developmental disorders from the one ring: distinct molecular pathways underlie the cohesinopathies. *Frontiers in Genetics.* **3,** 171.

Hou F & Zou H, 2005. Two human orthologues of Eco1/Ctf7 acetyltransferases are both required for proper sister-chromatid cohesion. *Molecular Biology of the Cell.* **16,** 3908-3918.

Hou, C., Dale, R., Dean, A., 2010. Cell type specificity of chromatin organization mediated by CTCF and cohesin. *Proceedings of the National Academy of Sciences of the United States of America.* **107,** 3651-3656.

Houtgraaf, J.H., Versmissen, J., van der Giessen, W.J., 2006. A concise review of DNA damage checkpoints and repair in mammalian cells. *Cardiovascular Revascularization Medicine.* **7,** 165-172.

Hoyt, M.A., Totis, L., Roberts, B.T., 1991. S. cerevisiae genes required for cell cycle arrest in response to loss of microtubule function. *Cell.* **66,** 507-517.

Hu, B., Itoh, T., Mishra, A., Katoh, Y., Chan, K., Upcher, W., Godlee, C., Roig, M.B., Shirahige, K., Nasmyth, K., 2011. ATP hydrolysis is required for relocating cohesin from sites occupied by its Scc2/4 loading complex. *Current Biology.* **21,** 12-24.

Huis in 't Veld,Pim J., Herzog, F., Ladurner, R., Davidson, I.F., Piric, S., Kreidl, E., Bhaskara, V., Aebersold, R., Peters, J., 2014. Characterization of a DNA exit gate in the human cohesin ring. *Science.* **346,** 968-972.

Hyman, T., Watanabe, Y., Yanagida, M., Hirano, T., 2005. Shugoshin protects cohesin complexes at centromeres - Discussion. *Philosophical Transactions of the Royal Society B-Biological Sciences.* **360,** 521-521.

Inoue, A., Li, T., Roby, S.K., Valentine, M.B., Inoue, M., Boyd, K., Kidd, V.J., Lahti, J.M., 2007. Loss of ChlR1 helicase in mouse causes lethality due to the accumulation of aneuploid cells generated by cohesion defects and placental malformation. *Cell Cycle.* **6,** 1646-1654.

Ishiguro, K. & Watanabe, Y., 2007. Chromosome cohesion in mitosis and meiosis. *Journal of Cell Science.* **120,** 367-369.

Ivanov, D. & Nasmyth, K., 2005. A topological interaction between cohesin rings and a circular minichromosome. *Cell.* **122,** 849-860.

Ivanov, D., Schleiffer, A., Eisenhaber, F., Mechtler, K., Haering, C.H., Nasmyth, K., 2002. Eco1 is a novel acetyltransferase that can acetylate proteins involved in cohesion. *Current Biology.* **12,** 323-328.

Jeong, A.L. & Yang, Y., 2013. PP2A function toward mitotic kinases and substrates during the cell cycle. *Bmb Reports.* **46,** 289-294.

Jiang, X.-., Jimenez, G., Chang, E., Frolkis, M., Kusler, B., Sage, M., Beeche, M., Bodnar, A.G., Wahl, G.M., Tlsty, T.D., Chiu, C.-., 1999. Telomerase expression in human somatic cells does not induce changes associated with a transformed phenotype. *Nature Genetics.* **21,** 111-1114.

Jin, H., Guacci, V., Yu, H., 2009. Pds5 is required for homologue pairing and inhibits synapsis of sister chromatids during yeast meiosis. *Journal of Cell Biology.* **186,** 713-725.

Juraj, G., Cornelia, R., Zhang, L., and Lubos, C., 2008. What makes centromeric cohesion resistant to separase cleavage during meiosis I but not during meiosis II? *Cell Cycle.* **7,** 151-153.

Kagey, M.H., Newman, J.J., Bilodeau, S., Zhan, Y., Orlando, D.A., van Berkum, N.L., Ebmeier, C.C., Goossens, J., Rahl, P.B., Levine, S.S., Taatjes, D.J., Dekker, J., Young, R.A., 2010. Mediator and cohesin connect gene expression and chromatin architecture. *Nature.* **467,** 430-435.

Kaiser, F.J., Ansari, M., Braunholz, D., Concepcion Gil-Rodriguez, M., Decroos, C., Wilde, J.J., Fincher, C.T., Kaur, M., Bando, M., Amor, D.J., Atwal, P.S., Bahlo, M., Bowman, C.M., Bradley, J.J., Brunner, H.G., Clark, D., Del Campo, M., Di Donato, N., Diakumis, P., Dubbs, H., Dyment, D.A., Eckhold, J., Ernst, S., Ferreira, J.C., Francey, L.J., Gehlken, U., Guillen-Navarro, E., Gyftodimou, Y., Hall, B.D., Hennekam, R., Hudgins, L., Hullings, M., Hunter, J.M., Yntema, H., Innes, A.M., Kline, A.D., Krumina, Z., Lee, H., Leppig, K., Lynch, S.A., Mallozzi, M.B., Mannini, L., McKee, S., Mehta, S.G., Micule, I., Care4Rare Canada Consortium, Mohammed, S., Moran, E., Mortier, G.R., Moser, J.S., Noon, S.E., Nozaki, N., Nunes, L., Pappas, J.G., Penney, L.S., Perez-Aytes, A., Petersen, M.B., Puisac, B., Revencu, N., Roeder, E., Saitta, S., Scheuerle, A.E., Schindeler, K.L., Siu, V.M., Stark, Z., Strom, S.P., Thiese, H., Vater, I., Willems, P., Williamson, K., Wilson, L.C., University of Washington Center for Mendelian Genomics, Hakonarson, H., Quintero-Rivera, F., Wierzba, J., Musio, A., Gillessen-Kaesbach, G., Ramos, F.J., Jackson, L.G., Shirahige, K., Pie, J., Christianson, D.W., Krantz, I.D., Fitzpatrick, D.R., Deardorff, M.A., 2014. Loss-of-function HDAC8 mutations cause a phenotypic spectrum of Cornelia de Lange syndrome-like features, ocular hypertelorism, large fontanelle and X-linked inheritance. *Human Molecular Genetics.* **23,** 2888-2900.

Kateneva, A. & Dresser, M., 2006. Sister chromatid cohesion remodeling and meiotic recombination. *Cell Cycle.* **5,** 467-471.

Katis, V.L., Galova, M., Rabitsch, K.P., Gregan, J., Nasmyth, K., 2004. Maintenance of cohesin at centromeres after meiosis I in budding yeast requires a kinetochore-associated protein related to MEI-S332. *Current Biology.* **14,** 560-572.

Kawashima, S.A., Tsukahara, T., Langegger, M., Hauf, S., Kitajima, T.S., Watanabe, Y., 2007. Shugoshin enables tension-generating attachment of kinetochores by loading Aurora to centromeres. *Genes & Development.* **21,** 420-435.

Kawauchi, S., Calof, A.L., Santos, R., Lopez-Burks, M.E., Young, C.M., Hoang, M.P., Chua, A., Lao, T., Lechner, M.S., Daniel, J.A., Nussenzweig, A., Kitzes, L., Yokomori, K., Hallgrimsson, B., Lander, A.D., 2009. Multiple organ system defects and transcriptional dysregulation in the Nipbl(+/-) mouse, a model of Cornelia de Lange Syndrome. *PLoS Genetics.* **5,** e1000650.

Keeling, J.W. & Miller, R.K., 2011. Indirect immunofluorescence for monitoring spindle assembly and disassembly in yeast. *Methods in Molecular Biology.* **782,** 231-244.

Kenna, M.A. & Skibbens, R.V., 2003. Mechanical link between cohesion establishment and DNA replication: Ctf7p/Eco1p, a cohesion establishment factor, associates with three different replication factor C complexes. *Molecular and Cellular Biology.* **23,** 2999-3007.

Kerr, G.W., Sarkar, S., Arumugam, P., 2012. How to halve ploidy: lessons from budding yeast meiosis. *Cellular and Molecular Life Sciences.* **69,** 3037-3051.

Kerrebrock, A.W., Moore, D.P., Wu, J.S., Orr-Weaver, T.L., 1995. Mei-S332, a Drosophila protein required for sister-chromatid cohesion, can localize to meiotic centromere regions. *Cell.* **83,** 247-256.

Kiburz, B.M., Amon, A., Marston, A.L., 2008. Shugoshin promotes sister kinetochore biorientation in Saccharomyces cerevisiae. *Molecular Biology of the Cell.* **19,** 1199-1209.

Kitajima, T.S., Kawashima, S.A., Watanabe, Y., 2004. The conserved kinetochore protein shugoshin protects centromeric cohesion during meiosis. *Nature.* **427,** 510-517.

Kitajima, T., Hauf, S., Ohsugi, M., Yamamoto, T., Watanabe, Y., 2005. Human Bub1 defines the persistent cohesion site along the mitotic chromosome by affecting shugoshin localization. *Current Biology.* **15,** 353-359.

Kitajima, T., Sakuno, T., Ishiguro, K., Iemura, S., Natsume, T., Kawashima, S., Watanabe, Y., 2006. Shugoshin collaborates with protein phosphatase 2A to protect cohesin. *Nature.* **441,** 46-52.

Kon, A., Shih, L.-., Minamino, M., Sanada, M., Shiraishi, Y., Nagata, Y., Yoshida, K., Okuno, Y., Bando, M., Nakato, R., Ishikawa, S., Sato-Otsubo, A., Nagae, G., Nishimoto, A., Haferlach, C., Nowak, D., Sato, Y., Alpermann, T., Nagasaki, M., Shimamura, T., Tanaka, H., Chiba, K., Yamamoto, R., Yamaguchi, T., Otsu, M., Obara, N., Sakata-Yanagimoto, M., Nakamaki, T., Ishiyama, K., Nolte, F., Hofmann, W.-., Miyawaki, S., Chiba, S., Mori, H.,

Nakauchi, H., Koeffler, H.P., Aburatani, H., Haferlach, T., Shirahige, K., Miyano, S., Ogawa, S., 2013. Recurrent mutations in multiple components of the cohesin complex in myeloid neoplasms. *Nature Genetics.* **45,** 1232-1237.

Kon, A., Shih, L., Minamino, M., Sanada, M., Shiraishi, Y., Nagata, Y., Yoshida, K., Okuno, Y., Bando, M., Ishikawa, S., Sato-Otsubo, A., Nagae, G., Haferlach, C., Nowak, D., Sato, Y., Alpermann, T., Nagasaki, M., Shimamura, T., Tanaka, H., Chiba, K., Yamamoto, R., Yamaguchi, T., Otsu, M., Obara, N., Sakata-Yanagimoto, M., Nakamaki, T., Ishiyama, K., Nolte, F., Hofmann, W., Miyawaki, S., Chiba, S., Mori, H., Nakauchi, H., Koeffler, H.P., Aburatani, H., Haferlach, T., Shirahige, K., Miyano, S., Ogawa, S., 2012. Recurrent Mutations of Multiple Components of Cohesin Complex in Myeloid Neoplasms. *Blood.* **120,** .

Kondo, T., Matsumoto, K., Sugimoto, K., 1999. Role of a complex containing Rad17, Mec3, and Ddc1 in the yeast DNA damage checkpoint pathway. *Molecular & Cellular Biology.* **19,** 1136-1143.

Kops, G.J.P.L., 2009. Dividing the goods: co-ordination of chromosome biorientation and mitotic checkpoint signalling by mitotic kinases. *Biochemical Society Transactions.* **37,** 971-975.

Koshland, D.E. & Guacci, V., 2000. Sister chromatid cohesion: the beginning of a long and beautiful relationship. *Current Opinion in Cell Biology.* **12,** 297-301.

Kouprina, N., Kroll, E., Bannikov, V., Bliskovsky, V., Gizatullin, R., Kirillov, A., Shestopalov, B., Zakharyev, V., Hieter, P., Spencer, F., 1992. CTF4 (CHL15) mutants exhibit defective DNA metabolism in the yeast Saccharomyces cerevisiae. *Molecular & Cellular Biology.* **12,** 5736-5747.

Krantz, I.D., McCallum, J., DeScipio, C., Kaur, M., Gillis, L.A., Yaeger, D., Jukofsky, L., Wasserman, N., Bottani, A., Morris, C.A., Nowaczyk, M.J.M., Toriello, H., Bamshad, M.J., Carey, J.C., Rappaport, E., Kawauchi, S., Lander, A.D., Calof, A.L., Li, H., Devoto, M., Jackson, L.G., 2004. Cornelia de Lange syndrome is caused by mutations in NIPBL, the human homolog of Drosophila melanogaster Nipped-B. *Nature Genetics.* **36,** 631-635.

Kueng, S., Hegemann, B., Peters, B.H., Lipp, J.J., Schleiffer, A., Mechtler, K., Peters, J.M., 2006. Wapl controls the dynamic association of cohesin with chromatin. *Cell.* **127,** 955-967.

Kulemzina, I., Schumacher, M.R., Verma, V., Reiter, J., Metzler, J., Failla, A.V., Lanz, C., Sreedharan, V.T., Raetsch, G., Ivanov, D., 2012. Cohesin Rings Devoid of Scc3 and Pds5 Maintain Their Stable Association with the DNA. *Plos Genetics.* **8,** e1002856.

Kuroda, M., Oikawa, K., Ohbayashi, T., Yoshida, K., Yamada, K., Mimura, J., Matsuda, Y., Fujii-Kuriyama, Y., Mukai, K., 2005. A dioxin sensitive gene, mammalian WAPL, is implicated in spermatogenesis. *FEBS Letters.* **579,** 167-172.

Kuzminov, A., 2013. The chromosome cycle of prokaryotes. *Molecular Microbiology.* **90,** 214-227.

Kwiatkowski, B.A., Ragoczy, T., Ehly, J., Schubach, W.H., 2004. Identification and cloning of a novel chromatin-associated protein partner of Epstein-Barr nuclear protein 2. *Experimental Cell Research.* **300,** 223-233.

Ladurner, R., Kreidl, E., Ivanov, M.P., Ekker, H., Idarraga-Amado, M.H., Busslinger, G.A., Wutz, G., Cisneros, D.A., Peters, J., 2016. Sororin actively maintains sister chromatid cohesion. *EMBO Journal.* **35,** 635-653.

Lafont, A.L., Song, J., Rankin, S., 2010. Sororin cooperates with the acetyltransferase Eco2 to ensure DNA replication-dependent sister chromatid cohesion. *Proceedings of the National Academy of Sciences of the United States of America.* **107,** 20364-20369.

Lara-Gonzalez, P., Westhorpe, F.G., Taylor, S.S., 2012. The Spindle Assembly Checkpoint. *Current Biology.* **22,** R966-R980.

Laugsch, M., Seebach, J., Schnittler, H., Jessberger, R., 2013. Imbalance of SMC1 and SMC3 cohesins causes specific and distinct effects. *PLoS ONE [Electronic Resource].* **8,** e65149.

Le Bot, N., 2007. Wapl takes cohesin off chromosome arms. *Nature Cell Biology.* **9,** 21-21.

Lee, J., Kumagai, A., Dunphy, W.G., 2001. Positive regulation of Wee1 by Chk1 and 14-3-3 proteins. *Molecular Biology of the Cell.* **12,** 551-563.

Lee, J.Y. & Orr-Weaver, T.L., 2001. The molecular basis of sister-chromatid cohesion. *Annual Review of Cell & Developmental Biology.* **17,** 753-777.

Lemaitre, J., Danis, E., Pasero, P., Vassetzky, Y., Mechali, M., 2005. Mitotic remodeling of the replicon and chromosome structure. *Cell.* **123,** 787-801.

Lengronne, A., Katou, Y., Mori, S., Yokobayashi, S., Kelly, G.P., Itoh, T., Watanabe, Y., Shirahige, K., Uhlmann, F., 2004. Cohesin relocation from sites of chromosomal loading to places of convergent transcription. *Nature.* **430,** 573-578.

Lengronne, A., McIntyre, J., Katou, Y., Kanoh, Y., Hopfner, K., Shirahige, K., Uhlmann, F., 2006. Establishment of sister chromatid cohesion at the S. cerevisiae replication fork. *Molecular Cell.* **23,** 787-799.

Li, Y., Gorbea, C., Mahaffey, D., Rechsteiner, M., Benezra, R., 1997. MAD2 associates with the cyclosome/anaphase-promoting complex and inhibits its activity. *Proceedings of the National Academy of Sciences of the United States of America.* **94,** 12431-12436.

Lightfoot, J., Testori, S., Barroso, C., Martinez-Perez, E., 2011. Loading of meiotic cohesin by SCC-2 is required for early processing of DSBs and for the DNA damage checkpoint. *Current Biology.* **21,** 1421-1430.

Lindqvist, A., Rodriguez-Bravo, V., Medema, R.H., 2009. The decision to enter mitosis: feedback and redundancy in the mitotic entry network. *Journal of Cell Biology.* **185,** 193-202.

Ling, Y., Liebes, L., Ng, B., Buckley, M., Elliott, P.J., Adams, J., Jiang, J., Muggia, F.M., Perez-Soler, R., 2002. PS-341, a novel proteasome inhibitor, induces Bcl-2 phosphorylation and cleavage in association with G2-M phase arrest and apoptosis. *Molecular Cancer Therapeutics.* **1,** 841-849.

Liu, H., Jia, L., Yu, H., 2013. Phospho-H2A and cohesin specify distinct tension-regulated Sgo1 pools at kinetochores and inner centromeres. *Current Biology.* **23,** 1927-1933.

Liu, H., Rankin, S., Yu, H., 2013. Phosphorylation-enabled binding of SGO1-PP2A to cohesin protects sororin and centromeric cohesion during mitosis. *Nature Cell Biology.* **15,** 40-49.

Liu, Q., Guntuku, S., Cui, X.-., Matsuoka, S., Cortez, D., Tamai, K., Luo, G., Carattini-Rivera, S., DeMayo, F., Bradley, A., Donehower, L.A., Elledge, S.J., 2000. Chk1 is an essential kinase that is regulated by Atr and required for the G2/M DNA damage checkpoint. *Genes and Development.* **14,** 1448-1459.

Liu, X., Lei, M., Erikson, R.L., 2006. Normal cells, but not cancer cells, survive severe Plk1 depletion. *Molecular and Cellular Biology.* **26,** 2093-2108.

Logarinho, E. & Bousbaa, H., 2008. Kinetochore-microtubule interactions "in check" by Bub1, Bub3 and BubR1: The dual task of attaching and signalling. *Cell Cycle.* **7,** 1763-1768.

Lopes, C. & Sunkel, C., 2003. The spindle checkpoint: From normal cell division to tumorigenesis. *Archives of Medical Research.* **34,** 155-165.

Lopez-Girona, A., Tanaka, K., Chen, X.B., Baber, B.A., McGowan, C.H., Russell, P., 2001. Serine-345 is required for Rad3-dependent phosphorylation and function of checkpoint kinase Chk1 in fission yeast. *Proceedings of the National Academy of Sciences of the United States of America.* **98,** 11289-11294.

Lopez-Serra, L., Lengronne, A., Borges, V., Kelly, G., Uhlmann, F., 2013. Budding Yeast Wapl Controls Sister Chromatid Cohesion Maintenance and Chromosome Condensation. *Current Biology.* **23,** 64-69.

Losada A, Hirano M, Hirano T, 1998. Identification of Xenopus SMC protein complexes required for sister chromatid cohesion. *Genes & Development.* **12,** 1986-1997.

Losada, A., Hirano, M., Hirano, T., 2002. Cohesin release is required for sister chromatid resolution, but not for condensin-mediated compaction, at the onset of mitosis. *Genes and Development.* **16,** 3004-3016.

Losada, A. & Hirano, T., 2005. Dynamic molecular linkers of the genome: the first decade of SMC proteins. *Genes & Development.* **19,** 1269-1287.

Losada, A., Yokochi, T., Kobayashi, R., Hirano, T., 2000. Identification and characterization of SA/Scc3p subunits in the Xenopus and human cohesin complexes. *Journal of Cell Biology.* **150,** 405-416.

Losada, A., 2014. Cohesin in cancer: chromosome segregation and beyond. *Nature Reviews.Cancer.* **14,** 389-393.

Lundberg, A.S. & Weinberg, R.A., 1998. Functional inactivation of the retinoblastoma protein requires sequential modification by at least two distinct cyclin-cdk complexes. *Molecular & Cellular Biology.* **18,** 753-761.

Luo, X. & Yu, H., 2012. Mitosis: short-circuiting spindle checkpoint signaling. *Current Biology.* **22,** R128-30.

Lyons, N.A. & Morgan, D.O., 2011. Cdk1-dependent destruction of Eco1 prevents cohesion establishment after S phase. *Molecular Cell.* **42,** 378-389.

MacAlpine, H.K., Gordan, R., Powell, S.K., Hartemink, A.J., MacAlpine, D.M., 2010. Drosophila ORC localizes to open chromatin and marks sites of cohesin complex loading. *Genome Research.* **20,** 201-211.

Macip, S., Igarashi, M., Fang, L., Chen, A., Pan, Z., Lee, S.W., Aaronson, S.A., 2002. Inhibition of p21-mediated ROS accumulation can rescue p21-induced senescence. *EMBO Journal.* **21,** 2180-2188.

Macy, B., Wang, M., Yu, H., 2009. The many faces of shugoshin, the "guardian spirit," in chromosome segregation. *Cell Cycle.* **8,** 35-37.

Mailand, N., Falck, J., Lukas, C., Syljuasen, R.G., Welcker, M., Bartek, J., Lukas, J., 2000. Rapid destruction of human Cdc25A in response to DNA damage. *Science.* **288,** 1425-1429.

Malumbres, M. & Barbacid, M., 2009. Cell cycle, CDKs and cancer: a changing paradigm. *Nature Reviews.Cancer.* **9,** 153-166.

Manning, A.L., Yazinski, S.A., Nicolay, B., Bryll, A., Zou, L., Dyson, N.J., 2014. Suppression of genome instability in pRB-deficient cells by enhancement of chromosome cohesion. *Molecular Cell.* **53,** 993-1004.

Mannini, L., Cucco, F., Quarantotti, V., Krantz, I.D., Musio, A., 2013. Mutation spectrum and genotype-phenotype correlation in Cornelia de Lange syndrome. *Human Mutation.* **34,** 1589-1596.

Marchisio, P.C. & Trusolino, L., 1999. Immunofluorescence of cultured cells. *Methods in Molecular Biology.* **96,** 85-92.

Marston, A.L., 2015. Shugoshins: tension-sensitive pericentromeric adaptors safeguarding chromosome segregation. *Molecular & Cellular Biology.* **35,** 634-648.

Marston, A.L. & Amon, A., 2004. Meiosis: cell-cycle controls shuffle and deal. *Nature Reviews Molecular Cell Biology.* **5,** 983-997.

Matsuoka, S., Huang, M., Elledge, S.J., 1998. Linkage of ATM to cell cycle regulation by the Chk2 protein kinase. *Science.* **282,** 1893-1897.

Matsuoka, S., Rotman, G., Ogawa, A., Shiloh, Y., Tamai, K., Elledge, S.J., 2000. Ataxia telangiectasia-mutated phosphorylates Chk2 in vivo and in vitro. *Proceedings of the National Academy of Sciences of the United States of America.* **97,** 10389-10394.

May, K.M. & Hardwick, K.G., 2006. The spindle checkpoint. *Journal of Cell Science.* **119,** 4139-4142.

Mayer, M.L., Gygi, S.P., Aebersold, R., Hieter, P., 2001. Identification of RFC(Ctf18p, Ctf8p, Dcc1p): an alternative RFC complex required for sister chromatid cohesion in S. cerevisiae. *Molecular Cell.* **7,** 959-970.

Mayer, M.L., Pot, I., Chang, M., Xu, H., Aneliunas, V., Kwok, T., Newitt, R., Aebersold, R., Boone, C., Brown, G.W., Hieter, P., 2004. Identification of protein complexes required for efficient sister chromatid cohesion. *Molecular Biology of the Cell.* **15,** 1736-1745.

McAleenan, A., Clemente-Blanco, A., Cordon-Preciado, V., Sen, N., Esteras, M., Jarmuz, A., Aragon, L., 2013. Post-replicative repair involves separase-dependent removal of the kleisin subunit of cohesin. *Nature.* **493,** 250-U270.

McGuinness, B., Hirota, T., Kudo, N., Peters, J., Nasmyth, K., 2005. Shugoshin prevents dissociation of cohesin from centromeres during mitosis in vertebrate cells. *Plos Biology.* **3,** 433-449.

McNairn, A.J. & Gerton, J.L., 2008. Cohesinopathies: One ring, many obligations. *Mutation Research.* **647,** 103-111.

Mehta, G.D., Kumar, R., Srivastava, S., Ghosh, S.K., 2013. Cohesin: Functions beyond sister chromatid cohesion. *FEBS Letters.* **587,** 2299-2312.

Mehta, G.D., Rizvi, S.M.A., Ghosh, S.K., 2012. Cohesin: A guardian of genome integrity. *Biochimica Et Biophysica Acta-Molecular Cell Research.* **1823,** 1324-1342.

Mendez, J. & Stillman, B., 2000. Chromatin association of human origin recognition complex, cdc6, and minichromosome maintenance proteins during the cell cycle: assembly of prereplication complexes in late mitosis. *Molecular & Cellular Biology.* **20,** 8602-8612.

Michaelis, C., Ciosk, R., Nasmyth, K., 1997. Cohesins: chromosomal proteins that prevent premature separation of sister chromatids. *Cell.* **91,** 35-45.

Miles, J. & Formosa, T., 1992. Evidence that POB1, a Saccharomyces cerevisiae protein that binds to DNA polymerase a, acts in DNA metabolism in vivo. *Molecular and Cellular Biology.* **12,** 5724-5735.

Minamino M, Ishibashi M, Nakato R, Akiyama K, Tanaka H, Kato Y, Negishi L, Hirota T, Sutani T, Bando M, Shirahige K, 2015. Esco1 Acetylates Cohesin via a Mechanism Different from That of Esco2. *Current Biology.* **25,** 1694-1706.

Mishiro, T., Ishihara, K., Hino, S., Tsutsumi, S., Aburatani, H., Shirahige, K., Kinoshita, Y., Nakao, M., 2009. Architectural roles of multiple chromatin insulators at the human apolipoprotein gene cluster. *EMBO Journal.* **28,** 1234-1245.

Misulovin, Z., Schwartz, Y.B., Li, X., Kahn, T.G., Gause, M., MacArthur, S., Fay, J.C., Eisen, M.B., Pirrotta, V., Biggin, M.D., Dorsett, D., 2008. Association of cohesin and Nipped-B with transcriptionally active regions of the Drosophila melanogaster genome. *Chromosoma.* **117,** 89-102.

Moldovan, G., Pfander, B., Jentsch, S., 2006. PCNA controls establishment of sister chromatid cohesion during S phase. *Molecular Cell.* **23,** 723-732.

Monahan, K., Rudnick, N.D., Kehayova, P.D., Pauli, F., Newberry, K.M., Myers, R.M., Maniatis, T., 2012. Role of CCCTC binding factor (CTCF) and cohesin in the generation of single-cell diversity of protocadherin-alpha gene expression. *Proceedings of the National Academy of Sciences of the United States of America.* **109,** 9125-9130.

Monnich, M., Kuriger, Z., Print, C.G., Horsfield, J.A., 2011. A zebrafish model of Roberts syndrome reveals that Esco2 depletion interferes with development by disrupting the cell cycle. *PLoS ONE [Electronic Resource].* **6,** e20051.

Moore, D.P., Page, A.W., Tang, T.T., Kerrebrock, A.W., Orr-Weaver, T.L., 1998. The cohesion protein MEI-S332 localizes to condensed meiotic and mitotic centromeres until sister chromatids separate. *Journal of Cell Biology.* **140,** 1003-1012.

Morgan, D.O., 2007. ***The Cell Cycle:*** *Principles of Control.* London: New Science Press Ltd.

Morgan, D.O., 1999. Regulation of the APC and the exit from mitosis. *Nature Cell Biology.* **1,** E47-53.

Muir, K.W., Kschonsak, M., Li, Y., Metz, J., Haering, C.H., Panne, D., 2016. Structure of the Pds5-Scc1 Complex and Implications for Cohesin Function. *Cell Reports.* **14,** 2116-2126.

Mullins, J.M., 1999. Overview of fluorochromes. *Methods in Molecular Biology.* **115,** 97-105.

Murayama, Y. & Uhlmann, F., 2015. DNA Entry into and Exit out of the Cohesin Ring by an Interlocking Gate Mechanism. *Cell.* **163,** 1628-1640.

Murayama, Y. & Uhlmann, F., 2014. Biochemical reconstitution of topological DNA binding by the cohesin ring. *Nature.* **505,** 367-371.

Murayama, Y. & Uhlmann, F., 2013. Chromosome segregation: how to open cohesin without cutting the ring? *Embo Journal.* **32,** 614-616.

Musacchio, A., 2011. Spindle assembly checkpoint: the third decade. *Philosophical Transactions of the Royal Society of London - Series B: Biological Sciences.* **366,** 3595-3604.

Musacchio, A. & Salmon, E.D., 2007. The spindle-assembly checkpoint in space and time. *Nature Reviews Molecular Cell Biology.* **8,** 379-393.

Musio, A., Selicorni, A., Focarelli, M.L., Gervasini, C., Milani, D., Russo, S., Vezzoni, P., Larizza, L., 2006. X-linked Cornelia de Lange syndrome owing to SMC1L1 mutations. *Nature Genetics.* **38,** 528-530.

Nagase, T., Seki, N., Ishikawa, K., Ohira, M., Kawarabayasi, Y., Ohara, O., Tanaka, A., Kotani, H., Miyajima, N., Nomura, N., 1996. Prediction of the coding sequences of unidentified human genes. VI. The coding sequences of 80 new genes (KIAA0201-KIAA0280) deduced by analysis of cDNA clones from cell line KG-1 and brain. *DNA Research.* **3,** 321-329.

Nakajima, H., Toyoshima-Morimoto, F., Taniguchi, E., Nishida, E., 2003. Identification of a consensus motif for Plk (Polo-like kinase) phosphorylation reveals Myt1 as a Plk1 substrate. *Journal of Biological Chemistry.* **278,** 25277-25280.

Nakajima, M., Kumada, K., Hatakeyama, K., Noda, T., Peters, J., Hirota, T., 2007. The complete removal of cohesin from chromosome arms depends on separase. *Journal of Cell Science.* **120,** 4188-4196.

Nasmyth, K., 2005. How might cohesin hold sister chromatids together? *Philosophical Transactions of the Royal Society of London - Series B: Biological Sciences.* **360,** 483-496.

Nasmyth, K., 2001. Disseminating the genome: joining, resolving, and separating sister chromatids during mitosis and meiosis. *Annual Review of Genetics.* **35,** 673-745.

Nasmyth, K., 2011. Cohesin: a catenase with separate entry and exit gates? *Nature Cell Biology.* **13,** 1170-1177.

Nasmyth, K. & Haering, C.H., 2009. Cohesin: its roles and mechanisms. *Annual Review of Genetics.* **43,** 525-558.

Nasmyth, K. & Haering, C.H., 2005. The structure and function of SMC and kleisin complexes. *Annual Review of Biochemistry.* **74,** 595-648.

Nativio, R., Wendt, K.S., Ito, Y., Huddleston, J.E., Uribe-Lewis, S., Woodfine, K., Krueger, C., Reik, W., Peters, J., Murrell, A., 2009. Cohesin is required for higher-order chromatin conformation at the imprinted IGF2-H19 locus. *PLoS Genetics.* **5,** e1000739.

Nigg, E.A., 2001. Mitotic kinases as regulators of cell division and its checkpoints. *Nature Reviews Molecular Cell Biology.* **2,** 21-32.

Nishiyama, T., Ladurner, R., Schmitz, J., Kreidl, E., Schleiffer, A., Bhaskara, V., Bando, M., Shirahige, K., Hyman, A.A., Mechtler, K., Peters, J., 2010. Sororin Mediates Sister Chromatid Cohesion by Antagonizing Wapl. *Cell.* **143,** 737-749.

Nishiyama, T., Sykora, M.M., Huis in 't Veld,Pim J., Mechtler, K., Peters, J., 2013. Aurora B and Cdk1 mediate Wapl activation and release of acetylated cohesin from chromosomes by phosphorylating Sororin. *Proceedings of the National Academy of Sciences of the United States of America.* **110,** 13404-13409.

Ocampo-Hafalla, M.T. & Uhlmann, F., 2011. Cohesin loading and sliding. *Journal of Cell Science.* **124,** 685-691.

Oikawa, K., Ohbayashi, T., Kiyono, T., Nishi, H., Isaka, K., Umezawa, A., Kuroda, M., Mukai, K., 2004. Expression of a novel human gene, Human wings apart-like (hWAPL), is associated with cervical carcinogenesis and tumor progression. *Cancer Research.* **64,** 3545-3549.

Oikawa, K., Akiyoshi, A., Tanaka, M., Takanashi, M., Nishi, H., Isaka, K., Kiseki, H., Idei, T., Tsukahara, Y., Hashimura, N., Mukai, K., Kuroda, M., 2008. Expression of various types of alternatively spliced WAPL transcripts in human cervical epithelia. *Gene.* **423,** 57-62.

Olins, A.L. & Olins, D.E., 1974. Spheroid chromatin units (v bodies). *Science.* **183,** 330-332.

Olins, D.E. & Olins, A.L., 2003. Chromatin history: our view from the bridge. *Nature Reviews Molecular Cell Biology.* **4,** 809-814.

Onn, I.*, et al*, 2008. Sister chromatid cohesion: A simple concept with a complex reality.

Orth, M., Mayer, B., Rehm, K., Rothweiler, U., Heidmann, D., Holak, T.A., Stemmann, O., 2011. Shugoshin is a Mad1/Cdc20-like interactor of Mad2. *EMBO Journal.* **30,** 2868-2880.

Ouyang, Z., Zheng, G., Song, J., Borek, D.M., Otwinowski, Z., Brautigam, C.A., Tomchick, D.R., Rankin, S., Yu, H., 2013. Structure of the human cohesin inhibitor Wapl. *Proceedings of the National Academy of Sciences of the United States of America.* **110,** 11355-11360.

Panizza, S., Tanaka, T., Hochwagen, A., Eisenhaber, F., Nasmyth, K., 2000. Pds5 cooperates with cohesin in maintaining sister chromatid cohesion. *Current Biology.* **10,** 1557-1564.

Parelho, V., Hadjur, S., Spivakov, M., Leleu, M., Sauer, S., Gregson, H.C., Jarmuz, A., Canzonetta, C., Webster, Z., Nesterova, T., Cobb, B.S., Yokomori, K., Dillon, N., Aragon, L., Fisher, A.G., Merkenschlager, M., 2008. Cohesins functionally associate with CTCF on mammalian chromosome arms. *Cell.* **132,** 422-433.

Parish, J.L., Rosa, J., Wang, X., Lahti, J.M., Doxsey, S.J., Androphy, E.J., 2006. The DNA helicase ChlR1 is required for sister chromatid cohesion in mammalian cells. *Journal of Cell Science.* **119,** 4857-4865.

Peng, C.Y., Graves, P.R., Thoma, R.S., Wu, Z., Shaw, A.S., Piwnica-Worms, H., 1997. Mitotic and G2 checkpoint control: regulation of 14-3-3 protein binding by phosphorylation of Cdc25C on serine-216. *Science.* **277,** 1501-1505.

Perrimon, N., Engstrom, L., Mahowald, A.P., 1985. Developmental genetics of the 2C-D region of the Drosophila X chromosome. *Genetics.* **111,** 23-41.

Peters JM, Tedeschi A, Schmitz J, 2008. The cohesin complex and its roles in chromosome biology. *Genes & Development.* **22,** 3089-3114.

Peters, J.M., 2006. The anaphase promoting complex/cyclosome: a machine designed to destroy. *Nature Reviews Molecular Cell Biology.* **7,** 644-656.

Peters, J.M., 2002. The anaphase-promoting complex: proteolysis in mitosis and beyond. *Molecular Cell.* **9,** 931-943.

Peters, J., 2012. The many functions of cohesin-different rings to rule them all? *Embo Journal.* **31,** 2061-2063.

Peters, J., 2010. Roles of Cohesin and Wapl in Sister Chromatid Cohesion, Chromatin Structure and Gene Regulation. *American Journal of Medical Genetics Part a.* **152A,** 1638-1638.

Peters, J. & Bhaskara, V., 2009. Cohesin Acetylation: From Antiestablishment to Establishment. *Molecular Cell.* **34,** 1-2.

Peters, J. & Nishiyama, T., 2012. Sister Chromatid Cohesion. *Cold Spring Harbor Perspectives in Biology.* **4,** a011130.

Petronczki, M., Siomos, M.F., Nasmyth, K., 2003. Un menage a quatre: the molecular biology of chromosome segregation in meiosis. *Cell.* **112,** 423-440.

Pfau, S.J. & Amon, A., 2012. Chromosomal instability and aneuploidy in cancer: from yeast to man. *EMBO Reports.* **13,** 515-527.

Pfleger, C.M. & Kirschner, M.W., 2000. The KEN box: an APC recognition signal distinct from the D box targeted by Cdh1. *Genes & Development.* **14,** 655-665.

Pinsky, B. & Biggins, S., 2005. The spindle checkpoint: tension versus attachment. *Trends in Cell Biology.* **15,** 486-493.

Pouwels, J., Kukkonen, A.M., Lan, W., Daum, J.R., Gorbsky, G.J., Stukenberg, T., Kallio, M.J., 2007. Shugoshin 1 plays a central role in kinetochore assembly and is required for kinetochore targeting of Plk1. *Cell Cycle.* **6,** 1579-1585.

Qi, W. & Yu, H., 2006. The spindle checkpoint and chromosomal stability. *Genome Dynamics.* **1,** 116-130.

Rabitsch, K.P., Gregan, J., Schleiffer, A., Javerzat, J., Eisenhaber, F., Nasmyth, K., 2004. Two fission yeast homologs of Drosophila Mei-S332 are required for chromosome segregation during meiosis I and II. *Current Biology.* **14,** 287-301.

Rankin, S., 2005. Sororin, the cell cycle and sister chromatid cohesion. *Cell Cycle.* **4,** 1039-1042.

Rankin, S., 2004. Sororin, a substrate of the anaphase promoting complex, is required for sister chromatid cohesion in vertebrates. *Molecular Biology of the Cell.* **15,** 240A-240A.

Rankin, S., Ayad, N., Kirschner, M., 2005. Sororin, a substrate of the anaphase-promoting complex, is required for sister chromatid cohesion in vertebrates. *Molecular Cell.* **18,** 185-200.

Rankin, S., 2006. A Wapl a day keeps the sisters apart: Wapl and cohesin dynamics. *Developmental Cell.* **11,** 754-755.

Reddy, S.K., Rape, M., Margansky, W.A., Kirschner, M.W., 2007. Ubiquitination by the anaphase-promoting complex drives spindle checkpoint inactivation. *Nature.* **446,** 921-925.

Remeseiro, S., Cuadrado, A., Losada, A., 2013. Cohesin in development and disease. *Development.* **140,** 3715-3718.

Remeseiro, S., Cuadrado, A., Carretero, M., Martinez, P., Drosopoulos, W.C., Canamero, M., Schildkraut, C.L., Blasco, M.A., Losada, A., 2012. Cohesin-SA1 deficiency drives aneuploidy and tumourigenesis in mice due to impaired replication of telomeres. *Embo Journal.* **31,** 2076-2089.

Remeseiro, S. & Losada, A., 2013. Cohesin, a chromatin engagement ring. *Current Opinion in Cell Biology.* **25,** 63-71.

Resnick, T.D., Satinover, D.L., MacIsaac, F., Stukenberg, P.T., Earnshaw, W.C., Orr-Weaver, T.L., Carmena, M., 2006. INCENP and Aurora B promote meiotic sister chromatid cohesion through localization of the Shugoshin MEI-S332 in Drosophila. *Developmental Cell.* **11,** 57-68.

Rhodes, J.M., McEwan, M., Horsfield, J.A., 2011. Gene regulation by cohesin in cancer: Is the ring an unexpected party to proliferation? *Molecular Cancer Research.* **9,** 1587-1607.

Riedel, C.G., Katis, V.L., Katou, Y., Mori, S., Itoh, T., Helmhart, W., Galova, M., Petronczki, M., Gregan, J., Cetin, B., Mudrak, I., Ogris, E., Mechtler, K., Pelletier, L., Buchholz, F., Shirahige, K., Nasmyth, K., 2006. Protein phosphatase 2A protects centromeric sister chromatid cohesion during meiosis I. *Nature.* **441,** 53-61.

Rieder, C.L., Schultz, A., Cole, R., Sluder, G., 1994. Anaphase onset in vertebrate somatic cells is controlled by a checkpoint that monitors sister kinetochore attachment to the spindle. *Journal of Cell Biology.* **127,** 1301-1310.

Rivera, T. & Losada, A., 2006. Shugoshin and PP2A, shared duties at the centromere. *Bioessays.* **28,** 775-779.

Rivera, T. & Losada, A., 2009. Shugoshin regulates cohesion by driving relocalization of PP2A in Xenopus extracts. *Chromosoma.* **118,** 223-233.

Rocquain, J., Gelsi-Boyer, V., Adelaide, J., Murati, A., Carbuccia, N., Vey, N., Birnbaum, D., Mozziconacci, M., Chaffanet, M., 2010. Alteration of cohesin genes in myeloid diseases. *American Journal of Hematology.* **85,** 717-719.

Rolef Ben-Shahar, T., Heeger, S., Lehane, C., East, P., Flynn, H., Skehel, M., Uhlmann, F., 2008. Eco1-dependent cohesin acetylation during establishment of sister chromatid cohesion. *Science.* **321,** 563-566.

Rowland, B.D., Roig, M.B., Nishino, T., Kurze, A., Uluocak, P., Mishra, A., Beckouet, F., Underwood, P., Metson, J., Imre, R., Mechtler, K., Katis, V.L., Nasmyth, K., 2009. Building sister chromatid cohesion: smc3 acetylation counteracts an antiestablishment activity. *Molecular Cell.* **33,** 763-774.

Ruchaud, S., Carmena, M., Earnshaw, W.C., 2007. Chromosomal passengers: conducting cell division. *Nature Reviews Molecular Cell Biology.* **8,** 798-812.

Ryu, B., Kim, D.S., Deluca, A.M., Alani, R.M., 2007. Comprehensive expression profiling of tumor cell lines identifies molecular signatures of melanoma progression. *PLoS ONE [Electronic Resource].* **2,** e594.

Sakuno, T. & Watanabe, Y., 2009. Studies of meiosis disclose distinct roles of cohesion in the core centromere and pericentromeric regions. *Chromosome Research.* **17,** 239-249.

Salic, A., Waters, J.C., Mitchison, T.J., 2004. Vertebrate shugoshin links sister centromere cohesion and kinetochore microtubule stability in mitosis. *Cell.* **118,** 567-578.

Samora, C.P., Saksouk, J., Goswami, P., Wade, B.O., Singleton, M.R., Bates, P.A., Lengronne, A., Costa, A., Uhlmann, F., 2016. Ctf4 Links DNA Replication with Sister Chromatid Cohesion Establishment by Recruiting the Chl1 Helicase to the Replisome. *Molecular Cell.* **63,** 371-384.

Sanchez, Y., Wong, C., Thoma, R.S., Richman, R., Wu, Z., Piwnica-Worms, H., Elledge, S.J., 1997. Conservation of the Chk1 checkpoint pathway in mammals: linkage of DNA damage to Cdk regulation through Cdc25. *Science.* **277,** 1497-1501.

Sanyal, S., Kovacikova, I., Gregan, J., 2013. Chromosome Segregation: Disarming the Protector. *Current Biology.* **23,** R236-R239.

Scheffner, M., 1998. Ubiquitin, E6-AP, and their role in p53 inactivation. *Pharmacology & Therapeutics.* **78,** 129-139.

Schmidt, D., Schwalie, P.C., Ross-Innes, C.S., Hurtado, A., Brown, G.D., Carroll, J.S., Flicek, P., Odom, D.T., 2010. A CTCF-independent role for cohesin in tissue-specific transcription. *Genome Research.* **20,** 578-588.

Schmiesing JA, Ball AR Jr, Gregson HC, Alderton JM, Zhou S, Yokomori K, 1998. Identification of two distinct human SMC protein complexes involved in mitotic chromosome dynamics. *Proceedings of the National Academy of Sciences of the United States of America.* **95,** 12906-12911.

Schmitz, J., Watrin, E., Lenart, P., Mechtler, K., Peters, J.M., 2007. Sororin is required for stable binding of cohesin to chromatin and for sister chromatid cohesion in interphase. *Current Biology.* **17,** 630-636.

Schüle, B., Oviedo, A., Johnston, K., Pai, S., Francke, U., 2005. Inactivating mutations in ESCO2 cause SC phocomelia and Roberts syndrome: No phenotype-genotype correlation. *American Journal of Human Genetics.* **77,** 1117-1128.

Sczaniecka, M.M. & Hardwick, K.G., 2008. The spindle checkpoint: how do cells delay anaphase onset? *SEB Experimental Biology Series.* **59,** 243-256.

Seitan, V.C. & Merkenschlager, M., 2012. Cohesin and chromatin organisation. *Current Opinion in Genetics & Development.* **22,** 93-100.

Shen, Z., 2011. Genomic instability and cancer: an introduction. *Journal of Molecular Cell Biology.* **3,** 1-3.

Sherwood, R., Takahashi, T.S., Jallepalli, P.V., 2010. Sister acts: coordinating DNA replication and cohesion establishment. *Genes & Development.* **24,** 2723-2731.

Shintomi, K. & Hirano, T., 2009. Releasing cohesin from chromosome arms in early mitosis: opposing actions of Wapl-Pds5 and Sgo1. *Genes & Development.* **23,** 2224-2236.

Shiomi, Y., Shinozaki, A., Nakada, D., Sugimoto, K., Usukura, J., Obuse, C., Tsurimoto, T., 2002. Clamp and clamp loader structures of the human checkpoint protein complexes, Rad9-1-1 and Rad17-RFC. *Genes to Cells.* **7,** 861-868.

Simon, A.C., Zhou, J.C., Perera, R.L., Van Deursen, F., Evrin, C., Ivanova, M.E., Kilkenny, M.L., Renault, L., Kjaer, S., Matak-Vinkovi, D., Labib, K., Costa, A., Pellegrini, L., 2014. A Ctf4 trimer couples the CMG helicase to DNA polymerase α in the eukaryotic replisome. *Nature.* **510,** 293-297.

Skibbens, R.V., Corson, L.B., Koshland, D., Hieter, P., 1999. Ctf7p is essential for sister chromatid cohesion and links mitotic chromosome structure to the DNA replication machinery. *Genes & Development.* **13,** 307-319.

Skibbens, R.V., 2009. Establishment of Sister Chromatid Cohesion Minireview. *Current Biology.* **19,** R1126-R1132.

Skibbens, R.V., 2004. Chl1p, a DNA helicase-like protein in budding yeast, functions in sister-chromatid cohesion. *Genetics.* **166,** 33-42.

Smith, J., Tho, L.M., Xu, N., Gillespie, D.A., 2010. The ATM-Chk2 and ATR-Chk1 pathways in DNA damage signaling and cancer. *Advances in Cancer Research.* **108,** 73-112.

Smits, V.A.J. & Gillespie, D.A., 2015. DNA damage control: regulation and functions of checkpoint kinase 1. *FEBS Journal.* **282,** 3681-3692.

Smits, V.A.J., Warmerdam, D.O., Martin, Y., Freire, R., 2010. Mechanisms of ATR-mediated checkpoint signalling. *Frontiers in Bioscience (Landmark Edition).* **15,** 840-853.

Sofueva, S., Yaffe, E., Chan, W., Georgopoulou, D., Vietri Rudan, M., Mira-Bontenbal, H., Pollard, S.M., Schroth, G.P., Tanay, A., Hadjur, S., 2013. Cohesin-mediated interactions organize chromosomal domain architecture. *EMBO Journal.* **32,** 3119-3129.

Solomon, D.A., Kim, J., Waldman, T., 2014. Cohesin gene mutations in tumorigenesis: from discovery to clinical significance. *BMB Reports.* **47,** 299-310.

Solomon, D.A., Kim, T., Diaz-Martinez, L.A., Fair, J., Elkahloun, A.G., Harris, B.T., Toretsky, J.A., Rosenberg, S.A., Shukla, N., Ladanyi, M., Samuels, Y., James, C.D., Yu, H., Kim, J., Waldman, T., 2011. Mutational inactivation of STAG2 causes aneuploidy in human cancer. *Science.* **333,** 1039-1043.

Song, J., Lafont, A., Chen, J., Wu, F.M., Shirahige, K., Rankin, S., 2012. Cohesin Acetylation Promotes Sister Chromatid Cohesion Only in Association with the Replication Machinery. *Journal of Biological Chemistry.* **287,** 34325-34336.

Stead, K., Aguilar, C., Hartman, T., Drexel, M., Meluh, P., Guacci, V., 2003. Pds5p regulates the maintenance of sister chromatid cohesion and is sumoylated to promote the dissolution of cohesion. *Journal of Cell Biology.* **163,** 729-741.

Stegmeier, F., Rape, M., Draviam, V.M., Nalepa, G., Sowa, M.E., Ang, X.L., McDonald, E.R.3., Li, M.Z., Hannon, G.J., Sorger, P.K., Kirschner, M.W., Harper, J.W., Elledge, S.J., 2007. Anaphase initiation is regulated by antagonistic ubiquitination and deubiquitination activities. *Nature.* **446,** 876-881.

Stemmann, O., Boos, D., Gorr, I.H., 2005. Rephrasing anaphase: separase FEARs shugoshin. *Chromosoma.* **113,** 409-417.

Strom, L., Lindroos, H.B., Shirahige, K., Sjogren, C., 2004. Postreplicative recruitment of cohesin to double-strand breaks is required for DNA repair. *Molecular Cell.* **16,** 1003-1015.

Strom, L., Karlsson, C., Lindroos, H.B., Wedahl, S., Katou, Y., Shirahige, K., Sjogren, C., 2007. Postreplicative formation of cohesion is required for repair and induced by a single DNA break. *Science.* **317,** 242-245.

Stursberg S, Riwar B, Jessberger R, 1999. Cloning and characterization of mammalian SMC1 and SMC3 genes and proteins, components of the DNA recombination complexes RC-1. *Gene.* **228,** 1-12.

Sudakin, V., Chan, G.K.T., Yen, T.J., 2001. Checkpoint inhibition of the APC/C in HeLa cells is mediated by a complex of BUBR1, BUB3, CDC20, and MAD2. *Journal of Cell Biology.* **154,** 925-936.

Suijkerbuijk, S.J.E. & Kops, G.J.P.L., 2008. Preventing aneuploidy: The contribution of mitotic checkpoint proteins. *Biochimica Et Biophysica Acta-Reviews on Cancer.* **1786,** 24-31.

Sumara, I., Vorlaufer, E., Gieffers, C., Peters, B.H., Peters, J.M., 2000. Characterization of vertebrate cohesin complexes and their regulation in prophase. *Journal of Cell Biology.* **151,** 749-762.

Sumara, I., Vorlaufer, E., Stukenberg, P.T., Kelm, O., Redemann, N., Nigg, E.A., Peters, J.M., 2002. The dissociation of cohesin from chromosomes in prophase is regulated by Polo-like kinase. *Molecular Cell.* **9,** 515-525.

Sutani, T., Kawaguchi, T., Kanno, R., Itoh, T., Shirahige, K., 2010. Budding Yeast Eco1 Counteracts Anti-"Cohesion Establishment" Function of Wpl1-Pds5 Complex. *American Journal of Medical Genetics Part a.* **152A,** 1639-1640.

Sutani, T., Kawaguchi, T., Kanno, R., Itoh, T., Shirahige, K., 2009. Budding yeast Wpl1(Rad61)-Pds5 complex counteracts sister chromatid cohesion-establishing reaction. *Current Biology.* **19,** 492-497.

Takagi, M., Bunai, K., Yanagi, K., Imamoto, N., 2008. Cloning of Xenopus orthologs of Ctf7/Eco1 acetyltransferase and initial characterization of XEco2. *FEBS Journal.* **275,** 6109-6122.

Takahashi, T.S., Yiu, P., Chou, M.F., Gygi, S., Walter, J.C., 2004. Recruitment of Xenopus Scc2 and cohesin to chromatin requires the pre-replication complex. *Nature Cell Biology.* **6,** 991-996.

Takahashi, T.S., Basu, A., Bermudez, V., Hurwitz, J., Walter, J.C., 2008. Cdc7-Drf1 kinase links chromosome cohesion to the initiation of DNA replication in Xenopus egg extracts. *Genes & Development.* **22,** 1894-1905.

Takaki, T., Trenz, K., Costanzo, V., Petronczki, M., 2008. Polo-like kinase 1 reaches beyond mitosis--cytokinesis, DNA damage response, and development. *Current Opinion in Cell Biology.* **20,** 650-660.

Takayama, Y., Kamimura, Y., Okawa, M., Muramatsu, S., Sugino, A., Araki, H., 2003. GINS, a novel multiprotein complex required for chromosomal DNA replication in budding yeast. *Genes & Development.* **17,** 1153-1165.

Tanaka, H., Katou, Y., Yagura, M., Saitoh, K., Itoh, T., Araki, H., Bando, M., Shirahige, K., 2009. Ctf4 coordinates the progression of helicase and DNA polymerase a. *Genes to Cells.* **14,** 807-820.

Tanaka, K., Hao, Z., Kai, M., Okayama, H., 2001. Establishment and maintenance of sister chromatid cohesion in fission yeast by a unique mechanism. *EMBO Journal.* **20,** 5779-5790.

Tanaka, K. & Watanabe, Y., 2008. Chromatid Cohesion: Acetylation Joins the Sisters. *Current Biology.* **18,** R917-R919.

Tanaka, T., Fuchs, J., Loidl, J., Nasmyth, K., 2000. Cohesin ensures bipolar attachment of microtubules to sister centromeres and resists their precocious separation. *Nature Cell Biology.* **2,** 492-499.

Tang, Z., Shu, H., Qi, W., Mahmood, N.A., Mumby, M.C., Yu, H., 2006. PP2A is required for centromeric localization of Sgo1 and proper chromosome segregation. *Developmental Cell.* **10,** 575-585.

Tang, Z., Sun, Y., Harley, S., Zou, H., Yu, H., 2004. Human Bub1 protects centromeric sister-chromatid cohesion through Shugoshin during mitosis. *Proceedings of the National Academy of Sciences of the United States of America.* **101,** 18012-18017.

Taylor, S. & Peters, J.M., 2008. Polo and Aurora kinases: lessons derived from chemical biology. *Current Opinion in Cell Biology.* **20,** 77-84.

Taylor, S., 1999. Chromosome segregation: Dual control ensures fidelity. *Current Biology.* **9,** R562-R564.

Tedeschi, A., Wutz, G., Huet, S., Jaritz, M., Wuensche, A., Schirghuber, E., Davidson, I.F., Tang, W., Cisneros, D.A., Bhaskara, V., Nishiyama, T., Vaziri, A., Wutz, A., Ellenberg, J., Peters, J.M., 2013. Wapl is an essential regulator of chromatin structure and chromosome segregation. *Nature.* **501,** 564-568.

Terret, M., Sherwood, R., Rahman, S., Qin, J., Jallepalli, P.V., 2009. Cohesin acetylation speeds the replication fork. *Nature.* **462,** 231-U106.

Thol F, Bollin R, Gehlhaar M, Walter C, Dugas M, Suchanek KJ, Kirchner A, Huang L, Chaturvedi A, Wichmann M, Wiehlmann L, Shahswar R, Damm F, Gohring G, Schlegelberger B, Schlenk R, Dohner K, Dohner H, Krauter J, Ganser A, Heuser M, 2014. Mutations in the cohesin complex in acute myeloid leukemia: clinical and prognostic implications. *Blood.* **123,** 914-920.

Thota S, Viny AD, Makishima H, Spitzer B, Radivoyevitch T, Przychodzen B, Sekeres MA, Levine RL, Maciejewski JP, 2014. Genetic alterations of the cohesin complex genes in myeloid malignancies. *Blood.* **124,** 1790-1798.

Tong, K. & Skibbens, R.V., 2015. Pds5 regulators segregate cohesion and condensation pathways in Saccharomyces cerevisiae. *Proceedings of the National Academy of Sciences of the United States of America.* **112,** 7021-7026.

Tonkin, E.T., Wang, T., Lisgo, S., Bamshad, M.J., Strachan, T., 2004. NIPBL, encoding a homolog of fungal Scc2-type sister chromatid cohesion proteins and fly Nipped-B, is mutated in Cornelia de Lange syndrome. *Nature Genetics.* **36,** 636-641.

Toth, A., Ciosk, R., Uhlmann, F., Galova, M., Schleiffer, A., Nasmyth, K., 1999. Yeast cohesin complex requires a conserved protein, Eco1p(Ctf7), to establish cohesion between sister chromatids during DNA replication. *Genes & Development.* **13,** 320-333.

Trinkle-Mulcahy, L. & Lamond, A.I., 2006. Mitotic phosphatases: no longer silent partners. *Current Opinion in Cell Biology.* **18,** 623-631.

Uhlmann, F., 2004. The mechanism of sister chromatid cohesion. *Experimental Cell Research.* **296,** 80-85.

Uhlmann, F., 2003. Chromosome cohesion and separation: from men and molecules. *Current Biology.* **13,** R104-14.

Uhlmann, F., 2000. Chromosome cohesion: a polymerase for chromosome bridges. *Current Biology.* **10,** R698-700.

Uhlmann, F., Lottspeich, F., Nasmyth, K., 1999. Sister-chromatid separation at anaphase onset is promoted by cleavage of the cohesin subunit Scc1. *Nature.* **400,** 37-42.

Uhlmann, F. & Nasmyth, K., 1998. Cohesion between sister chromatids must be established during DNA replication. *Current Biology.* **8,** 1095-1101.

Uhlmann, F., 2016. SMC complexes: from DNA to chromosomes. *Nature Reviews Molecular Cell Biology.* **17,** 399-412.

Unal, E., Arbel-Eden, A., Sattler, U., Shroff, R., Lichten, M., Haber, J.E., Koshland, D., 2004. DNA damage response pathway uses histone modification to assemble a double-strand break-specific cohesin domain. *Molecular Cell.* **16,** 991-1002.

Unal, E., Heidinger-Pauli, J.M., Kim, W., Guacci, V., Onn, I., Gygi, S.P., Koshland, D.E., 2008. A molecular determinant for the establishment of sister chromatid cohesion. *Science.* **321,** 566-569.

Unal, E., Heidinger-Pauli, J.M., Koshland, D., 2007. DNA double-strand breaks trigger genome-wide sister-chromatid cohesion through Eco1 (Ctf7). *Science.* **317,** 245-248.

Upton, A.L. & Sherratt, D.J., 2013. Breaking symmetry in SMCs. *Nature Structural & Molecular Biology.* **20,** 246-249.

van der Lelij, P., Chrzanowska, K.H., Godthelp, B.C., Rooimans, M.A., Oostra, A.B., Stumm, M., Zdzienicka, M.Z., Joenje, H., de Winter, J.P., 2010. Warsaw breakage syndrome, a cohesinopathy associated with mutations in the XPD helicase family member DDX11/ChlR1. *American Journal of Human Genetics.* **86,** 262-266.

van der Lelij, P., Godthelp, B.C., van Zon, W., van Gosliga, D., Oostra, A.B., Steltenpool, J., de Groot, J., Scheper, R.J., Wolthuis, R.M., Waisfisz, Q., Darroudi, F., Joenje, H., de Winter, J.P., 2009. The cellular phenotype of Roberts syndrome fibroblasts as revealed by ectopic expression of ESCO2. *PLoS ONE [Electronic Resource].* **4,** e6936.

Vanoosthuyse, V., Prykhozhij, S., Hardwick, K.G., 2007. Shugoshin 2 regulates localization of the chromosomal passenger proteins in fission yeast mitosis. *Molecular Biology of the Cell.* **18,** 1657-1669.

Varma, D., Wan, X., Cheerambathur, D., Gassmann, R., Suzuki, A., Lawrimore, J., Desai, A., Salmon, E.D., 2013. Spindle assembly checkpoint proteins are positioned close to core microtubule attachment sites at kinetochores. *Journal of Cell Biology.* **202,** 735-746.

Vaur, S., Feytout, A., Vazquez, S., Javerzat, J., 2012. Pds5 promotes cohesin acetylation and stable cohesin-chromosome interaction. *EMBO Reports.* **13,** 645-652.

Vega, H., Waisfisz, Q., Gordillo, M., Sakai, N., Yanagihara, I., Yamada, M., van Gosliga, D., Kayserili, H., Xu, C., Ozono, K., Jabs, E.W., Inui, K., Joenje, H., 2005. Roberts syndrome is caused by mutations in ESCO2, a human homolog of yeast ECO1 that is essential for the establishment of sister chromatid cohesion. *Nature Genetics.* **37,** 468-470.

Verni, F., Gandhi, R., Goldberg, M., Gatti, M., 2000. Genetic and molecular analysis of wings apart-like (wapl), a gene controlling heterochromatin organization in Drosophila melanogaster. *Genetics.* **154,** 1693-1710.

Vernos, I. & Peters, J., 2008. Twenty years of cell-cycle conferences in Roscoff. *Nature Cell Biology.* **10,** 877-880.

Visconti, R., Palazzo, L., Pepe, A., Monica, R.D., Grieco, D., 2013. The end of mitosis from a phosphatase perspective. *Cell Cycle.* **12,** 17-19.

Vogelstein, B., Pardoll, D.M., Coffey, D.S., 1980. Supercoiled loops and eukaryotic DNA replication. *Cell.* **22,** 79-85.

Waizenegger, I.C., Hauf, S., Meinke, A., Peters, J.M., 2000. Two distinct pathways remove mammalian cohesin from chromosome arms in prophase and from centromeres in anaphase. *Cell.* **103,** 399-410.

Wang, F., Yoder, J., Antoshechkin, I., Han, M., 2003. Caenorhabditis elegans EVL-14/PDS-5 and SCC-3 are essential for sister chromatid cohesion in meiosis and mitosis. *Molecular and Cellular Biology.* **23,** 7698-7707.

Wang, S.-., Read, R.L., Norbury, C.J., 2002. Fission yeast Pds5 is required for accurate chromosome segregation and for survival after DNA damage or metaphase arrest. *Journal of Cell Science.* **115,** 587-598.

Wang, X. & Dai, W., 2005. Shugoshin, a guardian for sister chromatid segregation. *Experimental Cell Research.* **310,** 1-9.

Wang, X., Yang, Y., Dai, W., 2006. Differential subcellular localizations of two human Sgo1 isoforms: implications in regulation of sister chromatid cohesion and microtubule dynamics. *Cell Cycle.* **5,** 635-640.

Wang, X., Yang, Y., Duan, Q., Jiang, N., Huang, Y., Darzynkiewicz, Z., Dai, W., 2008. sSgo1, a major splice variant of Sgo1, functions in centriole cohesion where it is regulated by Plk1. *Developmental Cell.* **14,** 331-341.

Wang, Z. & Christman, M.F., 2001. Replication-related activities establish cohesion between sister chromatids. *Cell Biochemistry & Biophysics.* **35,** 289-301.

Wassmann, K., 2013. Sister chromatid segregation in meiosis II: Deprotection through phosphorylation. *Cell Cycle.* **12,** 1352-1359.

Watanabe, Y., 2005. Shugoshin: guardian spirit at the centromere. *Current Opinion in Cell Biology.* **17,** 590-595.

Watanabe, Y., 2005. Sister chromatid cohesion along arms and at centromeres. *Trends in Genetics.* **21,** 405-412.

Watanabe, Y., 2004. Modifying sister chromatid cohesion for meiosis. *Journal of Cell Science.* **117,** 4017-4023.

Watanabe, Y. & Kitajima, T., 2005. Shugoshin protects cohesin complexes at centromeres. *Philosophical Transactions of the Royal Society B-Biological Sciences.* **360,** 515-520.

Watrin, E. & Peters, J.-., 2006. Cohesin and DNA damage repair. *Experimental Cell Research.* **312,** 2687-2693.

Wendt, K.S., Yoshida, K., Itoh, T., Bando, M., Koch, B., Schirghuber, E., Tsutsumi, S., Nagae, G., Ishihara, K., Mishiro, T., Yahata, K., Imamoto, F., Aburatani, H., Nakao, M., Imamoto, N., Maeshima, K., Shirahige, K., Peters, J., 2008. Cohesin mediates transcriptional insulation by CCCTC-binding factor. *Nature.* **451,** 796-801.

Whelan, G., Kreidl, E., Wutz, G., Egner, A., Peters, J., Eichele, G., 2012. Cohesin acetyltransferase Esco2 is a cell viability factor and is required for cohesion in pericentric heterochromatin. *EMBO Journal.* **31,** 71-82.

White, G.E. & Erickson, H.P., 2006. Sequence divergence of coiled coils--structural rods, myosin filament packing, and the extraordinary conservation of cohesins. *Journal of Structural Biology.* **154,** 111-121.

Williams, B.C., Garrett-Engele, C.M., Li, Z., Williams, E.V., Rosenman, E.D., Goldberg, M.L., 2003. Two putative acetyltransferases, san and deco, are required for establishing sister chromatid cohesion in Drosophila. *Current Biology.* **13,** 2025-2036.

Wu, F.M., Nguyen, J.V., Rankin, S., 2011. A conserved motif at the C terminus of sororin is required for sister chromatid cohesion. *Journal of Biological Chemistry.* **286,** 3579-3586.

Wu, N., Kong, X., Ji, Z., Yokomori, K., Potts, P.R., Yu, H., 2012. Scc1 sumoylation by Mms21 promotes sister chromatid recombination through counteracting Wapl. *Faseb Journal.* **26,** .

Xiong, B., Lu, S., Gerton, J.L., 2010. Hos1 is a lysine deacetylase for the Smc3 subunit of cohesin. *Current Biology.* **20,** 1660-1665.

Xu, H., Tomaszewski, J.M., McKay, M.J., 2011. Can corruption of chromosome cohesion create a conduit to cancer? *Nature Reviews.Cancer.* **11,** 199-210.

Xu, H., Boone, C., Brown, G.W., 2007. Genetic dissection of parallel sister-chromatid cohesion pathways. *Genetics.* **176,** 1417-1429.

Yamagishi, Y., Sakuno, T., Shimura, M., Watanabe, Y., 2008. Heterochromatin links to centromeric protection by recruiting shugoshin. *Nature.* **455,** 251-255.

Yang, J., Ikezoe, T., Nishioka, C., Yokoyama, A., 2013. A novel treatment strategy targeting shugoshin 1 in hematological malignancies. *Leukemia Research.* **37,** 76-82.

Yang, Y., Wang, X., Dai, W., 2006. Human Sgo1 is an excellent target for induction of apoptosis of transformed cells. *Cell Cycle.* **5,** 896-901.

Yao, S., Neiman, A., Prelich, G., 2000. BUR1 and BUR2 encode a divergent cyclin-dependent kinase-cyclin complex important for transcription in vivo. *Molecular & Cellular Biology.* **20,** 7080-7087.

Yao, Y. & Dai, W., 2012. Shugoshins function as a guardian for chromosomal stability in nuclear division. *Cell Cycle.* **11,** 2631-2642.

Yu, H., 2002. Regulation of APC-Cdc20 by the spindle checkpoint. *Current Opinion in Cell Biology.* **14,** 706-714.

Yu, H. & Tang, Z., 2005. Bub1 multitasking in mitosis. *Cell Cycle.* **4,** 262-265.

Zamariola, L., De Storme, N., Tiang, C.L., Armstrong, S.J., Franklin, F.C.H., Geelen, D., 2013. SGO1 but not SGO2 is required for maintenance of centromere cohesion in Arabidopsis thaliana meiosis. *Plant Reproduction.* **26,** 197-208.

Zhang, B., Jain, S., Song, H., Fu, M., Heuckeroth, R.O., Erlich, J.M., Jay, P.Y., Milbrandt, J., 2007. Mice lacking sister chromatid cohesion protein PDS5B exhibit developmental abnormalities reminiscent of Cornelia de Lange syndrome. *Development.* **134,** 3191-3201.

Zhang, N., Kuznetsov, S.G., Sharan, S.K., Li, K., Rao, P.H., Pati, D., 2008. A handcuff model for the cohesin complex. *Journal of Cell Biology.* **183,** 1019-1031.

Zhang, N. & Pati, D., 2009. Handcuff for sisters: A new model for sister chromatid cohesion. *Cell Cycle.* **8,** 399-402.

Zhang, N., Jiang, Y., Mao, Q., Demeler, B., Tao, Y.J., Pati, D., 2013. Characterization of the Interaction between the Cohesin Subunits Rad21 and SA1/2. *Plos One.* **8,** e69458.

Zhang, N., Panigrahi, A.K., Jiang, Y., Rao, P.H., Pati, D., 2010. Role of Sororin in sister chromatid cohesion and separation in vertebrates. *Faseb Journal.* **24,** .

Zhang, N., Panigrahi, A.K., Mao, Q., Pati, D., 2011. Interaction of Sororin Protein with Polo-like Kinase 1 Mediates Resolution of Chromosomal Arm Cohesion. *Journal of Biological Chemistry.* **286,** 41826-41837.

Zhang, N. & Pati, D., 2015. C-terminus of Sororin interacts with SA2 and regulates sister chromatid cohesion. *Cell Cycle.* **14,** 820-826.

Zhang, N. & Pati, D., 2012. Sororin is a master regulator of sister chromatid cohesion and separation. *Cell Cycle.* **11,** 2073-2083.

Zhang, S., Li, J., Zhou, G., Mu, D., Yan, J., Xing, J., Yao, Z., Sheng, H., Li, D., Lv, C., Sun, B., Hong, Q., Guo, H., 2016. Increased expression of ESCO1 is correlated with poor patient survival and its role in human bladder cancer. *Tumour Biology.* **37,** 5165-5170.

Zhang, Y., Huang, X., Qi, J., Yan, C., Xu, X., Han, Y., Wang, M., 2008. Correlation of genomic and expression alterations of AS3 with esophageal squamous cell carcinoma. *Journal of Genetics & Genomics = Yi Chuan Xue Bao.* **35,** 267-271.

Zhang, Z., Ren, Q., Yang, H., Conrad, M.N., Guacci, V., Kateneva, A., Dresser, M.E., 2005. Budding yeast PDS5 plays an important role in meiosis and is required for sister chromatid cohesion. *Molecular Microbiology.* **56,** 670-680.

Zhao, H. & Piwnica-Worms, H., 2001. ATR-mediated checkpoint pathways regulate phosphorylation and activation of human Chk1. *Molecular & Cellular Biology.* **21,** 4129-4139.

Zheng, G. & Yu, H., 2015. Regulation of sister chromatid cohesion during the mitotic cell cycle. *Science China.Life Sciences.* **58,** 1089-1098.

Zhou, J., Yao, J., Joshi, H.C., 2002. Attachment and tension in the spindle assembly checkpoint. *Journal of Cell Science.* **115,** 3547-3555.

Zuin, J., Dixon, J.R., van der Reijden,Michael I J A., Ye, Z., Kolovos, P., Brouwer, R.W.W., van de Corput,Mariette P C., van de Werken,Harmen J G., Knoch, T.A., van IJcken, W.F.J., Grosveld, F.G., Ren, B., Wendt, K.S., 2014. Cohesin and CTCF differentially affect chromatin architecture and gene expression in human cells. *Proceedings of the National Academy of Sciences of the United States of America.* **111,** 996-1001.

Chapter 7 - APPENDIX

A1

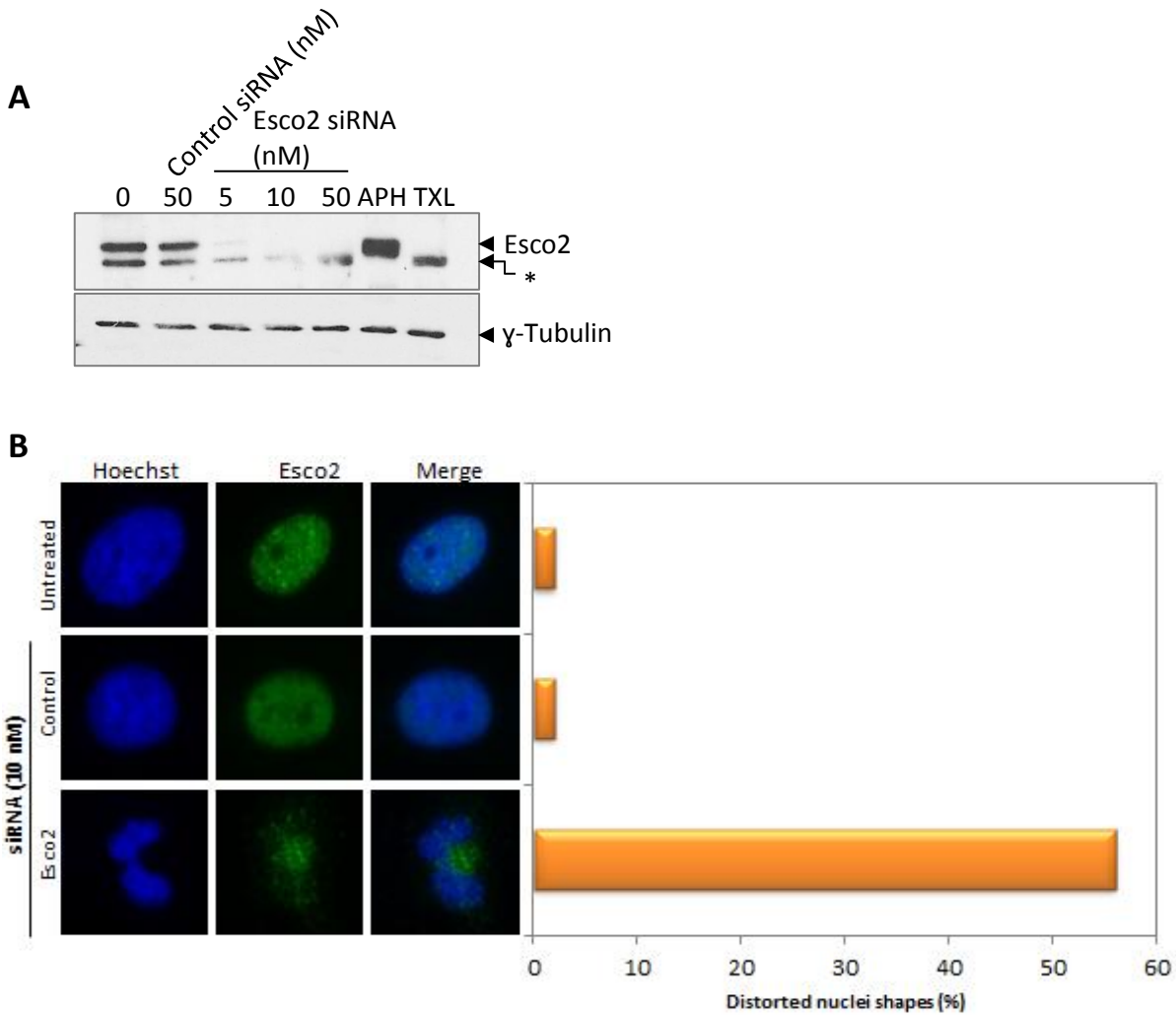

Figure 7.1 Depletion of Esco2 induces formation of multilobed nuclei

(**A**) Western blot of HeLa cell lysates following treatment with either control (50 nM) or Esco2 siRNA (5-50 nM) for 48 h. Control cells were also treated with Aphidicolin (APH, 5μg/ml) and Taxol (TXL, 1 μg/ml) for 24 h to arrest them at the G1/S or M-phase, respectively. Cells were lysed in RIPA buffer and Western blot was carried out using anti-Esco2 and anti-γ-Tubulin antibodies. (**B**) Immunofluorescence images and quantitation of asynchronous HeLa cells following a 48-h treatment with 10 nM of either control or Esco2 siRNAs. Cells were fixed in Methanol before being blocked with BSA (5 % w/v) and stained with the anti-Esco2 antibody (green). DNA was stained with Hoechst 33342 (blue). *= non-specific binding. Merged images are shown in the last panels in B. Scale bar: 10 μm.

A2

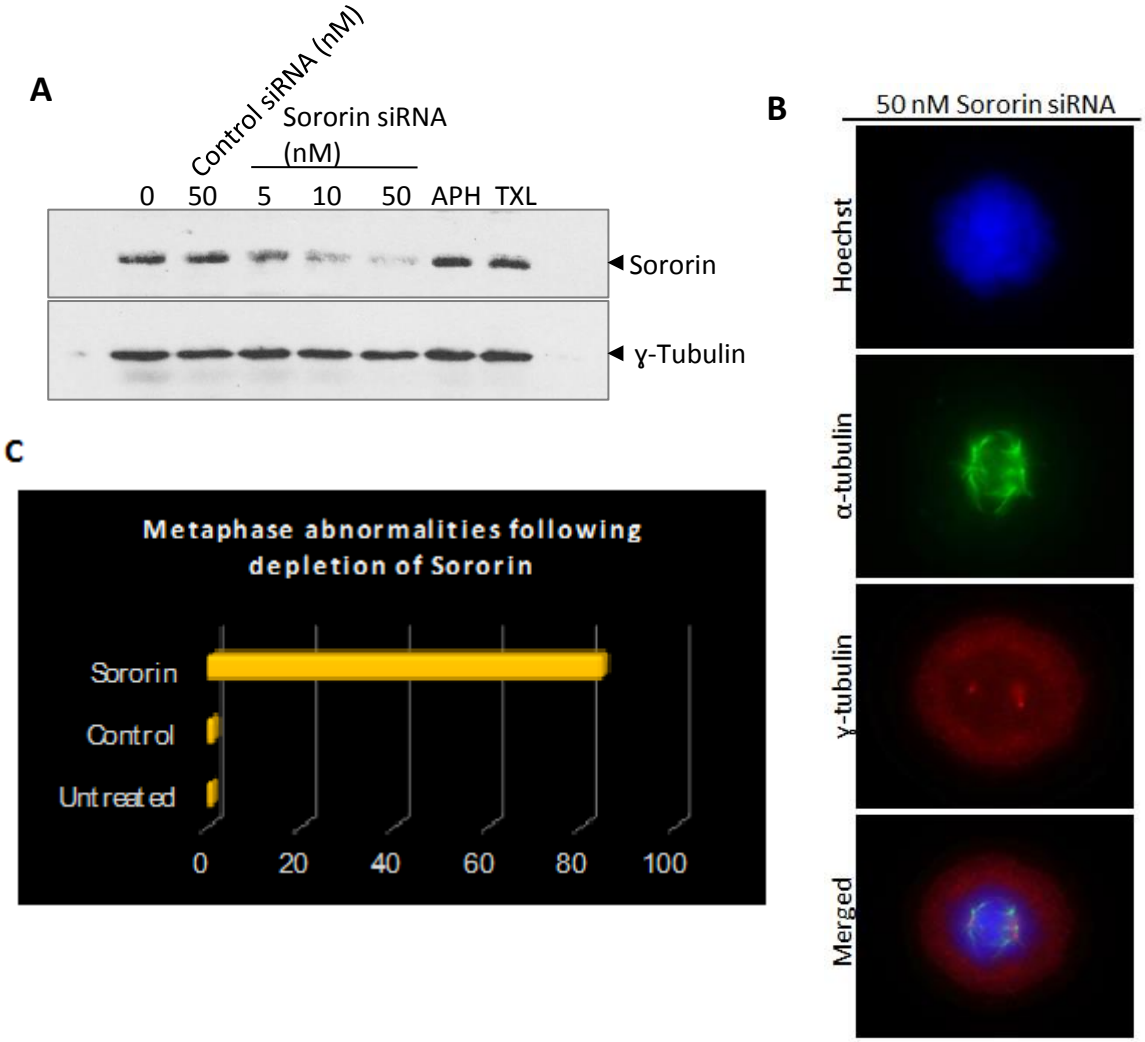

Figure 7.2 Depletion of Sororin results in abnormal metaphase

(**A**) Western blot of HeLa cell lysates following treatment with either control (50 nM) or Sororin siRNA (5-50 nM) for 48 h. Control cells were also treated with Aphidicolin (APH, 5μg/ml) and Taxol (TXL, 1 μg/ml) for 24 h to arrest them at the G1/S or M-phase, respectively. Cells were lysed in RIPA buffer and Western blot was carried out using anti-Sororin and anti-γ-Tubulin antibodies. (**B**) Immunofluorescence images of HeLa cells following a 48-h treatment with 50 nM of the Sororin siRNA. Cells were fixed in Methanol before being blocked with BSA (5 % w/v) and stained with the anti-α-Tubulin antibody (green) or anti-γ-Tubulin antibody (red). DNA was stained with Hoechst 33342 (blue). A merged image is shown in the bottom panel in B. Scale bar: 10 μm. (**C**) Histogram showing quantification of data in **B.**

A3

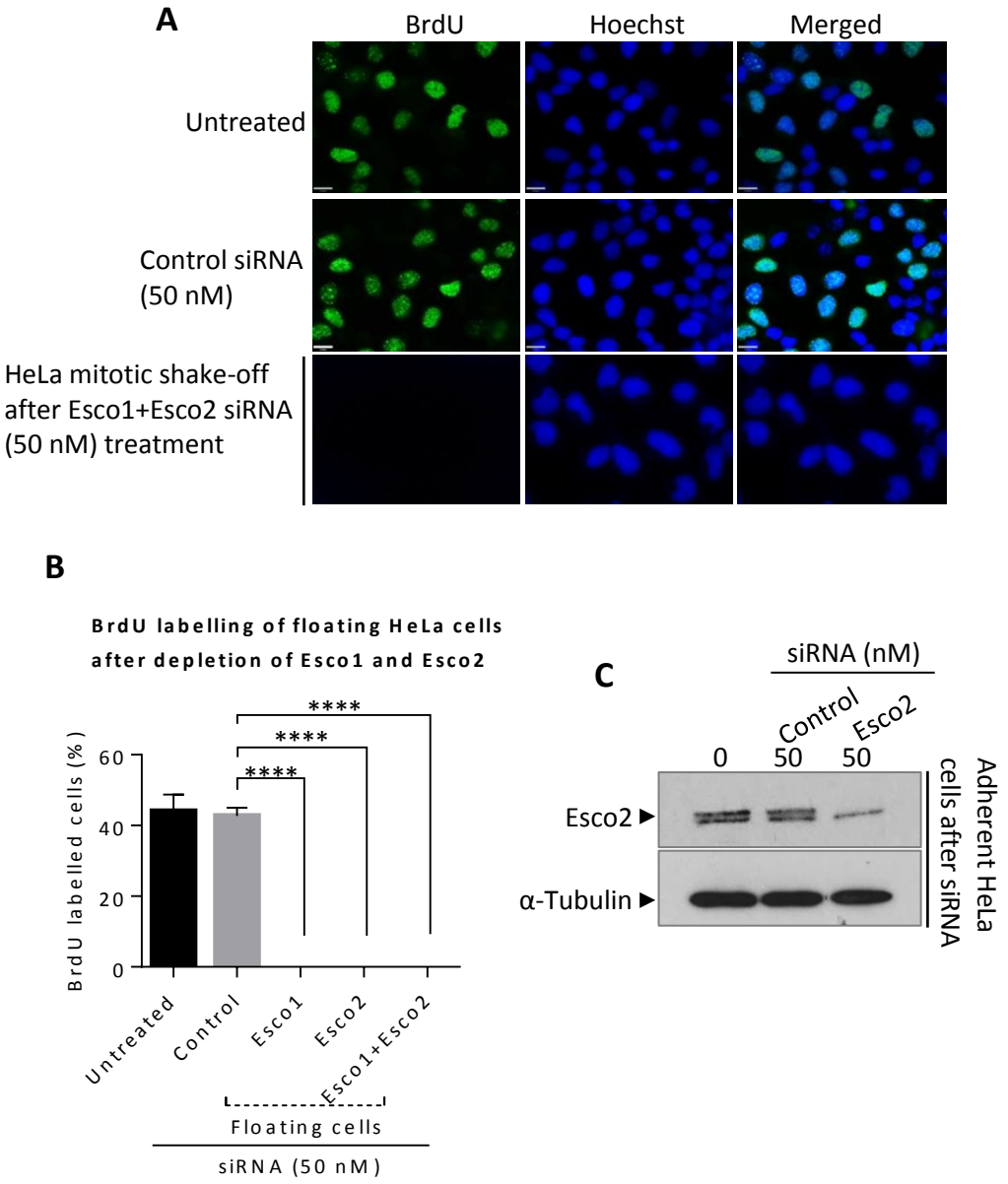

Figure 7.3 HeLa cells detaching from tissue culture plates following depletion of Esco1 and Esco2 cannot incorporate BrdU

(**A**) Immunofluorescence images of BrdU (1 μM)-labelled HeLa cells following a 48 h treatment with 50 nM of either control, Esco1, Esco2, or both Esco1 and Esco2 siRNAs. Cells were fixed in Methanol before being blocked with BSA (5 % w/v) and stained with the anti-BrdU antibody (green). DNA was stained with Hoechst 33342 (blue). Merged images are shown in the last panels. Scale bar: 10 μm. (**B**) Histogram showing quantitation of data in (**A**). The mean+s.e.m of at least 100 cells counted in randomly selected fields is shown. ****P < 0.0001. P values were calculated using a two-tailed Student t-test. (**C**) Western blot of adherent HeLa cell lysates after mitotic shake-off following treatment with either control (10 nM) or Esco2 siRNA (10 nM) for 48 h. Cells were lysed in RIPA buffer prior to Western blotting with the anti-Esco2 and anti-α-Tubulin antibodies.

A4

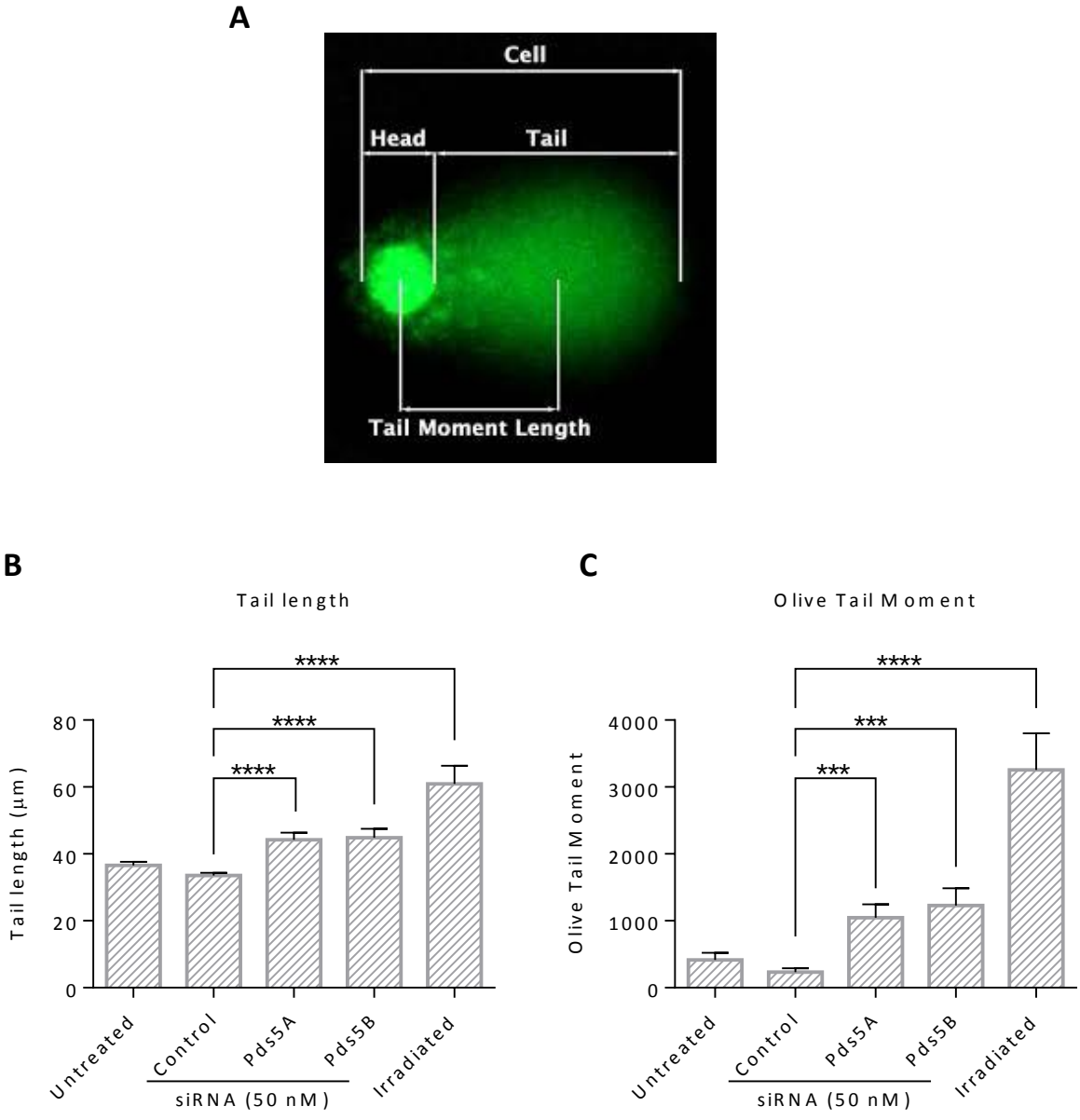

Figure 7.4 Depletion of Pds5 proteins induces DNA damage

(**A**) Representative image showing quantifiable parameters of a comet (adapted from Cell Biolabs, Inc. product data sheet). (**B** and **C**) Histograms showing quantitation of Tail Lengths and Olive Tail Moments, respectively, of comets derived from Propidium Iodide (1 mg/ml)-labelled HeLa cells following a 48 h-treatment with 50 nM of either control, Pds5A, or Pds5B siRNAs. Control cells were also X-Ray irradiated (195 kV) for 6 min and 19 s. The mean+s.e.m of at least 100 cells scored in randomly selected fields is shown. ***P < 0.001 ****P < 0.0001. P values were calculated using a two-tailed Student t-test. Prior to image analysis, cells were mixed with low melting point agarose and electrophoresis performed in ice-cold alkali buffer at 30V, 300mA for 20 min.